

Middlesex University Research Repository

An open access repository of

Middlesex University research

<http://eprints.mdx.ac.uk>

Abdullah Thani, Noor Azela (2016) Evaluation of the potential therapeutic effects of curcumin and lycopene in adult malignant brain tumour cells in vitro. PhD thesis, Middlesex University.
[Thesis]

Final accepted version (with author's formatting)

This version is available at: <https://eprints.mdx.ac.uk/21220/>

Copyright:

Middlesex University Research Repository makes the University's research available electronically.

Copyright and moral rights to this work are retained by the author and/or other copyright owners unless otherwise stated. The work is supplied on the understanding that any use for commercial gain is strictly forbidden. A copy may be downloaded for personal, non-commercial, research or study without prior permission and without charge.

Works, including theses and research projects, may not be reproduced in any format or medium, or extensive quotations taken from them, or their content changed in any way, without first obtaining permission in writing from the copyright holder(s). They may not be sold or exploited commercially in any format or medium without the prior written permission of the copyright holder(s).

Full bibliographic details must be given when referring to, or quoting from full items including the author's name, the title of the work, publication details where relevant (place, publisher, date), pagination, and for theses or dissertations the awarding institution, the degree type awarded, and the date of the award.

If you believe that any material held in the repository infringes copyright law, please contact the Repository Team at Middlesex University via the following email address:

eprints@mdx.ac.uk

The item will be removed from the repository while any claim is being investigated.

See also repository copyright: re-use policy: <http://eprints.mdx.ac.uk/policies.html#copy>

**Evaluation of the potential therapeutic effects
of curcumin and lycopene in adult malignant
brain tumour cells *in vitro***

Noor Azela Abdullah Thani



**A dissertation submitted in partial fulfilment of the
requirements of Middlesex University for the degree of
Doctor of Philosophy**

June 2015

Abstract

Glioblastoma multiforme are the most challenging of cancers to treat and even with recent advances in therapeutic approaches, the prognosis following diagnosis remains poor. Novel therapeutic approaches able to target such tumours without resulting in significant toxicity are needed. Micronutrients have been shown to exert potential therapeutic effects in cell culture and animal models which include anti-cancer activity and other functional properties such as anti-microbial and anti-oxidative effects. The aim of this research was to investigate the anti-cancer properties of curcumin (77% pure, derived from the ground rhizome of turmeric) and LycoRed powder (containing 10% lycopene from tomato extract) on four primary brain tumour-biopsy derived cell cultures (glioblastoma multiforme malignant cells) using a normal brain cell line as control (CC2565; passage 10 and above).

The morphological appearance of the normal brain cell line and glioblastoma cell cultures was compared under phase contrast microscopy. The cytotoxicity of curcumin and LycoRed was determined using a DRAQ 7 cell viability assay. Expression of antigens linked to invasive, angiogenic and apoptotic potential was studied using immunocytochemistry and flow cytometry. Induction of apoptosis was investigated using flow cytometry via Annexin-V staining. Anti-invasive and anti-angiogenic potentials were studied using a FluoroBlok invasion and angiogenesis assay (co-culture method) *in vitro*, respectively.

Brain tumour-biopsy derived cell cultures incubated for 24h with increasing concentrations of curcumin showed significant decreased in cell viability ($IC_{75,50,25}$ values 14.2 to 19.5 $\mu\text{g/ml}$). LycoRed was not found to affect the cell viability of tumour cells and no IC values could be established; only curcumin was therefore investigated in subsequent assays (using IC_{75} concentration). Neither curcumin nor LycoRed showed toxicity to normal brain cells.

No significant induction of apoptosis by curcumin was observed in the primary brain tumour cells studied. However, three of the primary brain tumour cell cultures investigated were high in invasive capacity and curcumin treatment at IC₇₅ concentration reduced the percentage of invasion after only 24 hours of incubation. In addition, curcumin was found to have anti-angiogenic properties *in vitro*. In the normal brain cell culture, each parameter (number of nodes, junctions and branches) was maintained when treated with increasing concentrations of curcumin (0 to 40µg/ml). When all glioblastoma cell cultures and normal brain cells showed strong positivity for GFAP confirming that they are astrocytic in origin, expression of other antigens studied (Beta-1-integrin, CD44, VEGF, MMP-14, NG2, GD3) varied between the primary brain tumour cell cultures. This suggests that the invasive or angiogenic capacity of the glioblastoma cell cultures investigated may not be attributable to one common factor as has been reported before, but perhaps an integration of many factors with overlapping functions.

In conclusion, the results indicate that curcumin may have anti cancer properties through inhibition of invasion and angiogenesis in these malignant glioblastomas. Further studies are necessary to establish whether LycoRed possesses therapeutic potential.

Contents

Abstract.....	i
Contents	iii
List of Figures and Tables	vii
Acknowledgements	xvi

Chapter 1: Introduction

1.1 Classification of brain tumour	1
1.2 Classification of astrocytoma	2
1.3 Glioblastoma Multiforme	2
1.4 Types of Glioblastoma Multiforme: primary (<i>de novo</i>) and secondary	3
1.5 Incidence of Glioblastoma Multiforme	4
1.6 Pathophysiology of Glioblastoma Multiforme	5
1.7 Diagnosis of Glioblastoma Multiforme	7
1.8 Aetiology of Glioblastoma Multiforme	8
1.9 Mortality/Morbidity caused by Glioblastoma Multiforme	10
1.10 Biological features of Glioblastomas at a molecular level	11
1.10.1 Invasion	12
1.10.2 Heterogeneity.....	16
1.10.3 Angiogenesis	17
1.11 Stem cells.....	20
1.12 Apoptosis as a targeted therapeutic approach.....	22
1.13 Current treatment options for Glioblastoma	24
1.13.1 Neurosurgery	24
1.13.2 Radiotherapy.....	25
1.13.3 Chemotherapy.....	25
1.13.3.1 Temozolomide	26
1.13.3.2 Gliadel wafer (Carmustine)	27
1.13.3.3 Chlorimipramine.....	28
1.13.3.4 Bevacizumab (Avastin)	29

1.14 Novel treatment in Glioblastoma therapy: natural occurring micronutrients as integrative treatment	30
1.14.1 Flavanoids.....	31
1.15 Curcumin as the therapeutic agent.....	32
1.15.1 Dietary sources of curcumin.....	32
1.15.2 Chemical structure and therapeutic properties	32
1.15.3 Absorption, metabolism and transport.....	38
1.15.4 Bioavailability with tissue distribution.....	38
1.15.5 Cytotoxicity of curcumin.....	39
1.16 Lycopene, a naturally occurring pigment with health benefits	40
1.16.1 Dietary sources of lycopene	40
1.16.2 Chemical structure and therapeutic properties	40
1.16.3 Absorption, metabolism and transport.....	42
1.16.4 Bioavailability of lycopene with tissue distribution	43
1.16.5 Cytotoxicity of lycopene	44
1.17 Aim and research objectives.....	45

Chapter 2: Materials and methods

2.1 List of materials	46
2.2 Methods	55
2.2.1 Purification of Tetrahydrofuran.....	55
2.2.2 Preparation of Curcumin and LycoRed concentrations.....	55
2.2.3 Cell culture maintenance	56
2.2.4 Population doubling time.....	58
2.2.5 Cell viability assays	60
2.2.5.1 Calcein AM cell viability assays	61
2.2.5.2 Cell viability assay using the flow cytometry (DRAQ 7)	62
2.2.6 Cell characterization of primary brain tumour cells.....	64
2.2.6.1 Immunocytochemistry (ICC).....	64
2.2.6.2 Flow cytometry	67
2.2.7 <i>In vitro</i> invasion assay	69
2.2.8 Apoptosis assay via flow cytometry analysis (Annexin V detection).....	70
2.2.9 <i>In vitro</i> angiogenesis assay (co-culture method)	72
2.2.10 Statistical analysis.....	75

Chapter 3: Results

3.1 Morphology of primary brain tumour cell cultures	76
3.2 Population doubling time of primary brain tumour cell cultures	79
3.3 Dimethyl sulphoxide and Tetrahydrofuran cytotoxicity	81
3.4 IC values of the Curcumin and LycoRed	83
3.5 Antigens expression in primary brain tumour cells.....	90
3.5.1 Qualitative analysis of antigen expression using immunocytochemistry.....	90
3.5.2 Quantitative analysis of antigen expression using flow cytometry	95
3.6 Curcumin anti-invasive property in primary brain tumour cells	101
3.7 Curcumin as a pro-apoptotic agent.....	103
3.8 Curcumin as a potential anti-angiogenic agent.....	119

Chapter 4: Discussions

128

Curcumin is cytotoxic to the primary brain tumour cells but not LycoRed.....	128
Curcumin's cytotoxicity induced via non-apoptotic pathway in the primary brain tumour cells.....	133
Curcumin suppressed angiogenic activity of primary brain tumour cells <i>in vitro</i>	137
The effect of curcumin on the invasive potential of glioblastoma cells.....	141
Variations in the antigen expression induced interplay of multitude events in glioblastoma cells	144
Heterogeneity of glioblastoma cells contributes to sophisticated expression of markers and varied population doubling time.....	157
Conclusions	161
Further studies of importance.....	162

References

168

Appendices

Lists of figures

Figure 1: Two biological forms of glioblastoma that exist, each with different pathways of pathogenesis and possible genetic evolution. Adapted from Pilkington, 2001	4
Figure 2: Schematic representation of the mechanism of glioma cell interaction with astrocytes for invasion. Taken from Bellail <i>et al.</i> , 2004	15
Figure 3: Pathways involved in apoptosis	23
Figure 4: Chemical structures of curcuminoids; A) Curcumin, B) Demethoxycurcumin C) Bisdemethoxycurcumin and D) Cyclocurcumin	33
Figure 5: Multiple molecular targets of curcumin	37
Figure 6: Metabolic pathways of curcumin in rodents and <i>in vitro</i> culture (rat and human hepatocytes). Taken from: Marczylo <i>et al.</i> , 2007	39
Figure 7: Lycopene with 40 carbon acyclic in structure	40
Figure 8: Caretenoid uptake by micelles following ingestion and its release into the bloodstream prior to deposition in the tissues (Yeum and Russel, 2002). GI: gastrointestinal, CAR: Carotenoids, apo-CAR: apo-carotenoids, VLDL: very low density lipoprotein, LDL: low density lipoprotein, HDL: high density lipoprotein, RAL: retinal	43
Figure 9: A sigmoidal curve showing three different phases in cell growth. The numbers of cells/ml obtained from the count are plotted against number of hours in culture.	59
Figure 10: A cell viability curve with % of viable cells (y axis) and concentration of micronutrient (x axis) shows IC values. The IC values are derived at the point where % of viable cells crossed the curve and marked down towards the x axis to determine the concentration of micronutrient, i.e. IC value.	60
Figure 11: Gating method in the DRAQ7 cell viability assay using controls as to establish the position of DRAQ7 positive and negative cells. This gating method is applied accordingly to each of the primary brain tumour cell cultures	63

Figure 12: Immunocytochemistry reaction using labelled secondary antibody (Alexa-Fluor 488-Streptavidin conjugated).

..... 65

Figure 13: A histogram shows a negative control in the flow cytometry analysis in which the primary antibody was omitted leaving only secondary antibody (with biotin conjugated) being incubated. M2 will represent the positive stained cells while M1 is negative in staining.

..... 68

Figure 14: A quadrant in the Annexin V apoptosis. Each region in the quadrant i.e. lower right, lower left, upper right and upper left represents the population of cells. Axis with FL3-H indicates PI and axis with FL4-H indicates Annexin V.

..... 71

Figure 15: The tubule network traced with Paint software (A and B) before analysed using Image J software (C). With the image J software, each colour represents a parameter measured in the angiogenesis. The four parameters are total length of the tubules, node and junction (red in blue circle) and branches (green)

..... 74

Figure 16: Phase contrast micrographs of the normal brain cell line; A) CC2565-passage 10 and primary brain tumour cell cultures (GB biopsy-derived); (B) MUBS-passage 6 (C) MUBP-passage 9 (D) MUTC-passage 8 and (E) MUP-passage 8. The different morphology of cells was shown by the colour coded arrows which include spindle (red), small star (green), large star (blue) and broad, straight and blunt end (purple) in shapes. All cell cultures were viewed and compared under phase contrast microscopy (20X magnification)

..... 77

Figure 17: Population doubling time of each primary brain tumour cell cultures. The x and y axis represent the doubling time (h) and cell cultures, respectively. Standard error of the mean is represented by the error bars. Data represents the mean \pm standard error of the mean for n=2 experiments with each experiment being carried out in duplicate. Statistical analysis was carried out using a 2 sample t-test analysis to obtain the *p* value (each group of treated cells were compared with the normal brain cells). * $p < 0.05$

..... 80

Figure 18: Cell viability of MUBS following treatment with DMSO at a range of concentrations at four different time points of incubation. DMSO is only cytotoxic to the primary brain tumour cell culture at a concentration of 0.5% and above. Residual cell viability is shown as a percentage of the untreated (control). Data represents the mean \pm standard error of the mean for n=2 experiments with each experiment being carried out in duplicate. (See chapter 2, section 2.2.5.1).

..... 82

Figure 19: Cell viability of the MUTC cells following treatment with THF at a range of concentrations at four different time point of incubation. THF is cytotoxic to the cells above concentration of 0.2%. Residual cell viability is shown as a percentage of the untreated (control). Data represents the mean \pm standard error of the mean for n=2 experiments with each experiment being carried out in duplicate. (See chapter 2, section 2.2.5.1).

..... 83

Figure 20 A-J: Percentage of live cells of each cell culture after 24hours treatment with Curcumin (A-E;yellow curves) or LycoRed (F-J;red curves). IC values are showed by the blue, green and purple lines representing IC₇₅, IC₅₀ and IC₂₅ respectively. Standard error of the mean is represented by the error bars. Data was taken from at least 3 sets of experiments in duplicate. Statistical analysis was carried out using a 2 sample t-test analysis to obtain the *p* value (each group of treated cells were compared with the untreated cells). * *p*<0.05. See chapter 2, section 2.2.5.2

..... 87

Figure 21: Antigen expression of CC2565 cell culture following staining with different antibodies via immunocytochemistry. A) GFAP B) GD3 C) NG2 D) CD44 E) Beta-1 integrin. F) Negative control.

..... 92

Figure 22: Antigen expression of MUBS cell culture following staining with different antibodies via immunocytochemistry. A) GFAP B) GD3 C) NG2 D) CD44 E) Beta-1 integrin. F) Negative control.

..... 92

Figure 23: Antigen expression of MUBP cell culture following staining with different antibodies via immunocytochemistry. A) GFAP B) GD3 C) NG2 D) CD44 E) Beta-1 integrin. F) Negative control.

..... 93

Figure 24: Antigen expression of MUTC cell culture following staining with different antibodies via immunocytochemistry. A) GFAP B) GD3 C) NG2 D) CD44 E) Beta-1 integrin. F) Negative control.

..... 93

Figure 25: Antigen expression of MUP cell culture following staining with different antibodies via immunocytochemistry. A) GFAP B) GD3 C) NG2 D) CD44 E) Beta-1 integrin. F) Negative control.

..... 94

Figure 26a: The level of Beta-1-integrin expression in control and primary brain tumour cells following 24h incubation. All cells were stained with each of the four antibodies followed by a secondary antibody with FITC conjugated in order to enable the visualization. Standard error of means was represented by the error bars. Data was taken from at least 3 sets of experiments in duplicate. Statistical analysis was carried out with 2 sample t-test analysis to obtain the *p* value (* *p*<0.05) which is the value of each brain tumour cell culture compared with the control cells.

..... 97

Figure 26b: The level of CD44 expression in control and primary brain tumour cells following 24h incubation. All cells were stained with each of the four antibodies followed by a secondary antibody with FITC conjugated in order to enable the visualization. Standard error of means was represented by the error bars. Data was taken from at least 3 sets of experiments in duplicate. Statistical analysis was carried out with 2 sample t-test analysis to obtain the *p* value (* *p*<0.05) which is the value of each brain tumour cell culture compared with the control cells.

..... 98

Figure 26c: The level of MMP-14 expression in control and primary brain tumour cells following 24h incubation. All cells were stained with each of the four antibodies followed by a secondary antibody with FITC conjugated in order to enable the visualization. Standard error of means was

represented by the error bars. Data was taken from at least 3 sets of experiments in duplicate. Statistical analysis was carried out with 2 sample t-test analysis to obtain the p value (* $p < 0.05$) which is the value of each brain tumour cell culture compared with the control cells.

..... 99

Figure 26d: The level of VEGF expression in control and primary brain tumour cells following 24h incubation. All cells were stained with each of the four antibodies followed by a secondary antibody with FITC conjugated in order to enable the visualization. Standard error of means was represented by the error bars. Data was taken from at least 3 sets of experiments in duplicate. Statistical analysis was carried out with 2 sample t-test analysis to obtain the p value (* $p < 0.05$) which is the value of each brain tumour cell culture compared with the control cells.

..... 100

Figure 27: 2 Dimensional invasion assay *in vitro* showed the percentage of invasion of each cell culture after 24h incubation. Data represents the mean \pm standard error of mean for $n=2$ experiments with each experiment being carried out in duplicate. Data was taken from at least 2 sets of experiments in duplicate. Statistical analysis was carried out with 2 sample t-test analysis to obtain the p value (* $p < 0.05$). [†] p value < 0.05 (significant different between untreated normal brain cells and untreated brain tumour cells). * p value < 0.05 (significant different between untreated and curcumin treated for each cell culture. Percentage of invasion is made by using HT1080 cells (positive control) that is known to be invasive, i.e. 100% invasion

..... 102

Figure 28 : Four representative diagrams from Annexin V apoptosis assay of normal brain cells at different hour of incubation (following curcumin treatment); 24h (upper left box), 48h (upper right box), 72h (lower left box) and 96h (lower right box). In a diagram, each quadrant represents viable cells (lower left), early apoptosis cells (lower right), late apoptotic cells (upper right) and necrotic cells (upper left). Percentage of cell gated in the quadrant is made by CellQuest software.

..... 105

Figure 29: Normal brain cells population from each quadrant (viable, early apoptotic, late apoptotic, necrotic) of every incubation time (following curcumin treatment) are represented in a bar graph. Error bars show standard error of mean. Data represents the mean \pm standard error of mean for $n=3$ experiments with each experiment being carried out in duplicate. Percentage of cell gated was followed by statistical analysis (one way ANOVA-Fisher comparison) as to obtain the p value (* p value < 0.05) and tabulated as below.

..... 106

Figure 30 : Four representative diagrams from Annexin V apoptosis assay of MUBS cells at different hour of incubation (following curcumin treatment); 24h (upper left box), 48h (upper right box), 72h (lower left box) and 96h (lower right box). In a diagram, each quadrant represents viable cells (lower left), early apoptosis cells (lower right), late apoptotic cells (upper right) and necrotic cells (upper left). Percentage of cell gated in the quadrant is made by CellQuest software 108

Figure 31: MUBS cells population from each quadrant (viable, early apoptotic, late apoptotic, necrotic) of every incubation time (following curcumin treatment) are represented in a bar graph. Error bars show standard error of mean. Data represents the mean \pm standard error of mean for $n=3$ experiments with each experiment being carried out in duplicate. Percentage of cell gated was

followed by statistical analysis (one way ANOVA-Fisher comparison) as to obtain the p value (* p value<0.05) and tabulated as below.

..... 109

Figure 32: Four representative diagrams from Annexin V apoptosis assay of MUBP cells at different hour of incubation (following curcumin treatment); 24h (upper left box), 48h (upper right box), 72h (lower left box) and 96h (lower right box). In a diagram, each quadrant represents viable cells (lower left), early apoptosis cells (lower right), late apoptotic cells (upper right) and necrotic cells (upper left). Percentage of cell gated in the quadrant is made by CellQuest software

..... 111

Figure 33: MUBP cells population from each quadrant (viable, early apoptotic, late apoptotic, necrotic) of every incubation time (following curcumin treatment) are represented in a bar graph. Error bars show standard error of mean. Data represents the mean \pm standard error of mean for $n=3$ experiments with each experiment being carried out in duplicate. Percentage of cell gated was followed by statistical analysis (one way ANOVA-Fisher comparison) as to obtain the p value (* p value<0.05) and tabulated as below.

..... 112

Figure 34: Four representative diagrams from Annexin V apoptosis assay of MUP cells at different hour of incubation (following curcumin treatment); 24h (upper left box), 48h (upper right box), 72h (lower left box) and 96h (lower right box). In a diagram, each quadrant represents viable cells (lower left), early apoptosis cells (lower right), late apoptotic cells (upper right) and necrotic cells (upper left). Percentage of cell gated in the quadrant is made by CellQuest software

..... 114

Figure 35: MUP cells population from each quadrant (viable, early apoptotic, late apoptotic, necrotic) of every incubation time (following curcumin treatment) are represented in a bar graph. Error bars show standard error of mean. Data represents the mean \pm standard error of mean for $n=3$ experiments with each experiment being carried out in duplicate. Percentage of cell gated was followed by statistical analysis (one way ANOVA-Fisher comparison) as to obtain the p value (* p value<0.05) and tabulated as below

..... 115

Figure 36: Four representative diagrams from Annexin V apoptosis assay of MUTC cells at different hour of incubation (following curcumin treatment); 24h (upper left box), 48h (upper right box), 72h (lower left box) and 96h (lower right box). In a diagram, each quadrant represents viable cells (lower left), early apoptosis cells (lower right), late apoptotic cells (upper right) and necrotic cells (upper left). Percentage of cell gated in the quadrant is made by CellQuest software

..... 117

Figure 37: MUTC cells population from each quadrant (viable, early apoptotic, late apoptotic, necrotic) of every incubation time (following curcumin treatment) are represented in a bar graph. Error bars show standard error of mean. Data represents the mean \pm standard error of mean for $n=3$ experiments with each experiment being carried out in duplicate. Percentage of cell gated was followed by statistical analysis (one way ANOVA-Fisher comparison) as to obtain the p value (* p value<0.05) and tabulated as below.-

..... 118

Figure 38: a) *In vitro* angiogenesis assay (co-culture) showed the tubule network analysed using Image J software. A= untreated, B=10µg/ml, C= 20µg/ml, D= 40µg/ml. b) Bar graphs showed normal brain cells (CC2565) treated with 0µg/ml (untreated)-blue, 10µg/ml- red, 20µg/ml-green and 40µg/ml curcumin-purple. Number of nodes, junctions, branches and total length of the tubules (µm) were quantified by Image J software analysis as demonstrated by the bar graphs. Data represents the mean ±standard error of mean for n=3 experiments with each experiment being carried out in triplicate. Statistical analysis (one way ANOVA and 2 sample t-test analysis) was carried out to obtain the *p* value (**p*<0.05). Normal brain cells were not affected by curcumin treatment at all concentrations studied due to the value that is not statistically different (*p*>0.05) compared to the untreated cells

122

Figure 39: a) *In vitro* angiogenesis assay (co-culture) showed the tubule network analysed using Image J software. A= untreated, B=10µg/ml, C= 20µg/ml, D= 40µg/ml. b) Bar graphs showed normal brain cells (CC2565) treated with 0µg/ml (untreated)-blue, 10µg/ml- red, 20µg/ml-green and 40µg/ml curcumin-purple. Number of nodes, junctions, branches and total length of the tubules (µm) were quantified by Image J software analysis as demonstrated by the bar graphs. Data represents the mean ±standard error of mean for n=3 experiments with each experiment being carried out in triplicate. Statistical analysis (one way ANOVA and 2 sample t-test analysis) was carried out to obtain the *p* value (**p*<0.05). In MUBP cells, curcumin treatment has affected all angiogenic parameters but only at highest concentration with *p* value <0.05

123

Figure 40: a) *In vitro* angiogenesis assay (co-culture) showed the tubule network analysed using Image J software. A= untreated, B=10µg/ml, C= 20µg/ml, D= 40µg/ml. b) Bar graphs showed normal brain cells (CC2565) treated with 0µg/ml (untreated)-blue, 10µg/ml- red, 20µg/ml-green and 40µg/ml curcumin-purple. Number of nodes, junctions, branches and total length of the tubules (µm) were quantified by Image J software analysis as demonstrated by the bar graphs. Data represents the mean ±standard error of mean for n=3 experiments with each experiment being carried out in triplicate. Statistical analysis (one way ANOVA and 2 sample t-test analysis) was carried out to obtain the *p* value (**p* value<0.05). With MUBS cells, reduction was noted significantly at each angiogenesis parameters and concentrations studied when compared between untreated and curcumin treated cells

124

Figure 41: a) *In vitro* angiogenesis assay (co-culture) showed the tubule network analysed using Image J software. A= untreated, B=10µg/ml, C= 20µg/ml, D= 40µg/ml. b) Bar graphs showed normal brain cells (CC2565) treated with 0µg/ml (untreated)-blue, 10µg/ml- red, 20µg/ml-green and 40µg/ml curcumin-purple. Number of nodes, junctions, branches and total length of the tubules (µm) were quantified by Image J software analysis as demonstrated by the bar graphs. Data represents the mean ±standard error of mean for n=3 experiments with each experiment being carried out in triplicate. Statistical analysis (one way ANOVA and 2 sample t-test analysis) was carried out to obtain the *p* value (**p* value<0.05) Three out of four parameters of angiogenesis were affected significantly by curcumin at all concentrations.

125

Figure 42: a) *In vitro* angiogenesis assay (co-culture) showed the tubule network analysed using Image J software. A= untreated, B=10µg/ml, C= 20µg/ml, D= 40µg/ml. b) Bar graphs showed normal brain cells (CC2565) treated with 0µg/ml (untreated)-blue, 10µg/ml- red, 20µg/ml-green and 40µg/ml curcumin-purple. Number of nodes, junctions, branches and total length of the tubules (µm) were quantified by Image J software analysis as demonstrated by the bar graphs. Data represents the

mean \pm standard error of mean for $n=2$ experiments with each experiment being carried out in triplicate. Statistical analysis (one way ANOVA and 2 sample t-test analysis) was carried out to obtain the p value (* p value <0.05). With MUTC cells, the numbers of branches were not statistically significant in difference following curcumin treatment as compared to the untreated cells.

..... 126

Figure 43: Positive (A)- Suramin treated) and negative (B)- VEGF treated) cells were used as controls. * p value <0.05 (significant different noted between untreated and curcumin treated cells at each angiogenesis parameters and cell culture studied).

..... 127

Lists of tables

Table 1: Genetic mutations identified in glioblastoma..... 6

Table 2: Working dilutions of the primary antibodies (*Abcam **Milipore ***Cancer Research UK (*Abcam **Milipore ***Cancer Research UK) 65

Table 3: Working dilutions of the primary antibodies (Abcam) 69

Table 4: A summary of the pathology and histopathology details of all biopsies studied. These details were provided by Kings College Hospital at an appropriate procedure. For the purpose of record, each biopsy was designated to an acronym according to the patient's first and last names... 78

Table 5: Statistical analysis (One way-ANOVA-Fisher comparison) to show differences in doubling time between brain tumour cell cultures (MUBP, MUBS, MUP and MUTC). The doubling time ranged between 80 to 208h between primary brain tumour cell cultures studied (MUBS<MUBP<MUP<MUTC). Data showed that there are significant differences between the cell cultures studied with $p<0.05$

..... 80

Table 6: IC values of each cell culture after 24 hour incubation with Curcumin. IC values were similar for all primary brain tumour cell cultures with Curcumin. See chapter 2, section 2.2.5.2..... 88

Table 7: Summary of immunocytochemistry results (qualitative) for antigen expression in normal brain cells (CC2565) compared to primary brain tumour cultures (MUBS, MUBP, MUTC and MUP)94

Table 8: Statistical analysis (One way-ANOVA-Fisher comparison) of each primary brain tumour cell culture against each other as well as against the control (after 24h incubation). The p value was denoted by* ($p<0.05$) indicated that the mean value for all cell cultures were statistically significant against each other cell culture (including when compared with the control) except for MUBS against MUP cell culture (each difference in mean value in bold has p value >0.05).-p97

..... 97

Table 9: Statistical analysis (One way-ANOVA-Fisher comparison) of each primary brain tumour cell culture against each other as well as against the control (after 24h incubation). The p value was denoted by* ($p<0.05$) indicated that the mean value for all cell cultures were statistically significant against each other cell culture (including when compared with the control) except for MUBS against control and MUTC against MUP cell culture (each difference in mean value in bold has p value >0.05)..... 98

Table 10: Statistical analysis (One way-ANOVA-Fisher comparison) of each primary brain tumour cell culture against each other as well as against the control (after 24h incubation). The p value was denoted by* ($p<0.05$) indicated that the mean value for all cell cultures were statistically significant against each other cell culture (including when compared with the control) except for MUBP against MUP (each difference in mean value in bold has $p\text{ value}>0.05$)

99

Table 11: Statistical analysis (One way-ANOVA-Fisher comparison) of each primary brain tumour cell culture against each other as well as against the control (after 24h incubation). The p value was denoted by* ($p<0.05$) indicated that the mean value for all cell cultures were statistically significant against each other cell culture (including when compared with the control) except for MUBP against MUBS and MUBP against MUP cells (each difference in mean value in bold has $p\text{ value}>0.05$)

100

Table 12(a-d): Statistical analysis (One way-ANOVA-Fisher comparison) of % cells gated for all incubation time; 24h-48h-72h-96h (against each other) for every quadrant, i.e. a) viable, b)early apoptotic, c) late apoptotic and d) necrotic quadrant. The p value was denoted by* ($p<0.05$) indicated that the mean value for all incubation time were statistically significant against each. Each difference in mean value in bold showed that $p\text{ value}>0.05$). Significant difference was noted between different incubation time studied in all quadrants except for late apoptotic cells quadrant

106&107

Table 13(a-d): Statistical analysis (One way-ANOVA-Fisher comparison) of % cells gated for all incubation time; 24h-48h-72h-96h (against each other) for every quadrant, i.e. a) viable, b)early apoptotic, c) late apoptotic and d) necrotic quadrant. The p value was denoted by* ($p<0.05$) indicated that the mean value for all incubation time were statistically significant against each. Each difference in mean value in bold showed that $p\text{ value}>0.05$). Significant difference was noted between different incubation time studied in all quadrants except for viable and late apoptotic cells quadrants

109&110

Table 14(a-d): Statistical analysis (One way-ANOVA-Fisher comparison) of % cells gated for all incubation time; 24h-48h-72h-96h (against each other) for every quadrant, i.e. a) viable, b)early apoptotic, c) late apoptotic and d) necrotic quadrant. The p value was denoted by* ($p<0.05$) indicated that the mean value for all incubation time were statistically significant against each. Each difference in mean value in bold showed that $p\text{ value}>0.05$). Significant difference was noted between different incubation time studied in all quadrants

112&113

Table 15(a-d): Statistical analysis (One way-ANOVA-Fisher comparison) of % cells gated for all incubation time; 24h-48h-72h-96h (against each other) for every quadrant, i.e. a) viable, b)early apoptotic, c) late apoptotic and d) necrotic quadrant. The p value was denoted by* ($p<0.05$) indicated that the mean value for all incubation time were statistically significant against each. Each difference in mean value in bold showed that $p\text{ value}>0.05$). Significant difference was noted between different incubation time studied in all quadrants except for viable and late apoptotic cells quadrants

115&116

Table 16(a-d): Statistical analysis (One way-ANOVA-Fisher comparison) of % cells gated for all incubation time; 24h-48h-72h-96h (against each other) for every quadrant, i.e. a) viable, b)early apoptotic, c) late apoptotic and d) necrotic quadrant. The p value was denoted by* ($p<0.05$) indicated that the mean value for all incubation time were statistically significant against each. Each

difference in mean value in bold showed that p value>0.05). Significant difference was noted between different incubation time studied in all quadrants except for necrotic cells quadrant
..... 118&119

ACKNOWLEDGEMENTS

First of all, I would like to express my deepest gratitude to my Almighty Lord, Allah SWT. Without His help, all of this would not be possible. With His guidance, He sends so many good people to help me through this challenging journey. Below are the lists of people and organizations that have helped me to get through in completing this thesis in the sequence of their appearance throughout the journey.

An appreciation goes to my sponsor, Ministry of Higher Education, MALAYSIA and the attaché university, University of Science MALAYSIA for giving me the opportunity hence the financial support and advice to ensure the doctoral thesis is completed.

A big thank you goes to my enthusiastic former supervisor, Dr Bali Rooprai. Having her as a friendly and wholehearted supervisor has been an amazing experience and I thank her, not only for her academic support, but also for giving me so many wonderful positive thoughts to be motivated in completing this thesis.

Similarly, profound gratitude goes to Derek Davies (Cancer Research UK), who has been a truly dedicated and helpful trainer in facilitating me on completing the flow cytometry work in the university. I am particularly indebted to Derek for his constant faith in my lab work, and for his support especially on analysing the flow cytometry data regardless his time that is fully-booked in Cancer Research in Holborn.

I am also hugely appreciative to my dedicated supervisors, Dr Celia Bell and Dr Frank Hills for their concern and motivation in assisting me to complete this thesis. Without their help, this thesis could not be moved forward to the extent that the content has been written up in a perfect condition and good quality.

An appreciation also goes to Dr Alan Cooper (Portsmouth University) for his witty and wise advice on some assays and providing continuous moral support throughout the challenging and hard time experiments.

Special mention goes to Hakim Abdullah who has been supporting me throughout the time on completing the thesis. Motivation and positive thinking that delivered made me realized that inner strengths like mind set is important to achieve anything in life. Another special gratitude goes to Mastura Salpidin, for her encouragement on me to keep trying and not to lose hope easily.

Finally, but by no means least, thanks go to my mother and my late father for constant undivided support and advice. They are the most important people in my world and I dedicate this thesis to them.

CHAPTER 1: Introduction

1.1 Classification of brain tumour

The World Health Organisation (WHO) classification of gliomas recognizes three histological types of infiltrative tumours: the astrocytomas, oligodendrogliomas and mixed gliomas tumours (Kleihues, Burger and Scheithauer, 1993; Louis *et al.*, 2007). They are classified histologically according to their degree of malignancy with grades that correlate well with survival times. Derived from glia, malignant gliomas are heterogeneous and invasive. Louis *et al.*, (2007) have classified astrocytomas on the basis of histological features into four prognostic grades: I (diffuse astrocytoma), II (pilocytic astrocytoma), III (anaplastic astrocytoma) and IV (glioblastoma). This was also described in the Daumas-Duport grading system (Daumas-Duport *et al.*, 1988) which is based on the histopathologic features of the tumour.

Tumours are graded from I to IV in increasing malignancy as determined by histological appearance. Four features are assessed: nuclear atypia, mitosis, necrosis and endothelial hyperplasia. Accordingly, Grade 1 lesions have none of these features, Grade 2 lesions have 1 feature and so on. Histological classification of gliomas is also based on perceived cell of origin plus the suffix “oma”, thus astrocytes give rise to astrocytomas, oligodendrocytes to oligodendrogliomas or ependymal cells to ependymomas. Neuronal derived tumours, however, are less frequent but generally seen in paediatric patients. Thus, in adults, glioblastoma has the most common occurrence and is the most malignant of the gliomas.

1.2 Classification of astrocytoma

60% of all primary brain tumours are neuroepithelial in origin and most of those arise from astrocytes. Also known as gliomas, 75% of astrocytomas are diffusely infiltrative tumours and vary from low grade diffuse astrocytomas (grade II) to high grade tumours such as anaplastic astrocytomas (grade III) and glioblastoma multiforme (grade IV), the latter having the worst prognosis.

Pilocytic astrocytoma and pleomorphic xanthoastrocytoma have a more favourable prognosis due to their limited invasive capacity and lower capacity for anaplastic progression. Glioblastoma is the most common primary brain tumour to occur in adults and results in a median survival of less than a year, despite extensive multi-modality approaches in diagnosis and management of the patients.

1.3 Glioblastoma Multiforme

Gliomas are the most frequently diagnosed central nervous system tumours, representing 50% of all gliomas. The most common type of glioma is glioblastoma multiforme (GB) and is classified as grade IV (WHO classification). A glioblastoma, technically known as glioblastoma multiforme, is the fastest growing type of astrocytoma, spreads quickly, invades nearby normal brain tissue and contains areas of dead cells (necrosis) in the center of the tumour.

GB is thought to arise from an astrocytic lineage, with the possibility that it originates from progenitor cells (Fan, Salford and Widegren, 2007). Apart from the four features described previously all being present, these malignant neoplasms are also characterized by having a highly active mitotic rate, being pleomorphic in cellularity and exhibiting the presence of multinucleated giant cells. In GB, pseudopalisade is a constant feature, surrounding the

necrotic areas as a result of hypoxia within the tumour bed. Cells with pseudopalisades may serve to promote angiogenesis of the tumour (Pilkington, 2001; Rong *et al.*, 2006; Jain *et al.*, 2007) by secreting vascular endothelial factor (VEGF).

1.4 Types of Glioblastoma Multiforme: Primary (de novo) and secondary

There are 2 forms of GB that are thought to exist biologically. One of them is the astrocytic tumour which progresses from a lower to higher grade, known as secondary GB, and which occur in younger patients.

The, *de novo* (primary) form of GB appears in older patients without first presenting as the lower grade astrocytic tumour. Unlike secondary GB, *de novo* type may involve progenitor cells of oligodendrocytes or astrocytes (Gupta, Djalivand and Brat, 2005; Ohgaki and Kleihues, 2013; Huang *et al.*, 2014). For both evolutions, genetic alteration and mutation may be involved in the pathways (Fig.1).

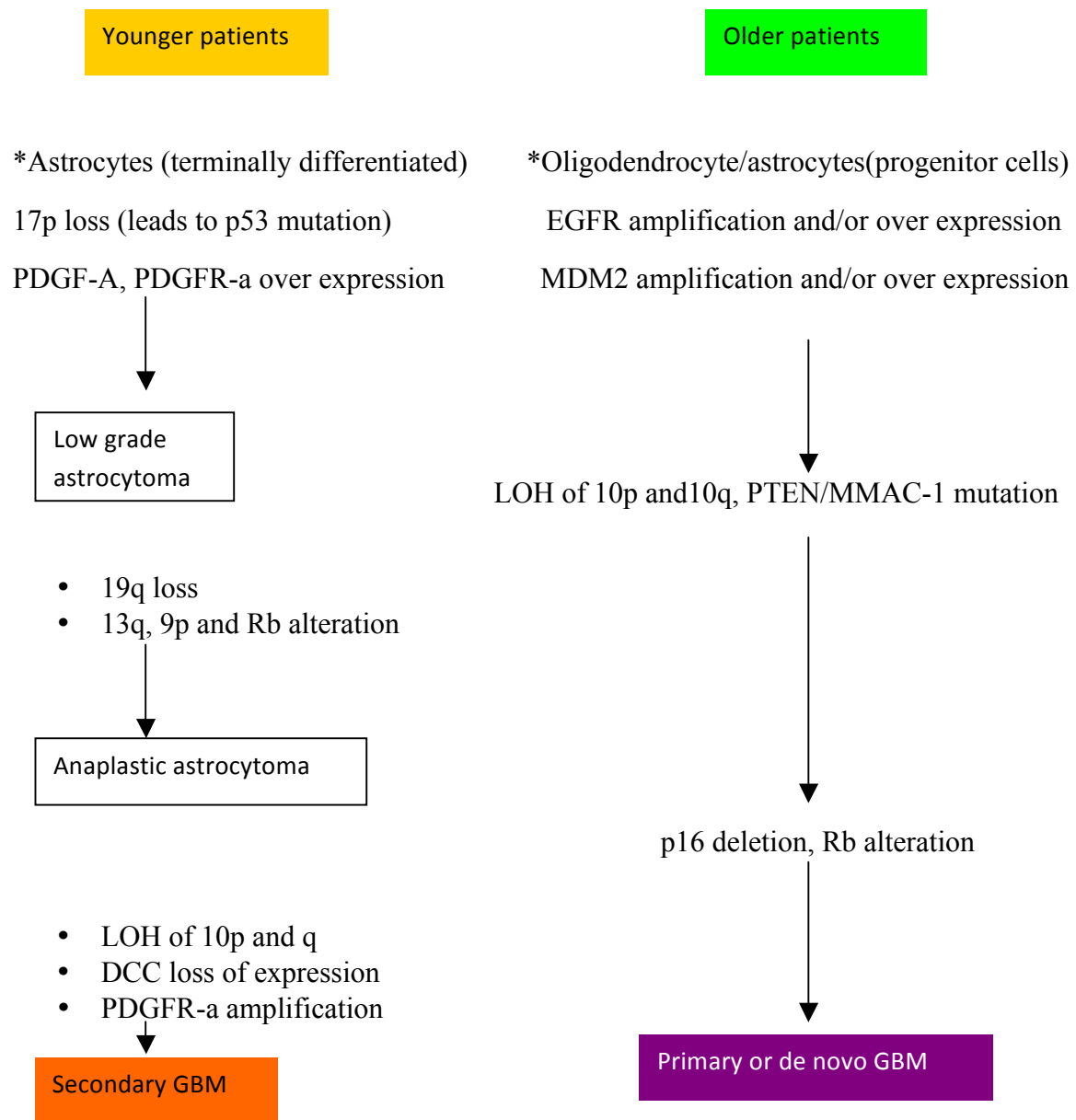


Figure 1: Two biological forms of glioblastoma that exist, each with different pathways of pathogenesis and possible genetic evolution. Adapted from Pilkington, 2001.

1.5 Incidence of Glioblastoma Multiforme

Glioblastomas account for 60-70% of malignant gliomas and the incidence has increased over the past 3 decades. Approximately 3,500 cases are reported in UK each year and they

represent 50-60% of all primary brain tumours. The incidence in England and Wales is 4 per 100,000 of the population (NHS, 2001) compared with approximately 5 cases per 100,000 people in the United States (Wen and Kesari, 2008).

GB is most commonly observed in adults aged 50 to 70 years and the median age of patients with glioblastomas at the time of diagnosis is 64 years, as reported by Wen and Kesari, (2008). Glioblastoma multiforme tends to occur more frequently in males than females by a ratio of about 3:2 in America; in the United Kingdom approximately 55% of patients with GBs are males. Burnet (2004) has emphasized life years that are lost, and has drawn a picture of the burden of the person affected person by a tumour. Tumours of the central nervous system were reported to account for approximately 20 years of life lost, the highest among any other adult tumour type studied.

1.6 Pathophysiology of Glioblastoma Multiforme

Arising from glial cells or their precursors within the central nervous system, the tumour occurs in the subcortical white matter of the cerebral hemispheres within the corticotemporal region of the brain. In terms of pathophysiology, GB is high in cellularity with poorly differentiated and pleomorphic cells (variation in the size and shape of cells or their nuclei) with occasional multinucleated cells and presence of mitotic activity. Besides nuclear atypia, GB cells are anaplastic by means of reversion of cells to an immature or a less differentiated form, as occurs in most malignant tumours. A GB also contains areas of microvascular proliferation, or necrosis, or both, which differentiates GB from anaplastic astrocytomas (AA).

Furthermore, a GB is extremely complex due to the genetic mutations that occur (Table 1). Variants of the tumour include gliosarcomas, giant cell glioblastomas, small cell

glioblastomas and glioblastoma with oligodendroglial features. All of these are uncommon glioblastoma which, respectively, contain a prominent sarcomatous element, multi-nucleated giant cells, are associated with amplification of epidermal growth factor receptor (EGFR) and may have better prognosis than standard glioblastomas (Wen and Kesari, 2008). Of all genetic mutations that occur, upregulation of vascular endothelial growth factor (VEGF) appears to be of utmost importance. Implicated in angiogenesis (formation of new blood vessels), VEGF ligands and receptors exist in extremely high concentrations compared to those in lower-grade tumours and even normal brain tissue (Pilkington, 2001; Popescu *et al.*, 2013). Hence, rapid growth of the tumour is permitted as a result of an increase in vascular permeability, endothelial gaps, and fenestrations.

Table 1: Genetic mutations identified in glioblastoma

EGFR: epidermal growth factor, VEGF: vascular endothelial growth factor, MDM2: murine double minute, MGMT: methylguanine methyltransferase (Wen and Kesari, 2008).

Mutations	Implications
EGFR	Affecting cell proliferations; upregulated in GBM
VEGF	Role in angiogenesis; upregulated in GBM
p53 deletion	Lack in tumour suppression
MDM2 amplification	Binding to p53 thus reduce p53 tumour suppressor activity
MGMT amplification	Upregulation in expression contribute to more DNA repair activity thus assists tumour to resistance in chemotherapy
Loss of heterozygosity on chromosome 10q	Associated with poor survival and appears to be a likely aid in the development of GBM

1.7 Diagnosis of Glioblastoma Multiforme

A convincing diagnosis is highly dependent on the morphological assessment of the stained tissue sections but should also be strengthened by other important perspectives which include the clinical presentation, imaging and molecular genetics. Glioblastoma is rarely seen in the spinal cord but frequently seen in the cerebral hemispheres of older adults. A variety of symptoms could be presented clinically and include headaches, seizures, memory loss and neurological deficits.

Neuronal imaging aids in providing essential information for a diagnosis such as the tumour site and details of the tumour characteristics. Thus, knowing about the exact locus of the tumour permits appropriate approaches for consideration. Moreover, enhancement in tumour characteristics may raise concerns about the true biological potential of the lesion which may not be assessed by other means. Thus, an ample representative nature of the biopsy could be determined and correlates with the histological feature or its microvascular proliferation (Kleihues and Cavenee, 2000).

Imaging techniques such as Magnetic Resonance Imaging (MRI) helps to show a heterogeneous tumour mass such as a glioblastoma when the central area of necrosis is surrounded with extensive oedema when compared to anaplastic gliomas. MRI is also increasingly used as a diagnostic tool in monitoring the response to therapy as it capable of measuring vessel permeability and relativity of cerebral blood volume and hence aid in planning of surgery. Indeed, neuronal imaging reveals the best set of anatomical, biochemical and molecular information on a specific tumor and, hence, its use in management of patients increases the understanding of the complex mechanism of glioma formation, behavior and migration. (Kleihues and Cavenee, 2000).

Genetic analysis could be distinctive in showing the genetic subtypes in tumours with the same morphology and reveal the probable pathways in tumour progression. Sequential accumulation of genetic aberrations and the deregulation of signaling pathways of growth factors could separate glioblastomas into 2 main subtypes and hence aid in the diagnosis. For example, as shown in figure 1, primary and secondary glioblastomas manifest different combinations of genetic mutations, and/or amplifications, despite being indistinguishable in morphology.

1.8 Aetiology of Glioblastoma Multiforme

An increase in the incidence of brain tumours over the past three decades has provoked the search for risk factors. Genetic alterations may permit cells to elude destruction by the immune system and evade the regulatory systems. Apart from molecular mechanisms, other sources such as chemical, physical or biological insults may exacerbate glioma-genesis.

Genetic factors

A number of familial syndromes are documented which may be associated with an increased incidence of brain tumours. Such inherited syndromes include neurofibromatosis types 1 and 2, Li Fraumeni syndrome and syndromes involving adenomatous polyps. Both types of neurofibromatosis are associated with GBs other than astrocytomas, but Li Fraumeni syndrome is mainly associated with astrocytic tumours and is involved with TP53 mutation on the long arm of chromosome 17 (Collins, 2004; Perfister, Hartmann and Korshunov, 2009). Indeed, the majority of human cancers are connected to mutation of this tumour suppressor gene. The p53 gene is important in guarding genome stability. It induces the cell cycle arrest at G1 (RNA and protein synthesis) by inhibiting retinoblastoma (RB) phosphorylation in the presence of cyclin dependent kinase 4 (CDK4).

p53 also stimulates bax and Fas protein expression in apoptosis induction. In GBs, about 30% of the genetic material was found to be lost on 17p. The allelic loss seems to occur at the initial stages of astrocytic tumour development as grade II and III were found to have higher genetic loss (Von Deimling *et al.*, 1992; Ohgaki and Kleihues, 2007). Thus, it was suggested that alteration of the p53 gene may have provoked the initial steps of astrocytoma tumourigenesis.

Neurocarcinogens

Other known risk factors are potential neurocarcinogens such as ionizing radiation, mobile phones, dietary additives, immune factors and chemicals. Radiation has long been suspected of increasing cancer incidence but no solid evidence has yet been provided to link radiation exposure with brain tumour development (Pilkington, 2001; Yasova *et al.*, 2009). The use of mobile phones has been brought up as a causative role in brain tumour aetiology in the past few years. However, increased risk was only found with the older analogue system; i.e. Nordic Mobile Telephony (NMT) system, and not the Global System for Mobile communication (GSM), but this remains to be confirmed (Hardell *et al.*, 1999).

In addition, attention has focused on aspartame (L-aspartyl-L-phenylalanine methyl ester), an artificial sweetener that is widely ingested and present mainly in our diet (soft drinks, confectionary etc.). Aspartame breakdown results in four main components which include methanol and formaldehyde, phenylalanine, aspartic acid and diketopiperazine (DKP). Nitrosation of aspartame, hence its components, was thought to cause an elevation in brain tumour risk by the nitroso-derivative products, by increasing aspartame's potential carcinogenic properties through inducing mutation of tumour suppressor genes. Pilkington (unpublished data) used the Comet assay to show that aspartame does not have an effect on

normal brain cells, thereby suggesting that aspartame may not cause tumours. However, if a pre-existing lesion is present, aspartame may speed up the progression of the tumour.

In addition, N-nitroso compounds are a group of neurocarcinogens that are present in cured meats and other food that have been preserved with nitrite and nitrosamides (Pilkington, 2001; McKinney, 2004). Such compounds are also found in green vegetables due to the use of crop fertilizers and pesticides.

Viruses

A number of viruses have been shown to cause brain tumours in animals but with the exception of studies in human immunodeficiency virus (HIV)-related brain lymphomas (Gavin and Yogeve, 1999; Taiwo, 2000), only a few (Kouhata *et al.*, 2001; Ceballos-Salobrena *et al.*, 2000; Corallini *et al.*, 1987b; Ka-Wei *et al.*, 2013) have been reported in humans. In addition, Pilkington (2001) has reported that SV40 (simian virus 40) was implicated in brain tumour aetiology in the 1950-1960s but that it was due to SV40 that contaminated the polio vaccine being administered. Indeed, McKinney (2004) reported that no virus has been consistently associated with or found in brain tumour tissue. Therefore, it is not definitely proven whether a virus can induce glioma in humans, and this is therefore an area that warrants further research.

1.9 Mortality/Morbidity caused by Glioblastoma Multiforme

There are many factors which account for the poor survival length for patients diagnosed with GB. Based on biological conditions and prognostic value, patients with GB have an average survival of between 9 to 11 months (despite intensive, multimodal treatment), much less than with low grade astrocytomas (Grade I-III); i.e. 3 -7 years (Fine, 2006). Hence, while other subtypes give a better prognosis, GB results in the poorest survival for all age groups. In

addition, the survival is known to differ by geographical region and between countries, e.g. in England, tumours that are classified as benign would not be registered in cancer registration schemes in the same way as they are in the USA. This results in lower rates of survival being recorded in the UK (McKinney, 2004).

1.10 Biological features of Glioblastomas at a molecular level

The biological properties of cell populations of intrinsic brain tumours, such as cellular heterogeneity and angiogenesis, have made effective treatment of gliomas challenging. Multiple processes of differentiation and anaplasia give rise to a heterogeneous cell population. Differences in morphology, genetics and immunological characteristics arise from the same neoplasm, rendering the tumour mass highly resistant to both radiotherapy and chemotherapy (Zhang and Barres 2010).

Solid tumour survival is dependent on angiogenesis which is the formation of new blood vessels to provide nutrients and oxygen and occurs in the presence of angiogenic factors such as VEGF. Proposed as a primary stimulant, VEGF at even nanomolar concentrations can induce microvascular permeability (Folkman and Haudenschild, 1980).

The most significant biological feature of GBs that preclude successful therapy is invasion, the process by which tumour cells infiltrate the normal brain in a complex way, thereby rendering all current forms of therapy ineffective (Bellail *et al.*, 2004). Various components, including cell adhesion molecules (Cluster of differentiation 44, CD44), proteases (such as matrix metalloproteinases –MMPS), extracellular matrix (ECM) components and growth factors are involved in this multi-step process and are studied as parameters of brain tumour invasion.

1.10.1 Invasion

A primary brain tumour is unique in its invasive behaviour as it does not metastasize outside of the brain but invades anywhere within the brain as single cells. In addition, unlike other systemic malignant tumours (carcinomas), they have the tendency to infiltrate the blood vessels walls along the periphery (but not into the blood vessels walls), subpial glial space or white matter tracts (corpus callosum) (Burger and Scheithauer, 1994; Kleihues and Cavenee, 2000). There are two important requisites for a malignant neoplasm of haematogenous origin (cancers originated from the blood) which allow metastasis and give the cells the capacity to invade through blood vessel walls and the lymphatic system for transportation. However, these are absent within the brain, thus may explain the reason why a primary brain tumour does not metastasise in nature. Moreover, primary brain tumours do not invade the bony calvarium (bones forming the convexity of the skull, periosteum, and soft tissue coverings) unlike other metastatic tumours which invade the calvarium and are also more sharply delineated from surrounding brain tissue (Bigner, McLendon, Brunner, 1998). Primary brain tumours are also short distance in invasive capacity and invade as a group of cells rather than as single cells. As a result, invasion is one of the critical prognostic factors for brain tumours (besides heterogeneity and angiogenesis) as this is associated with complications in surgical excision of the tumour mass in the brain (Bellail *et al.*, 2004).

In general, there are 3 steps in the model of invasion described for a variety of malignant cell types (Bellail *et al.*, 2004). Tumour cells (front) detach from the growing primary tumour mass and adhere to the extracellular matrix (ECM) via specific receptors. Tumour cells are believed to have the ability to degrade ECM components via matrix metalloproteinases, which are secreted by the tumour cells into the microenvironment. This will permit the neoplastic cells to migrate through the ECM and into the adjacent tissue.

However, the pathways created by glioma cells may be specific due to the unique composition of ECM of the brain (Bellail *et al.*, 2004).

Glycosaminoglycan hyaluronan is the major component of ECM within the brain, and attracts Na^+ and other cations required for osmotic influx of water. A variety of distinct proteoglycans are also present within the brain and have functions which include acting as de-adhesive proteins, growth factor modulators and cell cycle inhibitors. However, in the brain tumour microenvironment, hyaluronan and many other ECM components are upregulated in expression (Bellail *et al.*, 2004). Changes in proteoglycans such as vitronectin, osteopontin, tenascin-C, secreted protein acidic and rich in cysteine (SPARC) and brain enriched hyaluronic acid binding protein (BEHAB) may modulate the growth, proliferation and invasive activity of the tumour mass, but the exact mechanism(s) is yet unclear (Higuchi *et al.*, 1993; Zagzag *et al.*, 1996; Shi *et al.*, 2007). For instance, tenascin – C, SPARC and thrombospondin were found to be upregulated both within and surrounding the blood vessels walls hence suggesting that it has an impact on angiogenic activity (Higuchi *et al.*, 1993; Zagzag *et al.*, 1996).

Moreover, invasion *in vivo* and migration *in vitro* was found to be facilitated by an increase in hyaluronan (approximately 4 fold) through high expression of CD44 and RHAMM (Koochekpour, Pilkington and Merzak, 1995; Akiyama *et al.*, 2001; Kim and Kumar, 2014). Indeed, for the invasion to take place, it is critical for the neoplastic cells to interact with the ECM via specific receptors expressed on the cell surface (Hood and Cheresch, 2002). CD44 is the principal receptor for hyaluronan and plays a significant role in glioma cell-matrix adhesion, cell migration and regulation of tumour growth and metastasis (Ponta, Sherman and Herrlich, 2003). As a transmembrane glycoprotein belonging to the superfamily of immunoglobulin receptors, CD44 also has an additional role, a hyaluronan-independent role

in cell migration, as it can act as a cell surface anchor for matrix metalloproteinase 9 (MMP-9) (Yu and Stamenkovic, 1999; Wiranowska *et al.*, 2010). MMP-9 is one of the significant MMPs involved in proteolytic degradation of the ECM in brain tumours and has been strongly implicated in glioma invasion by several studies (Rao *et al.*, 1993; Kondraganti *et al.*, 2000; ; Murray, Morrin and McDonnell 2004; Hagemann *et al.*, 2010; Kenig *et al.*, 2010; Wiranowska and Rojiani, 2011)

It is necessary for malignant neoplasms to have specific extracellular matrix proteases that can degrade the ECM and thus allow invading tumour cells to get through to adjacent sites, hence tumour progression. MMPs are a large, diverse family of endopeptidases and are classified based on preferential substrate activity, protein domain similarity and sequence homology (Lee and Murphy, 2004). However, they do not necessarily have the substrate specificity as the proteolytic functions may overlap. Consisting of 25 members, they are produced in cells as pro-enzymes and require proteolytic cleavage for activation either by MMPs or serine protease (e.g. plasmin). They act as regulators to their inhibitors, tissue inhibitor of matrix metalloproteinases (TIMPs).

Over expression of MMPs has been widely documented in both *in vivo* and *in vitro* studies in numerous malignancies and are highly critical for invasion and metastasis (Egeblad and Werb, 2002; Brand, 2000; Rooprai *et al.*, 2007; Sohail *et al.*, 2008). MMP-2 and MMP-9 are the most debated and hence investigated for their roles in glioma invasion. Mechanisms on how MMPs are upregulated and activated in glioma include genetic, hypoxic and stromal contributions. Epidermal growth factor receptor variant III (EGFR vIII) amplification has appeared to promote the highest level of activated MMP-9 following constitutive EGFR tyrosine kinase activity (Choe *et al.*, 2002; Ohka, Natsume and Wakayabashi, 2011). Hypoxic GB cells *in vitro* were shown to secrete pro-MMP-2 in high levels which activated

MMP-2. This increased migratory properties by up to 60% more than normoxic cells (Brat et al., 2004; Brat and Van Meir, 2004). In addition, the urokinase pathway of plasminogen activation also led to activation of MMPs besides other cell surface receptors that transduce intracellular signaling for migration.

Known as urokinase-type plasminogen activator (uPA), it also includes urokinase receptor (uPAR) and plasminogen (Blasi and Carmeliet, 2002; Rao, 2003). uPA is first secreted as an inactive pro-enzyme that is activated once cleaved post binding to uPAR. Becoming an activated uPA, it then converts plasminogen to plasmin (a serine protease). Plasmin degrades ECM proteins, activates other MMPs (such as MMP-2, -3 and -9) and cell surface receptors that transduce intracellular signaling for migration as shown in figure 2 (Bellail *et al.*, 2004)(Fig.2).

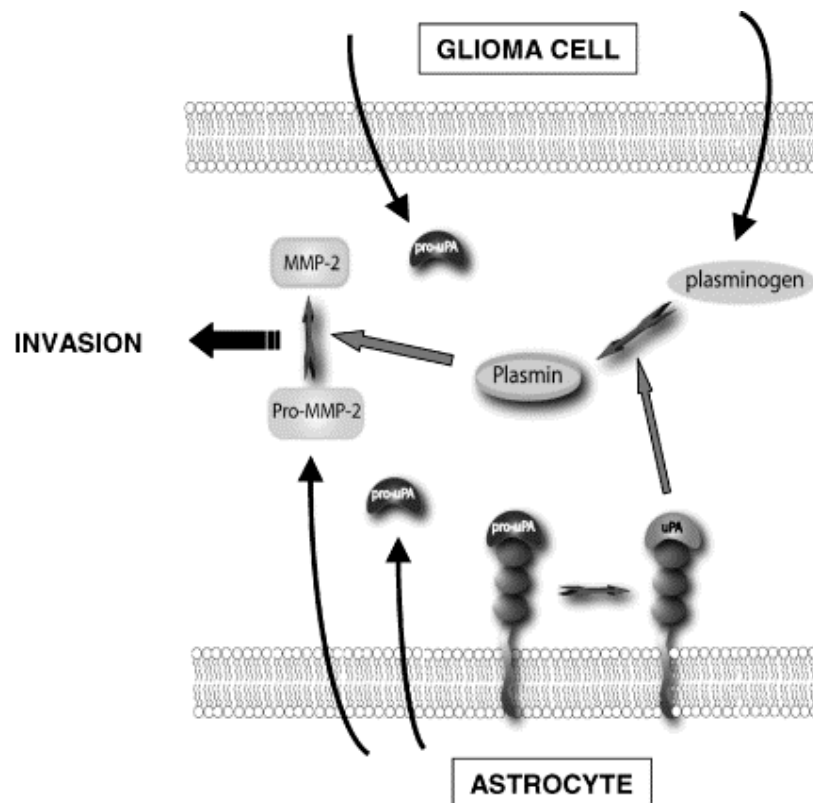


Figure 2: Schematic representation of the mechanism of glioma cell interaction with astrocytes for invasion. Taken from Bellail *et al.*, 2004.

1.10.2 Heterogeneity

The idea that astrocytes are a homogeneous group of cells was based historically on their appearance as star shaped (Greek root word 'astro') and is perhaps not appropriate as their morphology is extremely diverse. In the late 19th century and early 20th century the heterogeneity of astrocytes was documented but the function of astrocytes has only begun to be understood in the past 20 years. Astrocytes are heterogeneous across the brain regions as well as within the same regions of the brain. These cells differ in morphology, developmental origin, gene expression, physiology, functions and response towards injury and disease and are highly important in tumour occurrence which yet still in its rudimentary phase (Zhang and Barres, 2010) hence needs further investigation.

Astrocytes are found throughout the central nervous system but whether they originate from the same pool or distinct groups of progenitor cells is something that needs better understanding (Zhang and Barres, 2010). However, the spinal cord is at least one of the production sites of astrocytes although 3 positions of distinct groups of white matter astrocytes in the spinal cord derive from different progenitor domains (Hochstim et al., 2008).

In addition, astrocytes differ in proliferation activity based on locations in the brain. A population of astrocytes may appear homogenous but may contain hidden heterogeneity. The molecular mechanism that differentiates proliferative activity among astrocytes subtypes remains unclear (Fukuda et al., 2003; Ghashghaei et al., 2007).

Additionally, astrocytes are an extremely diverse group of cells with respect to gene expression and physiological properties (Sofroniew and Vinters, 2010). Diversity in the functionality of the astrocytes (astrocyte-neuron interactions or between astrocytes interactions) is due to the differences in surface glycoprotein expression. However, to date

heterogeneity in astrocytes is largely unexplored *in vitro* and warrants further research. In terms of connectivity of the networks, astrocytes were also thought to be uniform in negative resting membrane potential and extensive gap junctions with low input resistance. However, it has now been shown that they are diverse in gap junction coupling, calcium dynamicity and electrophysiological properties (Zhang and Barres, 2010).

Regional heterogeneity and diversity in immunoreactive surface markers and in chemokine and cytokines expressed (different brain regions cultured) implies differences in response towards disease and injury. Thus, heterogeneity must play additional roles in tractability (responsiveness to chemotherapy) of the tumour mass (Morga, Faber and Heuschling, 1999; Fitting et al., 2010). In fact, cultured astrocytes, in comparison with solid tumours, may become more sensitive to cytotoxic drugs due to external factors such as medium composition, inadequate growth factors and temperature which may not resemble the *in vivo* environment exactly (Szaakacs and Gottesman, 2004).

1.10.3 Angiogenesis

One of the features that are required for the tumour to grow and metastasize (for all solid tumours) is the formation of new blood vessels from the existing ones, a process known as angiogenesis. Brain tumours are particularly angiogenic and it has been reported that patients with high tumour microvascular densities have shorter post-operative survival durations in comparison with patients with low microvascular densities (Leon, Folkerth and Black, 1996; Carmeliet, 2003). A tumour mass that is expanding in size requires oxygen and a supply of nutrients for its continuing survival and growth. Thus, recruiting new blood vessels is important and occurs via angiogenesis.

Angiogenesis is normally controlled tightly by the balance of pro and anti-angiogenic factors. Both types of molecules are secreted by endothelial, stromal and blood cells, extracellular matrix and also cancer cells. A considerable amount of growth factors are pro-angiogenic in nature and include vascular endothelial growth factor (VEGF), acidic fibroblast growth factor, basic fibroblast growth factor (bFGF), placental growth factor, interleukins and angiopoietin-2. To counter-balance their activities in the cellular environment, anti-angiogenic factors such as angiostatin, endostatin, thrombospondin 1 and endothelial monocyte-activating polypeptide as well as some serine proteinases and metalloproteinases play their own role in suppressing angiogenic activity of the cells. A balanced expression between pro and anti-angiogenic factors is important for normal development and the well being of the cellular environment, but in tumourigenic conditions, an 'angiogenic switch' is turned on (Fidler and Ellis, 2004; Olson *et al.*, 2006). The tight regulation is disrupted and this leads to uncontrolled and disorganized angiogenesis.

It remains unclear how the signaling from the receptors on the cell surface to the nucleus in the cells controls the induction of angiogenesis in a cancerous environment. There is considerable progress in understanding angiogenesis regulation but the intracellular machinery of the angiogenic signaling needs further explanation (Castellino and Durden, 2007). It was suggested that most of the pathways in the regulation of angiogenesis are similar in that they regulate endothelial cell proliferation, migration and permeability. Thus, it is essential to implement the use of potential inhibitors to the fundamental principle of cell signaling (receptor interactions with the ligands) to combat angiogenesis in cancerous cells and hence inhibit brain tumour development (Deeken and Loscher, 2007).

Blood circulation in the central nervous system (CNS) is tightly regulated by the blood brain barrier (BBB). The BBB is a vasculature organization in the CNS which is highly

specialized and well distinguished by a unique structure of blood capillaries. Composed of walls of endothelial vessels with tight junctions in between, the BBB hence is both an anatomical and a physiological barrier as it limits blood vessel permeability, suppressing the flow of most substances from the blood stream to the neural system but sustaining the needs of brain cells with the required nutrients for continuous CNS function. It is selective to molecules of a certain molecular mass, not allowing molecules of more than 50kDa to pass through, and solubility, in which water-soluble molecules are unfavourable (Jain et al., 2007). The BBB is of primary concern as a barrier to the successfully delivery of drugs to a tumour mass. Moreover, the brain is confined in its space thus, breaking down the BBB and allowing leakage of fluid into the brain can lead to an undesirable increase in interstitial pressure. In fact, BBB architecture in brain tumours is tortuous, disorganized, and with high permeability due to abnormality of the endothelial walls. Thus, having more disruption in already disrupted structures of the BBB could result in oedema and cause increased morbidity in patients. Hence, it is important that anti-angiogenic therapy is not only aimed at preventing tumour angiogenic event but also suppresses the pathological damage following changes in tissue permeability.

Interventions aimed at preventing angiogenesis are high in importance when investigating the control of brain tumours. Indeed, in a study (Jain, Tong and Munn, 2007), expanding research on anti-angiogenic therapy for brain tumours either *in vivo* or *in vitro* has shown that regulating angiogenic activity may be promising in managing this deadly cancer. Such popular treatment is the use of Bevacizumab or Avastin, a humanized monoclonal antibody against VEGF, which is the prime target in angiogenesis.

A number of anti-angiogenic therapies such as sorafenib and sunitinib have been used for other solid cancers but not in gliomas, perhaps due to their non-specificity (Tourneau, Faivre

and Raymond, 2008). VEGF is known for its pivotal role in angiogenesis. The administration of Avastin as the main approach in anti-angiogenic therapy has shown Avastin to be an active regimen for recurrent grade III-IV glioma with acceptable toxicity (Vredenburgh et al., 2007). Based on VEGF signaling as the target (monoclonal antibody against VEGF approach), other inhibitors have been developed; tyrosine kinase inhibitors (against VEGFR2 tyrosine kinase activity) (Batchelor et al., 2007) and soluble decoy receptors VEGFR1-developed (against VEGF signaling) (Folkman, 2007). A potent $\alpha\text{v}\beta 3$ and $\alpha\text{v}\beta 5$ integrin inhibitor, cilengitide, has also been used in a clinical trial (Nabors *et al.*, 2007). It is a platelet-derived growth factor receptor (soluble decoy receptor) that inhibits alpha-V-beta-3 ($\alpha\text{v}\beta 3$) and alpha-V-beta-5 ($\alpha\text{v}\beta 5$) integrins. Both integrins are expressed by both the tumour-associated vasculature and tumour cells (Gladson, 1996; Bello, Francolini and Marthyn, 2001).

Nevertheless, despite all the possibilities that research into angiogenesis brings, there is a concern that anti-angiogenic therapy could lead to a transition phase of the tumour. It is a recurrence of the tumour growth after adaptation to the treatment. Evasive resistance and intrinsic resistance are possible occurrences, with cells developing alternative pathways to develop new blood vessels (Berges and Hanahan, 2008). However, this could be avoided by combining other therapies that are looking at another approach of killing the cells and thus may improve the efficacy of the treatment.

1.11 Stem cells

Stem cells are a primitive group of cells capable of reproducing themselves (self –renewal) and developing through cell division into specialized cells (potency) which make up the organs and tissues of the human body. In a normal state of functionality, the hallmark is haematopoietic stem cells (HSCs) of the bone marrow that are able to produce new blood

cells and immune cells over a long term, demonstrating potency. However, cancer stem cells (CSCs) are cancer cells that function likewise, but give rise to all cell types found in a particular cancer sample i.e. reinitiate the cancer (Eyler and Rich, 2008). CSCs are therefore tumourigenic either via self-renewal or differentiation into perhaps multiple cancer cell types.

In brain tumours, such cells are known as brain tumour stem cells (BTSCs) and have given new insights into chemo and radio resistance as the brain tumour stem cells persist as a distinct population hence surviving and initiating recurrence. Several studies have reported on a fraction of BTSCs found in brain tumours of most types including GBs. Clusters of differentiation 133 or CD133 was the first marker reported for hematopoietic stem/progenitor cells before becoming neural stem/progenitor stem cells.

It was identified (Singh et al., 2004) that as few as 100 cells with CD133⁺ cells derived from GB has adequately initiating GB in immunodeficient mice following injection, but shown to be lack of tumourigenic capacity when injected with CD133⁻ cells. Nevertheless, there could be differences between mice and humans, such as the metabolism, lifespan and length of telomeres and better insights could be gained by using an appropriate model. It is thought that BTSCs constitute only a small population of CD133⁺ cells and side population cells among the selected populations of cancer cells (Singh et al., 2004). Side population cells (SP) are the cells that appear on the lower left of the dot plot graph in flow cytometry and are known to possibly to have cancer stem cell characteristics as they have been identified in cancers (hepatocellular, gastrointestinal, ovarian cancers and glioma) (Haraguchi et al., 2006; Chiba et al., 2006; Szotek et al., 2006; Hide et al., 2008; Wu and Alman, 2008;) and may be the cells that efflux chemotherapy drugs and account for resistance of cancers to chemotherapy.

Besides the difficulties in purifying BTSCs from CD133⁺ fractions and SP cells, there are other complexities in the study. Hypothetical models of CD133 expression in BTSCs developed by Hide et al (2008) suggest that CD133 expression in BTSCs derived from GBs from patients is diverse depending on the origin of the cells and different mutations expressed and thus altering the growth pattern of the cells (Bar, Chaudhry and Lin, 2007).

Continuing study of BTSCs may increase our understanding of the development of brain tumours. BTSCs offer a potential target for cancer therapy with Sonic Hedgehog (Shh) and Notch pathways as the target. Due to their importance roles in brain development and sustaining the stem cell-like, Sonic Hedgehog and Notch pathways become a target by inhibiting the self-renewal functions and tumorigenicity in gliomas (Fan et al., 2006; Birlik, Canda and Ozer, 2006; Clement et al., 2007).

1.12 Apoptosis as a targeted therapeutic approach

Alterations in cell death and cell proliferation are essential determinants of the physiologic and homeostatic functions of normal tissues. The balance between the two is key to understanding the pathogenesis and progression of several diseases such as cancer. Greatly increased in importance in clinical management and human disease, apoptosis studies in cancer have been well documented as a potent mechanism in combating carcinogenesis and also as a target for an effective therapy (Fleischer et al., 2006).

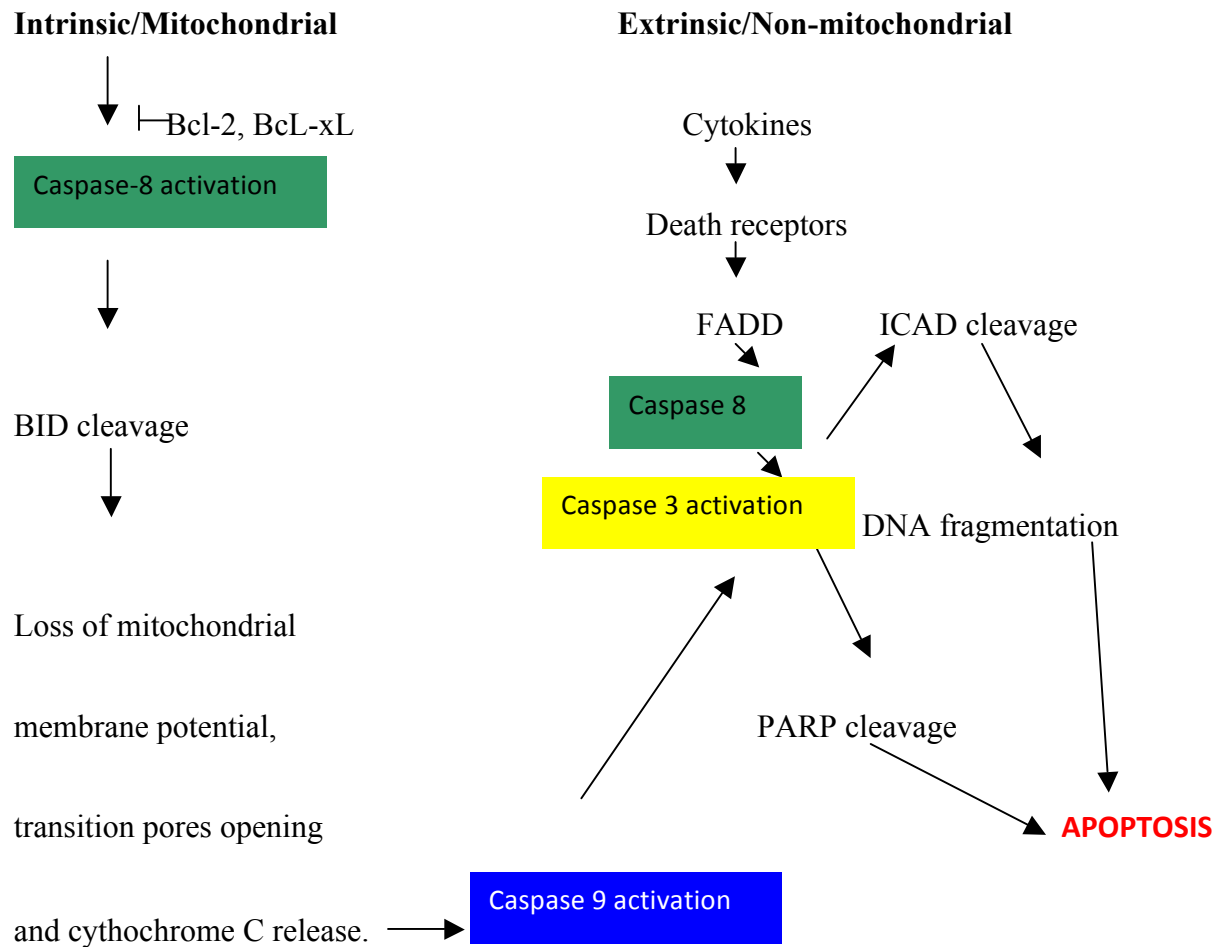


Figure 3: Pathways involved in apoptosis

The induction of apoptosis occurs along either the intrinsic or the extrinsic pathway. The intrinsic pathway (mitochondrial) is activated due to deprivation of growth factors and cytokines that result from DNA damage (Darzynkiewicz et al., 2004). Tumour suppressor p53 gene is responsible for the activation of genes transcribing pro-apoptotic Bcl-2 proteins. Dysregulation of its functions in cancer may interrupt the controlled ratio between pro- (Bax, Bad, Bik, Bcl-xs) and anti-apoptotic (Bcl-2, Bcl-xl) proteins (Darzynkiewicz et al., 2004).

The extrinsic pathway is activated by a tumour necrosis factor superfamily protein e.g. TNF- α post-binding to the death receptor on the cell surface (Darzynkiewicz et al., 2004). Following ligand binding, the receptor becomes trimerized which leads to recruitment of

death domain containing Fas-Associated Death Domain (FADD- an example of adapter protein molecules) at the end of the receptor, intracellularly. Initiator caspases such as caspase 8 is activated which in turn activates the other downstream effectors i.e. *caspase 3, 6 and 7*, eventually eliciting cell death (Darzynkiewicz et al., 2004). Many cytotoxic agents used in chemotherapy are thought to exert their therapeutic effects by inducing apoptosis in neoplastic cells, making them ideal anti-cancer agents.

1.13 Current treatment options for Glioblastoma Multiforme

GBs are the most challenging of cancers to treat and remain incurable. The prognosis of malignant brain tumours in man is dismal despite conventional therapeutic approaches such as radio and/or chemotherapy regimes and various novel surgical approaches that have been introduced for their management (Grossman and Batarra, 2004).

1.13.1 Neurosurgery

Neurosurgery is regarded as relatively safe with respect to procedures and has improved with the precision in tumour removal made possible by neuro-navigation and robotic surgery (Rampling, James and Papanastassiou, 2004; Grossman and Batarra, 2004). However, surgical resection as well as its effects remains controversial as this modality does not cure the patient due to the impossibility of debulking 100% of the tumour. The infiltrative nature of the tumour makes it difficult for the neurosurgeon to ascertain where the tumour ends and normal brain tissue starts. Single invading cells (“guerrilla” cells) tend to escape the surgeon’s knife, move a distance away into the normal brain and start proliferating (Pilkington, 1996).

Undoubtedly, the outlook for patients with GB remains dismal and adult patients usually die of within less than 1 year after first diagnosis (McKinney, 2004). As there has not been a

significant improvement in prognosis in 30 years, there is a very strong need for other therapeutic approaches in addition to conventional surgery and radio/chemotherapy.

1.13.2 Radiotherapy

Surgical procedure is usually followed by radiotherapy, which remains the most effective therapy for GB patients as it has been shown to prolong survival of the patients with malignant gliomas (Grossman and Batará, 2004; McKinney, 2004; Preusser *et al.*, 2011). However, this modality is not recommended for elderly patients as radiotherapy puts their life at greater risk (Combs *et al.*, 2008). It can only be given when the tumour cells are rapidly dividing and it is harmful to the normal brain cells. Radiotherapy also has some potential drawbacks, including resulting in learning difficulties in children or causing further tumours such as meningioma (Merchant, Pollack and Loeffler, 2010).

1.13.3 Chemotherapy

Chemotherapy is often given as an “adjuvant” to patients who are at a high risk of recurrence of the tumour. Chemotherapy may improve a patient’s survival, but it has been disappointing due to problems of drug delivery across the BBB (Regina *et al.*, 2001). As the tumour has a disrupted BBB, cytotoxic drugs can be delivered to it but this therapy cannot reach the guerrilla cells which are protected by the intact BBB in the normal brain (Merzak and Pilkington, 1997).

The use of Temozolomide (an oral alkylating agent) (Stupp *et al.*, 2005) and Carmustine or gliadel wafers (Westphal *et al.*, 2003) has been encouraging in recent years but there is still a strong need for novel therapeutic intervention.

1.13.3.1 Temozolomide

Temozolomide (TMZ) is the 3-methyl derivative of mitozolomide, a tirazinic compound which is active in various neoplasias and has shown the most encouraging results in treating high grade gliomas in the past 30 years. TMZ is a pro-drug that is rapidly converted through non-enzymatic processes to the active metabolite 5-(3-methyltriazen-1-yl)-imidazole-4-carboxamide (MTIC). Thus, without the need for hepatic metabolism, it transforms itself into MTIC (its active form) before being secreted by the kidneys and rapidly disappearing from the blood. Targeting the O⁶, N⁷ position of guanine, TMZ disables DNA repair enzymes. As a result, cells with unrepaired damaged DNA cannot pursue to the next phase of cell cycle i.e. cell cycle arrest occurs and apoptosis becomes a choice.

Furthermore, TMZ tissue distribution is excellent as it has 100% bioavailability as it is able to cross the BBB to reach a sufficient dose. TMZ is often given with radiotherapy or chemotherapy (either an injection or oral therapy) or to newly diagnosed patients (National Institute for Health and Clinical Excellence, 2007; Ohka, Natsume and Wakayabashi, 2011). Initial dosing consists of a 42-day concomitant phase of dosing while the patient receives radiation therapy. 6 dosing cycles are implemented following the completion of the concomitant phase with each cycle consisting of 28 days (5 days with therapy and 23 days without therapy). A complete blood count is taken within 48 hours of day 22 of the cycle as to assess for dosage modification (if required) due to toxicity. Post completion of the 6 dosing cycles, a re-evaluation is done to determine requirements for following therapy (if needed) (Schering-Plough Corporation, 2008).

However, a common adverse effect reported is an increased risk of the development of *Pneumocystis jiroveci* pneumonia (PCP) due to possible severe myelosuppression. Therefore, it is necessary for the patient to receive PCP prophylactic therapy alongside the 6 dosing cycles (Schering-Plough Corporation, 2008). Moreover, TMZ is toxic to organs that

have rapidly proliferating cells such as bone marrow, lymphatic and gastrointestinal systems (Avgeropoulus and Batchelor, 1999; Brandes and Pasetto, 2000). Stupp et al. (2005) in his study with newly diagnosed GB patients showed a clinically meaningful and statistically significant increase in survival following TMZ administration alongside radiotherapy. Radiotherapy alone showed only 10% increase in survival rate but 27% was achieved with TMZ alongside (Stupp et al., 2005; Brown, Eckley and Wargo, 2010).

Unfortunately, TMZ is not always effective in patients with GBM as the unsatisfactory outcome of chemotherapy with TMZ is mainly defined by the intrinsic or acquired chemoresistance of GB cells which include not just p53, proliferation rate and DSB repair but also O⁶-methylguanine-DNA methyltransferase (MGMT) level of activity (Capper et al., 2008; Lee et al., 2009; Glas et al., 2009).

It was postulated that MGMT removes the mutagenic and cytotoxic adducts from the O⁶-methylguanine in DNA which is the preferred point of attack of alkylating agents. Eventually, due to increased level of MGMT enzyme that present in the cells, it becomes irreversibly inactivated and consumed (Balana et al., 2008) and diminished after concentration of TMZ is increased. As a result, some cells die, while other, more resistant cells adapt and resume proliferation and evade apoptosis.

1.13.3.2 Gliadel wafer (Carmustine)

Westphal et al. (2006) have been researching the use of gliadel wafers in GBs for many years and these have now been used as a form of interstitial chemotherapy treatment. Following radiation, this biodegradable polymer containing 3.85% Carmustine or bis-chloronitrosourea (BCNU) is placed in the resection cavity at the time of craniotomy. Being implanted in the brain and lasting for 2-3 weeks, Carmustine is released into tumour sites, that cannot be removed surgically. In a long term study a reduction in the risk of death reported compared

with placebo of nearly 30% was noted. Indeed, patients who were treated with Carmustine have the advantage of 2 to 3 extra years of survival compared to patients given a placebo. Hence, it offers enormous hope of long term survival in malignant glioma patients but there could be potential adverse effects.

Another clinical study by Weber and Gobel, (2005) in GB management has introduced Carmustine wafers into the resection cavity when cerebral oedema occurrences following Gliadel implantation were experienced. Localized chemotherapy by wafers, together with other post-operative regimens reduced the systemic adverse effects but did not last for long as the patients developed neurological deficits gradually and these deteriorated over time. In one case, death followed as increased oedema developed. It is a fact of the infiltrative nature of the disease that some degree of cerebral oedema will develop in the malignant glioma where the resection has occurred, but it is usually around the adjacent areas of the craniotomy that corticosteroids are administered (Westphal et al., 2003; Weber and Goebel, 2005; ; Ohka, Natsume and Wakayabashi, 2011).

1.13.3.3 Chlorimipramine

Chlorimipramine (CIMP) or Anafranil is a tricyclic antidepressant that has been used widely for over 40 years (Peters, Davis and Austin, 1990; Trimble, 1990). It works by inhibiting the re-uptake of the neurotransmitters, norepinephrine and serotonin, by nerve cells. Following oral administration, CIMP is stored in high quantities in both the brain and lung and has a long half life of approximately 24 hours, increased to 40 hours once metabolized to its by product, desmethyl clomipramine. CIMP crosses the "blood-brain barrier" and therefore has an advantage in the treatment of brain tumours (Aitchison, et al., 2010).

CIMP mode of action is different from other cytotoxic drugs that are used in GB treatment (which act by damaging the DNA within the nucleus of the cells) as it acts through

mitochondria, which are responsible for production of energy for the cell's various activities. Therefore, it promotes programmed cell death (apoptosis) due to compromised respiratory function in cancer cells while leaving normal cells unaffected. In essence, the drug enters the mitochondria and affects complex III of the respiratory chain, reducing oxygen consumption, thereby increasing reactive oxygen species (ROS) and liberating cytochrome c as a consequence. This, in turn, activates a series of enzymes which results in programmed cell death (Daley et al., 2005).

1.13.3.4 Bevacizumab (Avastin)

Bevacizumab or Avastin is a humanized monoclonal antibody that prevents the formation of new blood vessels by targeting and inhibiting the function of vascular endothelial growth factor (Ferrara et al., 2004). Considered as one of the most vascularized cancerous tumours, GB over-expression of VEGF leads to increased microvascular density and increased angiogenesis (Sathornsumetee and Rich, 2007). By preventing VEGF association with its receptors, this disrupts new vessel formation and leads to inhibition of tumour growth (Friedman et al., 2009). First used as an angiogenic inhibitor in metastatic cancers such as colorectal, lung and breast cancers, Avastin was approved for GB treatment in 2009. The dose of Avastin used in GB is 10 mg/kg every 2 weeks, with the duration of therapy up to the discretion of the oncologist and patient (Genetech Inc., 2011).

The results of several clinical studies have been published and have shown positive effects for Avastin on GB progression. Avastin, with a combination of other regimes in chemotherapy, may be a more effective treatment in recurrent GB but warrants further studies on its survival perspective (Norden *et al.*, 2008; Kreisl *et al.*, 2009; Nghiemphu *et al.*, 2009; Readon *et al.*, 2009; Zuniga *et al.*, 2009). Vredenburgh et al. (2007) has combined Avastin

with Irinotecan, a topoisomerase 1 inhibitor involving patients with recurrent GB. This phase II trial has demonstrated that the combination is active against recurrent GB and yet the toxicity was acceptable. This was one of the first trials to show positive response rates and increased duration of life. At 6 months, the overall survival was found to be 77% and 20 of the 35 patients had at least a partial response as determined by MRI scans.

Friedman et al. (2009) compared treatment with Avastin alone and Avastin in combination with Irinotecan. At 6 months, of the 167 patients with recurrent GB randomised to the two groups, Avastin alone had a 42.6% survival rate compared with 50.3% in the combination therapy group. Moreover, as measured by MRI scan for tumour reduction assessment, 24 patients on monotherapy while 31 patients on combination therapy manifested a response to therapy. Despite the promise of Avastin for treating GB, there are drawbacks associated with side effects including gastrointestinal perforation, severe or fatal haemorrhage, and wound-healing complications (Sathornsumetee and Rich, 2007). In addition, hypertension has been observed in patients receiving this therapy as well as other common adverse events including thromboembolism formation, proteinuria/nephrotic syndrome, and reversible posterior leukoencephalopathy syndrome (Gressett and Shah, 2009).

1.14 Novel treatment in Glioblastoma therapy: natural occurring micronutrients as an integrative treatment

Naturally occurring agents such as micronutrients are being explored and researched as they have potential therapeutic effects on various tumours. It is also important to have novel therapeutic approaches which have an impact on the tumours without being toxic. For an agent to be of therapeutic value it should not only be cytotoxic, anti-invasive, anti-angiogenic or pro-apoptotic but most importantly it should be able to cross the BBB. Rooprai et al.

(2001) hypothesized that naturally occurring micronutrients found in citrus flavonoids (from tangerine peel) may have potential as anti-cancer agents in the treatment of malignant gliomas based on their ability to interfere with invasion.

Micronutrients are essential dietary components such as vitamins, minerals or other agents found in foods that are required in minute quantities for sustaining normal growth and development of living cells. Micronutrients have been shown to exert potentially therapeutic effects in cell culture and animal models which include anti-cancer activity and other functional properties such as anti-microbial and anti-oxidative effects. In addition, a combination of micronutrients or naturally occurring agents, known to have a variety of therapeutic properties such as anti- invasive and pro-apoptotic, has been suggested as one possible novel therapeutic approach to combat brain tumours. (Rooprai , Christidou and Pilkington, 2003;Rooprai et al., 2007).

1.14.1 Flavonoids

Flavonoids or bioflavonoids, are an extensive group of naturally occurring polyphenolic compounds and responsible for the pigments found in fruits, vegetables, wine and tea. Consisting of two benzene rings on either side of a 3-carbon ring , multiple combinations of hydroxyl groups, sugars, oxygens, and methyl groups attached to these structures create the various classes of flavonoids: flavanols, flavanones, flavones, flavan-3-ols (catechins), anthocyanins, and isoflavones (Miller,1997). Daily intake in the Western diet is approximately 20mg to 1g per day (Pierpoint, 1990; Hertog et al., 1995).

Increased interest in studies on flavonoids has been due to their proposed protective role in cancer prevention which includes pro-oxidant activity, mitochondrial toxicity (potential apoptosis-inducing properties), and interactions with drug-metabolizing enzymes (Galati and

O'Brien, 2004). Indeed, certain flavonoids have been found to exhibit anti-proliferative properties against some cancers and are known to cross the BBB (Datla et al., 2001; Zbarsky, et al., 2005).

Further research has now led to the inclusion of red clover extract, red grape seed extract, turmeric, chokeberry extract, lycopene and selenium. This combination of seven micronutrients has been carefully selected to target the tumours in different ways as a nutraceutical approach for a proposed clinical trial to treat malignant brain tumour patients (Rooprai, Christidou and Pilkington, 2003). Turmeric and chokeberry were included as part of a large study of flavonoids and other micronutrients screened *in vitro* to evaluate their ability to induce apoptosis in GBs.

1.15 Curcumin as a therapeutic agent

1.15.1 Dietary sources of curcumin

Curcumin (diferuloylmethane; 1,7-bis(4-hydroxy 3-methoxy phenyl)-1,6-heptadiene-3,5-dione) is a polyphenol derived from *Curcuma Longa*, a medicinal plant. Commonly called turmeric, it is an ancient spice with a distinct orange colour, which has been used for centuries in Asia, not just for indigenous medicine but also for colouring, food preservative and flavouring.

1.15.2 Chemical structure and therapeutic properties

Turmeric contains 3 main components; 77% curcumin (Fig. 4A), 17% demethoxycurcumin (Fig 4B) and 3% bisdemethoxycurcumin (Fig 4C). Together, they are referred to as curcuminoids (Aggarwal, Kumar and Bharti, 2003; Sharma, Gescher and Steward; 2005). More recently, it has been reported that a new component has been identified: cyclocurcumin

(Fig 4D). Curcumin has been identified as the most active component with several beneficial properties including anti-inflammatory, anti-oxidant, antibacterial, anti-amyloid and anti-angiogenic properties (Kunwar *et al.*, 2008; Jurenka, 2009).

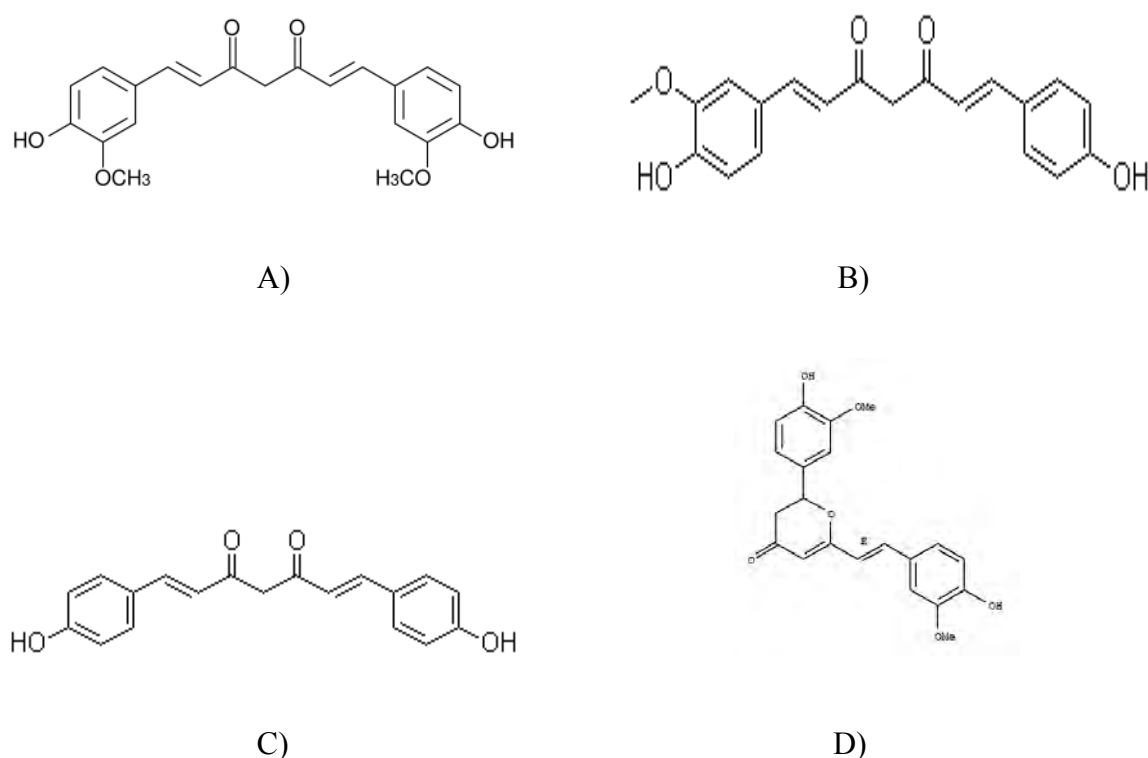


Figure 4: Chemical structures of curcuminoids; A) Curcumin, B) Demethoxycurcumin C) Bisdemethoxycurcumin and D) Cyclocurcumin

This phenolic compound has also been reported as having an anti-cancer chemopreventative role in tumour inhibition in breast, lung, colon and other types of somatic cancer (Simon *et al.*, 1998; Pillai *et al.*, 2004; Shi *et al.*, 2006). The powder is used to treat gastrointestinal inflammation, arthritic pain and as a tonic for the digestive system (Aggarwal, Kumar and Bharti, 2003). However, mechanisms underlying the actions of

curcumin in pathological conditions remain unclear, but extensive literature on this polyphenol (that based on *in vitro* and *in vivo* preclinical and clinical results) has suggested its potential in the prevention and treatment of cancer (Aggarwal, Kumar and Bharti, 2003; Sharma, Gescher and Steward, 2005; Wilken *et al.*, 2011).

Curcumin has an excellent safety profile and a number of potent pleiotropic actions for neuroprotective efficacy. Indeed, extensive research has reported that curcumin affects several targets (Fig. 5) including transcription factors, growth regulators, adhesion molecules, apoptotic genes, angiogenesis regulators and cellular signaling molecules (Anand *et al.*, 2008). Curcumin has been shown to downregulate the nuclear factor kappa B (NF- κ B), which is an inducible transcription factor. NF- κ B regulates genes expression as such involved in inflammation, cell proliferation and cell survival (Han, Seo and Surh, 2002; Aggarwal *et al.*, 2004; Bachmeier *et al.*, 2008; Panicker and Kartha, 2010). Transcription factors have pivotal roles in cellular processes as they regulate gene transcription necessary for normal conditions as well as the genes needed for tumours to form. For example, nuclear factor kappa B (NF- κ B) and activating protein-1 (AP-1) have been implicated in cell survival and tumour progression respectively (Sharma, Gescher and Steward, 2005). It has been reported that the activation of these two major transcription factors is inhibited by curcumin in leukaemic cells. Moreover, other researchers have documented that there could be involvement in the death receptor pathway through Fas-ligand interaction, caspase 3 activation (Duvoix *et al.*, 2005), caspase 8, BID cleavage, cytochrome c release and anti-apoptotic gene suppression (Bcl-2 and Bcl-xL) (Duvoix *et al.*, 2005; Anto *et al.*, 2002).

Reactive oxygen species (ROS) such as superoxide radical (O_2^-), hydrogen peroxide (H_2O_2), singlet oxygen (1O_2) and hydroxyl radical play important roles in initiating lipid peroxidation (Ahsan *et al.*, 1999). Lipid peroxidation has a significant impact, causing cell

cytotoxicity, as well as implications in inflammation, heart disease and carcinogenesis. Curcumin has been shown to scavenge the activated oxygen species which is an important mechanism in the prevention of cancer, thereby conferring its therapeutic advantages (Srejayan and Rao, 1994). Curcumin's potential as an anti-oxidant agent has been demonstrated in a wide range of pathological conditions. It was found that lipid peroxidation in rat brain homogenates and liver microsomes were inhibited by the three curcuminoids, compared with tocopherol (Srejayan and Rao, 1994). The effects were proposed to be due to phenolic hydroxyl and the methoxyl groups on the phenyl ring and the 1,3-diketone system that are present. Ahsan et al. (1999) have demonstrated that curcumin shows both pro-oxidant and anti-oxidant effects as in the presence of Cu (II), curcumin causes strand cleavage in DNA through the formation of hydroxyl radical.

Among the three components, curcumin was found to be the most effective in the reaction, followed by bis-demethoxycurcumin and demethoxycurcumin. Furthermore, an antioxidant behaviour of curcumin in protecting proteins was proposed by Kapoor and Priyadarsini (2001) who found that the reduction (at the disulphide bond) or oxidation (at amino acid site) of proteins is ultimately involved in controlling the vital processes such as gene expression and signaling pathways. In addition, long range electron transfer involved in the protein chain during the processes may extend to radiation which could damage the proteins sub-cellular fractions. As a result, oxidative damage that occurs may have initiated the progression of multi-stage carcinogenesis. Thus, curcumin with anti-oxidant activity provides protection from free radical attack to cells and ultimately proteins.

The anti-cancer properties of curcumin have been extensively reviewed with respect to duodenal, stomach, colon, esophageal and oral cancer (via animal tumour bioassay) (Maheshwari *et al.*, 2006). In addition, a study on mice has shown that curcumin treatment

could stop the progression of breast tumour growth (Shao *et al.*, 2002). Clinical trials on curcumin administration to patients with progressive, advanced colorectal cancer had promising results with patients experiencing longer stability post-radiotherapy (Kunwar *et al.*, 2008). Numerous molecular targets and different pathways of curcumin in combating large numbers of cancers have been reviewed by Anand *et al.* (2007).

Several mechanisms have been suggested in curcumin's actions against breast cancer. Curcumin has been shown to inhibit vascular endothelial growth factor (VEGF) and basic fibroblast growth factor (b-FGF) which are overexpressed and correlate with increased angiogenesis and hence poor prognosis of breast cancer. Its role in inducing p53 to regulate Bax expression and therefore to mediate apoptosis has also been widely debated (Schindler and Mentlein, 2006; Di *et al.*, 2003).

In addition, matrix metalloproteinases (MMPs), which have been strongly implicated as mediators of tumour invasion, have been shown to be down-regulated by curcumin in breast cancer. Concurrently, tissue inhibitor of MMP-1 (TIMP-1) is up-regulated. TIMPs play a critical role in the homeostasis of extracellular matrix (ECM) by regulating the activity of MMPs. Thus, the upregulation of TIMP activity enhances the anti-cancer properties of curcumin (Goel, Kunnumakkara and Aggarwal, 2008).

Gastrointestinal cancer studies suggest that a huge number of mechanisms may account for this effect. A wide range of transcription factors and enzymes involved in multistage-cancer progression have been modulated by curcumin. Curcumin was found to inhibit the cytokine-induced activation of NF- κ B in human pancreatic adenocarcinoma cells (Wang *et al.*, 1999; Khanbolooki *et al.*, 2006).

Others Similar therapeutic effect was observed in colorectal cancers (Reddy *et al.*, 2006), as well as in a number of bladder (Sun *et al.*, 2004; Kamat, Sethi and Aggarwal, 2007; Aggarwal *et al.*, 2007) prostate (Shi *et al.*, 2006), cervical (Divya and Pillai, 2006) and ovarian cancers (Zheng, Tong and Wu, 2002; Zheng, Tong and Wu, 2006), as well as in leukaemias (Sokoloski, Shyam and Satorelli, 1997; Bielak-Mijewska *et al.*, 2004; Mukherjee Nee Chakraborty *et al.*, 2007; Pae *et al.*, 2007), lymphomas (Wu *et al.*, 2002; Thompson *et al.*, 2004; Skommer *et al.*, 2006) and melanomas (Siwak *et al.*, 2005; Marin *et al.*, 2007).

Remarkably, curcumin has significantly down-regulated the levels of hypoxia-inducible factor-1 (HIF-1) which is important in stimulating genes that promote tumour angiogenesis (Bae *et al.*, 2006). This inhibition is thought to be via degradation of aryl hydrocarbon receptor nuclear translocator (ARNT), a sub-family of HIF-1 (Choi *et al.*, 2006) which has been seen in other cell lines such as prostate, cervical and lung cancers.

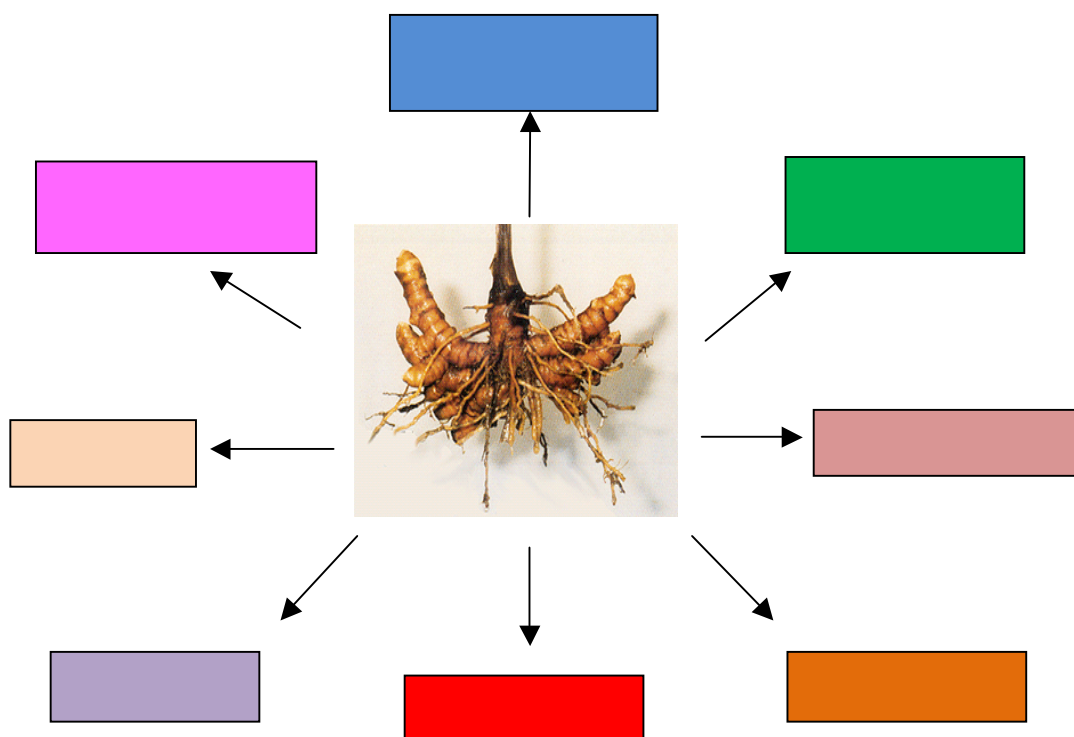


Figure 5: Multiple molecular targets of curcumin

1.15.3 Absorption, metabolism and transport

Clinical pharmacokinetic studies on curcumin have shown that curcumin has a rapid and extensive metabolism (Kunwar et al., 2008; Garcea et al., 2004; Garcea et al., 2005; Ireson et al., 2001; Ireson et al., 2002; Goel, Kunumakkara and Aggarwal, 2008). This may explain its poor bioavailability in plasma, urine and tissues in many pre-clinical studies (Strimpakos and Sharma, 2008; Sharma et al., 2001a; Sharma et al., 2001b). A study on hepatocellular and colorectal cancer suggested curcumin's poor availability, post-oral administration (450-3600mg daily) and the concentration achieved may not be sufficient to exert pharmacological activity in humans (Garcea et al., 2004).

1.15.4 Bioavailability with tissue distribution

Curcumin is highly prone to conjugation (via glucuronidation and sulfation) and reduction especially in humans (Fig. 6) thus resulting in a deficit at the systemic level (Marczylo et al., 2007). Marczylo et al. (2007) has also suggested that the preferential uptake of curcumin by tumour cells compared to normal cells is possibly due to differences in membrane structure, protein content and size between normal and tumour cells. Being a lipophilic molecule, curcumin is being transported inside the cells where toxicity of curcumin is increased with the increasing uptake. The research suggests that curcumin uptake is different in different cell types based on polarity and hydrophobicity of composition within the cells. Marczylo et al. (2007) showed that poorly absorbed drugs have been increased in bioavailability in plasma with the use of phosphatidylcholine. Therefore, due to curcumin better uptake following its formulation with phosphatidylcholine, a better systemic level in humans may be achieved.

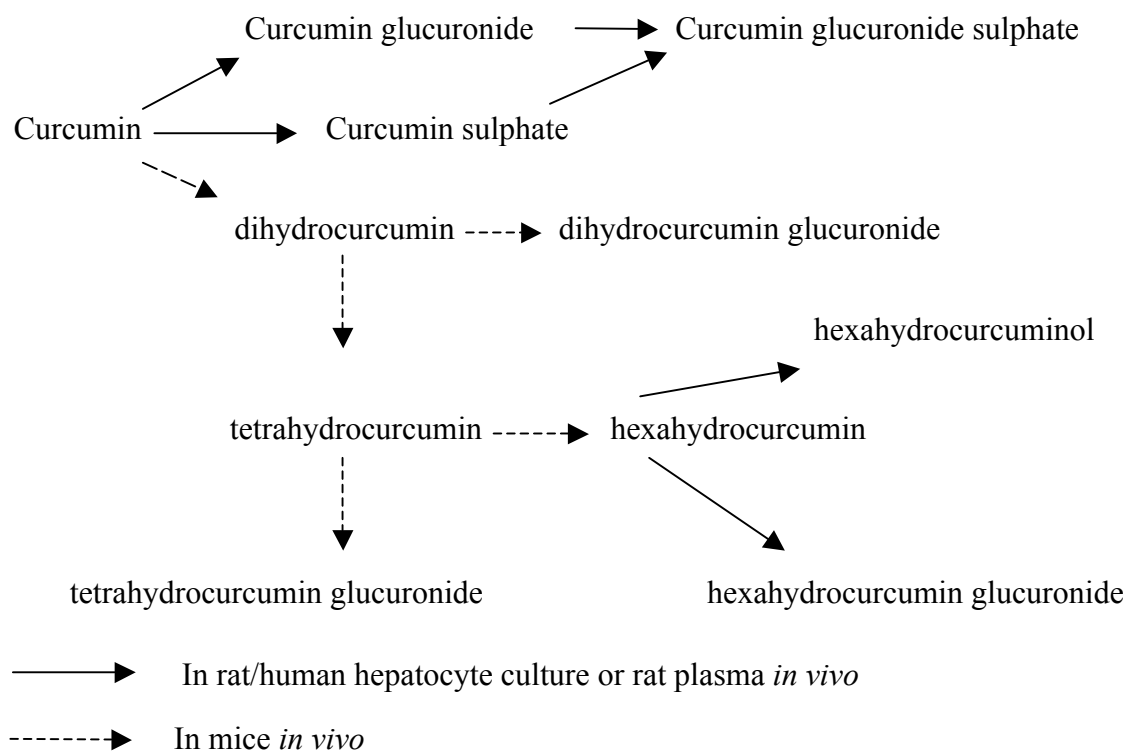


Figure 6: Metabolic pathways of curcumin in rodents and *in vitro* culture (rat and human hepatocytes). Taken from: Marczylo et al., 2007.

1.15.5 Cytotoxicity of Curcumin

Studies in which normal subjects were given doses of between 8g/day and 10g/day showed no toxic effects (Aggarwal, Kumar and Bharti, 2003). Furthermore, a review of a clinical trial by Goel, Kunnumakkara and Aggarwal (2008) has shown curcumin to be safe at a daily dose of 12g for 3 months. However, a clinical study that administered doses of up to 8000 mg daily for 4 months resulted in diarrhea and mild nausea but other toxicities were not reported (Hsu and Cheng, 2007).

Turmeric has most recently been reported to cross the rat BBB (Datla, Zbarsky and Dexter, 2006) which makes it ideal for use in the management of malignant brain tumours and neurological diseases. Extensive studies of anti-tumour activities of curcumin (described

earlier) have been reported in different types of cancer but those in malignant gliomas are still lacking.

1.16 Lycopene, a naturally occurring pigment with health benefits

1.16.1 Dietary sources of lycopene

Lycopene belongs to the carotenoid family which represents one of the most widespread groups of naturally occurring pigments. Tomatoes are the main source of lycopene besides apricots, guavas, papayas, rosehip, pink grapefruit and watermelon (Maiani *et al.*, 2009). However, gac fruit has been identified to have the highest content of lycopene, 70 times higher than tomatoes. Due to its rarity in availability (Ishida *et al.*, 2004) more than 85% of lycopene intake is from tomato-based juices and sauces for most people.

1.16.2 Chemical structure and therapeutic properties

Lycopene consists of 11 conjugated double bond in a 40 carbon acyclic with open chain structure (Fig. 7). Insoluble in water, its conjugated double bonds characterize its deep red colour and antioxidant activity which has led to preliminary research in cancer expanding to the investigation of a correlation between tomato consumption and risk of cancer which include research into the prevention and treatment of breast and prostate cancers (Sato *et al.*, 2002; Bureyko *et al.*, 2009; Wei and Giovannucci, 2012).

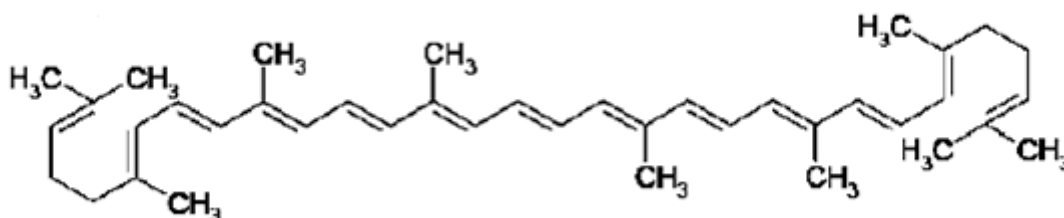


Figure 7: Lycopene with 40 carbon acyclic in structure

Carotenoids are one of the classes of micronutrients that have been studied extensively for their potential protective effects against cancer. One of the most active components in carotenoids is lycopene which has been suggested as having a role in preventing carcinogenesis and atherogenesis. Moreover, lycopene is proposed to have greater anti-oxidant properties and free radical scavenging activity compared to other carotenoids such as beta carotene or alpha tocopherol (Yeum and Russel, 2002). For example, despite having no variants in the protein levels, lycopene was found to have effects on mRNA levels of BRCA1 and BRCA2 genes and their splice variants in breast carcinogenesis (Chalabi *et al.*, 2004).

In addition, lycopene was found to inhibit the growth of human endometrial, mammary and lung cancer cells *in vitro* through reducing mutagenesis and improving anti-tumour immune response (Omoni and Aluko, 2005). Epidemiological studies on prostate cancer have shown that a higher consumption of tomato products results in a lower risk of prostate cancer in men and it has been suggested that this may be due to lycopene's health-protective effects that include strong anti-oxidant and anti-proliferative activity, growth factor inhibition and cell cycle arrest (Giovannucci, 2002; Teodoro *et al.*, 2012).

Lycopene exists in 'trans' forms in plants and this form is poorly absorbed. Bioavailability improves in human serum or plasma following heat-induced isomerization to the ('cis' forms) *in vivo* (Boileau and Erdman, 2002). Thus, lycopene is suggested for its efficacy in preventing carcinogenesis due to its enhancement in tissue uptake, metabolism and distribution while maintaining its anti-oxidant properties in the body. Furthermore, lycopene has been suggested as an inhibitor of insulin like growth factor-1 (IGF-1) signaling transduction hence delaying cell cycle progression (Karas *et al.*, 2000; Teodoro *et al.*, 2012). A study by Lo *et al.* (2007) has proposed that lycopene has anti-tumour activity, mediated through growth factor receptor inhibition in rat smooth muscle cells.

There is also compelling evidence (Yu, Ustach and Choi Kim, 2003) that platelet derived growth factor receptor BB (PDGFR-BB) overexpression occurs in diverse malignancies such as in breast cancer and brain tumours. It was found that lycopene inhibited PDGF-BB in human cultured skin fibroblasts via binding activity which could be a possible target for cancer. Therefore, inhibition or modulation of growth factor signaling may emerge as a possible mechanism for decreasing tumour progression hence designing better ways to treat the cancer.

1.16.3 Absorption, metabolism and transport

Growing interest in lycopene as a potential anti-cancer agent has followed from several studies on its disposition and distribution *in vivo*. Following ingestion, lycopene is solubilized by bile salts in the small intestine prior to incorporation with other lipids. Incorporated into lipid micelles, it is then transported to the liver in chylomicrons before being repackaged and transported through blood vessels in low and high density lipoproteins (Fig 8).

The processes by which the ingested lycopene is absorbed, transported in the body and deposited in tissues and organs are of fundamental importance in relation to any effect of lycopene on human health. One study looked at a physiological pharmacokinetic model in healthy subjects following ingestion of a tomato beverage formulation in different doses (Diwadkar-Navsariwala *et al.*, 2003). Comprised of seven compartments (gastrointestinal tract, enterocytes, chylomicrons, plasma lipoproteins, fast-turnover liver, slow-turnover tissues, and a delay compartment before the enterocytes) that were looked at, optimal percentage absorption of lycopene occurred at 10mg of physiological dose while higher doses of lycopene showed lower percentage in absorptive activity although the absolute amount (mg) of lycopene absorbed was not statistically different between doses. It was speculated

that there is possible saturation of lycopene at higher doses, indicating the importance of correctly planning clinical trials with multiple doses of lycopene in the treatment.

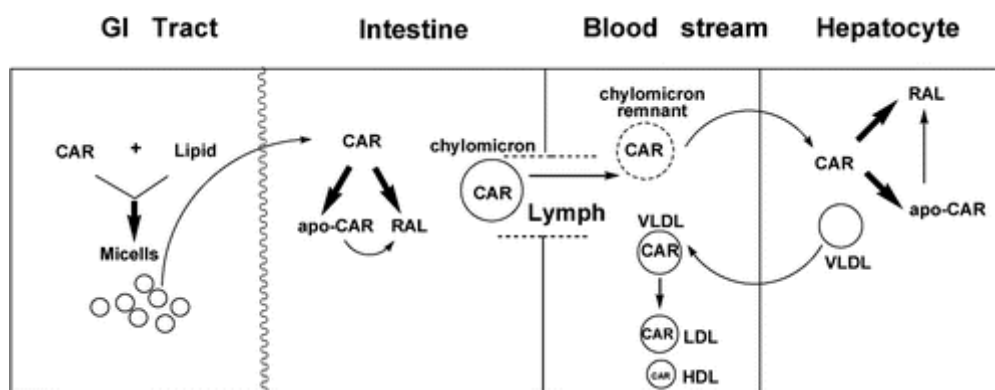


Figure 8: Carotenoid uptake by micelles following ingestion and its release into the bloodstream prior to deposition in the tissues (Yeum and Russel, 2002).

GI: gastrointestinal, CAR: Carotenoids, apo-CAR: apo-carotenoids, VLDL: very low density lipoprotein, LDL: low density lipoprotein, HDL: high density lipoprotein, RAL: retinal

1.16.4 Bioavailability of lycopene with tissue distribution

Despite growing studies in the role of lycopene in reducing the risks of certain malignancies, data on the mechanisms of absorption and bioavailability of this carotenoid is poorly explored (Diwadkar-Navsariwala *et al.*, 2003). Most of the studies on bioavailability are limited to crude food-based dietary supplements with less information available on the pure compound. Faisal, O'Driscoll and Griffin, (2010) in a study of bioavailability of lycopene in the rat and the role of intestinal lymphatic transport (as the major route for lycopene uptake) have found that the absolute bioavailability of lycopene after 8 hours was estimated to be as low as 1.85% as collected from the mesenteric lymph duct.

Another study investigating lycopene distribution in ferret and rat tissues (Ferreira *et al.* 2000) has measured the highest lycopene levels in liver where cis-lycopene and all-trans-lycopene are the predominant isomers in ferret and rat tissues, respectively. Due to the

highly lipophilic properties of lycopene, important factors could influence the absorption process such as the solubility in the physiological media, the uptake by intestinal cells and its release into the general circulation.

1.16.5 Cytotoxicity of lycopene

An excess intake of lycopene is not known for its toxicity but may cause a deep orange discoloration of the skin, a harmless condition called *lycopenemia* (Reich *et al.*, 1960). It was reported in a 61 year old woman who had consumed 2 litres of tomato juice everyday for several years, but was reversible after 3 weeks of consuming tomato-free juice with the discolouration fading.

There is a lack of data on the adverse effects of lycopene in either animal or healthy humans *in vivo* or *in vitro*, but Trumbo (2005) has reported that there were no adverse effects observed at intake levels up to 3g/(kg.d) of formulated lycopene in the diet. In addition, it was also suggested that there is neither tolerable intake of lycopene that standardized nor well documented by Institute of Medicine (Washington). Indeed in the UK, no definite recommendation for a dietary intake has been published to date for lycopene, presumably lycopene is present in so many food sources.

1.17 Aim and research objectives

The aims of this study were to investigate whether curcumin and lycopene have any potential therapeutic effects on a number of biopsy-derived GBs *in vitro*, as outlined below:

1. Determination of IC₂₅, ₅₀, and ₇₅ values (concentration that inhibits 25, 50 and 75% of cell viability of the tumour cells *in vitro*) of the 2 micronutrients using DRAQ7 cell viability assay (flow cytometry). Subsequent experiments were contingent upon obtaining this IC values.
2. Evaluation on the expression of parameters responsible for invasion, angiogenesis and apoptosis (e.g.MMPs, CD44, growth factors) using immunocytochemistry and flow cytometry.
3. Investigation of the ability of curcumin and lycopene to induce apoptosis in biopsy-derived GBs using flow cytometry via Annexin-V staining.
4. Determination of anti-invasive potential of micronutrients studied using an invasion *in vitro*.
5. Investigation of anti-angiogenic effects of micronutrients using an *in vitro* angiogenesis assay.

CHAPTER 2: Materials and Methods

2.1 List of materials

Equipment/ Labware

Flasks	Corning Life Sciences, Amsterdam, Netherlands
0.22µm Filter	Milipore, Watford, United Kingdom
6, 24 well plates	Thermo Scientific Nunclon, Langenselbold, Germany
Angiogenesis inserts	Corning Life Sciences, Amsterdam, Netherlands
Column chromatography	Fisher Scientific, Loughborough, United Kingdom
Centrifuge	ALC multispeed refrigerated centrifuge, PK13IR, DJB Labcare, Buckinghamshire, United Kingdom
Biofuge Fresco (microcentrifuge)	Heraeus Instrumetns, DJB Labcare, Buckinghamshire, United Kingdom
GX Microscope	GX Optical, Suffolk, United Kingdom
Ceti Microscope	Labmode, Borehamwood, United Kingdom
JB Aqua 26 waterbath	Grant, Cmabridgeshire, United Kingdom
Vortex-genie 2	Jencons Scientific Ltd, Bedfordshire, United Kingdom
ACCULAB weighing scale	VWR International Ltd, Leicestershire, United Kingdom
Clifton sonicator	Nickel-Electro Ltd, Weston-Super-Mare, United Kingdom
Fluo Satr Optima microplate reader	BMG Labtech, Bucks, United Kingdom

BD FACS Calibur	BD Biosciences, Oxford, United Kingdom
Cryogenics	Jencons Scientific Ltd, Bedfordshire, United Kingdom

Reagents

Purification of Tetrahydrofuran

THF (tetrahydrofuran)	Sigma-Aldrich, Dorset, United Kingdom
Aluminium oxide (alox)	Sigma-Aldrich, Dorset, United Kingdom

Preparation of Curcumin and LycoRed concentrations

DMSO (dimethyl sulphoxide)	Fisher Scientific, Loughborough, United Kingdom
THF (tetrahydrofuran)	Sigma-Aldrich, Dorset, United Kingdom
DMEM (Dulbecco's Modified Eagle Medium)	Invitrogen, Paisley, United Kingdom
FCS (Foetal calf serum)	Sigma-Aldrich, Dorset, United Kingdom
Antibiotic (Penicillin-Streptomycin) (500U/M)	Invitrogen, Paisley, United Kingdom

Cell culture maintenance

DMSO (dimethyl sulphoxide)	Fisher Scientific, Loughborough, United Kingdom
DMEM (Dulbecco's Modified Eagle Medium)	Invitrogen, Paisley, United Kingdom
FCS (Foetal calf serum)	Sigma-Aldrich, Dorset, United Kingdom
Antibiotic (Penicillin-Streptomycin) (500U/M)	Invitrogen, Paisley, United Kingdom
HUVEC (Human Umbilical Vein Endothelial Cells)	
Cell Growth Supplement	TCS Cellworks (Caltag Medsystem), Buckingham United Kingdom
HUVEC Media	TCS Cellworks (Caltag Medsystem), Buckingham, United Kingdom
Gelatin	Sigma-Aldrich, Dorset, United Kingdom

Population doubling time

Trypsin	Invitrogen, Paisley, United Kingdom
DMEM (Dulbecco's Modified Eagle Medium)	Invitrogen, Paisley, United Kingdom
FCS (Foetal calf serum)	Sigma-Aldrich, Dorset, United Kingdom
Antibiotic (Penicillin-Streptomycin) (500U/M)	Invitrogen, Paisley, United Kingdom

Calcein AM cell viability assay

Calcein AM	Invitrogen, Paisley, United Kingdom
DMEM (Dulbecco's Modified Eagle Medium)	Invitrogen, Paisley, United Kingdom
FCS (Foetal calf serum)	Sigma-Aldrich, Dorset, United Kingdom
Antibiotic (Penicillin-Streptomycin) (500U/M)	Invitrogen, Paisley, United Kingdom

Cell viability assay using flow cytometry (DRAQ 7)

DRAQ7	Biostatus Ltd, Leicestershire
DMEM (Dulbecco's Modified Eagle Medium)	Invitrogen, Paisley, United Kingdom
FCS (Foetal calf serum)	Sigma-Aldrich, Dorset, United Kingdom
Antibiotic (Penicillin-Streptomycin) (500U/M)	Invitrogen, Paisley, United Kingdom

Cell characterization via Immunocytochemistry (ICC)

Trypsin	Invitrogen, Paisley, United Kingdom
HBSS (Hanks Balance Salt Solution)	Invitrogen, Paisley, United Kingdom
Anti-mouse IgG (developed in rabbit) biotin conjugated	Sigma-Aldrich, Dorset, United Kingdom

Alexa fluor 488 streptavidin conjugated	Invitrogen, Paisley, United Kingdom
Mouse monoclonal anti-GFAP (Glial Fibrillary Acidic Protein)	Abcam plc, Cambridge, United Kingdom
PBS (phosphate buffer saline)	Invitrogen, Paisley, United Kingdom
Monoclonal anti-NG2 (neuron glial-2) antibody	Sigma-Aldrich, Dorset, United Kingdom
Mouse anti-human GD3 (ganglioside 3) monoclonal antibody	Milipore, Watford, United Kingdom
Mouse anti-human CD44 (cluster differentiation 44) monoclonal antibody	Milipore, Watford, United Kingdom
Mouse Anti-Beta-1-integrin monoclonal antibody	Abcam plc, Cambridge, United Kingdom
CDS (Cell Dissociation Solution)	Invitrogen, Paisley, United Kingdom
DMEM (Dulbecco's Modified Eagle Medium)	Invitrogen, Paisley, United Kingdom
FCS (Foetal calf serum)	Sigma-Aldrich, Dorset, United Kingdom
Antibiotic (Penicillin-Streptomycin) (500U/M)	Invitrogen, Paisley, United Kingdom

Cell characterization via Flow cytometry

Propidium iodide	Invitrogen, Paisley, United Kingdom
Mouse anti-human CD44 (cluster differentiation 44) monoclonal antibody	Milipore, Watford, United Kingdom
Mouse Anti-Beta-1-integrin monoclonal antibody	Abcam plc, Cambridge, United Kingdom
CDS (Cell Dissociation Solution)	Invitrogen, Paisley, United Kingdom
Mouse anti-MMP14 (matrix metalloproteinase 14) monoclonal antibody	Abcam plc, Cambridge, United Kingdom
Mouse Anti-VEGF (Vascular Endothelial Growth Factor) monoclonal antibody	Abcam plc, Cambridge, United Kingdom
Anti-mouse IgG (developed in rabbit) biotin conjugated DMEM (Dulbecco's Modified Eagle Medium)	Sigma-Aldrich, Dorset, United Kingdom Invitrogen, Paisley, United Kingdom
FCS (Foetal calf serum)	Sigma-Aldrich, Dorset, United Kingdom
Antibiotic (Penicillin-Streptomycin) (500U/M)	Invitrogen, Paisley, United Kingdom

Apoptosis assay via flow cytometry analysis (Annexin V detection)

Annexin V-Alexa fluor 647	Invitrogen, Paisley, United Kingdom
Propidium iodide	Invitrogen, Paisley, United Kingdom
Staurosporine	Sigma-Aldrich, Dorset, United Kingdom
DMEM (Dulbecco's Modified Eagle Medium)	Invitrogen, Paisley, United Kingdom
FCS (Foetal calf serum)	Sigma-Aldrich, Dorset, United Kingdom
Antibiotic (Penicillin-Streptomycin) (500U/M)	Invitrogen, Paisley, United Kingdom

In vitro invasion assay

DilC (1,1'-dioctadecyl-3,3,3',3'-tetramethylindocarbocyanine perchlorate)	BD Biosciences, Oxford, United Kingdom
BD Fluoroblok	BD Biosciences, Oxford, United Kingdom
DMEM (Dulbecco's Modified Eagle Medium)	Invitrogen, Paisley, United Kingdom
FCS (Foetal calf serum)	Sigma-Aldrich, Dorset, United Kingdom
Antibiotic (Penicillin-Streptomycin) (500U/M)	Invitrogen, Paisley, United Kingdom

HUVEC

(Human Umbilical Vein Endothelial Cells)

Cell Growth Supplement	TCS Cellworks (Caltag Medsystem), Buckingham, United Kingdom
HUVEC Media	TCS Cellworks (Caltag Medsystem), Buckingham, United Kingdom

In vitro angiogenesis assay

Trypan blue Sigma-Aldrich, Dorset, United Kingdom

DMEM

(Dulbecco's Modified Eagle Medium) Invitrogen, Paisley, United Kingdom

FCS (Foetal calf serum) Sigma-Aldrich, Dorset, United Kingdom

Antibiotic

(Penicillin-Streptomycin) (500U/M) Invitrogen, Paisley, United Kingdom

HUVEC

(Human Umbilical Vein Endothelial Cells)

Cell Growth Supplement	TCS Cellworks (Caltag Medsystem), Buckingham, United Kingdom
HUVEC Media	TCS Cellworks (Caltag Medsystem), Buckingham, United Kingdom
Matrigel (Extracellular matrix gel)	Sigma-Aldrich, Dorset, United Kingdom
Suramin	TCS Cellworks (Caltag Medsystem), Buckingham, United Kingdom
VEGF	TCS Cellworks (Caltag Medsystem), Buckingham, United Kingdom

Cell cultures

CC2565 Primary brain tumour cell cultures	Cambrex Biosciences Walkersville Inc. USA
MUBP, MUBS, MUP, MUTC, MUMG Designated cell cultures from Glioblastoma biopsy derived	Kings' College Hospital, London, United Kingdom
HT-1080 fibrosarcoma cell line	ATCC Middlesex, United Kingdom
HUVEC human umbilical vein endothelial cells	University of Portsmouth, United Kingdom

Micronutrients

Two micronutrients were used in this study, Curcumin extracted from turmeric and LycoRed (lycopene) extracted from tomato.

Curcumin

Curcumin was donated by Sabinsa Corporation, New Jersey USA (Sabinsa Corporation- appendix 1). It was 77% pure from the ground rhizome of turmeric, and produced by solvent extraction method (acetone solution). It was dissolved in 100% dimethyl sulphoxide prior to use and stored in room temperature.

LycoRed (lycopene)

Lycopene powder was kindly provided by LycoRed Israel (appendix 2). It contains 10% lycopene (via spectrophotometric method) from tomato extract and stored at -20°C in the dark. Other ingredients include maltodextrin, modified starch, gum acacia, sugar esters and

soy lecithin which amount were not provided. 500 μ M stock solutions were freshly prepared with purified tetrahydrofuran prior to use. Henceforth, lycopene used in this study will be referred to as LycoRed.

2.2 Methods

2.2.1 Purification of Tetrahydrofuran

THF is >99.9% pure and has the tendency to form highly explosive peroxides on storage in air. Thus, as to minimize this, commercially available THF has been added with 250ppm BHT (butylated hydroxyl-toluene) as an inhibitor of peroxides formation. Peroxides destroy the carotenoid as such in LycoRed hence purification of tetrahydrofuran is a requisite.

A layer of glass wool was placed at the bottom of the column (height 30cm, diameter 3cm) before filling the column with 20cm in height of aluminium oxide (Alox). Alox is a white, fine-grained powder that is generally used as a medium in column chromatography. As an activated basic alumina, it traps the peroxides that present in the THF. Therefore, 50ml THF was poured in the column packed with Alox and the first 10ml of eluent was discarded. The remaining eluent was collected in a dark glass bottle as THF can degrade plastic.

2.2.2 Preparation of Curcumin and LycoRed concentrations

A range of curcumin concentrations were prepared in DMEM with 20% fetal calf serum and 1% antibiotic (penicillin-streptomycin). 5mg curcumin was dissolved in 500 μ l DMSO and filtered by 0.22 μ m syringe driven filter to prepare the stock solution of 10mg/ml curcumin.

To ensure that any cytotoxicity observed was not due to DMSO activity, the 100% DMSO present in the curcumin stock solution was reduced to less than 1%. Therefore, 150 μ l of the

curcumin stock solution was dissolved in 49.85ml complete medium (20% fetal calf serum, 1% penicillin/streptomycin) to give 50ml in total volume. This is equivalent to 0.3% of DMSO present at 30µg/ml (highest concentration of curcumin used).

In order to see whether curcuminoids has any cytotoxicity effect on the normal brain cells (CC2565), a wide range of curcuminoids concentrations were prepared. From the 30µg/ml, a set of concentration was prepared in complete medium (20% fetal calf serum, 1% penicillin/streptomycin). These include 5 and 30ng/ml, 3, 5, 6, 9, 12, 15,18,20,21 and 24µg/ml.

Solutions of lycopene were prepared in purified tetrahydrofuran. Lycopene is highly hydrophobic resulting in low aqueous solubility. 3mg LycoRed was dissolved in 11ml THF (500µM). LycoRed solution was then vortexed and filled with nitrogen stream before sonication take in place for 30 minutes. Then it was diluted in complete medium (20% fetal calf serum, 1% penicillin/streptomycin) to 25µM resulting in a final concentration of 5% THF.

This was then filtered with a 0.22µm syringe driven filter (Milipore). From the filtered 25µM, a range of LycoRed concentrations were prepared in complete media; 20 (4% THF), 10 (2% THF), 5 (1% THF), 2(0.4% THF) and 1µM (0.2% THF) which are equivalent to 12, 6, 3, 1.2 and 0.6µg/ml LycoRed.

2.2.3 Cell culture maintenance

Normal astrocytes, (CC2565 cell line), at passage 11, were used as the control. This is a normal human brain cell population from an 18 year old male, purchased from Cambrex Biosciences. Brain tumour cultures for the study were obtained from craniotomy (removing

small window of bone from the cranium to allow the tumour section biopsied) of the glioblastoma patients in Kings College Hospital London (LREC protocols 02-056). Following each craniotomy, the tissue biopsy was placed in a universal bottle with complete medium (DMEM) before taken to Middlesex University about 30 minutes journey time in a sealed container. Five glioblastoma biopsy derived samples were used; MUBS, MUBP, MUMG, MUP and MUTC. These samples approximately 2 years to be obtained (hence gathered as number of samples for this study) as glioblastoma is quite a rare cancer. Each biopsy was immediately cultured as soon as it arrived at laboratory in Middlesex University. Using a sterile scalpel with an appropriate container, the biopsy was chopped into very small pieces as possible in the presence of the complete medium, i.e. DMEM contain 20% fetal calf serum and 1% penicillin/streptomycin. In order to achieve primary explant culture, each chopped biopsy was placed in a small flask in the complete medium as a monolayer and routinely passaged when it reached confluency. The physiological pH was maintained through equilibration with 5% CO₂ atmosphere in 37°C humidified incubator. For each biopsy collected, one small flask generated approximately 100,000 cells. When the cells were nearly confluent, they were harvested by trypsinization. The cells were passaged and more flasks were grown in order to have sufficient cells for all experiments. When necessary, the cells were frozen down for storage in the liquid nitrogen tank until required.

For *in vitro* angiogenesis and invasion assays, Human Umbilical Vein Endothelial Cells (HUVEC) was used (donated by Dr Alan Cooper from Portsmouth University at passage 2). HUVECs were maintained in HUVEC Complete Medium, supplemented with 0.2% of each Penicillin/Streptomycin, Heparin, EGF and 2% of FCS and 0.1% Hydrocortisone (TCS Cell Works). The cells were cultured in gelatin-coated flasks which were prepared one hour prior to culturing. Gelatin (1%) was prepared in sterile PBS autoclaved before use. In addition, a

fibrosarcoma cell line, designed as HT-1080, which is purchased from ATCC, was used as a positive control in the analysis due to its high invasive capacity (Rasheed, et al., 1974). The medium was changed approximately twice a week and trypsinized when nearly confluent.

2.2.4 Population doubling time

In order to study the population doubling time (PDT) or cell kinetics of a cell line, primary brain tumour cells were seeded, initially at 20 000 cells/well (in 2ml complete medium per well), in 6 well plates. The cells were incubated overnight, harvested and resuspended in 1ml of complete media from which 20µl of this cells suspension was combined with 20µl of trypan blue stain. 20µl of this solution was placed onto the haematocytometer prior to counting. This was carried out in triplicate, twice a day for up to 9-13 days. Trypan blue is a vital stain that selectively stains the dead cells but not the live ones. The cell count obtained by calculating the average of two counts (a and b) as in the equation as follow:

$$\text{Number of cells/ml} = \frac{(a + b) \times 2 \times 10,000}{2}$$

Population doubling time assess the time that cells take to double in number, determined by the growth curve plotted (Fig.9). The lag phase represents slow growth as cells adapt to the *in vitro* environment before moving on to the log phase (exponential phase) of rapid growth. This is also known as exponential phase, the duration where the population doubling time of cells was measured. A plateau phase takes place subsequently when nutrients become depleted and the cells space limited; under such conditions cell growth is reduced before cell senescence occurs. A Doubling Time software (Roth, 2006) was used to determine the PDT of cells on the log phase with the formula as below.

$$(t \log 2) / (\log N_t - \log N_i)$$

t= time period

N_t= number of cells at time t

N_i=initial number of cells

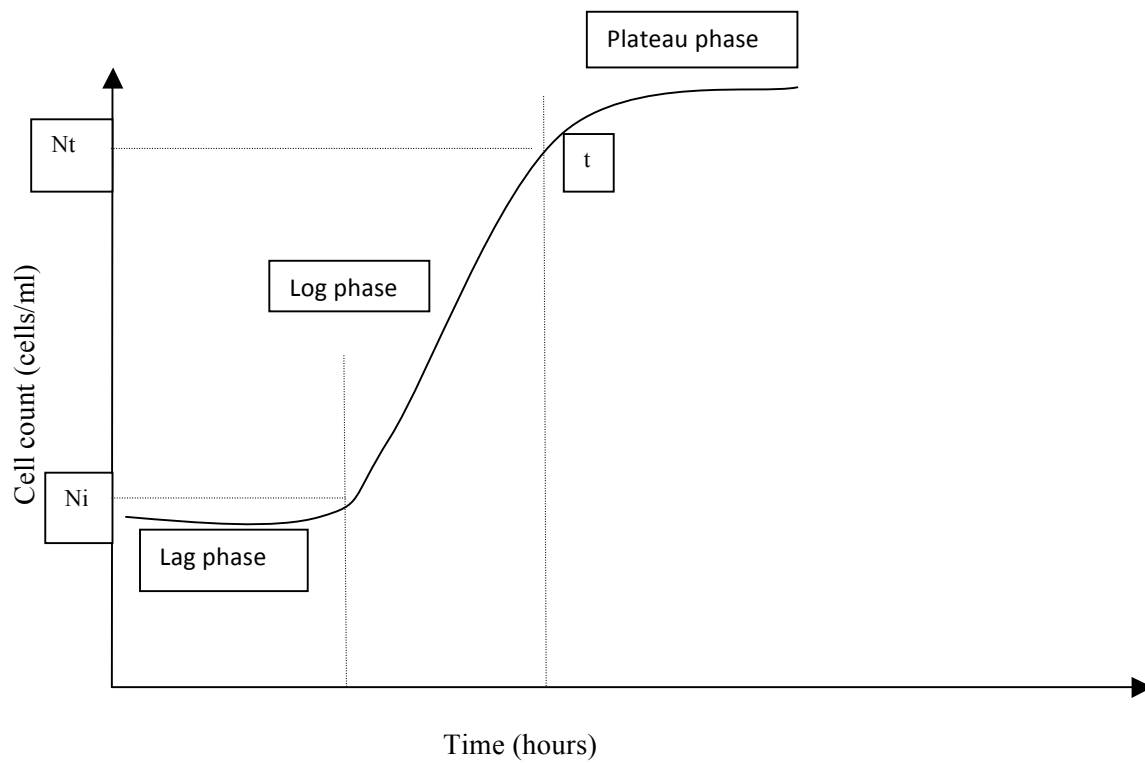


Figure 9: A sigmoidal curve showing three different phases in cell growth. The numbers of cells/ml obtained from the count are plotted against number of hours in culture.

2.2.5 Cell viability assays

A number of cell viability assays were used in measuring the cytotoxicity of the solvents (DMSO and THF) and the IC value of micronutrients studied. One small flask generated approximately 100,000 cells per biopsy and 10,000 cells were required for each well in cell viability plates. Therefore, prior to each set of experiment, it is important to ensure that more flasks (grown with confluent cells) per biopsy were available to provide enough number of cells.

IC₂₅, IC₅₀ and IC₇₅ are described as the concentration of the substance (i.e. micronutrient) required for 75%, 50% and 25% inhibition of the cell viability respectively. This study has used a cell viability graph with x axis as the concentrations of the micronutrient (or agent) studied and y axis as the percentage of cell that are viable (Fig 10). Therefore, the IC values were determined via the viability curve plotted. As it may be expected, IC₇₅ will result to the least while IC₂₅ to the most cytotoxic effect.

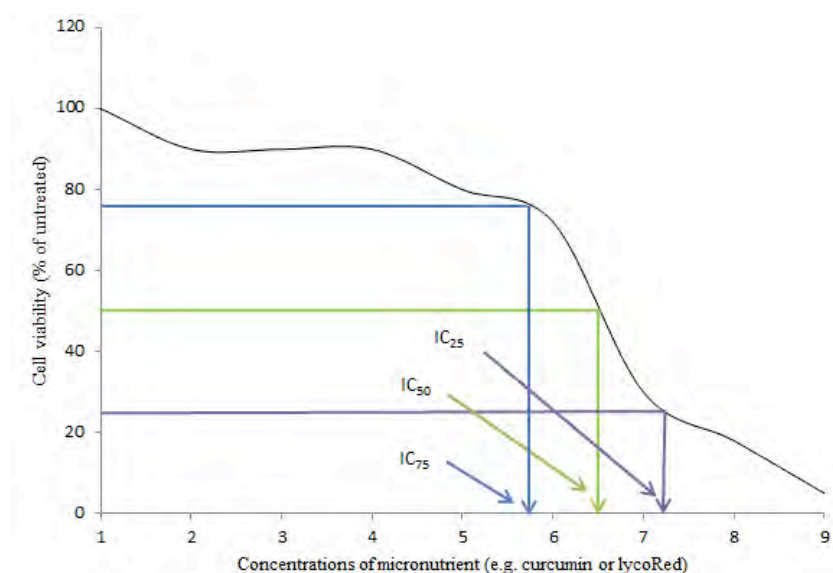


Figure 10: A cell viability curve with % of viable cells (y axis) and concentration of micronutrient (x axis) shows IC values. The IC values are derived at the point where % of viable cells crossed the curve and marked down towards the x axis to determine the concentration of micronutrient, i.e. IC value.

These values can be determined by a chemo-sensitivity assay, with either a colourimetric or a fluorometric method. However, throughout the experiment, it was noted that the distinct orange colour of curcumin affected the absorbance in the MTT assay and several washes as suggested by Peng et al (2005) had not resolved this problem. Indeed, adaptation and/or modification of cell viability assay is acceptable depending on the substance or micronutrient tested, as such MTT assay (3[4, 5-dimethylthiazole-2-yl]-2,5-diphenyltetrazolium bromide), has been modified and extensively used by other workers in the neuro-oncology field (Nikkah et al., 1992). Unlike MTT, which is a colourimetric, Calcein AM and DRAQ7 cell viability assays were used instead which are fluorescence dyes that are fluorometric in the detection. These allow less interference in the analysis and no solubilization step is required, unlike MTT.

2.2.5.1 Calcein AM cell viability assay

Calcein AM is a cell-permeant dye that can be used to determine cell viability in most eukaryotic cells. Once inside the cytoplasm of the cells, Calcein AM, a non-fluorescent molecule itself is hydrolyzed by endogenous esterase into the highly negatively charged green fluorescent Calcein (Brat-Boucher et al., 1995). The fluorescent Calcein is retained in the cytoplasm in live cells. The fluorescent signal is monitored using 492 nm excitation wavelength and 520 nm emission wavelength. This signal generated from the assay is proportional to the number of living cells in the sample.

The initial concentration of Calcein AM was 1mg/ml (1mM, molecular weight of 994.87) and diluted to 2 μ M/L in PBS for working concentration. 10,000 cells were grown in each well of the 96-well plate. A large number of cells were needed to run cell viability assay hence it is important to ensure that enough cells were available prior to setting up the experiment. Approximately 100,000 cells per biopsy will be collected from a small flask thus

preparing more flasks with grown, confluent cells beforehand is important. (see section 2.2.3). The medium was removed from each well (including control wells) and washed with PBS twice. 100µl of Calcein AM solution was pipetted into each well and the plates were incubated for 1 hour (37°C 5%, CO₂) prior to fluorescent spectrophotometer reading.

2.2.5.2 Cell viability assay using flow cytometry (DRAQ 7)

DRAQ 7 is a new Far-Red Fluorescent Live-Cell Impairment DNA dye (Biostatus Ltd) that only stains the nuclei in dead and permeabilized cells but not intact live cells. Unlike Propidium Iodide, DRAQ 7 has no ultra violet excitation and has far better spectral properties, (from the 488 nm, 568 nm and 633 nm lines, plus optimal 647 nm excitation, fluorescence emission from 665 nm into the low infra-red). Thus, problems such as overlapping with Green Fluorescence Protein (GFP)/Fluorescein isothiocyanate (FITC) or Phycoerythrin (PE) needs no compensation (Biostatus Ltd., 2011). DRAQ 7 fluorescent dye also requires no washing step which is helpful in preventing loss of cells due to washing.

Cells were harvested by trypsin and centrifuged at 800rpm for 5 minutes. The fluorescence dye DRAQ 7 was prepared (3µM) in PBS from the stock concentration (0.3mM) prior to use. For each of the primary brain tumour cell cultures, the cells pre-treated with sterile distilled water is positive control while negative control is untreated cells (with no either curcumin or LycoRed). The cells were not grown in the well of 96-well plates but small flasks due to higher number of cells required (100,000 cells) in FACS analysis. Each cell culture was carried out in triplicate. Therefore, prior to each set of experiment, more flasks with grown, confluent cells (per biopsy) were needed hence prepared beforehand.

To establish the position of DRAQ 7⁻ and DRAQ 7⁺ gates, each control (negative and positive controls) were divided into 2 eppendorf tubes; with and without DRAQ 7 staining

(Fig. 11). The other samples were resuspended in 100 μ l of the DRAQ 7 solution and incubated in the dark at room temperature for 15 minutes. The cells were analyzed by flow cytometry within one hour of staining.

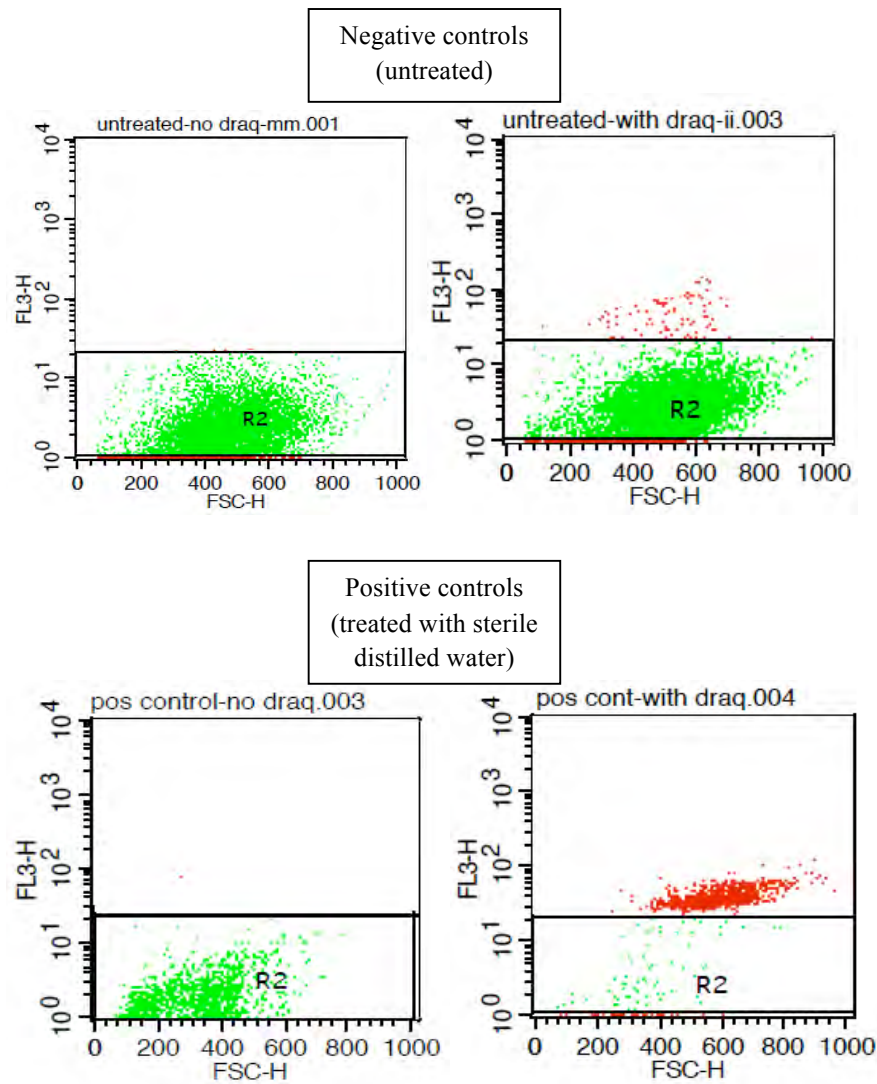


Figure 11: Gating method in the DRAQ7 cell viability assay using controls as to establish the position of DRAQ7 positive and negative cells. This gating method is applied accordingly to each of the primary brain tumour cell cultures.

These cell viability assays were then used to determine the IC values of each micronutrient via the viability curve plotted. Subsequent assays, such as Annexin-V-Alexa fluor 647 assay for detection of apoptosis by flow cytometry, are contingent upon the concentration (the IC

values) determined primarily in the cell viability assay. This was to confirm whether the IC values determined is inducing apoptosis or complete cell death. Essentially for apoptosis assay, IC₇₅ is selected to be used for their detection in inducing apoptosis, as it will results to the least cytotoxic effect on the cells hence to see the apoptotic induction rather than necrotic event in the occurrence. Another subsequent assays that also contingent upon the IC values obtained include *in vitro* invasion and angiogenesis assays.

2.2.6 Cell characterization of primary brain tumour cells

2.2.6.1 Immunocytochemistry (ICC)

Primary brain tumour cells were grown (10,000 cells) on autoclaved glass coverslips in a 6-well plate in growth medium DMEM through equilibration with 5% CO₂ atmosphere in 37°C humidified incubator until it reached 80-90% in confluency prior to trypsinization. Further analysis was carried out under non-sterile conditions and included a negative control (in the absence of primary antibody), in duplicate.

Primary antibody was prepared in Hanks Balance Salt Solution (HBSS -Sigma) or PBS according to manufacturer instructions (Table 2). Secondary antibody-biotin conjugated (developed in rabbit, monoclonal, Sigma) of 1:100 dilution was also diluted in HBSS (Invitrogen) and the other two were Alexa fluor 488-Streptavidin conjugated (Invitrogen) and Propidium Iodide (Invitrogen), each in 1:100 dilution.

Alexa fluor 488 that conjugated to a streptavidin is a fluorescence dye that is nearly identical to the spectral property and quantum yield of fluorescein isothiocyanate (FITC). It has brighter and more photo-stable conjugates with excitation and emission of 495 and 519nm respectively. Alexa fluor-488 enables superior photostability in comparison with FITC since it allows more time for image observation and capture, permitting greater

sensitivity. Streptavidin has a very high affinity for biotin, which commonly binds to variety of proteins and molecules such as the biotinylated secondary antibody used in the study. Therefore, the primary antibody that bound to the antigen on the cell surface can be detected via fluorescently labeled biotinylated secondary antibody.

Table 2: Working dilutions of the primary antibodies (*Abcam **Milipore ***Cancer Research UK

Primary antibodies (developed in mouse, monoclonal)	Working dilution
GFAP (Glial Fibrillary Acidic Protein) *	Used neat as pre-diluted (0.5µg/ml)
CD44 (Cluster Differentiation of 44)**	1:250 (0.4µg/ml)
Beta-1 integrin***	1:100 (1-10µg/ml)
NG2 (Neuron Glial 2) **	1:100 (20µg/ml)
GD3 (Gangliosides 3) **	1:250 (4µg/ml)

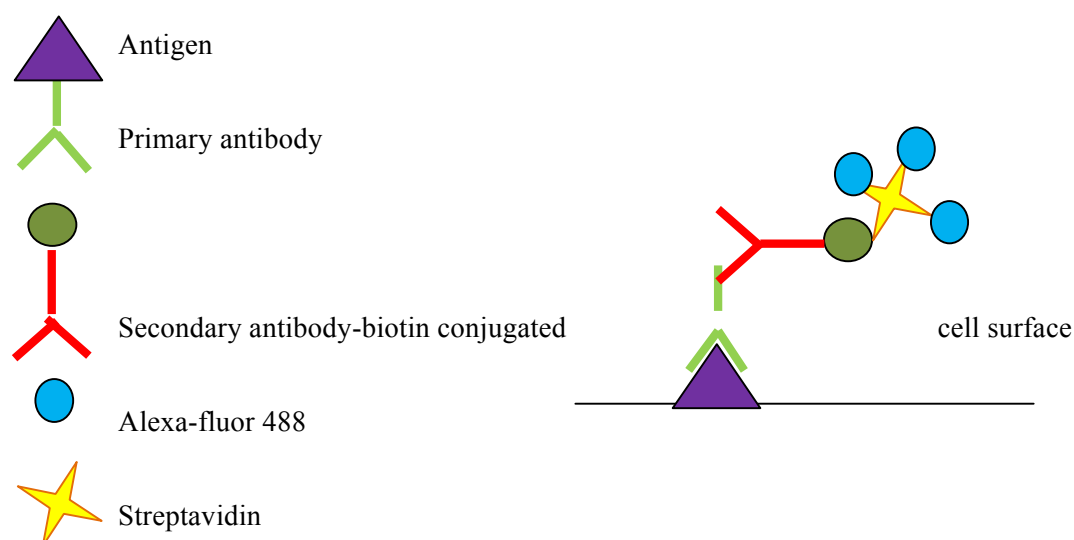


Figure 12: Immunocytochemistry reaction using labelled secondary antibody (Alexa-Fluor 488-Streptavidin conjugated).

After aspirating the medium from the petri dish, the cells were washed with Hanks for 1 minute. For accessing cytoplasmic antigen such as GFAP, acid alcohol (1 part concentrated hydrochloric acid in 99 parts of 70% ethanol) was added initially and left for 2 minutes to make the cell membrane permeable, allowing the primary antibody to be accessible to the antigenic sites. 2 ml of anti-GFAP solution was added to the corresponding cells. Addition of acid-alcohol solution is not applied to cell surface antigens (CD44, Beta-1 integrin, NG2 and GD3) studied thus this procedure was omitted. For cell surface antigens, 2 ml of each primary antibody was added to each corresponding well but not to the negative control. All primary antibodies added were left for one hour incubation at room temperature prior to washes with Hanks.

Then they were incubated with 2ml of secondary antibody (biotin conjugated) for 30 minutes at room temperature followed by washing with Hanks (three times). 2 ml of Alexa fluor 488-Streptavidin was added to it and left to incubate for 15 minutes in the dark. In between secondary antibody and Alexa fluor 488-Streptavidin addition, washing with Hanks was carried out. Subsequently, 1ml of Propidium Iodide was added to each well for 10 seconds exactly followed by the addition of excess Hanks.

For cells that were stained with cell surface antibody, acid-alcohol was added and left for 2 minutes before washing 3 times in Hanks. Propidium iodide then was added to counterstain the nucleus red. Cells stained with GFAP antibody were also stained with propidium iodide for the same principle. The cells were then washed with Hanks (three times for one minute each). Next, the coverslip was removed from each well and placed on a labeled glass slide prior to mounting with Citifluor (a mounting media), designed to reduce the fading (bleaching) of the fluorescence of fluorochromes. The slides were viewed under a confocal microscope (Leica TCS SP5) made together with control.

2.2.6.2 Flow cytometry

Primary brain tumour cultures were initially grown in 25cm² flask (Corning) until it reached 70-80% confluent, i.e 70,000 to 80,000 cells (37°C, 5% CO₂). Each primary brain tumour cell cultures were stained with four different antibodies investigated and this analysis was carried out in three sets of experiment in duplicate.

The cells were harvested by adding 1ml of Cell Dissociation Solution (CDS) for 10 minutes. CDS was used instead of trypsin as trypsin could damage the epitopes of the cell surface antigens. The cells suspension was centrifuged for 5 minutes at 800rpm. Following supernatant removal, the pellet was resuspended (in eppendorf tubes) in 100µl of primary antibody and incubated for 30minutes at room temperature.

The cells were then washed with PBS twice before resuspending in 100µl of secondary antibody-FITC conjugated (1:100 in PBS) and incubating for 30 minutes in the dark at room temperature. The cell suspension was transferred to FACS tubes. 50µl of Propidium Iodide at concentration of 50µg/ml was then added to the cell suspension prior to analysis. Simultaneously, the cell suspension that being aspirated for analysis was also undergoing statistical analysis carried out by Cell Quest Pro software.

For each antibody investigated, in order to differentiate the positive (M2) and negative (M1) sides of the histogram in the analysis, a negative control was also run alongside the other samples investigated in which primary antibody was omitted but secondary antibody-FITC conjugated was added (Fig 13).

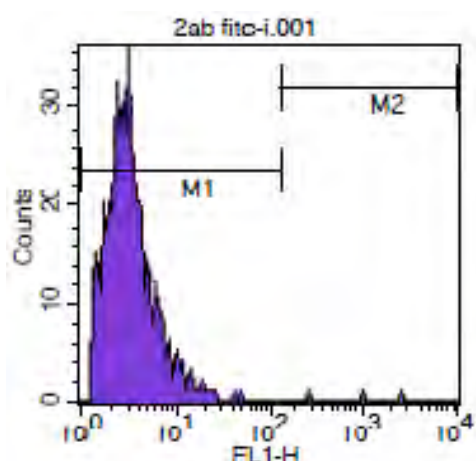


Figure 13: A histogram shows a negative control in the flow cytometry analysis in which the primary antibody was omitted leaving only secondary antibody (with biotin conjugated) being incubated. M2 will represent the positive stained cells while M1 is negative in staining.

In order to establish the positive control for each primary antibody studied, the cells that are known to be positive in its expression was sought to be analysed hence finding the optimal concentration to be used next, particularly for the primary brain tumour cells being investigated. For example, CD44 and Beta-1-integrin was known to be expressed by a breast cancer cell line, MCF-7 (Park et al 2006, Hiscox et al 2012) while MMP-14 and VEGF in U373 cells (Nuttal RK et al 2003, Feldkamp et al 1999), an established glioblastoma cell line.

The final concentration of primary antibody which prepared in PBS has been optimized initially. Each primary antibody was titrated using doubling dilutions (twofold) of the primary antibody and a standard number of cells ($\times 10^6$ in 100 μ l of buffer for each titration). Cells were stained with the isotype control or the primary antibody titrated separately, in which the concentration and conditions of both staining are the same. Isotype control used was the mouse IgG which acts as a reference population to estimate the non-specific binding (due to Fc receptor binding or other protein-protein interactions) of the primary antibodies to cell surface antigens. The optimal dilution chosen was based on the best separation between the isotype and the titrated antibody measured (the difference in the

fluorescence intensity) at a dilution point. A summary of concentrations used is tabulated in table 3.

Table 3: Working dilutions of the primary antibodies (Abcam).

Primary antibodies (monoclonal)	Working dilution
MMP-14 (Matrix metalloproteinase 14)	50µg/ml
CD44 (Cluster Differentiation of 44)	2.5µg/ml
Beta-1 integrin	10µg/ml
VEGF (Vascular Endothelial Growth Factor)	12.5µg/ml

2.2.7 *In vitro* invasion assay

Invasion assay *in vitro* by Albini et al (1987) has been widely used in the investigation of invasive capacity of most cancer cells which is based on the movement of cancer cells through a porous filter coated with Matrigel. BD Biocoat Fluoroblok invasion has made invasion assay *in vitro* easier and quantitative in the analysis.

The process of cellular invasion is comprised of distinct events which include attachment of cells into the basement membrane, secretion of enzymes which degrade the basement membrane and the migration of cells into the target tissue in response to specific chemotactic stimuli. Indeed, a similar system of invasion assay *in vitro* was applied in both invasion assay *in vitro* but with Fluoroblok system it is pre-coated with the Matrigel. This uniform layer of BD Matrigel Matrix serves as a reconstituted basement membrane *in vitro* providing a true barrier to non-invasive cells. BD Fluoroblok has a membrane which is

effectively blocks the passage of light from 490-700 nm. Indeed, fluorescently-labeled cells that have not invaded are not detected by a bottom-reading fluorescence plate reader.

Before use, each well in the invasion plate was rehydrated with 75µl serum free media for 2 hours (37°C, 5% CO₂). The cells were then incubated with DilC (a fluorescence dye that fluoresces inside the cells only) at 10µg/ml for 1 hour. HT1080 cells were used as the positive control and the invasive capacity of the untreated and IC₇₅ treated cells were compared. After 1 hour incubation with DilC dye, the cells were trypsinized and counted. After rehydration with the serum free medium, 25µl of serum free media were aspirated out. Then the cells were seeded on the Matrigel (12,500 cells in 25µl are needed for each insert) followed by addition of micronutrients studied. Finally, 200µl of chemoattractant (growth media at 5% fetal calf serum) was added to the base plate through the feeding hole next to the insert. The plate was incubated at 37°C, 5% CO₂ and read every 24hour with the plate reader at excitation of 450 and emission of 460 nm.

2.2.8 Apoptosis assay via flow cytometry analysis (Annexin V detection)

An important feature in apoptotic cells is the translocation of phosphatidylserine (PS) from the inner to the outer leaflet of the plasma membrane, exposing PS to the external cellular environment. Annexin-V is a Ca²⁺ dependent phospholipid binding-protein that has a high affinity with PS (Vermes et al., 1995).

Conjugation of Annexin-V with Alexa fluor 647, a fluorochrome, was used since it is a sensitive probe for flow cytometric analysis of cells that are undergoing apoptosis. Flow cytometers use separate fluorescence (FL) channels to detect light emitted. For example, Annexin-V Alexa fluor 647 conjugated (BD Biosciences) has maximal emission of 665nm which uses channel FL4 (FL4-H in the diagram) in the flow cytometer setup. Its staining

identifies early apoptosis PS externalization occurs at an early stage of apoptosis. Propidium iodide, with maximal emission of 617nm stains the nucleus of dead cells. This uses channel FL3 (FL3-H in the diagram) that represents late apoptosis. Thus, cells that are late in apoptosis will be positive in both Annexin-V and PI, while an early apoptotic event will be shown as positive for Annexin-V but negative for PI. For viable cells, Annexin-V and PI are both negative (Fig 14).

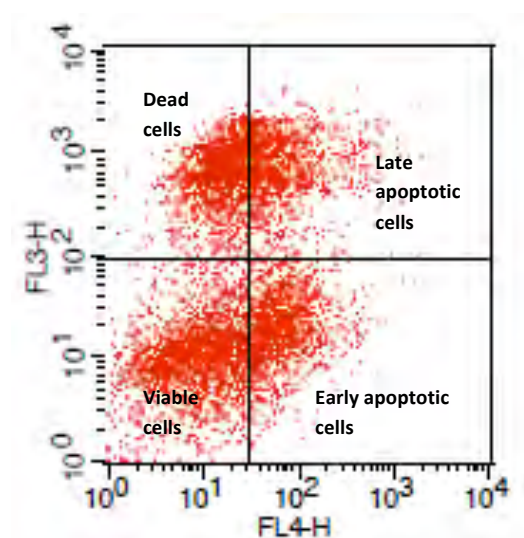


Figure 14: A quadrant in the Annexin V apoptosis. Each region in the quadrant i.e. lower right, lower left, upper right and upper left represents the population of cells. Axis with FL3-H indicates PI and axis with FL4-H indicates Annexin V.

Cells were incubated for 24, 48, 72 and 96 h with or without curcumin prior to analysis. The cells were harvested by adding 1ml of Cell Dissociation Solution (CDS) for 10 minutes. The cells suspension was centrifuged for 5 minutes at 800rpm. Following supernatant removal, the pellet was resuspended (in eppendorf tubes) in PBS for washing before resuspending in 5 μ l of Annexin-V-Alexa fluor-647 conjugated was added (prepared initially in 1x Annexin V binding buffer) and incubated at room temperature in the dark for 30 minutes. 50 μ l of Propidium Iodide at concentration of 50 μ g/ml was then added to the cell

suspension prior to analysis. A positive control for apoptosis used was staurosporine treated cells (1 μ M) in order to set up the quadrant of dead and live cells respectively.

2.2.9 *In vitro* angiogenesis assay (co-culture method)

Angiogenesis is a physiological process that occurs during wound healing and normal development which involves the growth of new blood vessels from pre-existing vessels. It is essential for normal growth and homeostasis yet can be altered in disease states with excessive or inadequate blood vessel occurrence (Kim and Lee, 2009). There are an abundance of angiogenesis assays available to screen various compounds in the analysis (exploiting the tubule formation of endothelial cells) but co-culture assay with the use of Matrigel (in transwell chamber) was selected to be carried out.

Following degradation of the capillary wall by extracellular proteinases, Human Umbilical Vein Endothelial Cells (HUVEC) respond to angiogenic factors secreted by the cancer cells prior to tubule formation. Starting with a branching point in the vessel wall, HUVEC cells will migrate into the extracellular matrix (ECM) towards the angiogenic stimulus, resulting in re-organization of endothelial cells to form tubules with a central lumen and hence a network (anastomosis).

Primary brain tumour cultures were harvested and seeded in 24-well plates in 500 μ l of DMEM with 20% foetal calf serum and 1% antibiotic (penicillin-streptomycin) at density of 100,000 cells per well. The physiological pH is maintained through equilibration with 5% CO₂ atmosphere in 37°C humidified incubator. Cells were incubated as to allow the cells to settle on the surface of the wells. Then, 8 μ m pore size inserts (Costar Corning, Netherlands) were coated with 100 μ l of undiluted (8-12mg/ml) Matrigel (Sigma) Matrigel is the extracellular matrix gel that prepared from Engelbreth-Holm Swarm (EHS) sarcoma

produced in mice and mainly contains laminin as a major component (Kleinman et al., 1993). Inserts were seeded with HUVEC at the cell density of 50,000 cells per insert in 300ul of HUVEC Complete Media which consisted of 2% fetal bovine serum, 0.1% of hydrocortisone and 0.2% each of penicillin and streptomycin, Epidermal Growth Factor (EGF) and heparin.

Matrigel coated inserts (which HUVEC were grown) were placed above the wells. Both negative (Suramin at 20µM) and positive (VEGF at 2ng/ml) controls were included. Suramin is an inhibitor of tubule formation while VEGF is act as a stimulant for it. Each concentration investigated was run in triplicate and experiments were repeated when necessary. This co-culture plate was incubated at 37°C for 6 to a maximum 16 hours as recommended by Becton Dickinson (BD Biocoat Angiogenesis Systems, 2006).

Medium was aspirated and each insert was then washed twice in PBS. HUVEC cells in the insert were fixed with 100% of methanol for 10 seconds and stained with crystal violet (1:1000 dilution in PBS) for 1 hour at 37°C. Six random fields of each insert were photographed under Ceti (10x10) microscope. Tubule networks were traced from these images using paint software. These were then analysed using Image J.

Image J software (Carpentier, Universite Paris Est) consists of segmentation of the cell areas followed by a skeletonization. Skeletonization includes the detection of pixels; extremities (one neighbor pixel), nodes (three neighbor pixels) and junctions (one or more nodes). Next, the pseudo vascular tree analysis was sorted into different pieces resulting to branches (pieces connected to one extremity, one node or junction) and segments (pieces connecting to two nodes or junctions). Once all the parameters read and analysed, all data obtained will be displayed and tabulated in an Excel (Microsoft). Of all the parameters measured, only four were taken into analysis which are mainly reported and representative in

angiogenesis analysis. Tubules that formed following curcumin treatment were quantified from the photograph captured and results were presented as mean and standard error of mean.

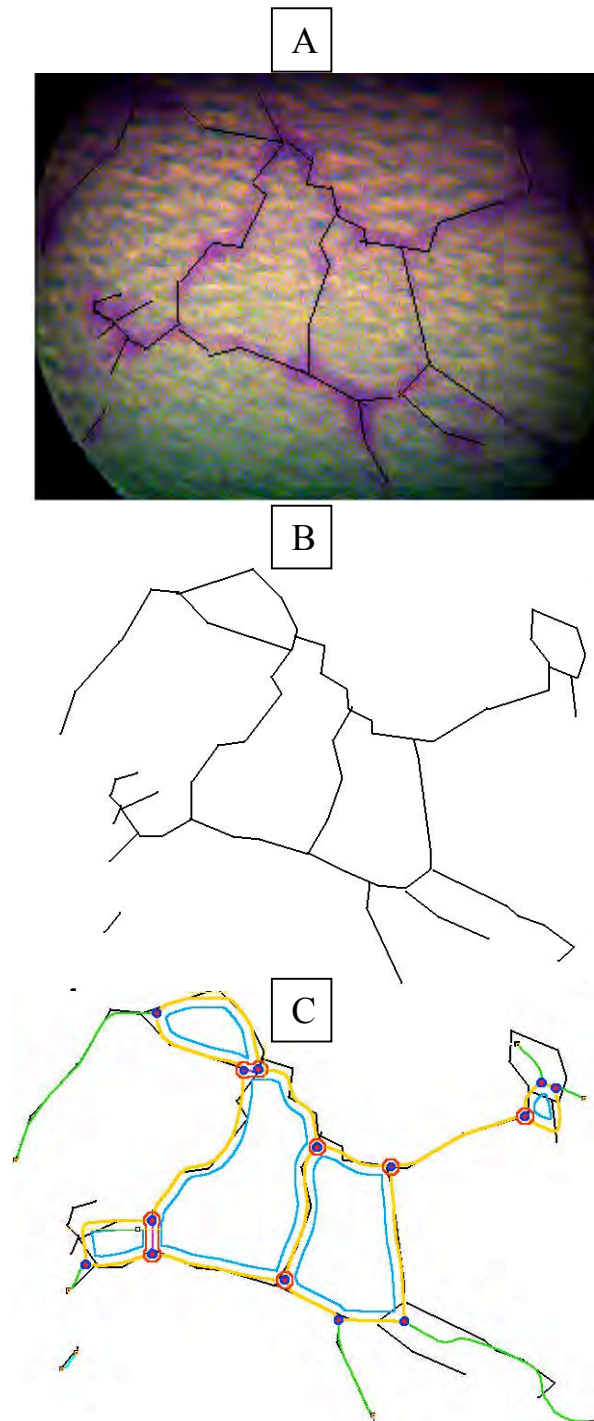


Figure 15: The tubule network traced with Paint software (A and B) before analysed using Image J software (C). With the image J software, each colour represents a parameter measured in the angiogenesis. The four parameters are total length of the tubules, node and junction (red in blue circle) and branches (green).

2.2.10 Statistical analysis

Statistical analysis was performed using Microsoft Excel 2007 and Minitab 16 to analyse the readings obtained from each assays being carried out; i.e. cell viability, flow cytometry, *in vitro* invasion and angiogenesis assays. One way ANOVA (Analysis of variation) was employed to determine whether differences exist among the means of the experimental data sets. If differences existed, 2 sample t-test analyses were carried out. *p* value obtained determined significance at value of <0.05 . Each concentration studied, either duplicate or triplicate (when required) was averaged. For cell viability, the mean value was then compared to the positive control (representing 100% cells that are viable as untreated) in order to get the percentage of residual viable cells (in cell viability assays). For flow cytometry analysis, Cell Quest Pro was used in order to get the data analysed and presented.

Chapter 3: Results

3.1 Morphology of primary brain tumour cell cultures

Glioblastoma multiforme is widely known for its characteristic of extensive heterogeneity not only at molecular but also at cellular levels, hence the word “multiforme”. Not only in brain tumours, this feature ascends in many types of other tumours which contribute to the general consequence of the malignancy such as tumour aggressiveness and creating hurdles for effective therapies to be achieved. Indeed, within the heterogenous cell population of glioblastoma, there are different sub populations of cells that respond differently towards the therapies (Bradford *et al*, 1997) hence surviving and growing in the tumour bed.

Morphological appearances of both the normal brain cell line and glioblastoma cell cultures were viewed and compared under phase contrast microscopy (200 x magnification). CC2565, the normal brain cell line was used as a control in this study (passage 10 and above) while the four primary cell cultures were glioblastoma-biopsy derived.

Each of the primary cell cultures showed some degree of heterogeneity. This is a feature of brain tumour cell cultures. Figures 16A-16E show the different population of cells within each cell line studied.

Normal brain cells (Fig 16A) showed less heterogeneity in the morphology with elongated spindle cells with few of small star shaped cells. MUBS cell primary cell culture was various in the shapes and cells size when it was not only comprised of small, large, star shaped cells but also some spindle shaped cells as indicated by the colour coded arrows in fig 16B. As with MUBP (Fig 16C) and MUP (Fig 16E) cell cultures, spindle, small and large star shaped cells were photographed by the phase contrast microscope. As indicated by the coloured arrows, MUTC cell culture was comprised with intermittently arranged of cells (Fig

16D) with a mixed morphology of spindle, small and large stars as well as broad, straight and blunt end shaped cells. Thus, based on the different cell morphology observed in a population of cells, it is suggested that in these primary cell cultures, they are more heterogenous in the morphology compared to the normal brain cells, CC2565.

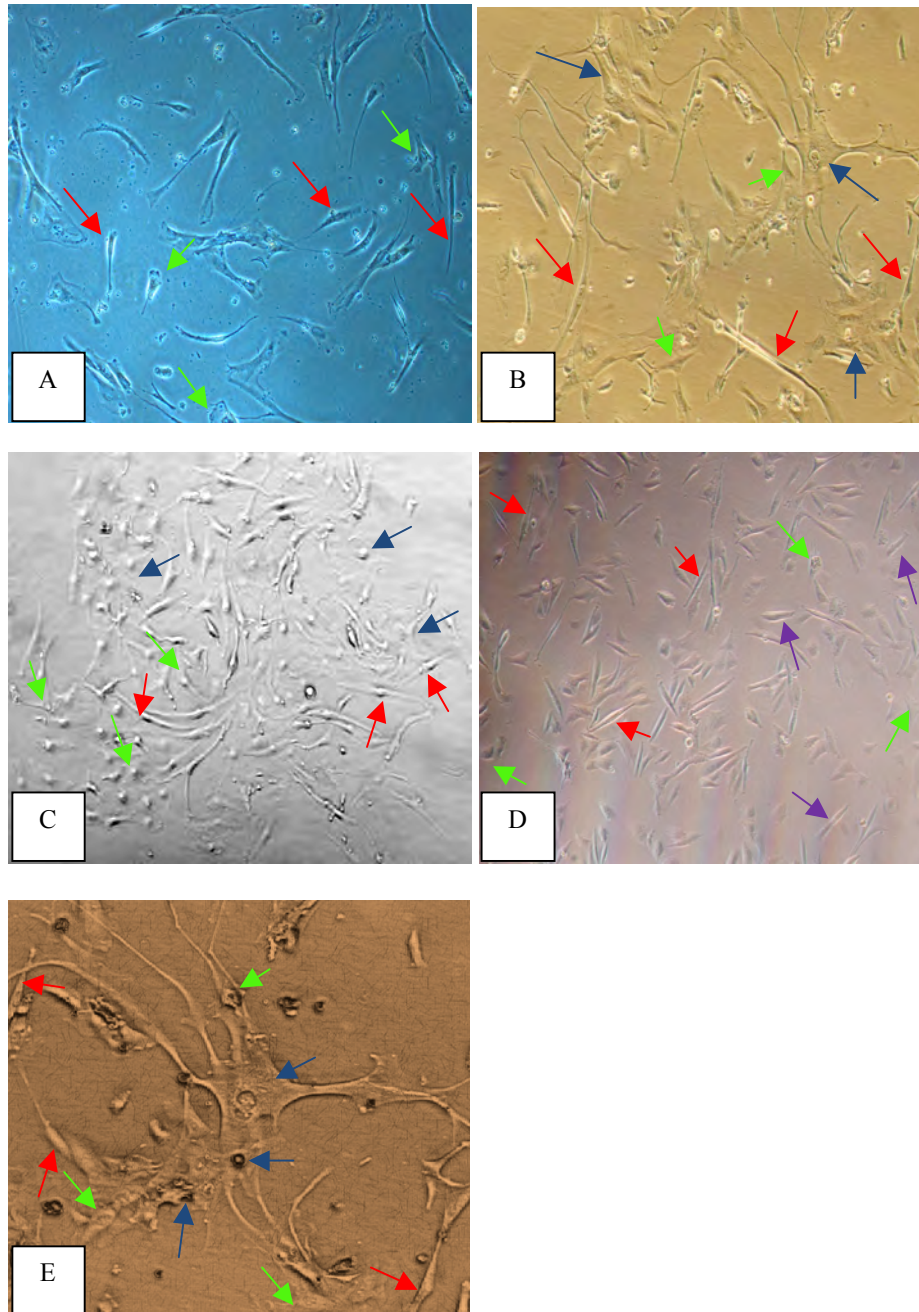


Figure 16: Phase contrast micrographs of the normal brain cell line; A) CC2565-passage 10 and primary brain tumour cell cultures (GB biopsy-derived); (B) MUBS-passage 6 (C) MUBP-passage 9 (D) MUTC-passage 8 and (E) MUP-passage 8. The different morphology of cells was shown by the colour coded arrows which include spindle (red), small star (green), large star (blue) and broad, straight and blunt end (purple) in shapes. All cell cultures were viewed and compared under phase contrast microscopy (20X magnification).

Below are the summary of the biopsy reports which were taken on the day the surgery was completed at Kings College Hospital at an appropriate procedure (as mentioned in the materials and methods chapter). Following surgeons' confirmation on Glioblastoma (grade IV), each biopsy was processed in Middlesex University in the tissue culture laboratory to generate a cell culture prior to be used in this study. See appendix for an example of the report (all details are confidential).

Designated Biopsy	Histology/Pathology details	Clinical details
MUBP	<ul style="list-style-type: none"> Multiple fragments of an extensive necrotic tumour. Hypercellularity with glial fibrillary background, increased mitotic activity and nuclear pleomorphism Endothelial hyperplasia with glomeruloid changes 	<ul style="list-style-type: none"> Headaches, confusion, 4 weeks of left sided weakness
MUP	<ul style="list-style-type: none"> No deletion of 1p and 19q Showed areas of fibrillary astrocytes and gemistocytic astrocytes Necrosis and vascular hyperplasia seen 	<ul style="list-style-type: none"> Not mentioned
MUBS	<ul style="list-style-type: none"> Pleomorphic cells seen Occasional giant cells and mitotic figures Cells with eosinophilic processes embedded within fibrillary background Florid vascular endothelial cell proliferation, necrotic areas with surrounding pseudopalisading of tumour cells 	<ul style="list-style-type: none"> Previously fit and well until experienced headache with incoordination of left side. Improve on steroids. MRI showed enhancement with gadolinium with central necrosis
MUTC	<ul style="list-style-type: none"> Pleomorphic, elongated, round nuclei, proliferation marker (Ki67) was expressed (35% of tumour cells) 	<ul style="list-style-type: none"> Not mentioned

Table 4: A summary of the pathology and histopathology details of all biopsies studied. These details were provided by Kings College Hospital at an appropriate procedure. For the purpose of record, each biopsy was designated to an acronym according to the patient's first and last names.

3.2 Population doubling time of primary brain tumour cell cultures

The doubling time of each cell culture was measured from the log phase of the growth curve using Doubling Time Calculator software (Roth, 2006). The PDT results obtained via Doubling Time Calculator software uses the same formula as in the principle of determining PDT in cells as described in section 2.24 in chapter 2. This was carried out during the log phase of the growth curve when the growth rate is constant, (see chapter 2, section 2.2.4). Each PDT of a primary brain tumour cells were compared to the normal brain cells.

Primary brain tumour cell cultures were relatively slow growing compared to the normal brain (40 hours) and established cell lines, as reported in two unpublished studies by other members (U373; PDT of 48 hours, IPSB-18; PDT of 16 hours). The PDT results ranged from 80 to 208 hours, in different cell cultures (Fig 17) and statistically analysed using One Way-ANOVA (with Fishers comparison) method as tabulated in table 5.

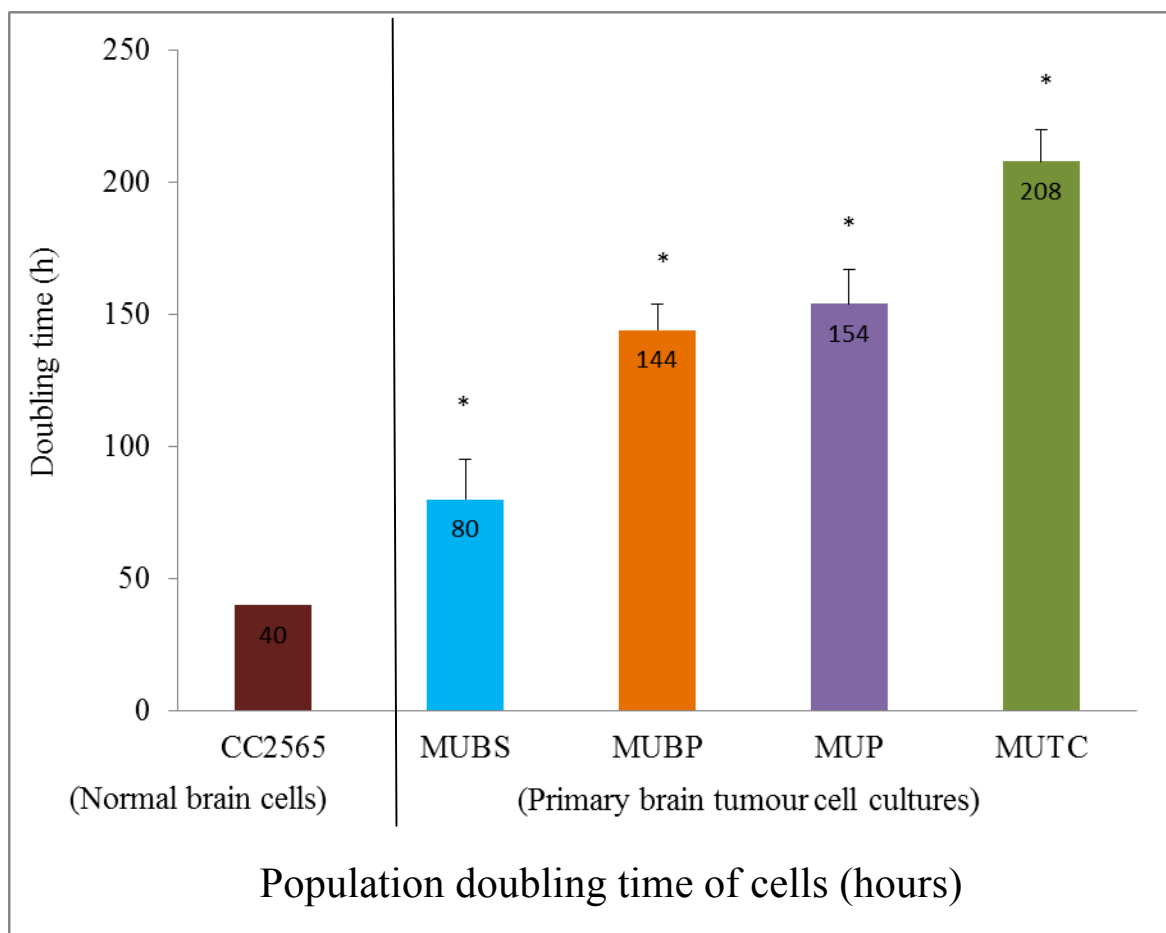


Figure 17: Population doubling time of each primary brain tumour cell cultures. The x and y axis represent the doubling time (h) and cell cultures, respectively. Standard error of the mean is represented by the error bars. Data represents the mean \pm standard error of the mean for $n=2$ experiments with each experiment being carried out in duplicate. Statistical analysis was carried out using a 2 sample t-test analysis to obtain the p value (each group of treated cells were compared with the normal brain cells). * $p<0.05$

Cell cultures	Mean	Standard deviation	Difference from control (95% CI)	P (vs control cell line)
CC2565 (control)	39.67	6.66	-	-
MUBS	80.00	38.5	40.3 (-18.9-99.6)	<0.05
MUBP	144.3	13.23	104.7 (45.4-163.9)	<0.05
MUP	154.3	45.0	114.7 (55.4-173.9)	<0.05
MUTC	208.3	39.7	168.7 (109.4-227.9)	<0.05

Table 5: Statistical analysis (One way-ANOVA-Fisher comparison) to show differences in doubling time between brain tumour cell cultures (MUBP, MUBS, MUP and MUTC). The doubling time ranged between 80 to 208h between primary brain tumour cell cultures studied (MUBS<MUBP<MUP<MUTC). Data showed that there are significant differences between the cell cultures studied with $p<0.05$

3.3 Dimethyl sulphoxide and Tetrahydrofuran cytotoxicity

Dimethyl sulphoxide (DMSO) and tetrahydrofuran (THF) are the organic solvents used to dissolve curcumin and lycopene respectively. In order to confirm that any cytotoxicity seen during experimentation is due to the effect of micronutrients rather than the solvents used, cell viability assays were carried out initially using DMSO and THF in the Calcein AM assay for cell viability. Different cells were used to test the toxicity of these 2 solvents, i.e. MUBS with DMSO and MUTC with THF. Due to limitation of the cells to grow in the same rate of doubling time, any cells that were readily confluent at the time were used as not all brain tumour cells samples were established at the same time.

Cell viability of a representative cell culture (MUBS) remained at 80 to 100% following treatment with DMSO for the range of concentrations used (Fig 18) at four different incubation periods (between 24 and 96 h), suggesting that DMSO is not cytotoxic to the cells at these concentrations. However, a decrease in cell viability was seen with DMSO at a concentration of 0.5% and higher. At the highest concentration used (3.84 %) cell viability was significantly decreased at each time point tested when compared to viability in the absence of DMSO.

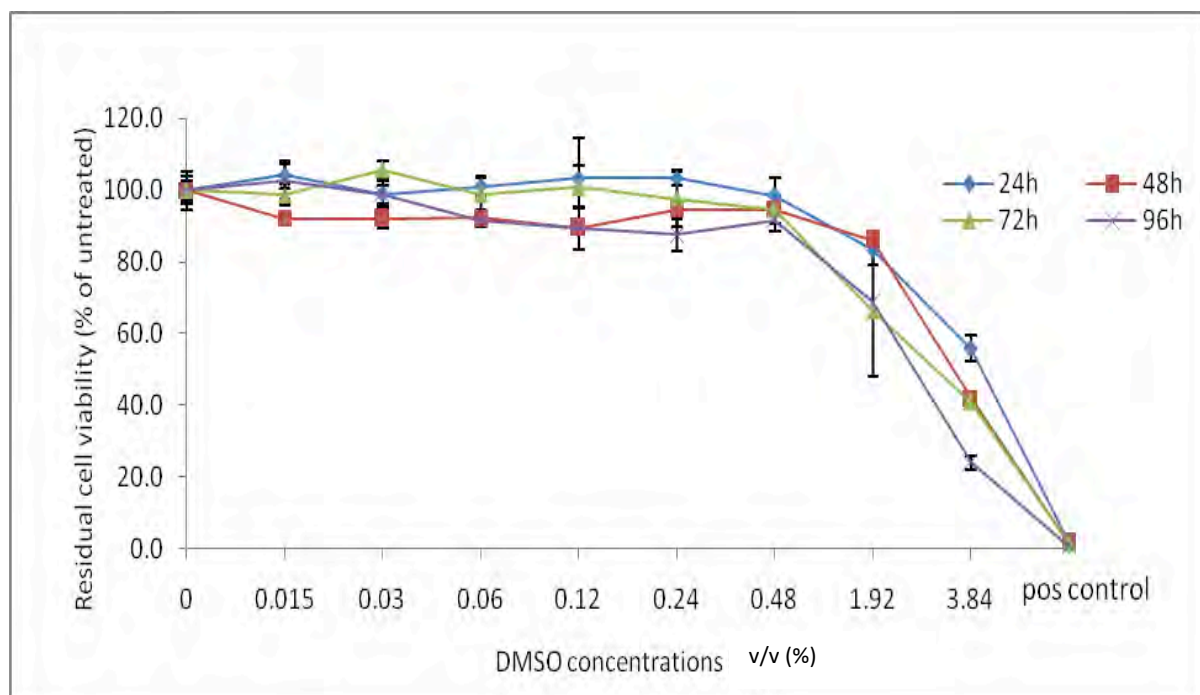


Figure 18: Cell viability of MUBS following treatment with DMSO at a range of concentrations at four different time points of incubation. DMSO is only cytotoxic to the primary brain tumour cell culture at a concentration of 0.5% and above. Residual cell viability is shown as a percentage of the untreated (control). Data represents the mean \pm standard error of the mean for $n=2$ experiments with each experiment being carried out in duplicate. (See chapter 2, section 2.2.5.1).

For determination of THF cytotoxicity to the cells, cell viability was again measured using the Calcein AM assay on the MUTC cell culture (Fig.19). A range of THF concentrations was used; (0.2 to 25.6%). It was found that above 0.2 % THF, cell viability decreased to about 80% of that seen in the absence of THF. This decrease was statistically significant at each time point measured ($p<0.05$), suggesting that THF is toxic to the cells at a concentration of 0.2% and higher. A further decrease in cell viability was seen at concentrations of 6.4% and above (figure 19) The final concentration of THF used in the assays was 4% due to the fact that it was the initial point to prepare the working concentrations yet to see if the same toxicity effect is demonstrated with the presence of LycoRed in the solution.

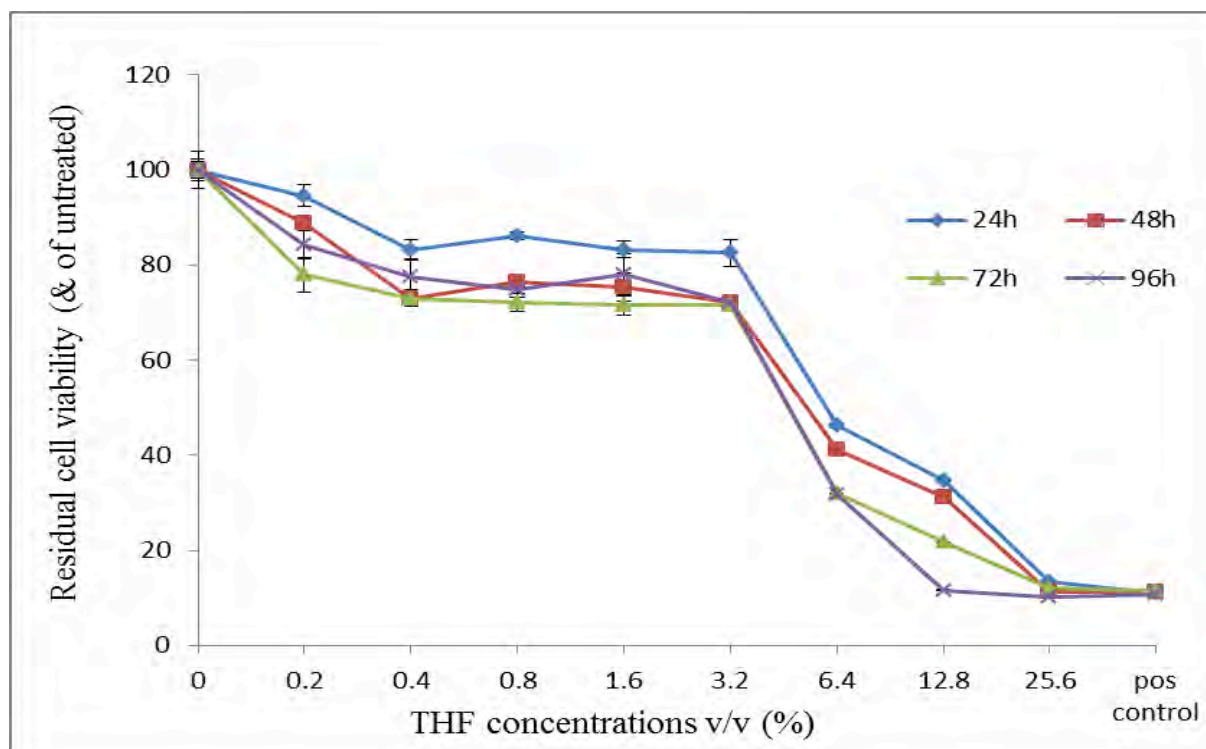


Figure 19: Cell viability of the MUTC cells following treatment with THF at a range of concentrations at four different time point of incubation. THF is cytotoxic to the cells above concentration of 0.2%. Residual cell viability is shown as a percentage of the untreated (control). Data represents the mean \pm standard error of the mean for $n=2$ experiments with each experiment being carried out in duplicate. (See chapter 2, section 2.2.5.1).

Thus, DMSO was used to dissolve curcumin (contained in the curcumin solution 0.3% DMSO) and THF for dissolving lycoRed (4% concentration of THF) in all further assays.

3.4 IC values of the Curcumin and LycoRed

The cytotoxicity of Curcumin or LycoRed was determined using a DRAQ 7 cell viability assay. Four different incubation periods were carried out (24, 48, 72 and 96 h) with the IC values (IC_{25} , IC_{50} and IC_{75}) determined at each time point.

In the normal brain cells (Fig 19A), curcumin effect on the cell viability at 5ng/ml is similar to the effect seen with 5 μ g/ml (cell viability remained at 90%). Higher concentrations of curcumin decreased the cell viability to 60 and 30% compared to the untreated cells (absence of curcumin). In figure 19A, the graph was plotted in a log scale due to the wide range of curcumin concentrations that studied (5ng/ml to 30 μ g/ml). Therefore, in order to

illustrate the effect of curcumin (wide range of concentrations) in normal brain cells, a log scale (x axis) has been chosen to demonstrate the cell viability graph (Fig 20A). Each log point represents a concentration of curcumin as showed in the graph. For example, as demonstrated in figure 20A, 0.7 at x axis represents 5ng/ml curcumin, 1.5 for 30ng/ml, 3.7 for 5000ng/ml (5 µg/ml), 4.2 for 15000ng/ml (15 µg/ml) and 4.5 for 30000ng/ml (30 µg/ml).

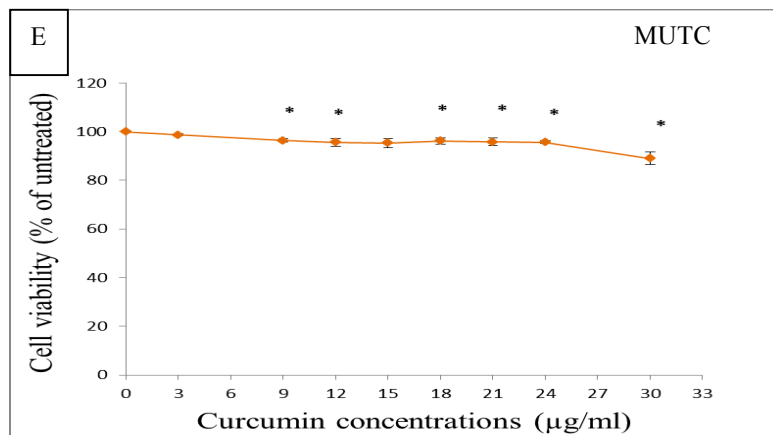
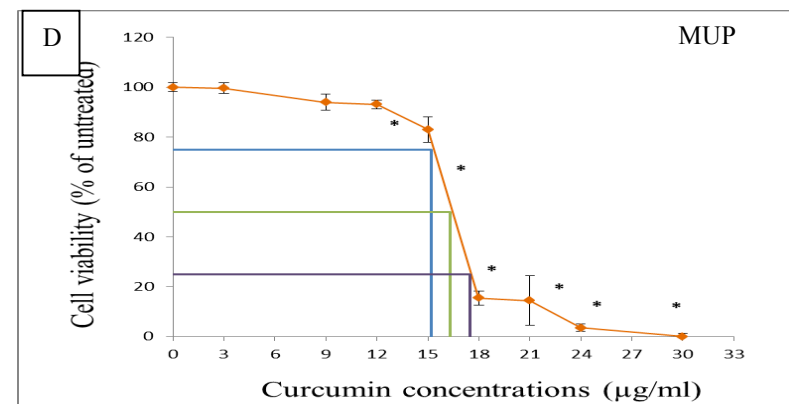
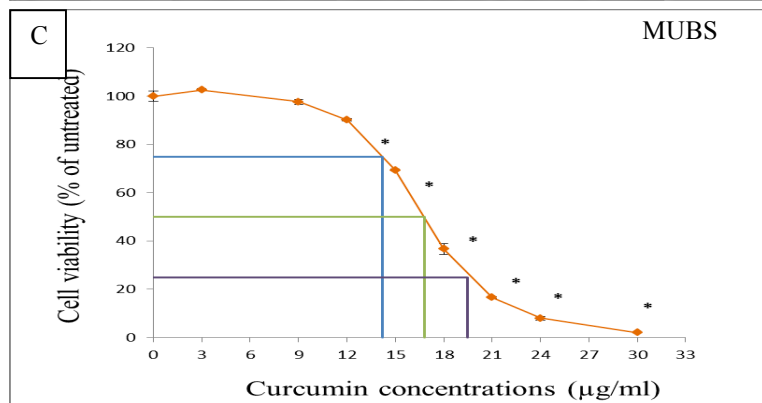
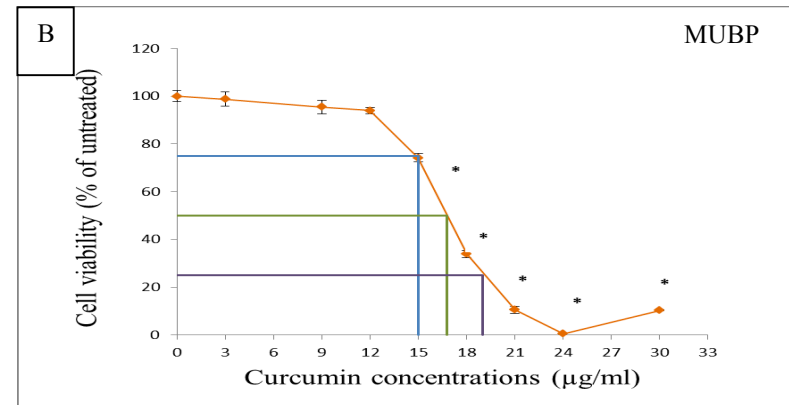
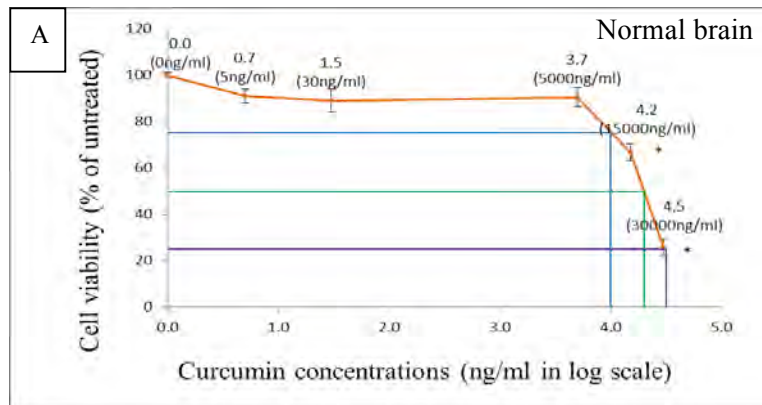
Incubation with curcumin has significantly decreased the cell viability of MUBP cells. Curcumin decreased the cell viability of MUBP cells by 50% at 16.8 µg/ml (Fig 20B). 19 µg/ml of curcumin has significantly decreased it further, leaving only 25% cells that are viable. Likewise, MUBS and MUP cell viability was also significantly decreased. The cell viability in MUBS primary cell cultures (Fig 20C) was decreased to 75% when treated with 14.2 µg/ml curcumin while 15.2 µg/ml in MUP cells (Fig 20D). However, with MUTC cells, the cells remain viable (95-100%) throughout the concentrations of curcumin studied which may reflected its resistance towards curcumin treatment.

The dose response curve plotted determined the IC values of each primary cell cultures studied. For example, the blue, green and purple arrow (Fig 20A-20D) indicated the IC₇₅, IC₅₀ and IC₂₅, respectively. MUBP cells have the IC values of 15, 16.8 and 19 µg/ml, each corresponds to the IC₇₅, IC₅₀ and IC₂₅, respectively (Fig 20B). MUBS cells have 14.2, 16.8 and 19.5 µg/ml while MUP cells with 15.2, 16.3 and 17.5 µg/ml for the respective IC₇₅, IC₅₀ and IC₂₅ values. These IC values were approximately similar among primary brain tumour cell cultures studied except with MUTC cells which were tabulated in table 4 as follows.

For each primary brain tumour cell cultures, no cytotoxicity was detected for LycoRed at any length of incubation. In addition, normal brain cells (CC2565) remained viable at all concentrations and incubation time (Fig. 20F) which suggested that LycoRed is

not toxic to normal brain cells. Hence no IC value could be detected for LycoRed in normal brain and all primary brain tumour cells (see Figure 20F-20J for indicative results).

Increasing the length of incubation had negligible impact on cell viability and therefore a single length of incubation is used to illustrate the findings. For each cell culture, all IC values were determined from the viability curve plotted and the results are shown in table 6. Thus, figure 20 (A-J) shows the cell viability of normal brain and primary brain tumour cell cultures, following 24 hours incubation with Curcumin or LycoRed.



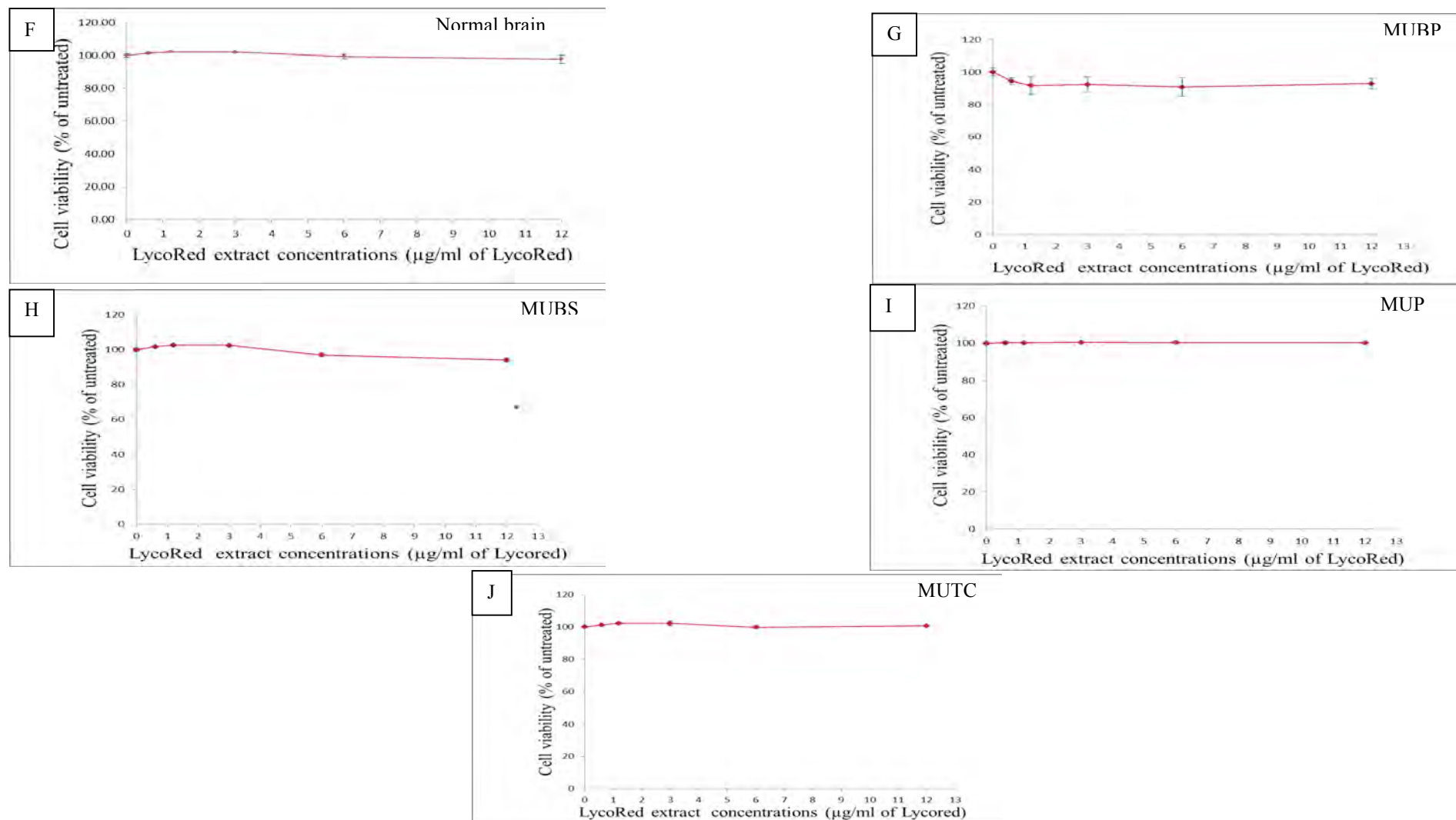


Figure 20 A-J: Percentage of live cells of each cell culture after 24hours treatment with Curcumin (A-E;yellow curves) or LycoRed (F-J;red curves). IC values are showed by the blue, green and purple lines representing IC₇₅, IC₅₀ and IC₂₅ respectively. Standard error of the mean is represented by the error bars. Data was taken from at least 3 sets of experiments in duplicate. Statistical analysis was carried out using a 2 sample t-test analysis to obtain the *p* value (each group of treated cells were compared with the untreated cells). * *p*<0.05. See chapter 2, section 2.2.5.2

Table 6: IC values of each cell culture after 24 hour incubation with Curcumin. IC values were similar for all primary brain tumour cell cultures with Curcumin. See chapter 2, section 2.2.5.2.

Cell cultures /IC values in µg/ml	Normal brain	MUBP	MUBS	MUP	MUTC
	Curcumin treated	Curcumin treated	Curcumin treated	Curcumin treated	Curcumin treated
IC ₇₅ (blue arrow)	10	15	14.2	15.2	ND
IC ₅₀ (green arrow)	20	16.8	16.8	16.3	ND
IC ₂₅ (purple arrow)	32	19	19.5	17.5	ND

ND=no detectable effect

Table 6 demonstrated that the IC values of curcumin were in the same range among primary brain tumour cell cultures studied. The IC values ranged from 14 to 19 $\mu\text{g/ml}$ (at 24 h of incubation) and addition of curcumin concentrations decreased the cell viability significantly. Due to the findings that there was no significant difference between IC_{75} and IC_{50} values, either one was chosen to be used in the following assays. The IC_{25} was rejected, as at this concentration incubation with curcumin led to significant cell death which might have resulted in cell loss before detection as early as 24 hour incubation. Hence, IC_{75} value obtained were used in subsequent analysis in the insight of it is lower in concentration to avoid less cell death which is useful particularly in compromising antigen detection experimentation.

3.5 Antigens expression in primary brain tumour cells

It is good to know the character of the tumour being sampled as to see their invasive, angiogenic and apoptotic potentials through the antigens expressed. The antigens expressed in each cell culture were studied by two methods; immunocytochemistry (qualitative) and flow cytometry (semi-quantitative). Expressions in primary brain tumour cell cultures were compared with the negative control, i.e. normal brain cell culture, CC2565. No specific positive control was used in this experiment as it is purely to compare the presence of these antigens in the tumour samples as opposed to the normal brain cells. In addition, the choices of antigens used were established previously by former brain tumour (associated to this study) researches thus expanding the finding in brain-tumour biopsy derived with the same setting of methodology. The experiments were repeated 3 times with each experiment being carried out in duplicate. See chapter 2, section 2.2.6.1 for immunocytochemistry and section 2.2.6.2 for flow cytometry methods.

3.5.1 Qualitative analysis of antigen expression using immunocytochemistry

The antigen expression of each cell culture was measured using immunocytochemistry (ICC). All cells were stained with each of the five antibodies followed by secondary antibody conjugated with Alexa fluor-488 for visualization showed by bright fluorescent green. Propidium iodide was applied to stain the nucleus of the cells, as showed by the bright red that fluoresced (see chapter 2 section 2.2.6.1). The 5 micrographs (A-F) in each (Figs 21 to 25) represent a primary brain tumour cell culture that was stained by 5 different antibodies as follows; A) GFAP B) GD3 C) NG2 D) CD44 E) Beta-1 integrin. A negative control (F) was also included where the primary antibody was omitted. Therefore, in the negative control, where the antibody was omitted, no Alexa fluor-488 but Propidium

iodide staining only was seen. The staining was quantified by scoring with respect to the staining intensity. All staining were compared to normal brain cells as showed in Table 7.

All cell cultures expressed GFAP, an establish marker of astrocytes, including normal brain cells, confirming that all primary brain tumour cell cultures being investigated are of astrocytic origin. Figure 21 shows normal brain cell culture (CC2565) stained with the five antibodies and a negative control (F). A high intensity of GFAP (A) staining, a marker of astrocytes was noted as well as significant CD44 (D) staining, while GD3 (B), NG2 (C) and Beta-1-integrin (E) were negligible in expression.

In comparison with normal brain cells, MUBS cell cultures (Fig 22) showed a slightly higher expression of CD44 (D). MUBS cells showed increased expression of NG2, CD44 and Beta-1-integrin compared to normal brain cells due to the higher in intensity of green fluorescence that observed in this population of cells hence suggesting that MUBS may have a high invasive capacity.

MUBP (Fig 23) and MUTC cell cultures (Fig 24) showed similar pattern of antigen expression compared with normal brain cells. The expression of CD44 (D) and NG2 (C) were slightly higher in intensity in MUBS cells than in normal brain cells which suggests the invasive and angiogenic potential of MUBS cell cultures.

MUP cells shown in figure 23 exhibited greater CD44 expression (D) than normal brain cells, but less GD3 (B) and Beta-1-integrin expression (E). In addition, NG2 expression was high which may indicate MUP cells are angiogenic and proliferative in the capacity.

The invasive, proliferative and angiogenic capacity of the primary brain tumour cell cultures are varied, demonstrated by the level of antigens that were expressed as compared with the normal brain cells. Each primary brain tumour cell culture may have either invasion or angiogenic potential or perhaps both due to the variation in the expression of CD44, Beta-1-integrin, GD3 and NG2.

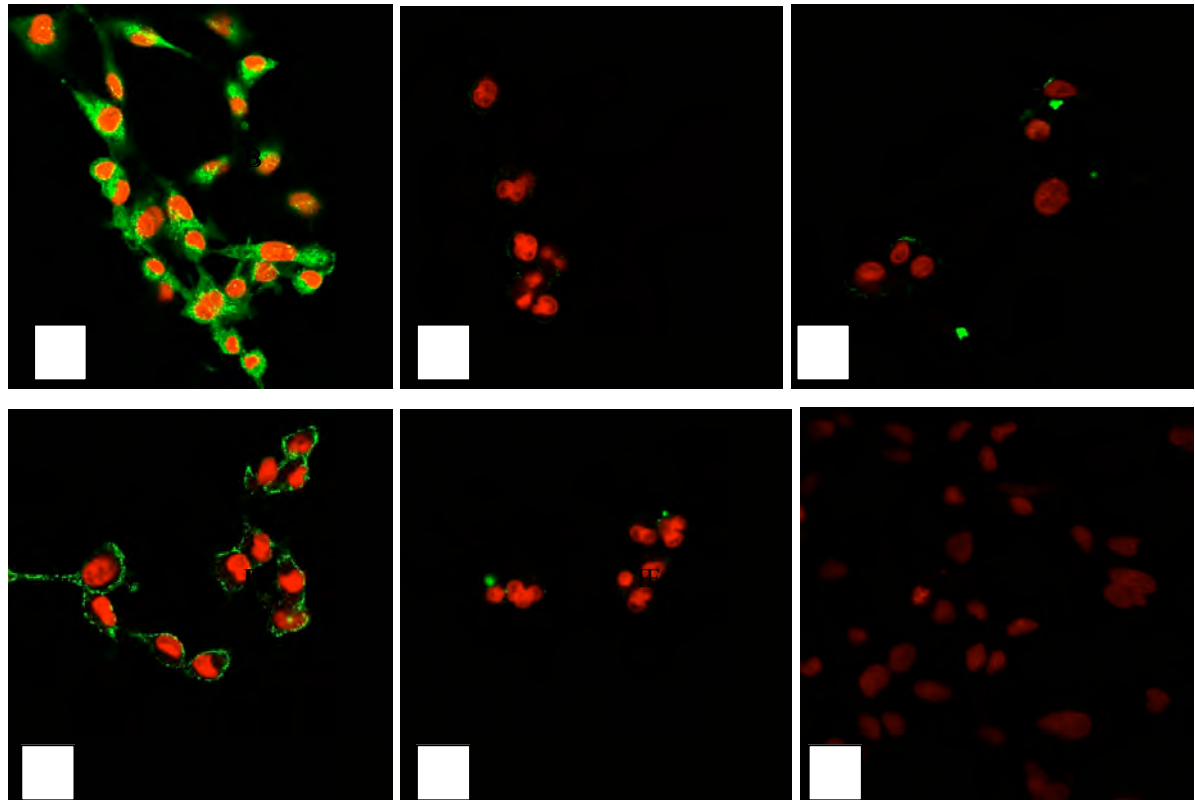


Figure 21: Antigen expression of CC2565 cell culture following staining with different antibodies via immunocytochemistry. A) GFAP B) GD3 C) NG2 D) CD44 E) Beta-1 integrin. F) Negative control.

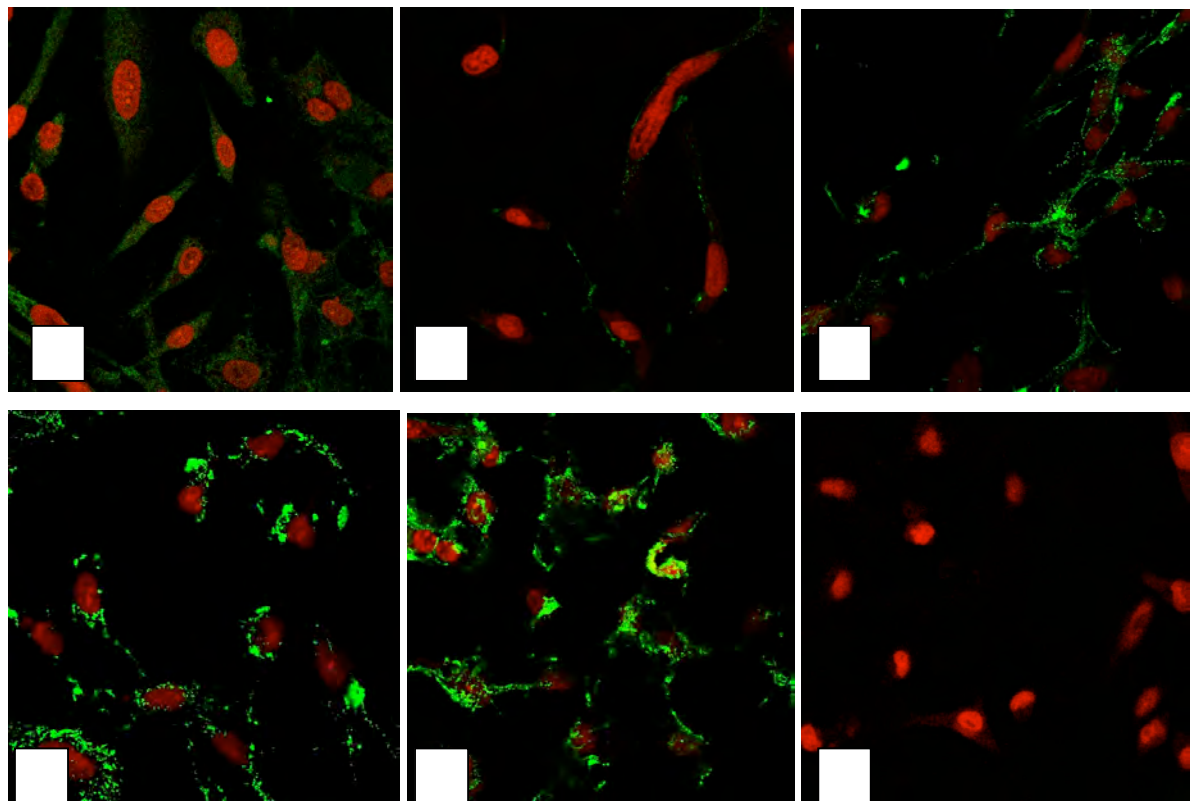
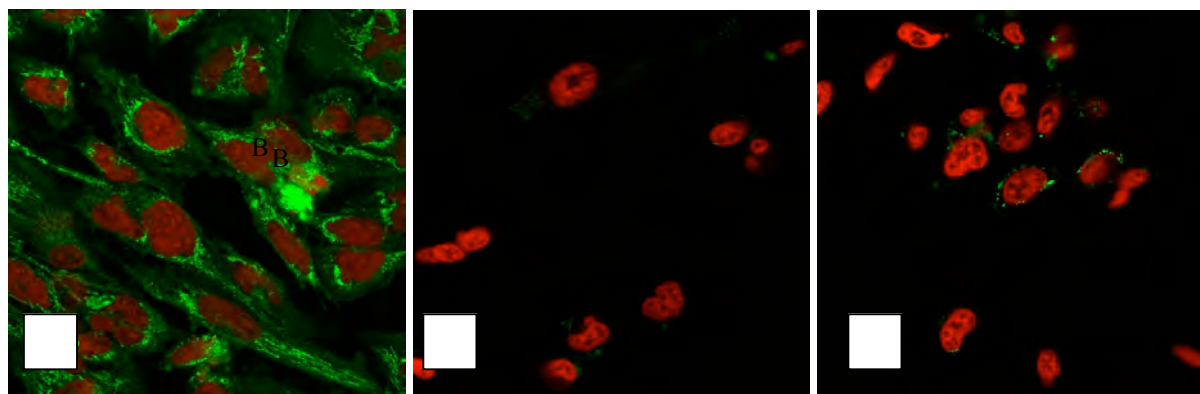


Figure 22: Antigen expression of MUBS cell culture following staining with different antibodies via immunocytochemistry. A) GFAP B) GD3 C) NG2 D) CD44 E) Beta-1 integrin. F) Negative control.

A



D

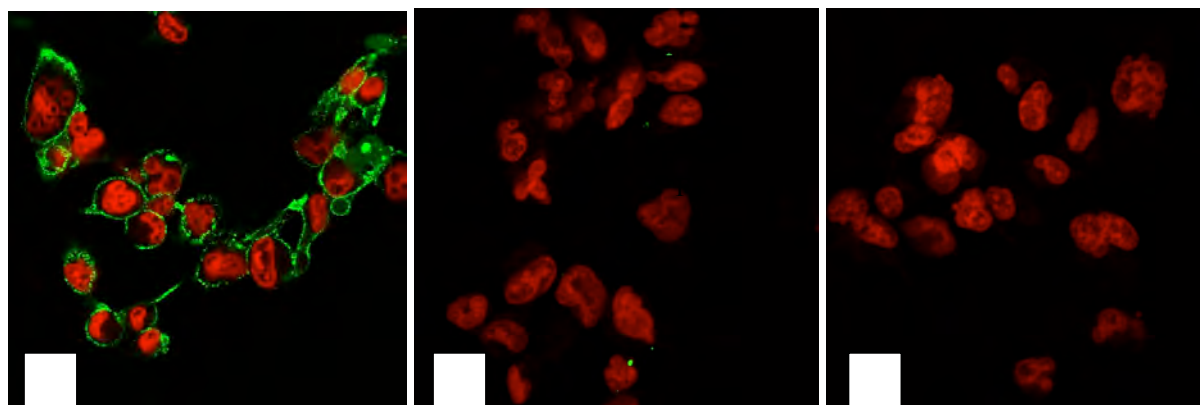


Figure 23: Antigen expression of MUBP cell culture following staining with different antibodies via immunocytochemistry. A) GFAP B) GD3 C) NG2 D) CD44 E) Beta-1 integrin. F) Negative control.

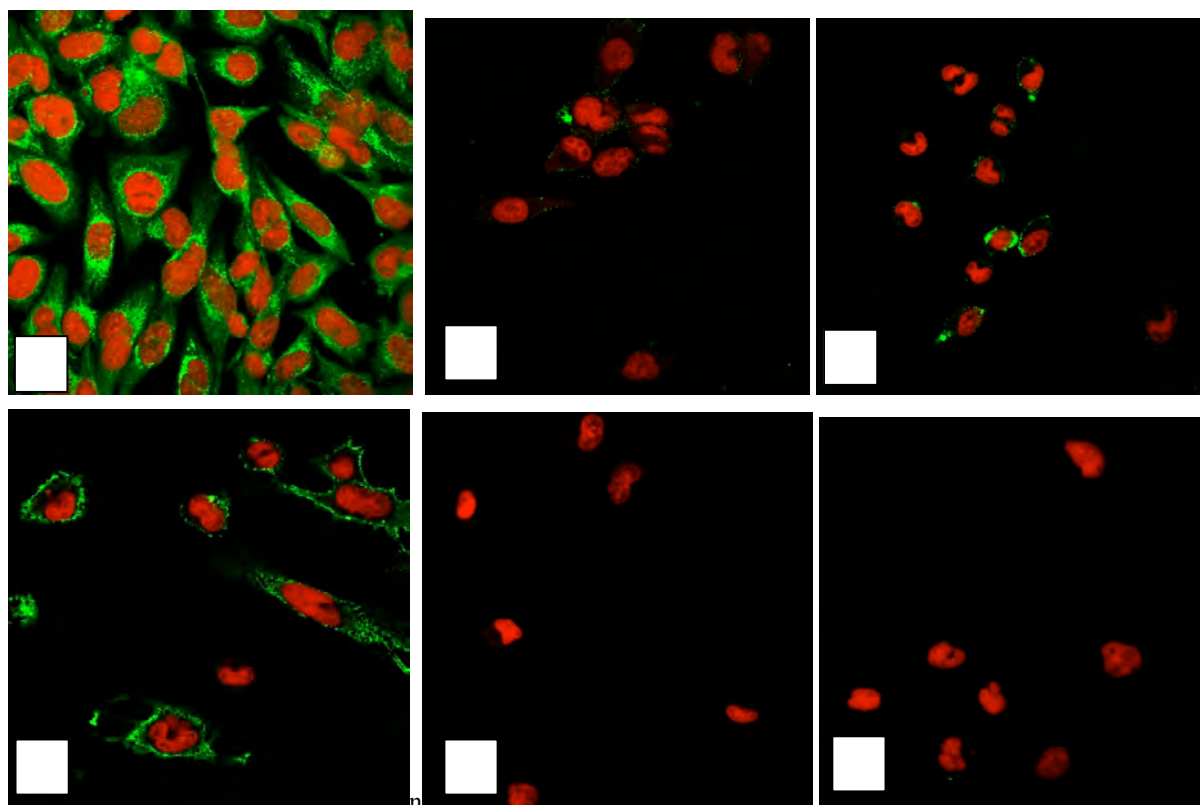
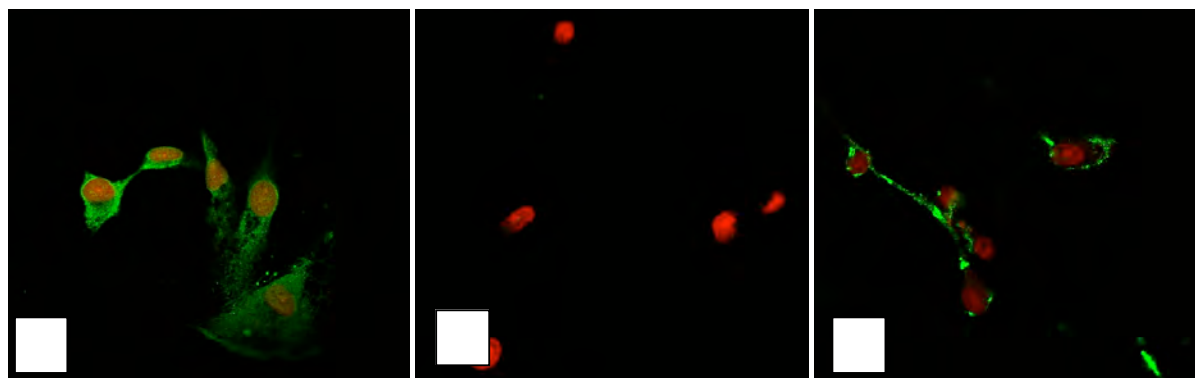


Figure 24: Antigen expression of MUTC cell culture following staining with different antibodies via immunocytochemistry. A) GFAP B) GD3 C) NG2 D) CD44 E) Beta-1 integrin. F) Negative control.

A



D

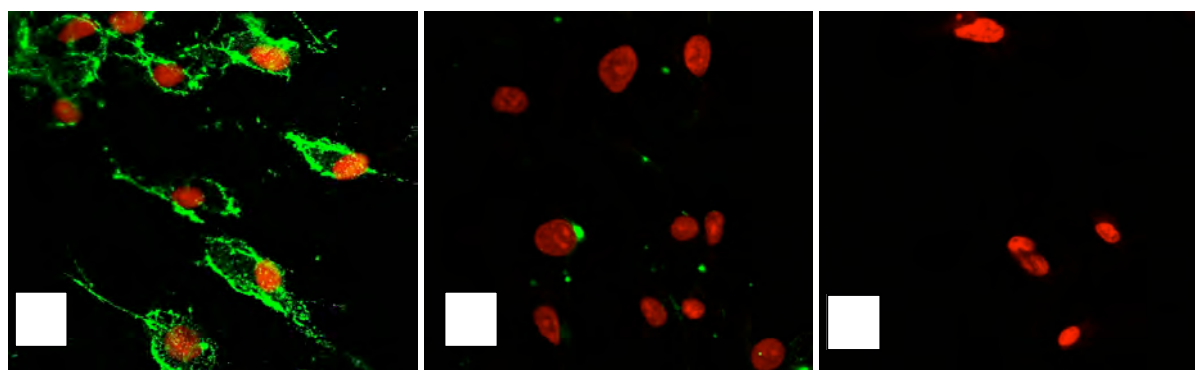


Figure 25: Antigen expression of MUP cell culture following staining with different antibodies via immunocytochemistry. A) GFAP B) GD3 C) NG2 D) CD44 E) Beta-1 integrin. F) Negative control.

Table 7: Summary of immunocytochemistry results (qualitative) for antigen expression in normal brain cells (CC2565) compared to primary brain tumour cultures (MUBS, MUBP, MUTC and MUP)

Antigens/Cell line	CC2565	MUBS	MUBP	MUTC	MUP
Beta-1-integrin	-	++	-	-	-
CD44	+	++	+	+	++
GD3	-	-	-	-	-
NG2	-	+	-	-	+
GFAP	+++	++	+++	+++	++
Negative control	-	-	-	-	-

+++ = strong positivity ++ = positive + = weak positivity - = negative

3.5.2 Quantitative analysis of antigen expression using flow cytometry

A semi quantitative analysis was carried out to determine the level of antigen expression in all primary brain tumour cell cultures investigated. Four antibodies were investigated; Beta-1-integrin, CD44, MMP-14 and VEGF. These antigens overexpression often associate in promoting invasion and angiogenesis in glioma as with most other cancers. For an example, MMP-14 was overexpressed in both primary cells and established cell line of glioblastoma by several studies (Fillmore et al., 2001; Hagemann et al., 2010; Hagemann et al., 2012). GD3 and NG2 were not able to be investigated due to time that constraint as well as not enough cells that were readily available at the time of investigation. Each primary brain tumour cell culture was stained with the respective antibodies (MUBP at passage 9-12; MUP at passage 8-14; MUBS at passage 6-9; MUTC at passage 8-10). To visualize the antibody stained, secondary antibody fluorescein isothiocyanate (FITC) conjugated was applied and the relative FITC intensity was measured by the bright green colour that fluoresced (see chapter 2 section 2.2.6.2). The results are summarised in figure 25a-c and table 8-11.

Markers of invasion in glioblastoma include Beta-1-integrin, MMP-14 and CD44. After 24h incubation, Beta-1-integrin was increased significantly in MUBP cells compared to control cells (normal brain cells) but lower levels were detected in other cell cultures studied (Fig 26a). However, no significant difference was noted in the level of expression between MUTC and normal brain cells. Using the ANOVA with Fisher post hoc test, mean value of Beta-1-integrin was significantly different among the 4 primary brain tumour cell cultures as well as when compared with the control cells but not between MUBS and MUP cell cultures with p value >0.05 (table 8).

After 24h incubation, when compared to normal brain cells (control), all three primary brain tumour cell cultures expressed significant levels of CD44 with p value <0.05 (Fig 26b) except for MUBS cells (via ANOVA with Fishers post hoc test in table 9) . The highest level

was detected in MUTC cells followed by MUP and MUBP cells. Further statistical analysis via Fishers comparison showed that the mean value of CD44 was significantly different among the primary brain tumour cell cultures studied but exclusively not between MUTC and MUP cell cultures with p value >0.05

MMP-14 (a membrane type MMP; MT1-MMP) is known to be highly expressed in glioblastoma. As one of the matrix metalloproteinases that degrades the extracellular matrix in infiltrating tumours it was surprising that a low level of MMP-14 was detected in three out of four cell cultures studied. Only MUTC cells expressed a high level of MMP-14 at approximately twice that of control cells (Fig 26c). As established via Fishers statistical analysis, the mean value of MMP-14 was significantly different among the primary brain tumour cell cultures studied except between MUBP and MUP cell cultures (table 10).

In addition to high level of MMP-14, MUTC cells also have much higher levels of VEGF than the other tumour cells studied. This was almost three times higher than the control cells but the level of expression was significantly lower in MUBS cell culture compared to normal brain cells (Fig 26d). However, the level of VEGF in MUBP and MUP cells was similar with the control cells. However, there was no statistically significance in VEGF mean values between MUBP and MUBS as well as between MUBP and MUP cell cultures due to their p value >0.05 (table 11).

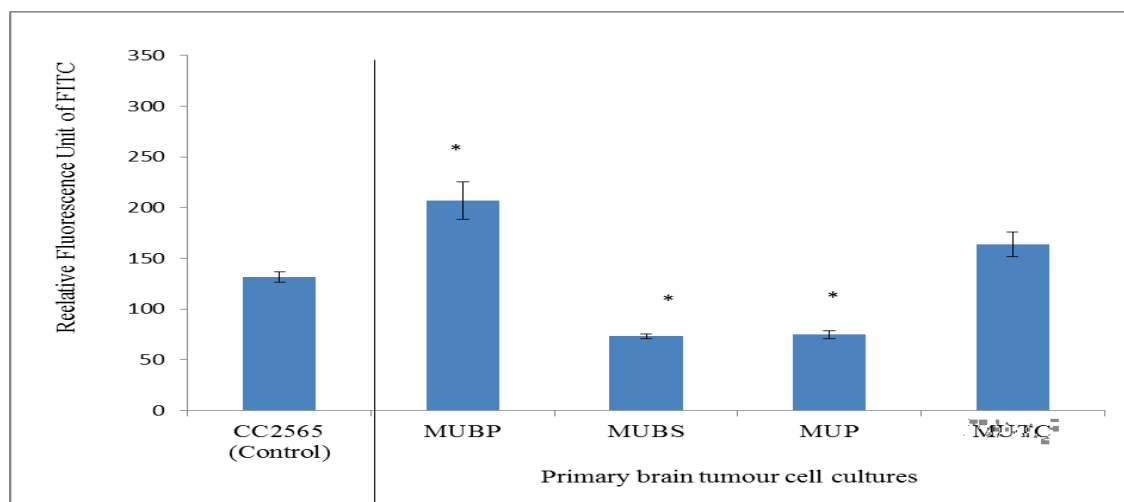


Figure 26a: The level of Beta-1-integrin expression in control and primary brain tumour cells following 24h incubation. All cells were stained with each of the four antibodies followed by a secondary antibody with FITC conjugated in order to enable the visualization. Standard error of means was represented by the error bars. Data was taken from at least 3 sets of experiments in duplicate. Statistical analysis was carried out with 2 sample t-test analysis to obtain the *p* value (* *p*<0.05) which is the value of each brain tumour cell culture compared with the control cells.

Cell cultures	Mean	Difference from cell culture (95% CI)				
		CC2565	MUBP	MUBS	MUP	MUTC
CC2565 (control)	131.55	-	75.5* (44.4-106.5)	58.3* (-89.3- [-27.2])	56.6* (-87.6- [-25.5])	32.1* (3.4-60.9)
MUBP	207.0	75.5*(44.4-106.5)	-	133.7*(-166.9-[-100.5])	132.1*(-165.3-[-98.8])	43.3*(-74.4-[-12.3])
MUBS	73.29	58.3*(-89.3- [-27.2])	133.7*(-166.9-[-100.5])	-	1.7(-31.5-34.9)	90.4*(59.3-121.5)
MUP	74.96	56.6*(-87.6- [-25.5])	132.1*(-165.3-[-98.8])	1.7(-31.5-34.9)	-	88.7*(57.6-119.8)
MUTC	163.7	32.1*(3.4-60.9)	43.3*(-74.4-[-12.3])	90.4*(59.3-121.5)	88.7*(57.6-119.8)	-

Table 8: Statistical analysis (One way-ANOVA-Fisher comparison) of each primary brain tumour cell culture against each other as well as against the control (after 24h incubation). The *p* value was denoted by* (*p*<0.05) indicated that the mean value for all cell cultures were statistically significant against each other cell culture (including when compared with the control) except for MUBS against MUP cell culture (each difference in mean value in bold has *p* value>0.05).

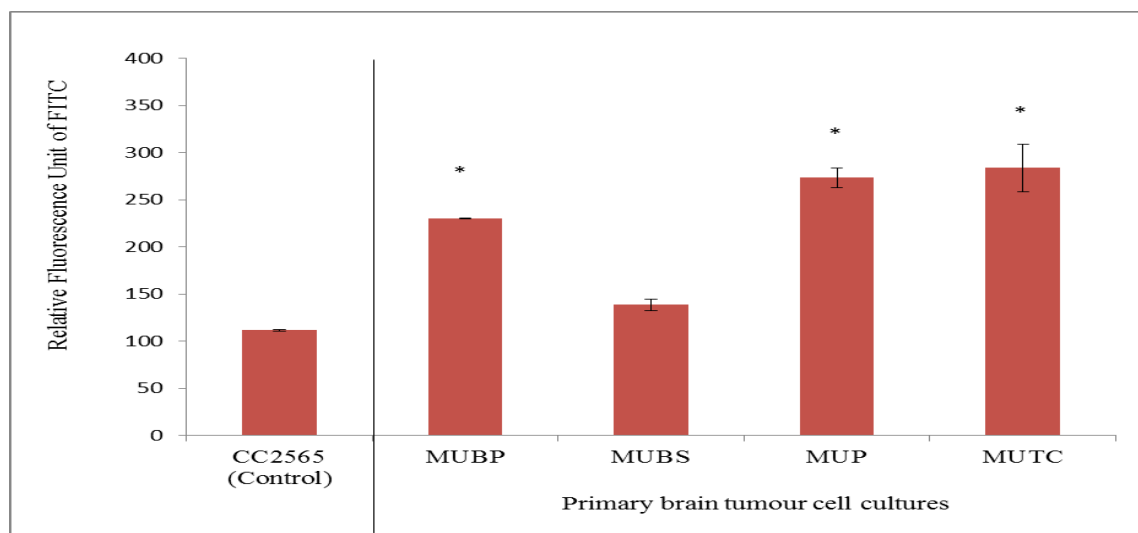


Figure 26b: The level of CD44 expression in control and primary brain tumour cells following 24h incubation. All cells were stained with each of the four antibodies followed by a secondary antibody with FITC conjugated in order to enable the visualization. Standard error of means was represented by the error bars. Data was taken from at least 3 sets of experiments in duplicate. Statistical analysis was carried out with 2 sample t-test analysis to obtain the p value (* $p<0.05$) which is the value of each brain tumour cell culture compared with the control cells.

Cell cultures	Mean	Difference from cell culture (95% CI)				
		CC2565	MUBP	MUBS	MUP	MUTC
CC2565 (control)	111.90*	-	118.2*(83.2-153.3)	26.6(-8.4-61.7)	161.5*(126.4-196.6)	171.9*(136.8-206.9)
MUBP	230.133*	118.2*(83.2-153.3)	-	91.6*(-129.1-[-54.1])	43.3*(5.8-80.8)	53.6*(16.1-91.1)
MUBS	138.53*	26.6(-8.4-61.7)	91.6*(-129.1-[-54.1])	-	134.9*(97.4-172.4)	145.2*(107.7-182.7)
MUP	273.4*	161.5*(126.4-196.6)	43.3*(5.8-80.8)	134.9*(97.4-172.4)	-	10.4(-27.1-47.9)
MUTC	283.8*	171.9*(136.8-206.9)	53.6*(16.1-91.1)	145.2*(107.7-182.7)	10.4(-27.1-47.9)	-

Table 9: Statistical analysis (One way-ANOVA-Fisher comparison) of each primary brain tumour cell culture against each other as well as against the control (after 24h incubation). The p value was denoted by* ($p<0.05$) indicated that the mean value for all cell cultures were statistically significant against each other cell culture (including when compared with the control) except for MUBS against control and MUTC against MUP cell culture (each difference in mean value in bold has p value >0.05)

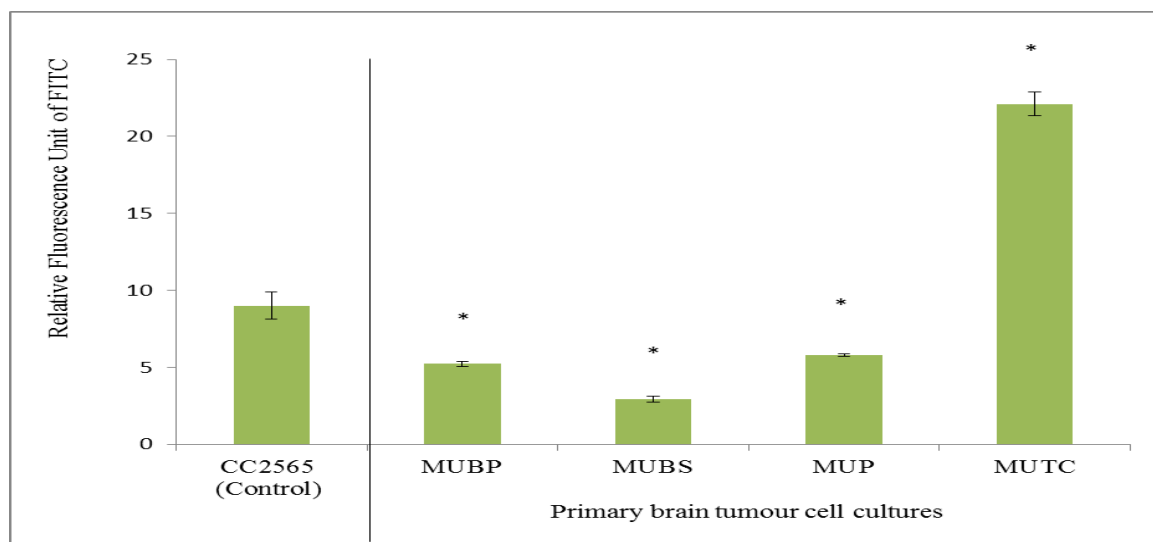


Figure 26c: The level of MMP-14 expression in control and primary brain tumour cells following 24h incubation. All cells were stained with each of the four antibodies followed by a secondary antibody with FITC conjugated in order to enable the visualization. Standard error of means was represented by the error bars. Data was taken from at least 3 sets of experiments in duplicate. Statistical analysis was carried out with 2 sample t-test analysis to obtain the *p* value (* $p < 0.05$) which is the value of each brain tumour cell culture compared with the control cells.

Cell cultures	Mean	Difference from cell culture (95% CI)				
		CC2565	MUBP	MUBS	MUP	MUTC
CC2565 (control)	9.008	-	3.793*(-5.417-[-2.168])	6.072*(-7.697-[-4.448])	3.230*(-4.855-[-1.605])	13.102*(11.478-14.727)
MUBP	5.215	3.793*(-5.417-[-2.168])	-	2.28*(-3.905-[-0.655])	0.562(-1.062-2.187)	16.895*(15.270-18.520)
MUBS	2.935	6.072*(-7.697-[-4.448])	2.28*(-3.905-[-0.655])	-	2.842*(1.218-4.467)	19.175*(17.550-20.800)
MUP	5.7775	3.230*(-4.855-[-1.605])	0.562(-1.062-2.187)	2.842*(1.218-4.467)	-	16.333*(14.708-17.957)
MUTC	22.110	13.102*(11.478-14.727)	16.895*(15.270-18.520)	19.175*(17.550-20.800)	16.333*(14.708-17.957)	-

Table 10: Statistical analysis (One way-ANOVA-Fisher comparison) of each primary brain tumour cell culture against each other as well as against the control (after 24h incubation). The *p* value was denoted by* ($p < 0.05$) indicated that the mean value for all cell cultures were statistically significant against each other cell culture (including when compared with the control) except for MUBP against MUP (each difference in mean value in bold has p value > 0.05).

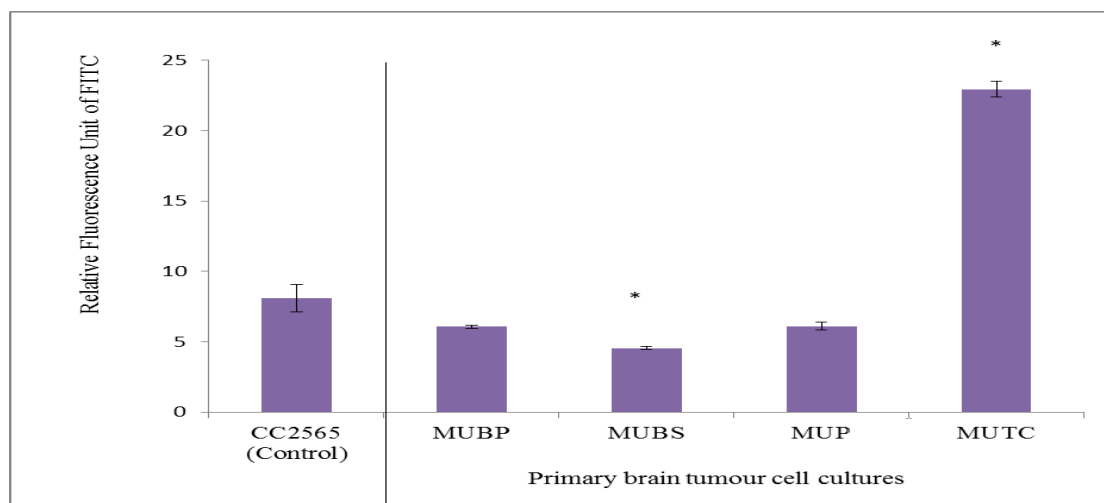


Figure 26d: The level of VEGF expression in control and primary brain tumour cells following 24h incubation. All cells were stained with each of the four antibodies followed by a secondary antibody with FITC conjugated in order to enable the visualization. Standard error of means was represented by the error bars. Data was taken from at least 3 sets of experiments in duplicate. Statistical analysis was carried out with 2 sample t-test analysis to obtain the *p* value (* *p*<0.05) which is the value of each brain tumour cell culture compared with the control cells.

Cell cultures	Mean	Difference from cell culture (95% CI)				
		CC2565	MUBP	MUBS	MUP	MUTC
CC2565 (control)	8.080*	-	2.005*(-3.591-[-0.419])	3.535*(-5.121-[-1.949])	1.975*(-.3561-[-0.389])	14.867*(13.282-16.453)
MUBP	6.075*	2.005*(-3.591-[-0.419])	-	1.53(-3.116-0.056)	0.03(-1.556-1.616)	16.872*(15.287-18.458)
MUBS	4.545*	3.535*(-5.121-[-1.949])	1.53(-3.116-0.056)	-	1.56(-0.026-3.146)	18.402*(16.817-19.988)
MUP	6.105*	1.975*(-.3561-[-0.389])	0.03(-1.556-1.616)	1.56(-0.026-3.146)	-	16.842*(15.257-18.428)
MUTC	22.947*	14.867*(13.282-16.453)	16.872*(15.287-18.458)	18.402*(16.817-19.988)	16.842*(15.257-18.428)	-

Table 11: Statistical analysis (One way-ANOVA-Fisher comparison) of each primary brain tumour cell culture against each other as well as against the control (after 24h incubation). The *p* value was denoted by* (*p*<0.05) indicated that the mean value for all cell cultures were statistically significant against each other cell culture (including when compared with the control) except for MUBP against MUBS and MUBP against MUP cells (each difference in mean value in bold has *p* value>0.05).

3.6 Curcumin anti-invasive property in primary brain tumour cells

Invasive potential of each primary brain tumour cell culture was measured using an *in vitro* 2 dimensional invasion assay (see chapter 2 section 2.2.7). The cells were stained with DilC, a fluorescence dye prior to seeding onto the wells of 96 well format plate. The intensity of the staining was measured by the fluorometric plate reader. A fibrosarcoma cell line, HT-1080, purchased from ATCC, was selected as a positive control for the invasion assay as it is known to be invasive. Normal brain cells were also included as a negative control (CC2565).

The invasive potential of the primary brain tumour cell cultures (MUBP, MUBS and MUP) were found to be significantly higher than in the normal brain cells (Fig 27). However, after 24 hour of curcumin treatment, there was a significant reduction of 13-16% in the invasive potential of these cells.

However, this was not observed in the MUTC cells in which the percentage of invasion was maintained at 30% after treatment with curcumin. It is of interest to note that of the four cancer cell cultures, this showed the lowest invasive potential in the absence of curcumin. This suggests that the MUTC cell culture may not show invasive potential and indeed, that the invasive potential may be lower than that of the normal brain cells.

With longer incubation periods of 48, 72 and 96 hours, all of the primary brain tumour cell cultures showed the same pattern of invasive potential with no changes seen in the reduction of invasion (data not shown). Thus, although the invasion data suggests that the level of invasive capacity present in these cell cultures varied, curcumin decreased the invasion to the same extent regardless of the cell cultures and length of incubation.

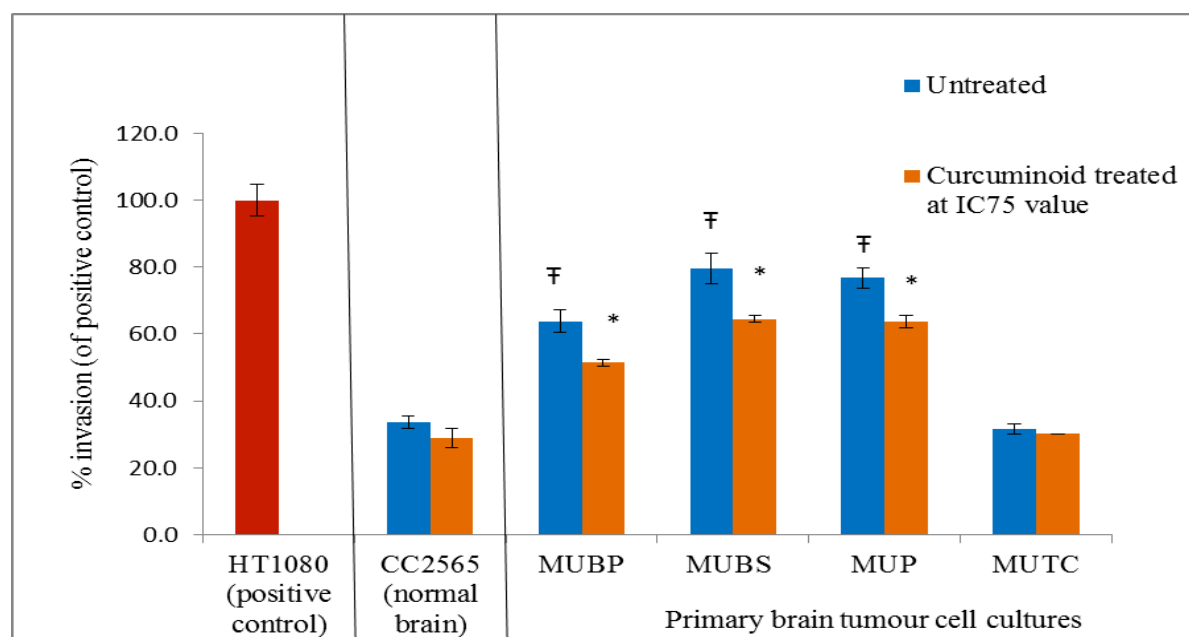


Figure 27: 2 Dimensional invasion assay *in vitro* showed the percentage of invasion of each cell culture after 24h incubation. Data represents the mean \pm standard error of mean for n=2 experiments with each experiment being carried out in duplicate. Data was taken from at least 2 sets of experiments in duplicate. Statistical analysis was carried out with 2 sample t-test analysis to obtain the *p* value (* $p < 0.05$). [‡] *p* value < 0.05 (significant different between untreated normal brain cells and untreated brain tumour cells). ^{*} *p* value < 0.05 (significant different between untreated and curcumin treated for each cell culture. Percentage of invasion is made by using HT1080 cells (positive control) that is known to be invasive, i.e. 100% invasion.

3.7 Curcumin as a pro-apoptotic agent

The apoptotic potential of curcumin was measured using Annexin V assay via flow cytometry. Apoptosis induces a variety of changes in the plasma cell membrane which includes permeability changes and membrane lipid alterations. Membrane lipid alterations occur when the phosphatidylserine residues are externalized; Annexin V has high affinity to these residues hence detected via flow cytometry.

Each primary brain tumour cells were treated with curcumin prior to staining with Annexin V which has Alexa fluor 647 (a bright green fluorescence dye) conjugated. Propidium iodide (bright red fluorescence dye) was also added to the staining to distinguish between viable and dead cells. The cells were gated into viable, early apoptotic and dead population of cells (see chapter 2 section 2.2.8). A positive control for apoptosis used was staurosporine treated cells (1 μ M) in order to set up the quadrant of dead and live cells respectively (the quadrants not shown here).

The following quadrants (Figs 28, 30, 32, 34, 36) represent population of cells gated after curcumin treatment at different time of incubation (24, 48, 72 and 96h). From the quadrants, four bar graphs showed each cell population; viable, early apoptotic, late apoptotic and necrotic cells, for each brain tumour cell cultures studied.

In the normal brain cells population, although early apoptotic cells population increased as the incubation time increased, this is negligible as only 3 to 8 % cells were gated. More than 40% of cells remained viable after 24 hour of incubation (figure 29) yet curcumin treatment at the IC₇₅ value improved the viability of normal brain cells, as demonstrated by the live cell population that was improved after 48 hour of incubation. This improvement was maintained after treatment throughout the incubation time studied, up to 96 hour. Normal brain cells were not significant in late apoptotic cells population only when the *p* value is more than 0.05 (fig 29, table 12c).

Among all primary brain tumour cell cultures investigated, MUTC cells showed significant amount of early apoptotic cells gated at 24h incubation (approximately 22%) before declined to 17% at 48h (Fig 37). This was not shown by other cell cultures studied as less than 12% of cells were gated following curcumin treatment as different hour of incubation (Figs. 31, 33, 35). However, for all brain tumour cell cultures studied, necrotic cells population gated were profound except for MUTC cells that were not significant (Fig 37, table 16d).

In addition, for most of the primary brain tumour cell cultures investigated, the cell viability remained between 40 to 60% and necrotic event was seen more than apoptotic occurrence. It could be suggested that the IC_{75} value of curcumin may have not cytotoxic enough in initiating the apoptotic occurrence in these primary brain tumour cell cultures. However, the remaining 40 to 60% were non-viable cells which are mainly composed of necrotic cells which may suggests that curcumin even at low concentration is already cytotoxic to the primary brain tumour cells.

Normal brain

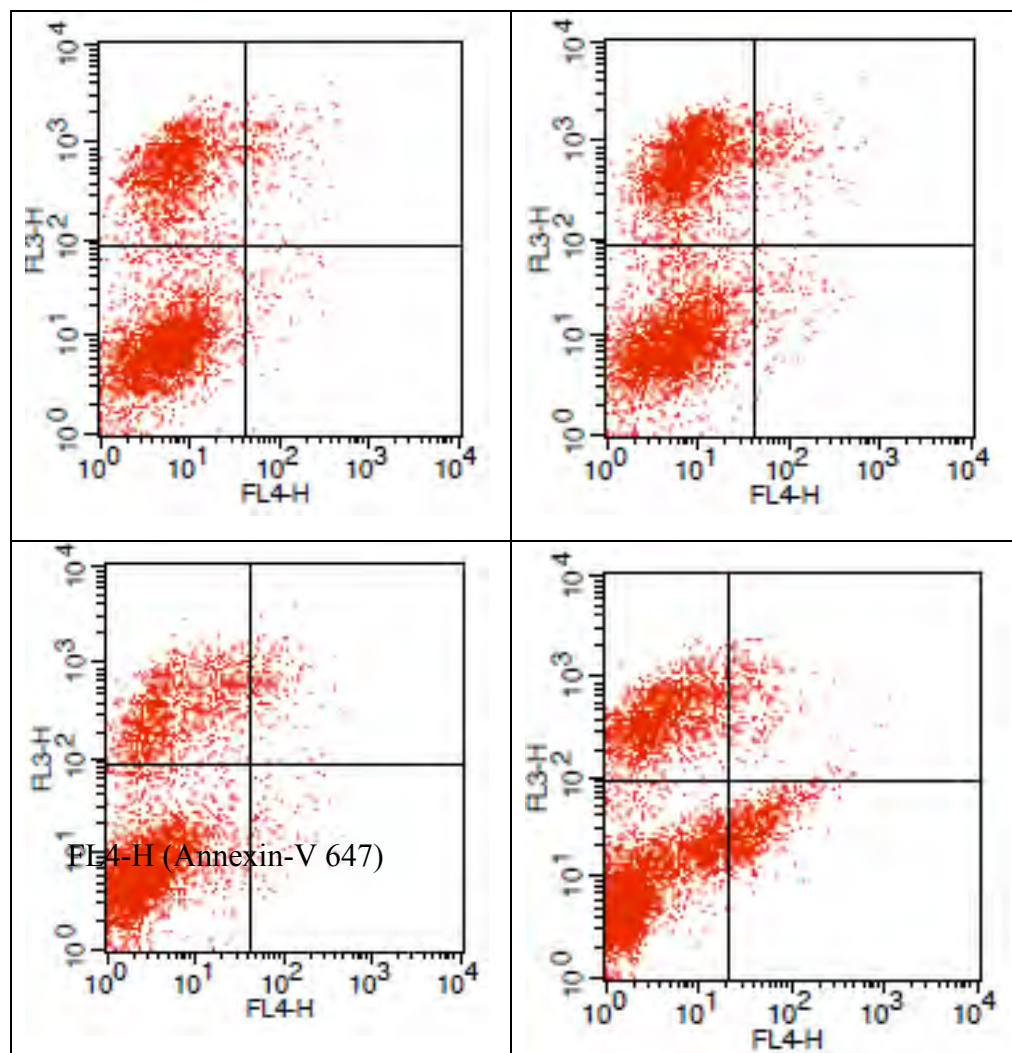


Figure 28 : Four representative diagrams from Annexin V apoptosis assay of normal brain cells at different hour of incubation (following curcumin treatment); 24h (upper left box), 48h (upper right box), 72h (lower left box) and 96h (lower right box). In a diagram, each quadrant represents viable cells (lower left), early apoptosis cells (lower right), late apoptotic cells (upper right) and necrotic cells (upper left). Percentage of cell gated in the quadrant is made by CellQuest software.

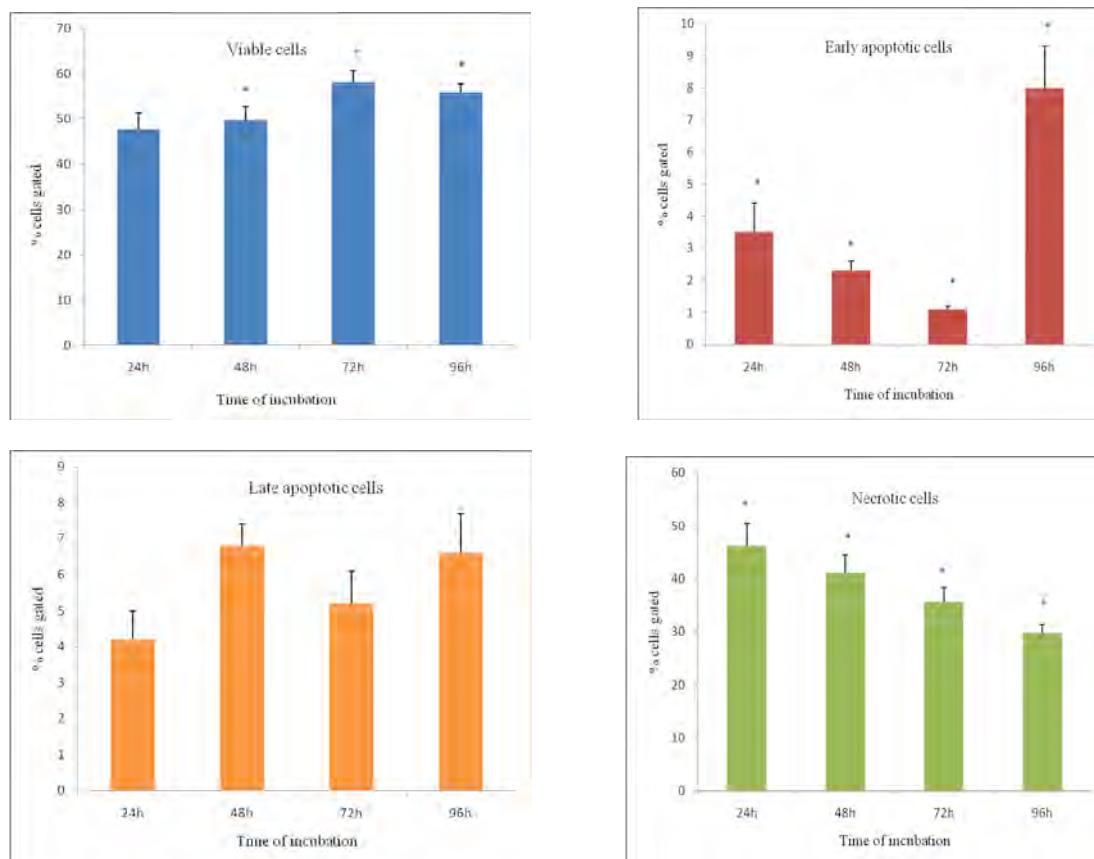


Figure 29: Normal brain cells population from each quadrant (viable, early apoptotic, late apoptotic, necrotic) of every incubation time (following curcumin treatment) are represented in a bar graph. Error bars show standard error of mean. Data represents the mean \pm standard error of mean for $n=3$ experiments with each experiment being carried out in duplicate. Percentage of cell gated was followed by statistical analysis (one way ANOVA-Fisher comparison) as to obtain the p value (* p value < 0.05) and tabulated as below.

a)Viable quadrants	Mean	Difference from time of incubation			
		24h	48h	72h	96h
24h	47.78	-	1.92 (-6.14-9.98)	10.27 (2.43-18.12)	8.02 (0.18-15.87)
48h	49.70	1.92 (-6.14-9.98)	-	8.35 (0.29-16.42)	6.11 (-1.95-14.17)
72h	58.05	10.27 (2.43-18.12)	8.35 (0.29-16.42)	-	-2.25 (-10.09-5.60)
96h	55.80	8.02 (0.18-15.87)	6.11 (-1.95-14.17)	-2.25 (-10.09-5.60)	-

b)Early apoptotic quadrants	Mean	Difference from time of incubation			
		24h	48h	72h	96h
24h	3.528	-	-1,190 (-3.3735-1.354)	-2.383 (-4.833-0.068)	4.427 (1.977-6.877)
48h	2.338	-1,190 (-3.3735-1.354)	-	-1.192 (-3.602-1.218)	5.617 (3.208-8.027)
72h	1.146	-2.383 (-4.833-0.068)	-1.192 (-3.602-1.218)	-	6.809 (4.499-9.120)
96h	7.955	4.427 (1.977-6.877)	5.617 (3.208-8.027)	6.809 (4.499-9.120)	-

c)Late apoptotic quadrants	Mean	Difference from time of incubation			
		24h	48h	72h	96h
24h	4.202	-	2.638 (0.28-5.149)	1.023 (-1.421-3.467)	2.349 (-0.095-4.793)
48h	6.841	2.638 (0.28-5.149)	-	-1.615 (-4.126-0.895)	-0.289 (-2.800-2.221)
72h	5.225	1.023 (-1.421-3.467)	-1.615 (-4.126-0.895)	-	1.326 (-1.118-3.770)
96h	6.551	2.349 (-0.095-4.793)	-0.289 (-2.800-2.221)	1.326 (-1.118-3.770)	-

d)Necrotic quadrants	Mean	Difference from time of incubation			
		24h	48h	72h	96h
24h	46.24	-	-5.15 (-14.15-3.85)	-10.66 [(-19.42-(-1.90))]	-16.55 [(-25.31-(-7.79))]
48h	41.09	-5.15 (-14.15-3.85)	-	-5.51 [(-14.51-3.49)]	-11.40 [(-20.40-(-2.40))]
72h	35.58	-10.66 [(-19.42-(-1.90))]	-5.51 [(-14.51-3.49)]	-	-5.89 (-14.65-2.87)
96h	29.69	-16.55 [(-25.31-(-7.79))]	-11.40 [(-20.40-(-2.40))]	-5.89 (-14.65-2.87)	-

Table 12(a-d) : Statistical analysis (One way-ANOVA-Fisher comparison) of % cells gated for all incubation time; 24h-48h-72h-96h (against each other) for every quadrant, i.e. a) viable, b)early apoptotic, c) late apoptotic and d) necrotic quadrant. The p value was denoted by* (p<0.05) indicated that the mean value for all incubation time were statistically significant against each. Each difference in mean value in bold showed that p value>0.05). Significant difference was noted between different incubation time studied in all quadrants except for late apoptotic cells quadrant.

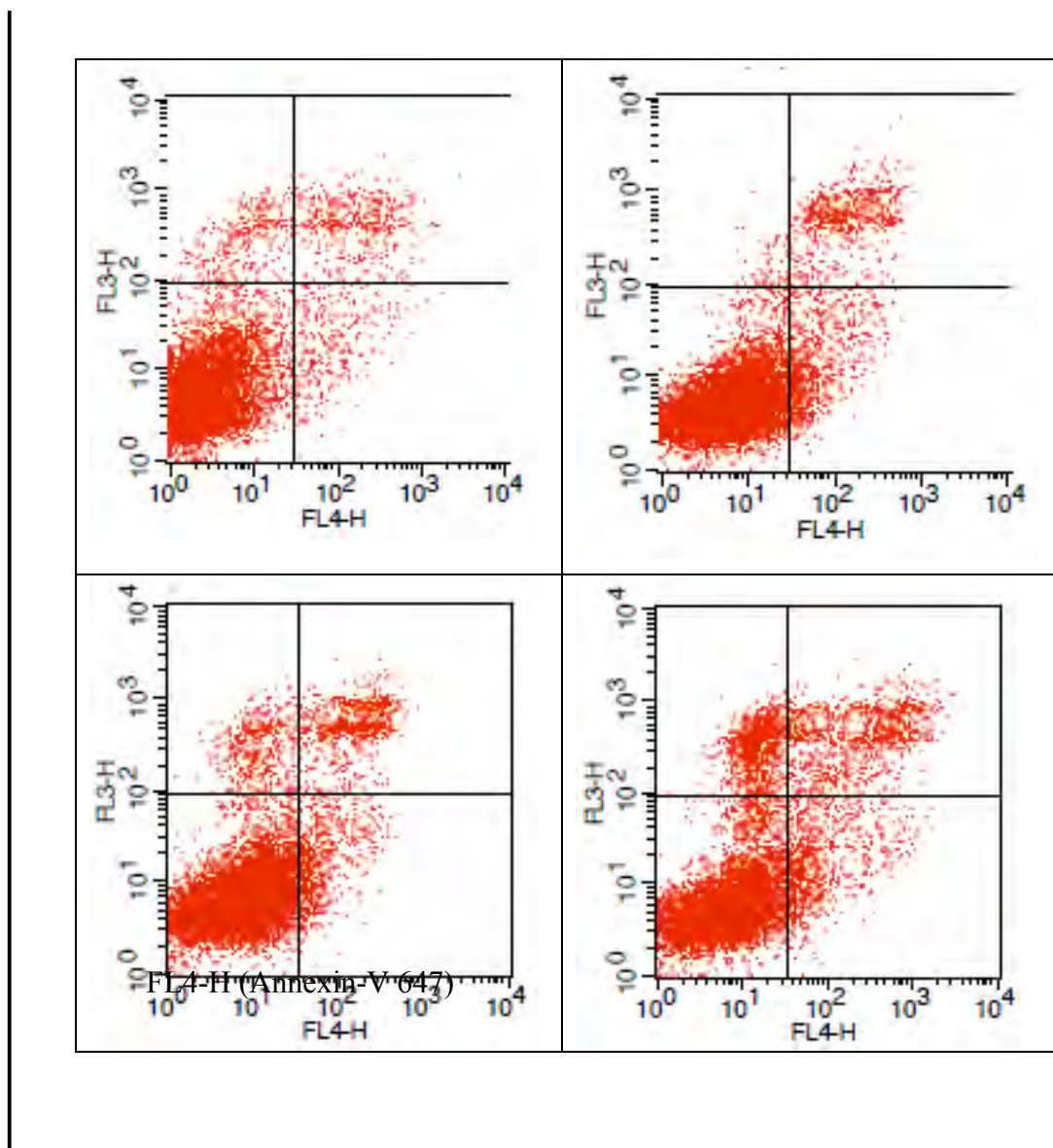


Figure 30 : Four representative diagrams from Annexin V apoptosis assay of MUBS cells at different hour of incubation (following curcumin treatment); 24h (upper left box), 48h (upper right box), 72h (lower left box) and 96h (lower right box). In a diagram, each quadrant represents viable cells (lower left), early apoptosis cells (lower right), late apoptotic cells (upper right) and necrotic cells (upper left). Percentage of cell gated in the quadrant is made by CellQuest software

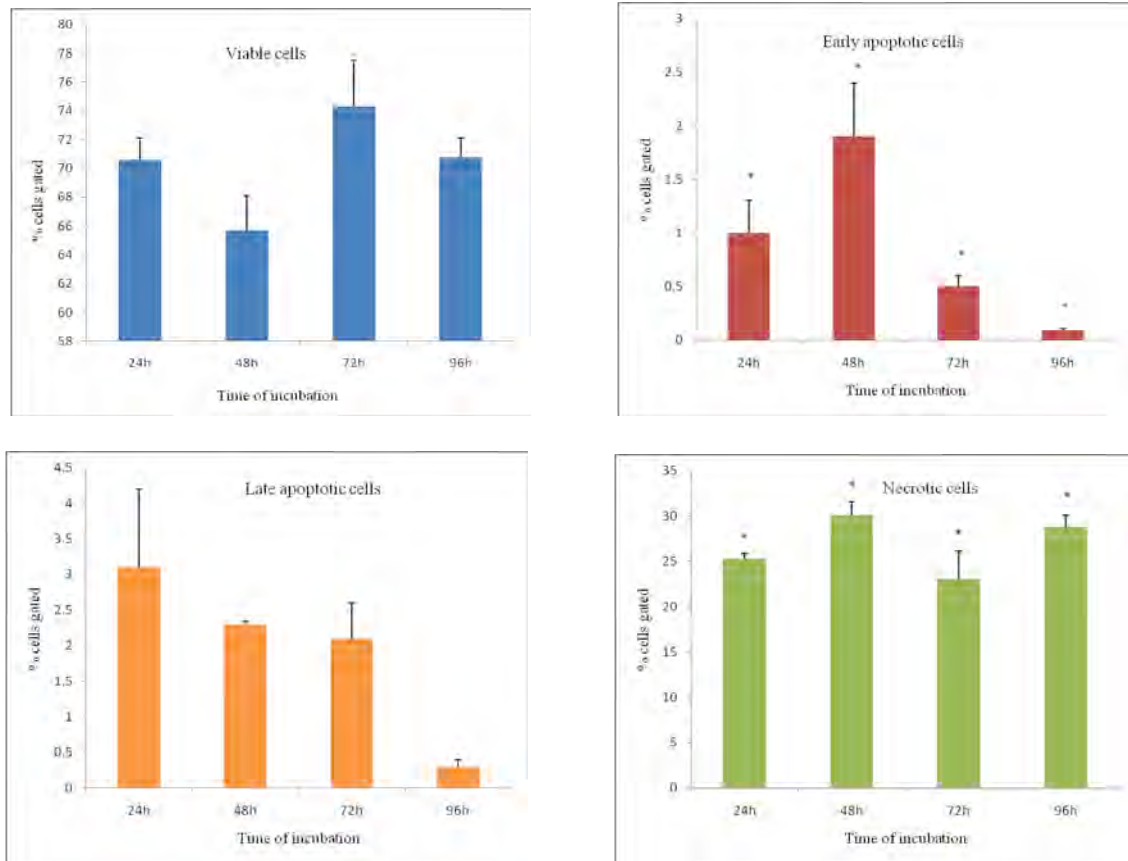


Figure 31: MUBS cells population from each quadrant (viable, early apoptotic, late apoptotic, necrotic) of every incubation time (following curcumin treatment) are represented in a bar graph. Error bars show standard error of mean. Data represents the mean \pm standard error of mean for $n=3$ experiments with each experiment being carried out in duplicate. Percentage of cell gated was followed by statistical analysis (one way ANOVA-Fisher comparison) as to obtain the p value (* p value < 0.05) and tabulated as below.

a)Viable quadrants	Mean	Difference from time of incubation			
		24h	48h	72h	96h
24h	70.648	-	-4.996 (-10.824-0.832)	3.649 (-2.179-9.477)	0.200 (-5.628-6.028)
48h	65.653	-4.996 (-10.824-0.832)	-	8.645 (2.261-15.029)	5.196 (-1.188-11.580)
72h	74.298	3.649 (-2.179-9.477)	8.645 (2.261-15.029)	-	-3.449 (-9.833-2.935)
96h	70.848	0.200 (-5.628-6.028)	5.196 (-1.188-11.580)	-3.449 (-9.833-2.935)	-

b)Early apoptotic quadrants	Mean	Difference from time of incubation			
		24h	48h	72h	96h
24h	0.966	-	0.940 (0.060-1.820)	-0.432 (-1.312-0.448)	-0.896 [(-1.776-(-0.017))]
48h	1.906	0.940 (0.060-1.820)	-	-1.372 [(2.336-(-0.409))]	-1.837 [(-2.800-(-0.873))]
72h	0.533	-0.432 (-1.312-0.448)	-1.372 [(2.336-(-0.409))]	-	-0.464 (-1.428-0.500)
96h	0.069	-0.896 [(-1.776-(-0.017))]	-1.837 [(-2.800-(-0.873))]	-0.464 (-1.428-0.500)	-

c)Late apoptotic quadrants	Mean	Difference from time of incubation			
		24h	48h	72h	96h
24h	3.086	-	-0.784 (-3.082-1.515)	-0.970 (-3.268-1.329)	-2.796 [(-5.095-(-0.498))]
48h	2.302	-0.784 (-3.082-1.515)	-	-0.186 (-2.704-2.332)	-2.013 (-4.530-0.505)
72h	2.116	-0.970 (-3.268-1.329)	-0.186 (-2.704-2.332)	-	-1.827 (-4.344-0.691)
96h	0.289	-2.796 [(-5.095-(-0.498))]	-2.013 (-4.530-0.505)	-1.827 (-4.344-0.691)	-

d)Necrotic quadrants	Mean	Difference from time of incubation			
		24h	48h	72h	96h
24h	25.300	-	4.840 (0.404-9.276)	-2.245 (-6.681-2.191)	3.492 (-0.944-7.927)
48h	30.140	4.840 (0.404-9.276)	-	-7.085 [(-11.94-(-2.226))]	-1.348 (-6.207-3.511)
72h	23.055	-2.245 (-6.681-2.191)	-7.085 [(-11.94-(-2.226))]	-	5.737 (0.878-10.596)
96h	28.792	3.492 (-0.944-7.927)	-1.348 (-6.207-3.511)	5.737 (0.878-10.596)	-

Table 13(a-d) : Statistical analysis (One way-ANOVA-Fisher comparison) of % cells gated for all incubation time; 24h-48h-72h-96h (against each other) for every quadrant, i.e. a) viable, b)early apoptotic, c) late apoptotic and d) necrotic quadrant. The p value was denoted by* (p<0.05) indicated that the mean value for all incubation time were statistically significant against each. Each difference in mean value in bold showed that p value>0.05). Significant difference was noted between different incubation time studied in all quadrants except for viable and late apoptotic cells quadrants.

MUBP cells

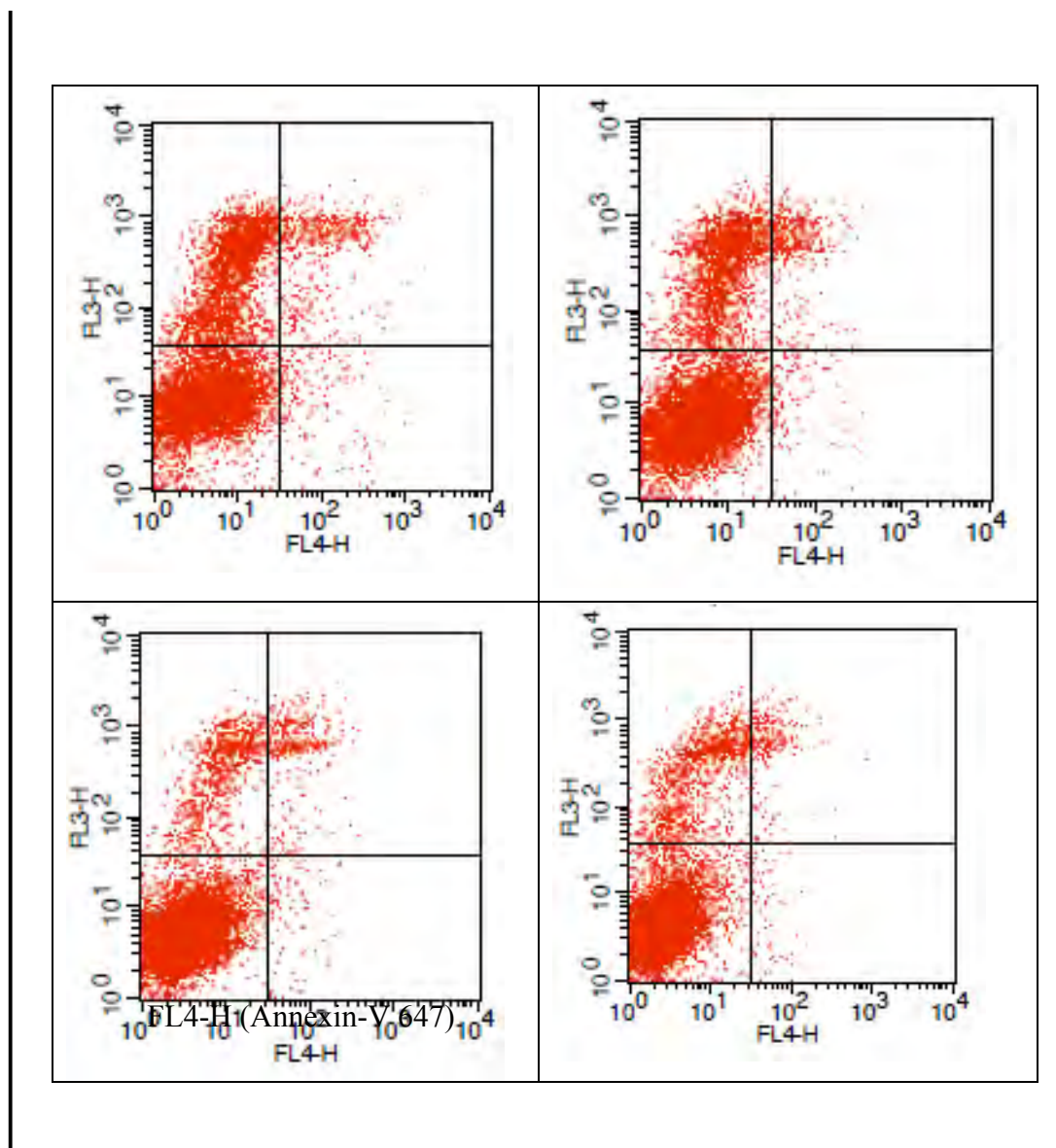


Figure 32 : Four representative diagrams from Annexin V apoptosis assay of MUBP cells at different hour of incubation (following curcumin treatment); 24h (upper left box), 48h (upper right box), 72h (lower left box) and 96h (lower right box). In a diagram, each quadrant represents viable cells (lower left), early apoptosis cells (lower right), late apoptotic cells (upper right) and necrotic cells (upper left). Percentage of cell gated in the quadrant is made by CellQuest software

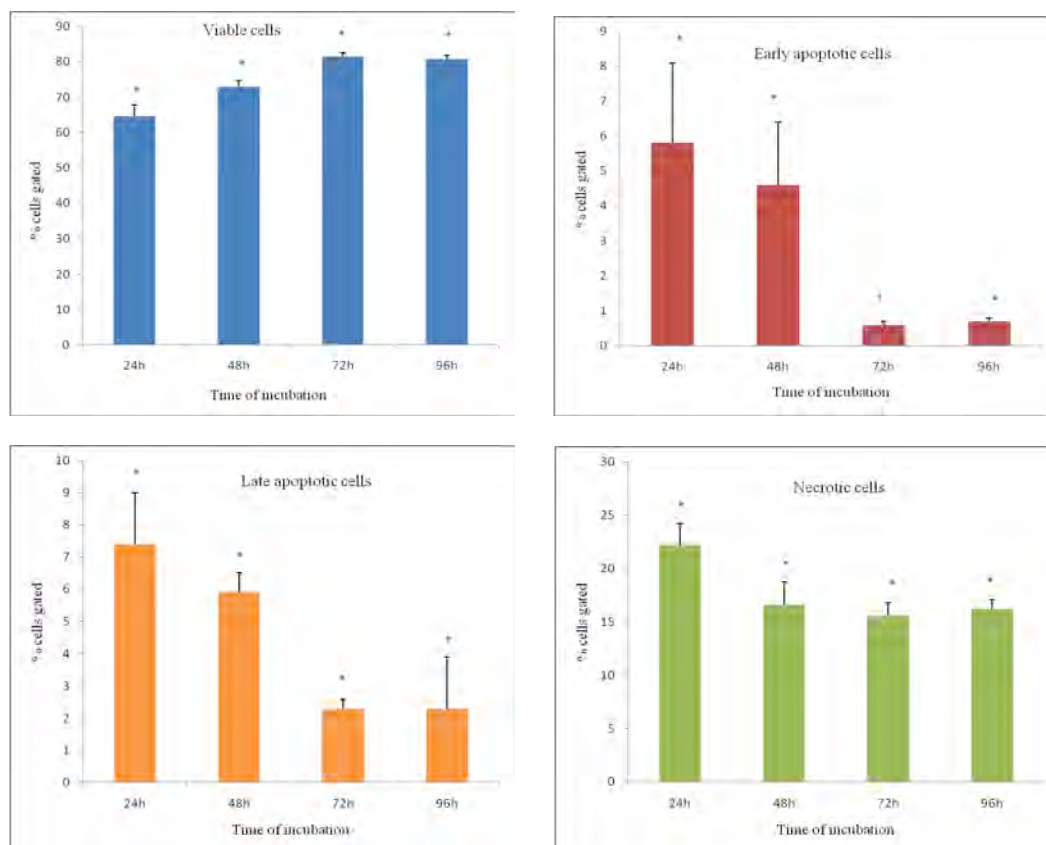


Figure 33: MUBP cells population from each quadrant (viable, early apoptotic, late apoptotic, necrotic) of every incubation time (following curcumin treatment) are represented in a bar graph. Error bars show standard error of mean. Data represents the mean \pm standard error of mean for $n=3$ experiments with each experiment being carried out in duplicate. Percentage of cell gated was followed by statistical analysis (one way ANOVA-Fisher comparison) as to obtain the p value (* p value < 0.05) and tabulated as below.

a)Viable quadrants	Mean	Difference from time of incubation			
		24h	48h	72h	96h
24h	64.488	-	8.447 (2.926-13.968)	16.984 (11.463-22.506)	16.297 (10.776-21.818)
48h	72.935	8.447 (2.926-13.968)	-	8.537 (3.016-14.058)	7.849 (2.328-13.371)
72h	81.472	16.984 (11.463-22.506)	8.537 (3.016-14.058)	-	-0.688 (-6.209-4.833)
96h	80.784	16.297 (10.776-21.818)	7.849 (2.328-13.371)	-0.688 (-6.209-4.833)	-

b)Early apoptotic quadrants	Mean	Difference from time of incubation			
		24h	48h	72h	96h
24h	5.840	-	-1.276 (-5.433-2.882)	-5.222 [(-9.380-(-1.065))]	-5.131 [(-9.289-(-0.974))]
48h	4.564	-1.276 (-5.433-2.882)	-	-3.947 [(-8.104-0.211)]	-3.856 (-8.013-0.302)
72h	0.618	-5.222 [(-9.380-(-1.065))]	-3.947 [(-8.104-0.211)]	-	0.091 (-4.066-4.249)
96h	0.709	-5.131 [(-9.289-(-0.974))]	-3.856 (-8.013-0.302)	0.091 (-4.066-4.249)	-

c)Late apoptotic quadrants	Mean	Difference from time of incubation			
		24h	48h	72h	96h
24h	7.429	-	-1.553 (-4.122-1.015)	-5.085 [(-7.653-(-2.517))]	-5.164 [(-7.732-(-2.595))]
48h	5.876	-1.553 (-4.122-1.015)	-	-3.532 [(-6.100-(-0.963))]	-3.611 [(-6.179-(-1.042))]
72h	2.344	-5.085 [(-7.653-(-2.517))]	-3.532 [(-6.100-(-0.963))]	-	-0.079 (-2.647-2.490)
96h	2.266	-5.164 [(-7.732-(-2.595))]	-3.611 [(-6.179-(-1.042))]	-0.079 (-2.647-2.490)	-

d)Necrotic quadrants	Mean	Difference from time of incubation			
		24h	48h	72h	96h
24h	22.243	-	-5.624 [(-10.193-(-1.056))]	-6.677 [(-11.245-(-2.109))]	-6.003 [(-10.571-(-1.435))]
48h	16.619	-5.624 [(-10.193-(-1.056))]	-	-1.053 (-5.621-3.515)	-0.378 (-4.946-4.190)
72h	15.566	-6.677 [(-11.245-(-2.109))]	-1.053 (-5.621-3.515)	-	0.674 (-3.894-5.243)
96h	16.241	-6.003 [(-10.571-(-1.435))]	-0.378 (-4.946-4.190)	0.674 (-3.894-5.243)	-

Table 14(a-d) : Statistical analysis (One way-ANOVA-Fisher comparison) of % cells gated for all incubation time; 24h-48h-72h-96h (against each other) for every quadrant, i.e. a) viable, b)early apoptotic, c) late apoptotic and d) necrotic quadrant. The p value was denoted by* (p<0.05) indicated that the mean value for all incubation time were statistically significant against each. Each difference in mean value in bold showed that p value>0.05). Significant difference was noted between different incubation time studied in all quadrants.

MUP cells

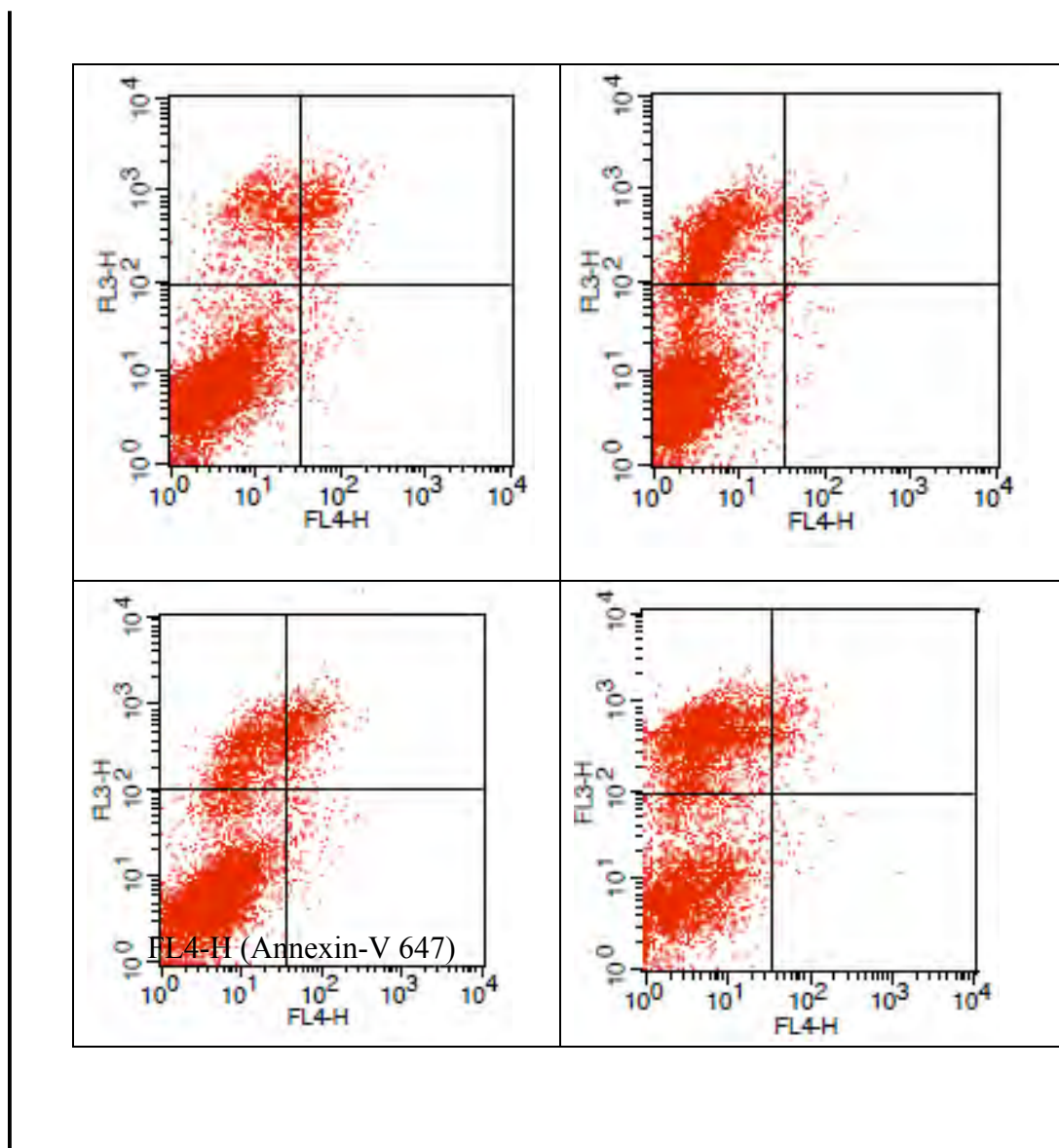


Figure 34: Four representative diagrams from Annexin V apoptosis assay of MUP cells at different hour of incubation (following curcumin treatment); 24h (upper left box), 48h (upper right box), 72h (lower left box) and 96h (lower right box). In a diagram, each quadrant represents viable cells (lower left), early apoptosis cells (lower right), late apoptotic cells (upper right) and necrotic cells (upper left). Percentage of cell gated in the quadrant is made by CellQuest software

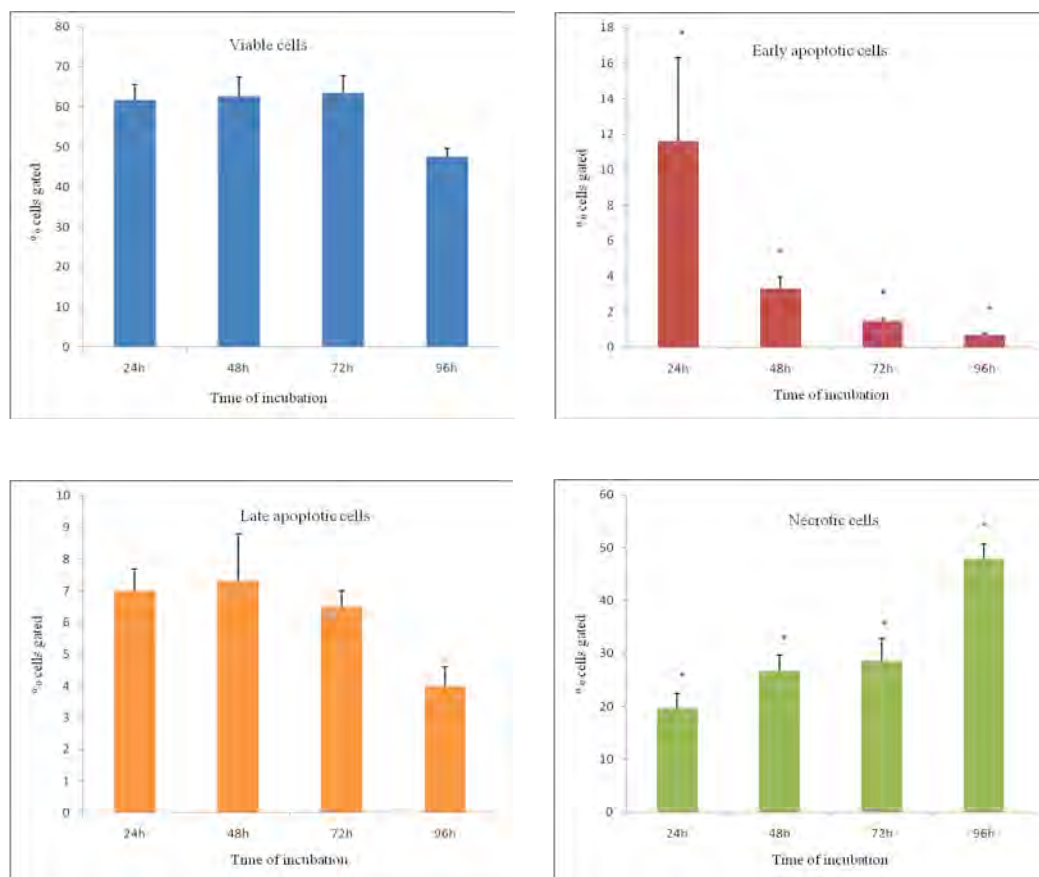


Figure 35: MUP cells population from each quadrant (viable, early apoptotic, late apoptotic, necrotic) of every incubation time (following curcumin treatment) are represented in a bar graph. Error bars show standard error of mean. Data represents the mean \pm standard error of mean for $n=3$ experiments with each experiment being carried out in duplicate. Percentage of cell gated was followed by statistical analysis (one way ANOVA-Fisher comparison) as to obtain the p value (* p value < 0.05) and tabulated as below.

a)Viable quadrants	Mean	Difference from time of incubation			
		24h	48h	72h	96h
24h	61.72	-	1.01 (-10.48-12.50)	1.72 (-9.77-13.21)	-14.26 [(-27.91-(-0.61))]
48h	62.73	1.01 (-10.48-12.50)	-	0.71 (-11.32-12.74)	-15.28 [(-29.39-(1.17))]
72h	63.44	1.72 (-9.77-13.21)	0.71 (-11.32-12.74)	-	-15.99 [(-30.10-(-1.88))]
96h	47.45	-14.26 [(-27.91-(-0.61))]	-15.28 [(-29.39-(1.17))]	-15.99 [(-30.10-(-1.88))]	-

b)Early apoptotic quadrants	Mean	Difference from time of incubation			
		24h	48h	72h	96h
24h	11.64	-	-8.33 [(-16.62-(-0.04))]	-10.14 [(-18.44-(-1.85))]	-10.98 [(-20.83-(-1.13))]
48h	3.31	-8.33 [(-16.62-(-0.04))]	-	-1.82 (-10.50-6.87)	-2.65 (-12.83-7.53)
72h	1.49	-10.14 [(-18.44-(-1.85))]	-1.82 (-10.50-6.87)	-	-0.84 (-11.02-9.35)
96h	0.66	-10.98 [(-20.83-(-1.13))]	-2.65 (-12.83-7.53)	-0.84 (-11.02-9.35)	-

c)Late apoptotic quadrants	Mean	Difference from time of incubation			
		24h	48h	72h	96h
24h	7.006	-	0.328 (-2.295-2.951)	-0.507 (-3.130-2.116)	-3.042 (-6.158-0.074)
48h	7.334	0.328 (-2.295-2.951)	-	-0.835 (-3.582-1.912)	-3.370 [(-6.591-(-0.149))]
72h	6.499	-0.507 (-3.130-2.116)	-0.835 (-3.582-1.912)	-	-2.535 (-5.756-0.686)
96h	3.964	-3.042 (-6.158-0.074)	-3.370 [(-6.591-(-0.149))]	-2.535 (-5.756-0.686)	-

d)Necrotic quadrants	Mean	Difference from time of incubation			
		24h	48h	72h	96h
24h	19.65	-	6.97 (-2.00-15.95)	8.92 (-0.06-17.90)	28.28 (17.61-38.94)
48h	26.62	6.97 (-2.00-15.95)	-	1.95 (-7.46-11.35)	21.30 (10.28-32.33)
72h	28.57	8.92 (-0.06-17.90)	1.95 (-7.46-11.35)	-	19.36 (8.33-30.38)
96h	47.93	28.28 (17.61-38.94)	21.30 (10.28-32.33)	19.36 (8.33-30.38)	-

Table 15(a-d) : Statistical analysis (One way-ANOVA-Fisher comparison) of % cells gated for all incubation time; 24h-48h-72h-96h (against each other) for every quadrant, i.e. a) viable, b)early apoptotic, c) late apoptotic and d) necrotic quadrant. The p value was denoted by* (p<0.05) indicated that the mean value for all incubation time were statistically significant against each. Each difference in mean value in bold showed that p value>0.05). Significant difference was noted between different incubation time studied in all quadrants except for viable and late apoptotic cells quadrants.

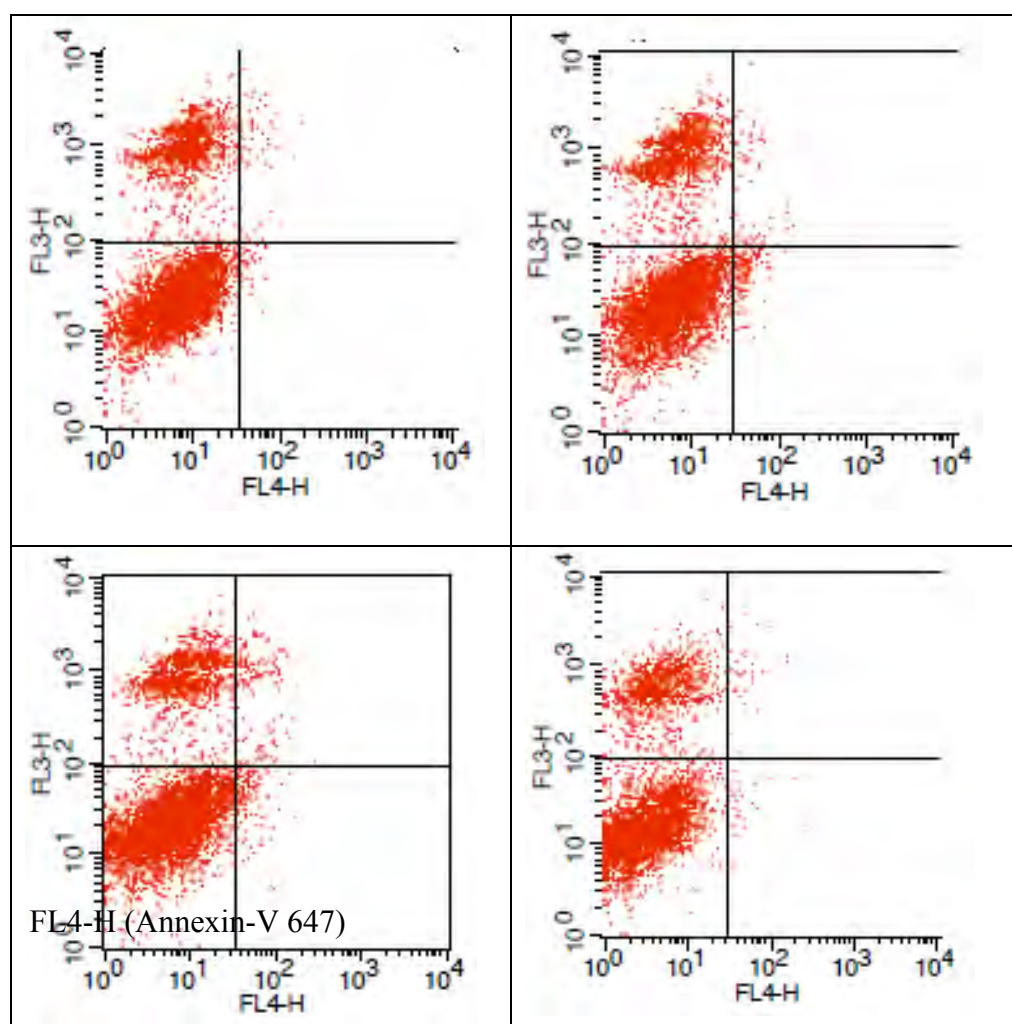


Figure 36: Four representative diagrams from Annexin V apoptosis assay of MUTC cells at different hour of incubation (following curcumin treatment); 24h (upper left box), 48h (upper right box), 72h (lower left box) and 96h (lower right box). In a diagram, each quadrant represents viable cells (lower left), early apoptosis cells (lower right), late apoptotic cells (upper right) and necrotic cells (upper left). Percentage of cell gated in the quadrant is made by CellQuest software

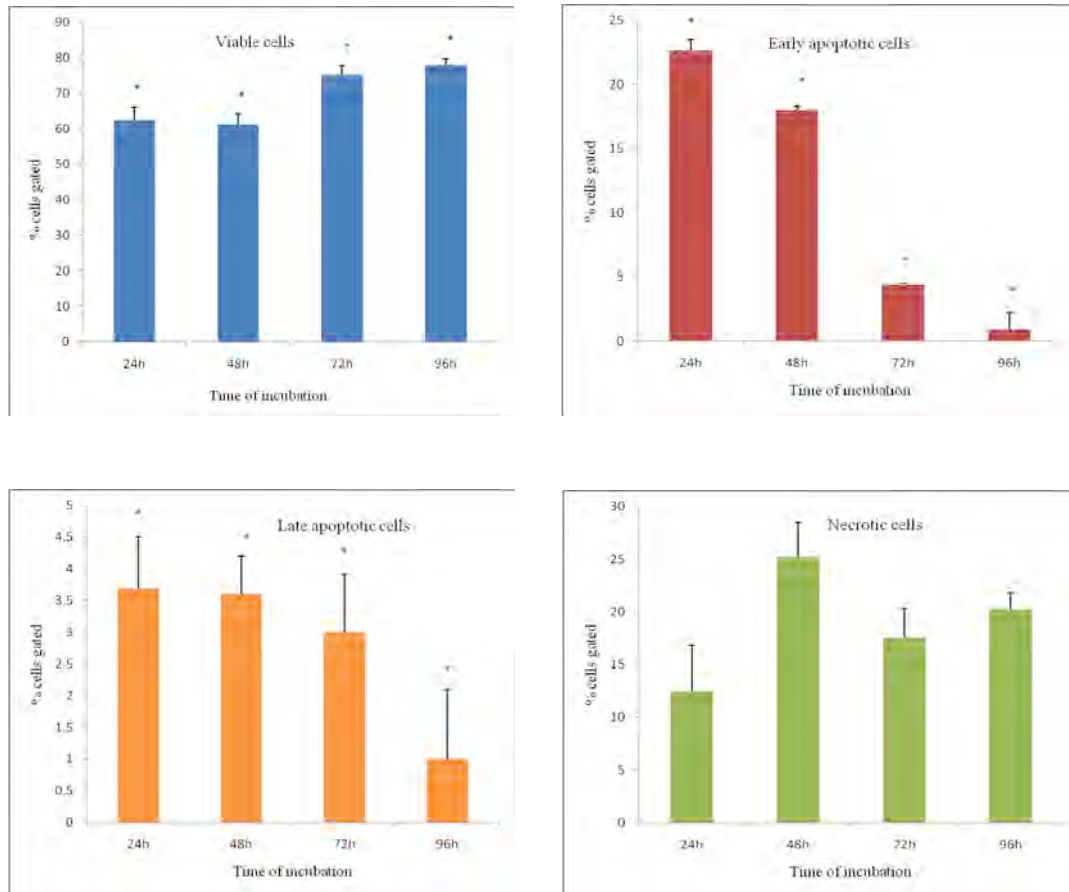


Figure 37: MUTC cells population from each quadrant (viable, early apoptotic, late apoptotic, necrotic) of every incubation time (following curcumin treatment) are represented in a bar graph. Error bars show standard error of mean. Data represents the mean \pm standard error of mean for $n=3$ experiments with each experiment being carried out in duplicate. Percentage of cell gated was followed by statistical analysis (one way ANOVA-Fisher comparison) as to obtain the p value (* p value < 0.05) and tabulated as below.

a)Viable quadrants	Mean	Difference from time of incubation			
		24h	48h	72h	96h
24h	62.510	-	-1.323 (-9.482-6.835)	12.561 (3.660-21.462)	15.375 (6.474-24.276)
48h	61.187	-1.323 (-9.482-6.835)	-	13.884 (6.763-21.005)	16.699 (9.577-23.820)
72h	75.071	12.561 (3.660-21.462)	13.884 (6.763-21.005)	-	2.814 (-5.147-10.776)
96h	77.875	15.375 (6.474-24.276)	16.699 (9.577-23.820)	2.814 (-5.147-10.776)	-

b)Early apoptotic quadrants	Mean	Difference from time of incubation			
		24h	48h	72h	96h
24h	22.62	-	-4.62 (-13.26-4.03)	-18.22 [(-27.65-(-8.80))]	-21.74 [(-31.17-(-12.31))]
48h	18.00	-4.62 (-13.26-4.03)	-	-13.61 [(-21.15-(-6.07))]	-17.12 [(-24.67-(-9.58))]
72h	4.39	-18.22 [(-27.65-(-8.80))]	-13.61 [(-21.15-(-6.07))]	-	-3.52 (-11.95-4.92)
96h	0.88	-21.74 [(-31.17-(-12.31))]	-17.12 [(-24.67-(-9.58))]	3.52 (-11.95-4.92)	-

c)Late apoptotic quadrants	Mean	Difference from time of incubation			
		24h	48h	72h	96h
24h	3.691	-	-0.057 (-1.442-1.328)	-0.721 (-2.232-0.790)	-2.667 [(-4.178-(-1.156))]
48h	3.635	-0.057 (-1.442-1.328)	-	-0.665 (-1.873-0.544)	-2.610 [(-3.819-(-1.401))]
72h	2.970	-0.721 (-2.232-0.790)	-0.665 (-1.873-0.544)	-	-1.946 [(-3.297-(-0.594))]
96h	1.024	-2.667 [(-4.178-(-1.156))]	-2.610 [(-3.819-(-1.401))]	-1.946 [(-3.297-(-0.594))]	-

d)Necrotic quadrants	Mean	Difference from time of incubation			
		24h	48h	72h	96h
24h	12.45	-	12.74 (-7.01-32.48)	5.11 (-16.42-26.65)	7.76 (-13.78-29.30)
48h	25.19	12.74 (-7.01-32.48)	-	-7.62 (-24.85-9.61)	-4.98 (-22.21-12.21)
72h	17.56	5.11 (-16.42-26.65)	-7.62 (-24.85-9.61)	-	2.64 (-16.62-21.91)
96h	20.21	7.76 (-13.78-29.30)	-4.98 (-22.21-12.21)	2.64 (-16.62-21.91)	-

Table 16(a-d) : Statistical analysis (One way-ANOVA-Fisher comparison) of % cells gated for all incubation time; 24h-48h-72h-96h (against each other) for every quadrant, i.e. a) viable, b)early apoptotic, c) late apoptotic and d) necrotic quadrant. The p value was denoted by* (p<0.05) indicated that the mean value for all incubation time were statistically significant against each. Each difference in mean value in bold showed that p value>0.05). Significant difference was noted between different incubation time studied in all quadrants except for necrotic cells quadrant

3.8 Curcumin as a potential anti-angiogenic agent

The anti-angiogenic property of curcumin was measured using an *in vitro* angiogenesis assay with the use of co-culture. This included an extracellular matrix gel (or also commercially known as matrigel) which mainly contains laminin and type IV collagen (see chapter 2 section 2.2.9). The insert was coated with matrigel prior to HUVEC seeding. HUVEC that grown on the matrigel surface were examined as to see if they form networking of tubules when co-culturing with primary brain tumour cells that grown in the well, which located underneath the insert.

In the co-culture setting, each normal brain and primary brain tumour cell culture was treated with different concentrations of curcumin over 16 hours prior to analysis. Each insert

containing HUVEC was processed as described in the chapter 2, section 2.2.9 before photographed. For each insert, randomly, 6 areas were captured under the magnification of 100 x. This include the inserts of both controls, Suramin (negative) and VEGF (positive) but not displayed in the graphs plotted (Fig 28). Each photograph was traced with Paint software (Microsoft) before quantification with Image J software (see chapter 2, section 2.2.9).

Normal brain cells showed almost equal number of nodes, junctions and branches at each of the curcumin doses used. Nodes are the points where branches intersect; they are an important feature in quantifying angiogenic tubule formation. In comparison with the HUVECS treated with normal brain cells, the number of nodes was increased with MUBS, MUTC and MUP untreated primary brain tumour cells. However, the number of nodes in MUBP cells prior to curcumin treatment was not significantly different from normal brain cells (CC2565). The number of nodes in MUBS, MUTC and MUP then decreased when treated with curcumin and greater in reduction was seen as the concentration of curcumin increased. At concentrations of 20µg/ml and above the number of nodes was significantly lower than in untreated normal brain cells.

Total length of the tubules was measured based on the whole areas analysed by the software used. This is another important feature in the quantification of potential angiogenesis activity. Similarly to the finding for nodes, MUTC (figure 28e), MUP (figure 28d) and MUBS (figure 28c) cell cultures showed increased values in the total length of the tubule as compared to the normal brain cells (figure 28a). The length of tubules decreased with the treatment of curcumin at all concentrations studied.

Junctions (the points where groups of nodes were formed) is another parameter measured in angiogenesis potential. The number of junctions was increased on co-culture with all three primary cell cultures as compared to the normal brain. However, this difference

did not reach statistical significance. However, curcumin treatment has significantly decreased the number of junctions present in each of the tumour cell lines.

The number of branches in all untreated primary brain tumour cells investigated was lower (from 11 to 17 branches) than what has been quantified in the normal brain cells (18 branches). Incubation with curcumin decreased the number of branches in each primary brain tumour cell culture at concentration as low as 10µg/ml. The anti-angiogenic effect of curcumin was also demonstrated by the number of junctions, nodes and total tubule length, that reduced after incubation with curcumin at each concentration studied.

Results are suggestive that MUBP cell culture might not have the angiogenic potential as compared to the other primary cell cultures studied due to the findings that seen. All the angiogenic parameters investigated in MUBP cell culture showed lower values than was perceived in the normal brain cells.

All remaining primary cell cultures may suggested to be pro-angiogenic based on the number of nodes and total tubule length that were high in the untreated ones. However, the angiogenic potential was reduced markedly when treated with curcumin hence demonstrated curcumin suggesting an anti-angiogenic property for curcumin in these primary brain tumour cells.

Normal brain cells (CC2565)

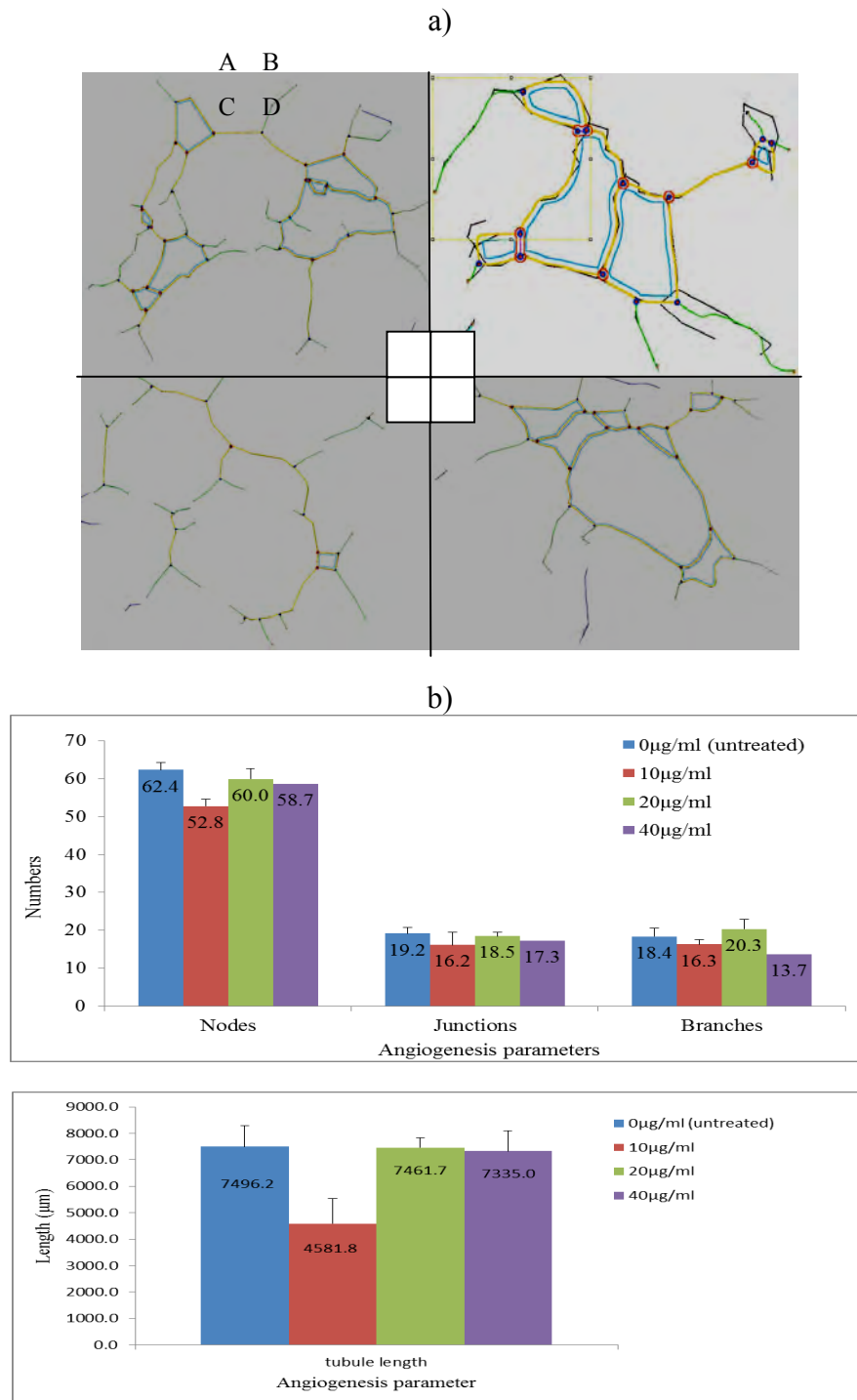
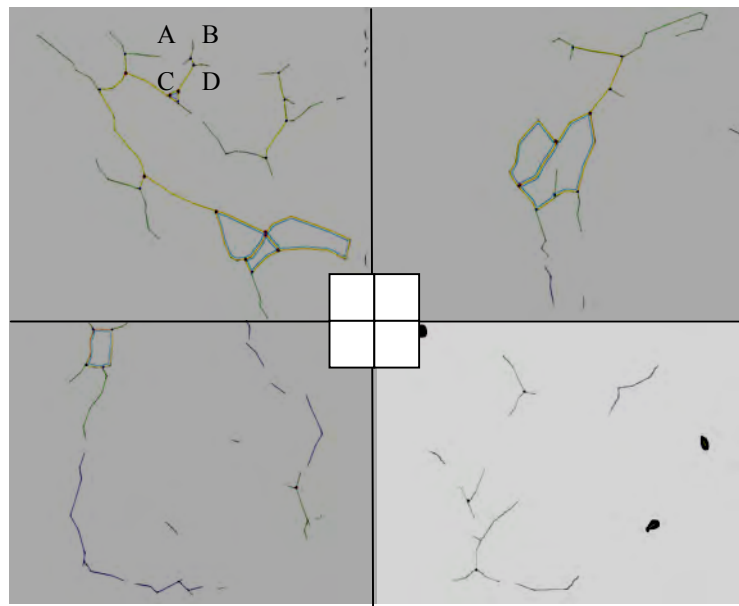


Figure 38: a) *In vitro* angiogenesis assay (co-culture) showed the tubule network analysed using Image J software. A= untreated, B=10 µg/ml, C= 20 µg/ml, D= 40 µg/ml. b) Bar graphs showed normal brain cells (CC2565) treated with 0 µg/ml (untreated)-blue, 10 µg/ml- red, 20 µg/ml-green and 40 µg/ml curcumin-purple. Number of nodes, junctions, branches and total length of the tubules (µm) were quantified by Image J software analysis as demonstrated by the bar graphs. Data represents the mean \pm standard error of mean for n=3 experiments with each experiment being carried out in triplicate. Statistical analysis (one way ANOVA and 2 sample t-test analysis) was carried out to obtain the *p* value (**p*<0.05). Normal brain cells were not affected by curcumin treatment at all concentrations studied due to the value that is not statistically different (*p*>0.05) compared to the untreated cells.

a)



b)

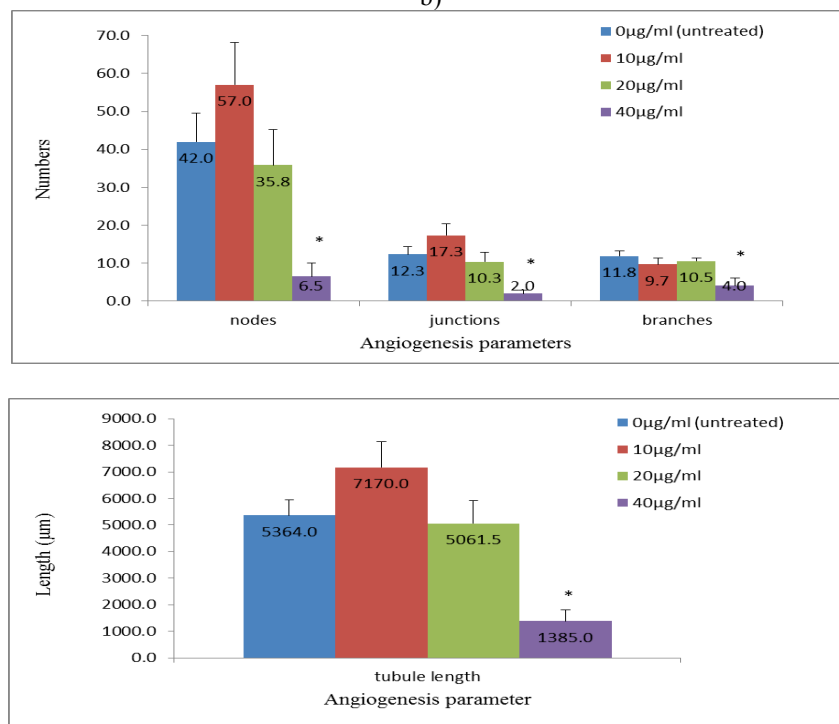


Figure 39: a) *In vitro* angiogenesis assay (co-culture) showed the tubule network analysed using Image J software. A= untreated, B=10 µg/ml, C= 20 µg/ml, D= 40 µg/ml. b) Bar graphs showed normal brain cells (CC2565) treated with 0 µg/ml (untreated)-blue, 10 µg/ml- red, 20 µg/ml-green and 40 µg/ml curcumin-purple. Number of nodes, junctions, branches and total length of the tubules (µm) were quantified by Image J software analysis as demonstrated by the bar graphs. Data represents the mean \pm standard error of mean for n=3 experiments with each experiment being carried out in triplicate. Statistical analysis (one way ANOVA and 2 sample t-test analysis) was carried out to obtain the *p* value (**p*<0.05). In MUBP cells, curcumin treatment has affected all angiogenic parameters but only at highest concentration with *p* value <0.05.

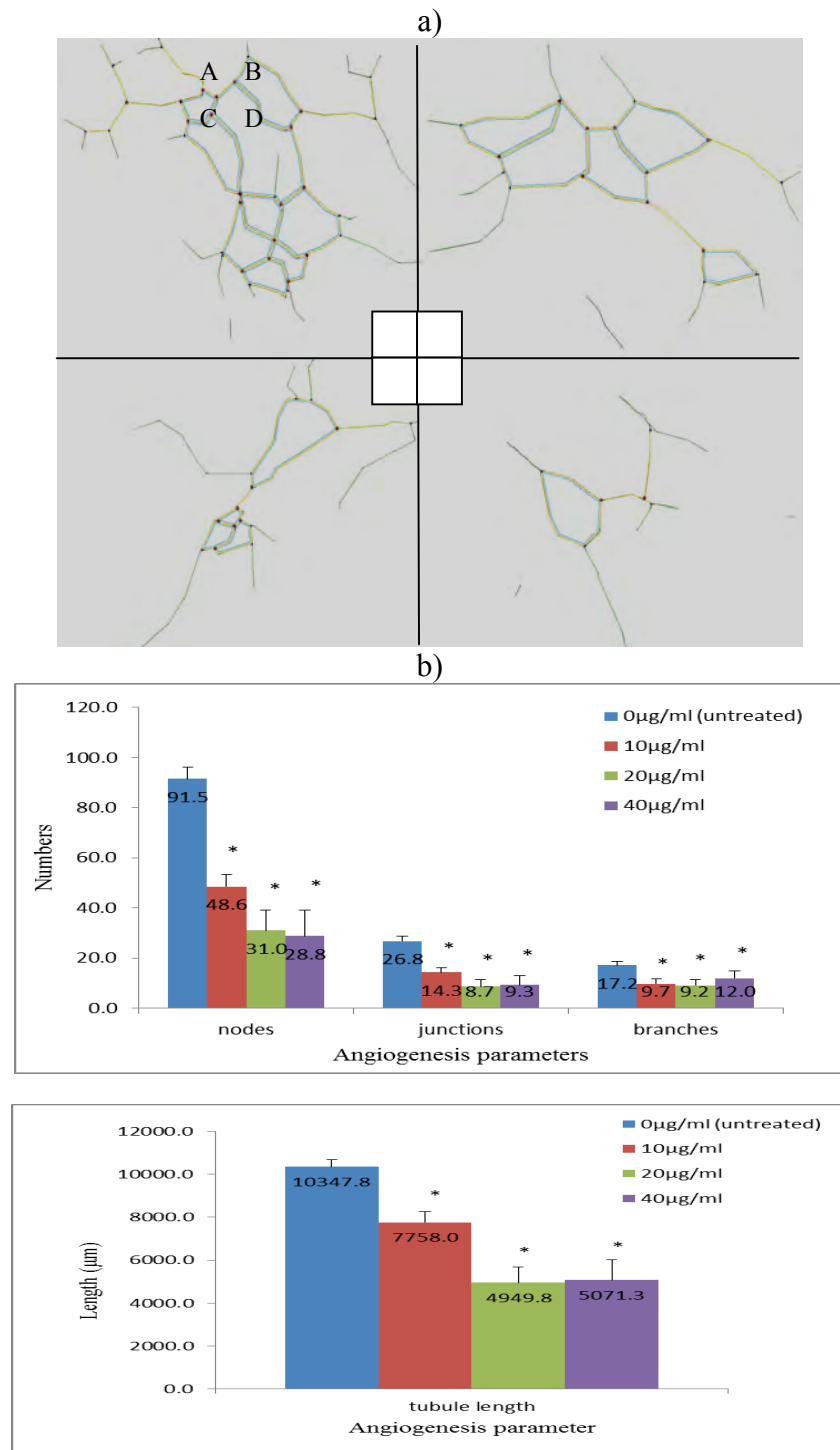


Figure 40: a) *In vitro* angiogenesis assay (co-culture) showed the tubule network analysed using Image J software. A= untreated, B=10 $\mu\text{g/ml}$, C= 20 $\mu\text{g/ml}$, D= 40 $\mu\text{g/ml}$. b) Bar graphs showed normal brain cells (CC2565) treated with 0 $\mu\text{g/ml}$ (untreated)-blue, 10 $\mu\text{g/ml}$ - red, 20 $\mu\text{g/ml}$ -green and 40 $\mu\text{g/ml}$ curcumin-purple. Number of nodes, junctions, branches and total length of the tubules (μm) were quantified by Image J software analysis as demonstrated by the bar graphs. Data represents the mean \pm standard error of mean for n=3 experiments with each experiment being carried out in triplicate. Statistical analysis (one way ANOVA and 2 sample t-test analysis) was carried out to obtain the *p* value (**p* value<0.05). With MUBS cells, reduction was noted significantly at each angiogenesis parameters and concentrations studied when compared between untreated and curcumin treated cells.

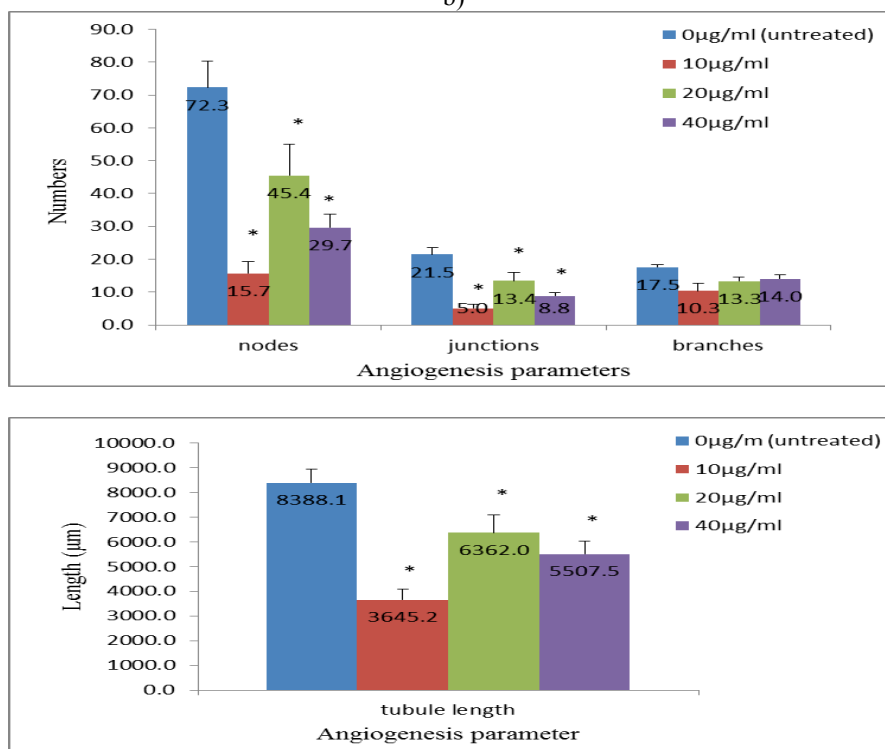
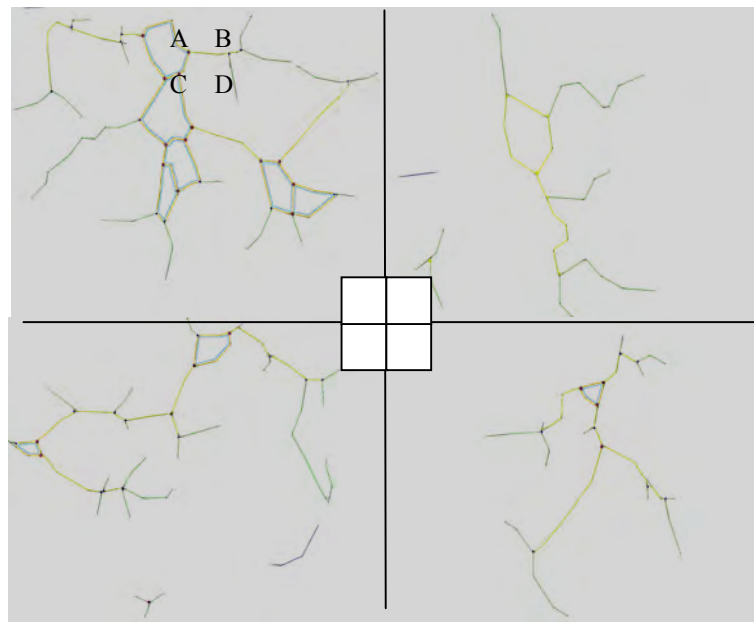


Figure 41: a) *In vitro* angiogenesis assay (co-culture) showed the tubule network analysed using Image J software. A= untreated, B=10µg/ml, C= 20µg/ml, D= 40µg/ml. b) Bar graphs showed normal brain cells (CC2565) treated with 0µg/ml (untreated)-blue, 10µg/ml- red, 20µg/ml-green and 40µg/ml curcumin-purple. Number of nodes, junctions, branches and total length of the tubules (µm) were quantified by Image J software analysis as demonstrated by the bar graphs. Data represents the mean \pm standard error of mean for n=3 experiments with each experiment being carried out in triplicate. Statistical analysis (one way ANOVA and 2 sample t-test analysis) was carried out to obtain the *p* value (**p* value<0.05) Three out of four parameters of angiogenesis were affected significantly by curcumin at all concentrations.

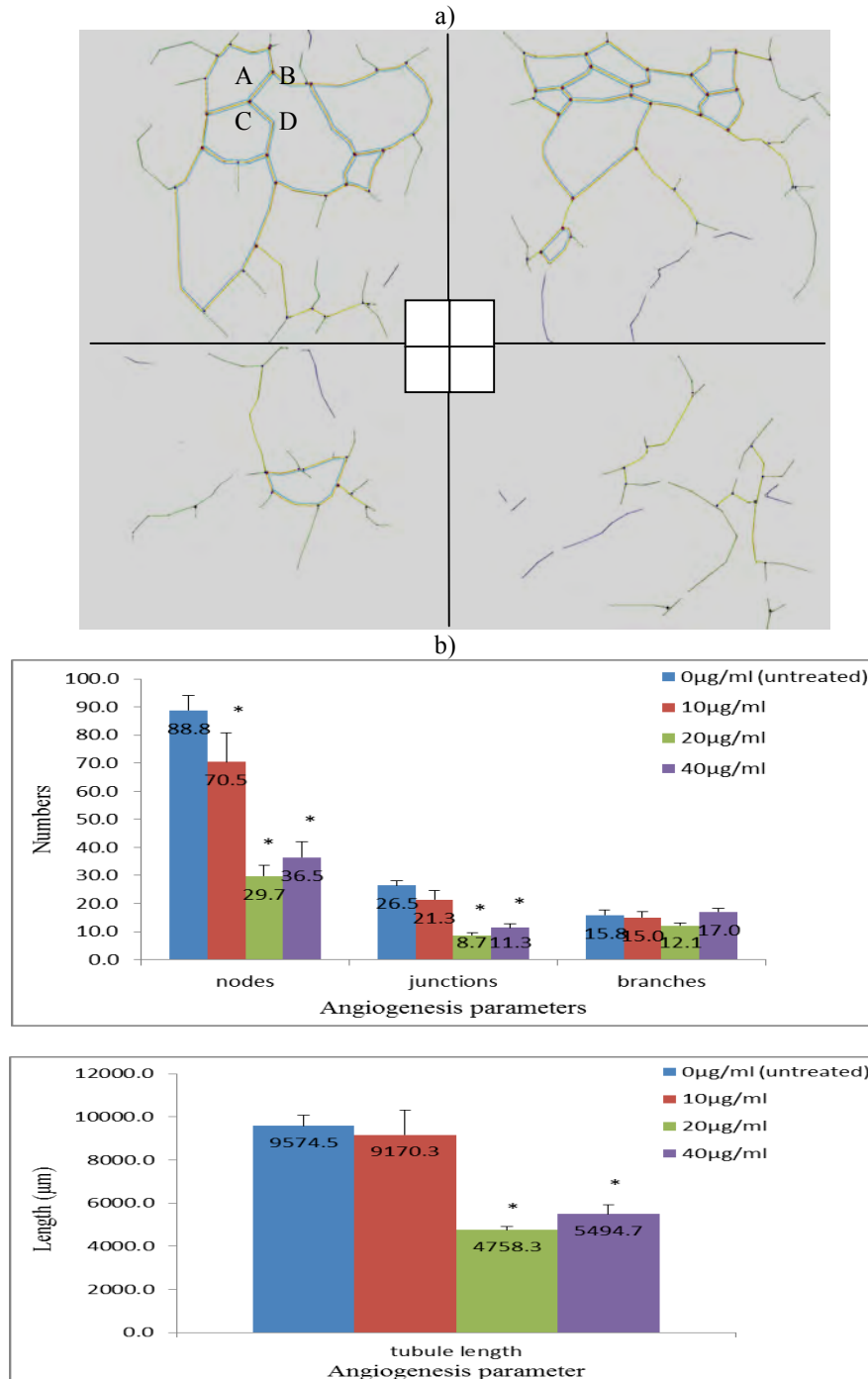


Figure 42: a) *In vitro* angiogenesis assay (co-culture) showed the tubule network analysed using Image J software. A= untreated, B=10µg/ml, C= 20µg/ml, D= 40µg/ml. b) Bar graphs showed normal brain cells (CC2565) treated with 0µg/ml (untreated)-blue, 10µg/ml- red, 20µg/ml-green and 40µg/ml curcumin-purple. Number of nodes, junctions, branches and total length of the tubules (µm) were quantified by Image J software analysis as demonstrated by the bar graphs. Data represents the mean \pm standard error of mean for n=2 experiments with each experiment being carried out in triplicate. Statistical analysis (one way ANOVA and 2 sample t-test analysis) was carried out to obtain the *p* value (**p* value<0.05). With MUTC cells, the numbers of branches were not statistically significant in difference following curcumin treatment as compared to the untreated cells.

Controls (Suramin /VEGF)

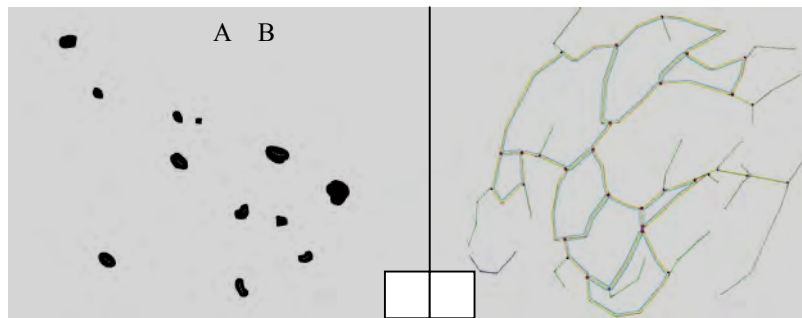


Figure 43: Positive (A)- Suramin treated) and negative (B)- VEGF treated) cells were used as controls. *p value<0.05 (significant different noted between untreated and curcumin treated cells at each angiogenesis parameters and cell culture studied).

Chapter 4: Discussion

Despite decades of major investigations for better understanding of the mechanisms underlie the development of cancers in recent years, the treatment and diagnosis of glioblastoma multiformes continues to harbour significant challenges hence remain incurable. Due to the exceptionally infiltrative nature of glioblastoma multiforme together with the scarcity in effective therapies, any new modality to replace or support current treatments would be helpful in improving the prognosis, to the least. In this study, we evaluated the potential therapeutic effects of 2 micronutrients; curcumin and lycoRed, on primary brain tumour cells (biopsy derived). We believed that this is the first study that did not use established glioma cell lines (unlike in other studies) in elucidating the potential therapeutic roles of both curcumin and lycoRed on malignant glioblastoma multiforme.

Curcumin is cytotoxic to the primary brain tumour cells but not LycoRed

Our results show that curcumin is cytotoxic the primary brain tumour cell cultures studied. Consistently with what we have demonstrated in this study, other previous studies on curcumin have also showed its cytotoxic effects but in different types of cell line *in vitro*. These include curcumin at a concentration of 4 µg/ml which produced 50% cytotoxicity in Dalton's lymphoma ascites cells, inhibition in the growth of Chinese hamster ovary cells and human leukemic lymphocytes in culture (Kuttan et al., 1985) and 50% growth arrest in K-562 human chronic myelogenousleukemia cells (Anuchapreeda et al., 2006) at a concentration of 20 µg/ml. Moreover, the anti-proliferative action of curcumin is mediated by suppression of the hepatocyte growth factor (HGF) and its receptor c-met.184 in the human hepatoma G2 cell line (Seol, 2000). In some other cell lines, curcumin potent therapeutic action in targeting cancer was reported to be mediated by its capability in generating reactive oxygen species (ROS) at a very low concentration (15 µM) which then caused damage to mitochondria, as demonstrated by decrease in the mitochondrial membrane potential and externalization of

phosphatidylserine, and the whole process eventually ended up in the initiation of apoptosis (Atsumi, 2006). It is suggested that this multifaceted anti-cancer effects by curcumin are predominantly mediated through various transcription factors, growth factors, oncogenic molecules, protein kinases and cytokines (Shanmugam et al., 2015).

It is crucial for an agent or micronutrient to be cytotoxic to the tumour cells and at the same time is safe to the normal cells during the treatment. For most of the concentration studied, curcumin is not cytotoxic to the normal brain cells. Indeed, the pharmacological safety of curcumin is well documented and demonstrated due to its natural occurrence, well established and long history of dietary use (Aggarwal, Kumar, Bharti, 2003). However, our finding of normal brain cells fragility towards higher concentration of curcumin may suggest that the toxicity level of curcumin reached may not be safe per se to be used *in vitro*. With respect to *in vivo* studies, although it has stated that beyond 8000 mg daily, curcumin is physiologically unattainable due to its average peak serum level that reach only up to $1.77 \pm 1.87 \mu\text{M}$ yet its serum level gradually declined within 12 hours after an oral intake, thus suggesting its poor bioavailability (Cheng et al., 2001). More extensive clinical and metabolic studies have reported that 8 to 12g/day is safe to be consumed (Aggarwal et al., 2003; Anand et al., 2007) though its level was reported to either undetected or extremely low $0.006 \pm 0.005 \mu\text{g/mL}$ at 1 h serum levels (Shoba et al., 1998). In a pancreatic cancer study, curcumin was well-tolerated as an adjuvant when studies conducted on combination therapy using 8 g oral curcumin daily with gemcitabine-based chemotherapy was safe and feasible (Rahmani et al., 2014).

The IC values obtained for these three primary brain tumour cells (MUBS, MUBP and MUP) were in the similar range between 14.2-15.2 $\mu\text{g/ml}$ for the IC_{75} , 16.3-16.8 $\mu\text{g/ml}$ for the IC_{50} and 17 -19.5 $\mu\text{g/ml}$ for the IC_{25} values. Thus, the IC values of curcumin for these primary brain tumour cell cultures lie between 14.2 and 19.5 $\mu\text{g/ml}$ which is limited in range

but it does show that curcumin has a significant effect on causing cytotoxicity to these malignant brain tumour cells by 25 to 75% inhibition of the cell viability. With respect to the normal brain cells, they remained viable when treated with the same concentrations of curcumin up to 5µg/ml before declining in the percentage of cell viability when treated with higher concentrations of curcumin. It is likely that the normal brain cells tend to become vulnerable to curcumin concentration at higher doses due to the nature of these cells which are fragile in *ex vivo*, especially during resuscitation from frozen and high maintenance during passaging *in vitro*.

24-hours incubation time was chosen to demonstrate the effect of each potential therapeutic agent studied; curcumin, LycoRed. As with previous studies, 48-hours period of incubation was set up as the standard. However, at earlier stage of this study, at 48-hours incubation, most of these treated biopsy-derived cells experienced necrotic event as gated via flow cytometry (DRAQ7 assay). Thus 24 hours was preferred. This is also to prevent the loss of cells during incubation (easily prone to contamination). Indeed, the period of incubation has been set out on different assays hence has to be standardised for all experiments that were carried out.

Curcumin has been studied in many cancer clinical trials such as oral, breast, bladder, colorectal, cervical, liver and skin cancer. Initiation of clinical studies in human were concurrent with clinical trials implemented *in vivo* as in animal studies, exhibiting chemopreventative effects against carcinogen (arsenic) in most cancers in mammals.. Clinical trials against cancers in human have mostly involved pharmacodynamic and pharmacokinetic effects of oral dose curcumin (Cheng et al., 2001). It is demonstrated that multi-targeted actions of curcumin are more effective than the most current anti-cancer therapies which are mostly mono-targeted. An example of mono targeted therapy is sorafenibin used to treat renal cell carcinoma (RCC) via the inhibition of platelet derived growth factor (PDGF) which

resulted to decreased in tumour angiogenesis in RCC (Ibrahim et al., 2012). Hence, this pleiotropic molecule may serve as a single drug that potentially acts on different type of cancers and studies, both *in vivo* and *in vitro*, have demonstrated curcumin's therapeutic value. There have been several mechanisms proposed for the action of curcumin in targeting multiple pathways in inflammatory diseases and carcinogenesis. Such mechanisms involve invasion and angiogenesis which are the hallmarks of human malignant gliomas (Jain et al., 2007). The mechanisms by which curcumin exerts its anti-cancer effects are extensive and varied. This includes many levels of regulation in the downstream processes of cellular growth. Curcumin effects on various transcription factors, oncogenes and signalling proteins. These include NF- κ B, AP-1, p53 gene, c-myc, Bcl-2, COX-2, NOS, Cyclin D1, TNF- α , interleukins and MMP-9. Curcumin also acts at various sequential stages of carcinogenesis such as mutagenesis, cell cycle regulation, apoptosis, and metastasis (Wilken et al., 2011).

In contrast, LycoRed failed to demonstrate any cytotoxic effects to these primary brain tumour cells. The data presented here demonstrated that exposure of LycoRed to primary brain tumour cell cultures grown *in vitro* did not cause the cytotoxic effect even though these were higher concentrations of lycopene than the normal physiological range for humans. The normal brain cells remained viable at a very wide range of concentrations studied (5ng/ml-24 μ g/ml) thus indicated that LycoRed also is not cytotoxic to the normal brain cells. Indeed, the viability of each cell line was increased compared to that seen where diluent (THF) was added in the absence of LycoRed. Thus, it appears from our studies that LycoRed has a protective effect on cells and may inhibit cytotoxic effects. As shown in Figure 18 in section 3.3 (result chapter), although the concentration of THF present was in the range of 0.2 to 3.2%, approximately 70% of the primary brain tumour cells remained viable following THF treatment. However, when these primary brain tumour cells were treated with LycoRed concentrations (dissolved in THF), 80 to 90% of the cells remained

viable which is believed that LycoRed may have a protective role on the cells from THF cytotoxicity.

Although the safety profile of lycopene as supplements has not been thoroughly studied, there are many reviews and scientific literatures available on tomatoes and tomato-based products. For instance, a report has investigated a range of botanical herbs which has included tomato extract in the randomized controlled trial and has endowed a safety dietary supplement of these herbs including the tomato extract. In addition, they have showed that tomato extract which was part of the combination is also effective in modulating the oxidation indices values as well as lowering the increased low density lipoprotein cholesterol values (Gupta et al., 2012).

Lycopene is the predominant carotenoid in tomato products after phytoene, phytofluene, and β -carotene (Wyss et al., 2001). In addition, lycopene rapidly oxidizes and degrades in cell culture systems, making it difficult to interpret results of *in vitro* studies. Variability in cell lines, culture conditions, solvents used to deliver lycopene as well as the source of lycopene, may contribute to different findings seen among *in vitro* researches conducted. Furthermore, a lycopene study (Ford et al., 2011) has demonstrated that oxidative metabolites of lycopene released *in vitro* and/or metabolic products of lycopene secreted by DU145 cells (prostate cancer cells) reduce the proliferation of prostate cancer cells, more than lycopene alone.

Although there are epidemiological studies that shown a relationship between diets rich in tomato and/or lycopene and a reduction in cancer rates (Gann et al., 1999; Giovannucci et al., 2002; Jian et al., 2005), unfortunately, it has not been upheld if lycopene alone is the sole compound suggested to reduce cancer rates (Bosetti et al., 2004). Perhaps, it is not the lycopene alone but rather the group of carotenoids and nutrients that may responsible for the

lower cancer rates seen in the epidemiological. Thus, LycoRed may not be exclusively responsible for the effects seen *in vivo* or in cell culture systems. As an anti-carcinogenic compound, LycoRed may not relate to the consumption of the whole tomato or other fruit in order to contribute to potential therapeutic effects for brain tumour.

The source of lycopene used in this study (commercially available as LycoRed) contained only 10% of lycopene (via spectrophotometric method) with the other ingredients including maltodextrin, modified gum starch, sugar esters, soya lecithin and gum acacia (see appendix). Thus, it is a mixture of other components yet only 10% lycopene is present. Indeed, difficulties with stability and solubility of lycopene in cell culture systems make it difficult to elucidate the mechanisms of action. Therefore, the results for LycoRed remain inconclusive and only curcumin findings will be discussed in further.

Curcumin's cytotoxicity induced via non-apoptotic pathway in the primary brain tumour cells

Although curcumin clearly showed a decrease in cell viability in our studies, we did not observe a significant induction of apoptosis by curcumin in the primary brain tumour cells studied. Thus, it is likely to be a non-apoptotic pathway triggered by curcumin in these malignant primary brain tumour cells. Although a contradictory report has stated previously that curcumin induced apoptosis in brain tumour cells via telomerase shortening (Khaw et al, 2013), it is not comparable to this study which have used primary brain tumour cell cultures (GBM, biopsy-derived) instead. The telomerase shortening study by curcumin used established cell lines; ONS-76- a medulloblastoma, KNS60- not astrocytic in origin (GFAP negative) unlike the four primary brain tumour cell cultures used in this study, which are astrocytomas. According to Li et al (2008), established cell lines may not represent primary

cell cultures at best thus established glioma cell lines are poorly representative of primary human gliomas. Moreover, unlike primary cells, cell lines have been *in vitro* and *in vivo* environment for more than two decades thus may have extensively changed in cellular or genomic level.

Progress has been made in understanding the route of apoptosis induced by curcumin, yet the primary site of its action remains elusive. It is well documented that survival signalling and apoptosis resistance are major regulators of cancer survival in glioblastoma. Both of these have to be targeted at the same time for the therapeutics to be effective (Krakstad and Chekenya, 2010). Curcumin's ability to induced programme cell death includes three pathways; I (apoptosis), II (autophagy) and III (necrosis). In a previous report, it was documented that curcumin induced G2/M cell cycle arrest and non-apoptotic autophagic death in malignant glioma cells (Aoki et al, 2007). Although the mechanism of autophagy on cell death by curcumin remains unclear, this protein degradation system of the cell's own lysosomes (autophagy) mediated the growth inhibition of malignant gliomas both *in vivo* and *in vitro*. Moreover, a number of reports have documented that malignant glioma cells are very resistant to apoptosis but that they undergo autophagy in response to anticancer therapies such as radiation, temozolomide, and ceramide (Daido et al., 2004, 2005; Kanzawa et al., 2004; Ito et al., 2005; Jo et al., 2014; Noack et al., 2014). Thus, it could be the same scenario with these primary brain tumour cells but with different treatments involved. While the current debates on autophagy and cancer is far from providing a conclusion, regulation of autophagy may contribute to an improved response to therapy hence warrant further investigations.

Initial assays established an IC₇₅ value for curcumin i.e, a concentration at which 75% of cells that were viable and 25% that were dead. However, in a subsequent assay to measure apoptosis, it was observed that curcumin treatment at its IC₇₅ value did not alter the viable

population of the primary tumour cells throughout the incubation time studied, i.e. between 40-60% viable cells remained. As expected in cell viability assay, IC₇₅ value resulted to the least cells cytotoxicity (25% cells inhibition) thus chosen to be used in Annexin V assay i.e. minimising cell death hence increasing probabilities to apoptosis occurrence.

However, with Annexin V assay, curcumin appeared to be non-apoptotic at its IC₇₅ value, but the same IC value is cytotoxic to the primary brain tumour cells as seen in the previous assay. One could speculate that the concentration of curcumin used in this study may be too low to elicit apoptosis or that it may be high enough to result in necrosis.

The IC₇₅ value (with the least cell death among other IC values studied) caused less cytotoxicity (more viable cells remained). Less cytotoxic level of curcumin concentration may have directed the unhealthy cells (not viable) to either undergo early or late apoptotic or necrotic event according to the condition of the cells at cellular level. Cells that were gated via flow cytometry analysis were mostly necrotic and very slightly in apoptotic areas (early and late quadrants). The necrotic event seen may be the outcome of the serial passage of the biopsy-derived cells. These fragile cells may have changed in durability while experienced difference microenvironment when propagated *in vitro*. Therefore, via flow cytometry analysis, most of the cells were gathered in the necrotic quadrant rather than apoptotic ones. It is also plausible that among the unhealthy cells, there was other proportion of cells that become externalized hence exposed the phosphatidylserine (PS) to be recognized by Annexin-V molecule. This may be little yet not significant to conclude that curcumin induced apoptosis occurrence but requires further investigation.

Indeed, there is no cut off point that is certain to hold on that will definitely trigger apoptosis to occur. The IC values used to investigate apoptosis may thus reflect curcumin cytotoxicity via non-apoptotic pathways. As seen in the initial assays, cell viability decreased

as the concentration of curcumin increased, suggesting that very high concentrations of curcumin could have been toxic to the cells which reflects an inhibition of cell growth but did not result to apoptosis to occur in the cells. It is also possible that the inhibitory action of curcumin to these primary brain tumour cells is due to arrest of the cell cycle. This is supported by a curcumin study which showed that the percentage of U251 cells (malignant glioma cell line) in G0/G1 and G2/M were decreased and increased respectively, after treated with curcumin (4 or 10 μ M) (Liu et al, 2007). Another study has also demonstrated that 15 μ M curcumin induced cell cycle arrest at G2/M phase in U251 cells (Wang et al., 2015).

Although in the previous study, curcumin at the same range of concentration was noted to induce apoptosis in an established malignant glioblastoma cell line (Abdullah Thani et al., 2012), this was not the case in the primary brain tumour cells in this study. There may be underlying features that are responsible for the evasion of apoptosis in the microenvironment. It has been reported in both neurons and prostate cancer studies that evasion of apoptosis occurred due to the cancerous cells that produce Insulin growth factor (IGF) survival factors, proteins with high sequence similarity to insulin. Furthermore, IGF proteins used by cells to communicate with their physiological environment which resulted in increased cell proliferation and decreased apoptosis (Chung et al., 2007; Tu et al., 2010).

In contrast, compelling scientific and dietary evidence has demonstrated the potential of curcumin to induce apoptosis in various cancer cells. Indeed, curcumin has been widely reported for its pro-apoptotic potential in various tumour cells, both *in vitro* and *in vivo*. This includes induction of several mechanisms responsible for curcumin pro-apoptotic activity such as caspase-cascade and mitochondria-dependent pathways, production of superoxide anions and involvement of p53 as well as inhibition of many other cell signalling pathways. Curcumin's roles in anti-cancer activity also include the inactivation of Activator Protein-1, Phosphatidylinositol 3-kinases, enzymes (Cyclooxygenase-2, MMPs), cell cycle arrest

(cyclin D1), proliferation (Epidermal Growth Factor Receptor and Akt), survival pathways (β -catenin and adhesion molecules), and Tumour Necrosis Factor. PI-3 kinase activity produced growth factor and regulators upon its activation. Akt-pathway or protein kinases B/RAC inactivate pro-apoptotic factors like Bad as well as anti-apoptotic genes (Dorai, 2004).

However, the apoptotic occurrence may be limited by other factors and cellular event in the microenvironment. For example, curcumin's pleiotropic roles in anti-cancer activity have been reported (Dorai, 2004) mainly on inactivation of transcription factor, NF- κ B. In various cancers NF- κ B is deregulated with increased expression of anti-apoptotic proteins. Thus, an interplay of a multitude of factors are thought to be unsolved but not elucidated yet. A critical review on emerging literatures regarding survival and apoptosis signalling in GBM has highlighted experimental, preclinical and recent clinical trials attempting to target these pathways. It has been suggested that combining the therapies of targeting apoptosis and survival signalling defects might result in greater cytotoxic effect and inevitable apoptosis. The review has taken vast collection of studies which has used glioblastoma cell line such as U87MG, D54MG. It has been suggested that targeting apoptosis resistance would likely resulted to efficacy in increasing survival. Therefore, combining these two targets (apoptosis resistance and survival signalling) might be associated with greater therapeutic benefits (Krakstad and Chekenya, 2010).

Curcumin suppressed angiogenic activity of primary brain tumour cells in vitro

The results of this study have shown that curcumin has demonstrated the anti-angiogenic effect towards these malignant glioma cells (MUBS, MUP and MUTC) *in vitro*. Indeed, angiogenesis is one of the most important parameters involved in tumour developments which accompany glioblastoma progression through the development of a new vascular

network for the glioma cells to survive in the tumour microenvironment. Angiogenesis can be divided into 3 stages: endothelial cell (EC) proliferation, EC migration and vessel morphogenesis which results in polygons or honeycomb patterns in the formation of a complex mesh. An animal study (Perry et al., 2010) has shown that curcumin inhibited tumour growth and angiogenesis in glioblastoma as indicated by the decreased endothelial cell marker from newly formed vessels and by the reduction of the haemoglobin concentration. Another animal study has also shown that curcumin suppressed angiogenesis in the ovarian carcinoma by inhibiting the transcription factor nuclear kappa B (NF- κ B) (Yvonne et al., 2007). Particularly in GBM which is highly vascularized within the hypoxic region, angiogenesis is mediated by vascular endothelial growth factor (VEGF), a factor that has been demonstrated to be present in the cyst fluid from glioma at high concentration (Takano et al., 2010).

However, it has been debated in the literatures that VEGF is not the only factor responsible for angiogenesis to occur in tumour cells. Numerous previous studies have demonstrated curcumin's potential therapeutic effect in regulating a variety of pro-angiogenic factors, enzymes and transcription factors which include bFGF, angiopoietin-1 and 2, COX-2, matrix metalloproteinase-9 (MMP-9), activator protein-1 (AP-1) and NF- κ B (Gururaj et al., 2002; Mohan et al., 2000; Yoysungnoen et al., 2006). Other factors such as integrins, adhesion molecules and proteases also have an integrated role in permitting and mediating angiogenic potential in many malignant tumours (Ray et al., 2003). Moreover, another animal study has also presented that curcumin exerts *in vitro* anti-angiogenic and *in vivo* anti-tumour properties through combined PDE2 and PDE4 (Cyclic nucleotide phosphodiesterases 2 and 4) inhibitions. Their up regulations in human umbilical vein endothelial cells are implicated in VEGF-induced angiogenesis. Thus, inhibition of PDE2 and PDE4 activities increased

cAMP level which in turn inhibited VEGF-induced endothelial cell proliferation and migration (Abusnina et al., 2015).

Our results showed that in the primary brain tumour cell cultures studied, the number of nodes decreased when treated with increased concentration of curcumin. Of all primary brain tumour cell cultures, MUBS cell cultures was the only cells that decreased significantly in all angiogenic parameters (nodes, junctions, branches, total tubule length) at all concentrations studied. Besides the number of nodes, other angiogenic measures such as the total length of tubules had high values but curcumin treatment reduced the formation of tubules. While this may suggest curcumin anti-angiogenic potential in the treatment of glioblastoma, it also had indicated curcumin's safety profile. In the normal brain cells, each parameter (number of nodes, junctions and branches) was maintained with increasing concentrations of curcumin (0 to 40µg/ml) hence depicted curcumin efficacy as a highly pleiotropic molecule as well. Moreover, its long history of medicinal use, especially for the treatment of inflammation and many of other traditional therapeutic uses have been extensively demonstrated in cellular systems as well as in animal models of disease (Aggarwal, 2009).

There are a lot of divergent opinions published in earlier years which have suggested the best method (both *in vitro* and *in vivo*) in analysing angiogenesis (Aeurbach and Polakowski, 1991; Fan and Polverini, 1997; Bishop et al., 1999). Several steps exist in angiogenesis, i.e. proliferation, migration and invasion, sprouting and vessel formation, and vessel modelling and reorganisation. Therefore, these key events neither are reflected in an *in vitro* assay alone nor *in vivo* study. For that reason, in this study, Matrigel assay was chosen for angiogenesis *in vitro* assay. Moreover, according to a review on bioassays involving brain tumour- induced angiogenesis, with an *in vitro* setting, certain key events are measureable in a short period of time while leaving other parameters not detected (Hock et al., 2013). Indeed, this study

investigated the efficacy of a potential anti-angiogenic agent, i.e. curcumin, which is easy to perform via *in vitro* assay as to prevent certain aspects of the *in vivo* condition, such as artificial cells responses towards treatment, i.e. considering the complexity of glioma cells microenvironment.

The *in vitro* angiogenesis assay described in this study offered the simplicity and speed in measuring the angiogenic event which could not be achieved through *in vivo* assays. The tubules network formed by endothelial cells may not a resemblance to the capillaries formed *in vivo*. This is due to the fact that this *in vitro* assay was shorter in time for completion hence the endothelial cells activity (perhaps proliferation, migration as well as differentiation) may not be greater as compared to the long run of *in vivo* angiogenesis assays. Moreover, while *in vivo* assay requires higher demand in time, material as well as maintenance, surgical skills are also needed and result can be inaccurately interpreted.

For both *in vivo* and *in vitro* settings, parameters such as branching, sprouting, tubule length or number of connecting tubules (junctions) are common and widely used for the estimation of angiogenic capacity of the tumour cells to form tubules. However, not all of the parameters may be necessarily applied as it can also depend on the type of cells and analysis. It was observed that in kidney cells, tubule formation on matrigel was no longer occurred unless the medium was further supplemented with epidermal growth factor (Taub et al., 1990). In addition, the morphology of tubules may vary between different types of assays as demonstrated in another study (Donovan et al., 2001). Thus, the consideration of which parameters to be used in angiogenesis assay is depending on the types of analysis (*in vitro* or *in vivo*) and cells.

For most of *in vitro* angiogenesis assays involving cancer cells, number of junctions, branches and nodes and total length of tubules were chosen to be used. However, the first two

measures (number of junctions and branches) were not demonstrated as they were negligible and insignificant in values as compared to the normal brain cells hence were not considered relevant to be studied further in demonstrating the angiogenic capacity in this study.

In summary, normal brain cell in a co-culture angiogenesis assay model showed no dose response to curcumin. Moreover values for the main tubule network parameters were lower than those achieved where co-culture with the neoplastic cells MUBS and MUTC were involved. Cell cultures MUP and MUBP gave intermediate overall readings. As the HUVEC cells and the brain cells were separated by a membrane, the effect is mediated by soluble factors rather than cell contact.

Corresponding to the overall picture, dose responsiveness to curcumin was also strongest with MUBS and MUTC, increasing doses of agent further inhibiting angiogenic parameters. MUBP showed increased tubule formation at the lowest curcumin dose tested (10µg/ml) but an inhibitory dose response thereafter. The dose responsiveness of MUP cells was less smooth, but inhibition was seen.

Patterns of inhibition were similar with all of the tubule network parameters measured. There is a strong indication from these experiments that curcumin might have anti-angiogenic properties that are relatively specific for at least some tumour cell types. The caveat is, of course, that HUVECs are not representative of all endovascular cell types and that the angiogenesis assay itself is a simple monoculture, albeit on Matrigel, an artificial 3-dimensional substrate including basement membrane components.

The effect of Curcumin on the invasive potential of glioblastoma cells

In addition to curcumin's potential therapeutic effects on angiogenesis, our results have also demonstrated that curcumin has the potential to affect the invasive potential of these

malignant gliomas. Three of the primary brain tumour cell cultures investigated (MUBS, MUBP and MUP), were high in the invasive capacity but curcumin treatment at IC₇₅ concentration reduced the percentage of invasion as early as 24 hours of incubation (fig 27, section 3.6 in chapter 3). MUTC cells however did not show invasive potential and curcumin treatment demonstrated no significant change in the reduction of invasive capacity of the cells. An alternative scratch assay was not chosen here as motility of the cells was not the parameter to be investigated. Moreover, a pilot study with scratch assay was carried out by others which always give consistent results (e.g. distinct area) for migration however resulted to qualitative and subjective in interpretation.

Glioblastoma rarely metastasizes to the periphery but there is a high propensity for these tumours to invade locally (Holland, 2000). This invasion occurs along the white matter tracts, with GBMs often crossing the midline via the corpus callosum. The tumour cells also migrate by direct invasion into the adjacent brain parenchyma, involving progressive replacement of normal brain tissue (Mikkelsen and Bjerkvig, 1998). Moreover, previously this series of processes has involved the redistribution of protease receptors to sites of dynamic change in neural cell processes, and in invading cell processes in cancer cells (Deryugina et al., 1997; Binder and Berger, 2002). Invasion is the most significant biological feature of glioblastoma multiformes that precludes successful therapy. The tumour cells infiltrate the normal brain in a complex way, thereby rendering all current forms of therapy ineffective. Invasion in glioblastoma includes three different but interrelated pathways; proteolytic alteration of the extracellular matrix, secretion of new extracellular structural proteins, and adhesion to elements of the matrix for which membrane-bound receptors exist (Pilkington, 1994). Thus, the cross-talk between cell-surface receptors and the redundancy of downstream effectors make analysis of invasive signals even more complex.

The anti-invasive potential of curcumin identified in this research is supported by other studies suggesting pathways or downstream events have been affected by curcumin. Indeed, these effects are facilitated through curcumin's regulation on various transcription factors, growth factors, inflammatory cytokines, protein kinases, and other enzymes. For examples, results of a downstream effect study (Senft et al., 2010) involving glioblastoma cell proliferation, migration and invasion was suggested to be hampered by curcumin through JAK/STAT3 pathway. It was also demonstrated in an animal model that curcumin attenuated glioma growth by inhibiting the JAK1, 2/STAT3 signalling pathway (Weissenberger et al., 2010) which holds promise for clinical application in glioma therapy.

There are many reports have documented curcumin anti-invasive potential in various signalling pathways in cancers. Curcumin was shown to inhibit JAK/STAT signalling via phosphorylation of STAT hence resulting in a significant reduction in nuclear phosphorylated-STAT-1 (Wang et al., 2009) which resulted in inhibited cell proliferation and apoptosis in hepatoma cell line. Curcumin has also significantly inhibited JAK2/STAT3 signalling in laryngeal squamous cell carcinoma which resulted to inhibition of invasion and vasculogenic mimicry *in vitro* (Hu et al., 2015). The anti-inflammatory property of curcumin was delivered through the inhibition of JAK1 and JAK2 phosphorylation via the increased phosphorylation of SHP-2 and its association with JAK1/2 (Kim et al., 2002). Phosphorylation of SHP-2 makes it a negative regulator of the JAK-STAT pathway (Kim et al., 2003). It has also been demonstrated that curcumin inhibits STAT3 phosphorylation in ovarian cancer cells (Seo et al., 2010). Moreover, a previous study of human lung adenocarcinoma cells has reported that 1–20 μ mol curcumin inhibited cancer cell invasion and metastasis through activation of the tumor suppressor DnaJ-like heat shock protein 40 (HLJ1) hence leading to activation of the JNK/JunD pathway (Chen et al., 2008). In addition, curcumin has been shown in microglia in which the JAK/STAT pathways were inhibited.

Therefore, it could be suggested that our previous finding on curcumin cytotoxicity effect on the cells integrity has interrupted the transmitting signals from the cell membrane to the nucleus following response to extracellular growth factors and cytokines. The activation of this series of pathways has been found in many tumours including in brain tumours (Tu et al., 2011) and lung cancer (Ye et al., 2012).

Variations in the antigen expression induced interplay of multitude events in glioblastoma cells

In this study, the results have also indicated that there were variances in the level of expressions of antigens studied which observed among the four primary brain tumour cells via immunocytochemistry and flow cytometry techniques. Differences in morphology, genetic and immunology arise from the same neoplasm, rendering the tumour mass highly resistant to both radiotherapy and chemotherapy. Published research has indicated that every cancer cells expresses specific proteins either inter or intra-cellularly with distinct functions and characteristics (Aplin et al., 1998; Ponta, Sherman and Herrlich, 2003; Luque-García et al., 2010). Thus, all findings obtained were linked together from this point onwards as to understand the whole picture of the study conducted.

For all glioblastoma cell cultures and normal brain cells, our results from the immunocytochemistry analysis with Alexa fluor 488 and PI staining showed strongly positive for GFAP (glial fibrillary acidic protein), a cellular antigen. GFAP has been selected as a positive control as it is widely known to be expressed in gliomas and can be regarded as a sensitive and reliable marker of astrocytes. Although there are still debates on GFAP existence either in oligodendrocytes or astrocytes, GFAP has been widely acknowledged and demonstrated as a positive control in this study due to its reliable and representative staining. A review on astrocyte biology and pathology has regarded GFAP as a sensitive and

reliable marker for astrocytic tumour (overexpressed) and normal astrocytes (consistently expressed) (Sofroniew and Vinters, 2010). Hence, this 47 kDa protein is widely used to confirm the astrocytic nature of glioblastoma which originate from astrocytic lineage. This is, usually done by immunostaining analysis with antibody against GFAP which is the classic intermediate filament contained within the cytoplasm of both astrocytic tumour and normal astrocytes. GFAP is heavily and specifically expressed in astrocytes, non-myelinating Schwann cells in peripheral nerves, peripheral ganglia (in satellite cells) and neural stem cells. However, many types of brain tumour (most probably astrocytic cell- derived) profoundly express GFAP (Knott et al., 1990; Hadjipanayis and Van Meir, 2009). Therefore, all primary brain tumour cells (biopsy derived) in this study are confirmed to be astrocytic in origin as demonstrated via immunocytochemistry analysis.

In our study, no NG2 results were available from the flow cytometry data due to time constraints. Moreover, not enough cells were harvested for additional staining at the time when flow cytometry assay was conducted. In addition, with the time that is limited, cell loss (as cells become fragile with passaging) was experienced and growing back the cells made such experiments unnecessary. However, it is suggested that there is an association between NG2 that expressed with angiogenesis that demonstrated *in vitro*. Prior to curcumin treatment in the angiogenesis assay *in vitro*, both MUBS and MUP cells (fig 28, section 3.8) were angiogenic in comparison with normal brain cells as shown by the high number of nodes and total length of tubules. Indeed, both cell cultures were also positive though weak in NG2 staining as seen in the immunocytochemistry analysis. Thus, it is suggested that NG2 is linked with the promotion of angiogenesis. It was reported that NG2's role in angiogenesis is due to its interaction with plasminogen and angiostatin in which modulation of the functional properties of both angiostatin and plasminogen resulted to cell migration and proliferation in the tumour cells (Chekenya et al., 2002a; Goretzki, 2000).

The same primary cell cultures (MUBS and MUP), were also found to have the shortest population doubling times (80 h and 154 h respectively). This finding is supported by a published study which reported that NG2 is present in GBM with high rates of cell proliferation *in vitro* (Chekenya et al., 2002a). NG2's role in tumourigenecity was investigated in an *in vivo* animal study involving implanting tumour spheroids (U251N cell line) intracerebrally into immunodeficient nude rats to see whether cell proliferation supported by NG2 activity *in vitro* would have the same effect *in vivo*. In the NG2-transfected U251N, it was observed that NG2 has increased the GBM tumourigenicity *in vivo* by 87.5%, compared to 40% in wild type (without NG2 being transfected) (Chekenya et al., 2002a). This implies that NG2's expression may correlate with an aggressive course when expressed on tumour cells. Therefore, high NG2 expression observed in both MUBS and MUP cell cultures may indicate that MUBS and MUP cells are angiogenic besides found to be proliferative in the capacity. This has been demonstrated in a study of tumour growth of central nervous system that NG2 promotes tumour angiogenesis *in vivo* by binding and sequestering endogenous angiostatin hence leading to increased tumour neovascularization (Chekenya et al., 2002).

A further study on NG2 expression in GBM has shown vascular leakiness, oedema and high microvascular density in comparison with the control. Intracranial distribution and volume of the tumour were reported as higher cellular densities with more mitotic figures that present as demonstrated via contrast-enhanced MRI (magnetic resonance imaging) analysis. Thus it is likely that NG2 has the capability to recruit neo-vasculature as well as regulating cell morphology thus suggested that NG2 might have been associated with cross-talk between tumour cells and cellular environment (Brekke et al., 2006; Caspani et al., 2014).

Initially, Chekenya et al. (1999) has been reported that NG2 expression is inversely related to the invasive capacity of the tumour cells. It was demonstrated in the migration and

invasion assays that NG2 positive glioma cells migrated more efficiently on collagen IV while NG2 negative cells were more invasive than the NG2 positive cells. NG2 is responsible in modulating both cell-extracellular matrix and cell-cell adhesion molecule hence it may have supporting migration in glioma but perhaps not invasion. NG2 positivity has also been reported in the normal human adult brain and peripheral tissues in which NG2 roles are not only in migration but also adhesion and differentiation of cells. However, (Chekenya and Pilkington, 2002) in an experiment of xenografting Ki-67-labelled cells into nude rat brains showed that NG2 is important in proliferation rather than migration or invasion activity in human glioma cells.

Taken together on NG2's various roles in tumourigenicity, our results showed weak positivity in NG2 expression in MUBS and MUP cell cultures and negative in other cell cultures. NG2, as with most studies (Burg et al., 1997, 1998; Wiranowska et al., 2006) is a cell surface marker was first identified in immature glial cells and has been shown to have strong associations with ECM ligands such as collagen IV and cellular ligands such as CD44. In another study, it was suggested that not only CD44, NG2 is also an invasive marker in gliomas which both demonstrated to aid the tracing and targeting the invading cells (Wiranowska et al., 2006). Thus, it is likely that NG2 has an indirect role in mediating invasion by interacting with certain adhesion molecules like CD44 to various ECM components. Unfortunately, via immunocytochemistry assay, NG2 was not detected in MUBP and MUTC cells and weakly positive in MUBS and MUP cells. It could be suggested that MUBS and MUP cell cultures (besides MUBP) that showed invasive potential via the invasion assay *in vitro* may not necessarily due to the role of NG2 but perhaps there are other antigens present that may have contributed to proliferation, survival, migration, invasion and angiogenesis in these glioblastoma cells. Therefore, the results obtained in this study may

suggest that the invasive capacity in these cells may be regulated by expression of multiple factors by different cells that overlap in the malignant microenvironment.

Indeed, the cross talk of signalling network transmitted between these antigens may be responsible for the contradictory seen in this study. Such example is CD44, one of the major categories of adhesion molecules besides integrins immunoglobulin superfamily and selectins (Aplin et al., 1998). They are expressed on the extracellular surface of the cell via a complex interaction between the tumour cell and the glial limitans externa, the brain parenchyma and the vascular basement membrane. With respect to CD44, our results from the qualitative immunocytochemistry may have only showed two cell cultures (MUBP and MUBS) that were intense in CD44 staining compared to the normal brain cells. However, the quantitative flow cytometry analysis demonstrated that the level of CD44 expressed were significantly high in all glioblastoma cells investigated. CD44 immunostaining may not correlated with flow cytometry analysis but both confirmed the expression of the antigen though not in all cells and it so happened that with flow cytometry technique is a better assay to determine the level of antigen expression of such as CD44.

Thus, the invasive potential determined in these glioblastoma cell cultures (MUBP, MUBS and MUP) are suggested to be indirectly co-ordinated by the CD44 positive cells that present. This is consistent with studies (Radotra, 1997; Ji et al., 2009) suggested that glioma invasion *in vitro* is mediated by hyaluronan interaction with CD44. Overexpression of CD44 in glioma is related to invasion in which the receptor binds with hyaluronic acid (HA) in the extracellular matrix, leading to cells detachment induction and stimulates migration and invasion of glioma cells *in vitro* (Merzak et al., 1994; Koochekpour, et al., 1995; Radotra et al., 1997; Bouterfa et al., 1997; Knupfer et al., 1999; Ranuncolo et al., 2002; Ji et al., 2009). Therefore, the increase in the expression of CD44 observed in these glioblastoma cells may add to the potential migration and invasion capacity of the cells. It is possible that there

would have been molecular events that have modulated the migration in these primary brain tumour cells at any stage of growth, hence contributed to the highly infiltrative nature characteristic of a glioblastoma multiforme. Indeed, migration and invasion are co-ordinated and integrated events identified by Liotta (1986) in the sense that extracellular matrix proteolysis and migration is mutually dependent. Although migration and invasion are often used interchangeably in the perspective of malignant gliomas, migration refers to the locomotive capacity of the tumour cells while invasion includes degradation of extracellular matrix barriers by proteases.

It is tempting to suggest that the angiogenesis activity detected in these two glioblastoma cell cultures (MUP and MUTC) may be due to the role(s) of CD44 that measured in flow cytometry assay. Indeed, CD44 is also responsible for mediating angiogenesis indirectly in addition to its role in promoting invasion in glioma cells. It is possible that CD44 positive cells detected in all four primary brain tumour cells studied may have produced high amount of hyaluronic acid (HA). As one of the main components in the extracellular matrix of the brain, high production of hyaluronic acid provides hydrated spaces that support glioma cell migration and angiogenesis. Both processes are under the tight regulation of a balance between stimulating and inhibiting factors. This is supported by a number of studies on CD44 positive glioma cells that interacts with hyaluronic acid produced angiogenesis *in vivo* and further promoted tumour establishment (Wiranowska et al., 2010; Onishi et al., 2011; Park et al., 2012). It is feasible that there is an association and alteration of glioma environment which requires a complex cross-talking between endothelial and tumour cells, extracellular matrix components, and cellular elements of the host microenvironment.

From the flow cytometry analysis, MUBP cells have high level of beta-1-integrin and CD44 level. As demonstrated in a glioma study, it appears that integrins are fundamental in

the process of tumour cell invasion, in which perturbation of integrin function can inhibit invasion *in vitro*. Integrins are crucial for cell invasion and migration, not only for physically tethering cells to the matrix, but also for sending and receiving molecular signals that regulate these processes (Rooprai et al., 1999). This may mean that there is a possible interaction between the two protein families on promoting invasion activity in the glioblastoma cells. In comparison, MUBS and MUP cells showed high level of CD44 expression (as with MUBP and MUTC), but the level of beta-1-integrin was much lower. However, these cells showed a high invasive capacity as measured via *in vitro* invasion assay. Hence, the level of beta-1-integrin was greatly varied among cell cultures studied. It could be suggested that the invasive capacity possessed by these two cell cultures (MUBS and MUP) was promoted by beta-1-integrin which was highly expressed in the immunocytochemistry analysis.

In addition, previous studies have indicated that beta-1-heterodimers are over-expressed in glioma primary cultures. Blocking its function with specific antisera decreased the ability of glioma cells to adhere to, and invade through many different extracellular matrix proteins *in vitro* (VanMeter et al., 2001). Furthermore, increased expression of certain integrins and of CD44, has been associated with glioma malignancy hence play a role in migration of gliomas *in vitro* (Giese and Westphal, 1996; Rooprai et al., 1999; Stivarou and Patsavoudi, 2015).

Among the eight Beta sub-units integrin members, Beta-1 is the most important one to glioma biology in which its expression has been correlated with the invasive behaviour of glioma (Paulus et al., 1996). An altered integrin expression was suggested to contribute an influence on the development of the malignant phenotype via many fundamental processes which include proliferation, resistance to apoptosis, genomic instability, MMP expression and invasion (Jones, 1999). Previously, it has been reported that neutralizing antibodies directed towards beta-1-integrin result in suppression of glioma migration *in vitro* (Tysnes

et. al., 1996). *In vivo* overexpression of beta-1-integrin in rat glioma cells (C6) implanted intracranially into the brain of nude mice leads to diffuse invasion in the brain (Paulus et.al, 1996). Integrins, cell surface receptors mediate the physical and functional interactions between a cell and its surrounding extracellular matrix (ECM). Hence, its role has been ascribed to anchoring cells to the ECM. Indeed, the role of specific integrins in tumourigenesis has been demonstrated in numerous cancer types which include breast and lung cancer (Taherian et al., 2011; Morello et al., 2011). Integrins, such as beta-1-integrin, due to their location on the cell surface and interactions with the extracellular matrix proteins, are known to be ideal candidates to mediate both migration and invasion.

As in these primary brain tumour cell cultures, none of them expressed GD3 as demonstrated via immunocytochemistry. GD3 belongs to gangliosides that are normally present at high concentration in the brain and ubiquitous in the body but over-expressed in malignant gliomas (Berra, 1985; Gaini et al., 1988; Ohkawa et al., 2015) in which correlates with the degree of biological aggressiveness. A study (Koochekpour, 1996) has shown that 100% positive in immunoreactivity in GBM but only 70% in grade III gliomas. GD3 is clearly seen in the perivascular areas including cytoplasm and endothelial cells. This may suggests that GD3 expression is correlated well with the degree of malignancy and potential involvement in neovascularization.

Neovascularization or angiogenesis is a hallmark in gliomas when GD3 was suggested to be a potent stimulator of VEGF release in human glioma cell lines and demonstrated to be highly expressed in hypervascularised areas of high grade gliomas (Koochekpour and Pilkington, 1996). However, acetylation of GD3 (addition of an acetyl group to the terminal sialic acid of GD3) by specific sialate -9-0-acetyl transferase renders apoptosis not to occur and reversal of it made the cells undergo apoptosis (Birks et al., 2011). It is possible that GD3 in these cells is either not being expressed or have been acetylated

thus resulted to GD3 negative cells detected in these glioblastoma cells. Therefore, in addition to the proposed non-apoptotic mechanisms that may have occurred (as discussed), acetylation or particularly the absence of GD3 in these glioblastoma cells may have resulted apoptosis not to take in place as demonstrated by Annexin V staining via flow cytometry. GD3 is a major ganglioside constituent of the embryonic brain that mediates migration as well as inducing apoptosis in the progenitor cells (Ogiso et al., 1991). Increase of GD3 in a variety of cell lines has been shown to facilitate apoptosis to occur which includes direct interaction with the mitochondrial permeability transition pore (MPTP), enhanced production of reactive oxygen species, suppression of the NF κ -B survival pathway, and promotion of CD95/Fas-mediated apoptosis (Colell et al., 2001; Chakrabandhu et al., 2008).

Our results have also demonstrated that MMP-14 was highly expressed in one of the glioblastoma cell culture, MUTC, by two-fold from that detected in normal brain cells (Fig 26, section 3.5.2 in results chapter). The other three primary brain tumour cells were either similar to MMP-14 measured in the normal brain cells or low in the expression of MMP-14 suggesting that they were not as invasive as MUTC. However, via invasion assay *in vitro*, MUTC cells that were found to show high MMP-14 in immunostaining (flow cytometry) were not invasive as compared to normal brain tumour cells. Moreover, MUTC level of invasion remained unaltered before and after treatment of curcumin. The remaining glioblastoma cells (MUBS, MUBP and MUP) expressed low level of MMP-14 as measured by flow cytometry, but in contrary, high level of invasion activity was detected in the *in vitro* invasion assay. Thus, to suggest that MMP-14 is inversely related to the invasion activity in cancer cells is somewhat contradict to what have reported in other studies. Overexpression of MMP-14 in human glioma samples was determined by several studies which include MMPs expression (including MMP-14) in both primary cells and established cell line of glioblastoma (Fillmore et al., 2001; Hagemann et al., 2010; Hagemann et al., 2012). Other

studies have shown that MMP-14 is expressed highly in tumour samples derived from higher grades of malignancy (Van Meter et al., 2001; Fillmore et al., 2001). MMP-14 mRNA level was significantly higher in malignant glioblastomas as detected via Northern blot and real-time PCR analysis but it was not detectable in normal brain tissues (VanMeter et al., 2001; Nakada et al., 1999; Nakada et al., 2001; Nuttall et al., 2003).

Membrane type matix metalloproteinase (MT1-MMP or also known as MMP-14) is involved in different pathophysiology of gliomas which include not only invasive property of the malignant gliomas but also angiogenesis activity of the tumour (Forsyth et al., 1999; Deyrugina, Soroceanu and Strongin, 2002; Deyrugina and Quigley, 2015). A correlation between MMP-14 and MMP-2 has long been established when a previous study showed that U251MG glioma cells transfected with MT1-MMP resulted in cell surface expression of MT1-MMP and constitutive activation of MMP-2. MMP-14 transfectants also caused increased migration in spheroid outgrowth assays and this effect was enhanced on collagen than fibronectin and vitronectin (Deyrugina et al., 1997). Furthermore, it is well documented that high levels of MT-MMPs, such as MMP-14 are expressed by gliomas and promote MMP-2 activation hence playing a role in the regulation of invasiveness (Nakada et al., 2001; Hakulinen et al., 2008).

Therefore, with respect to MMP-14 correlation with invasiveness of glioma, our immunostaining (flow cytometry) finding is not in agreement with the invasion activity detected via *in vitro* invasion assay. The reason for this is not immediately apparent but can be the subject of future investigations. Lower passage of cell cultures may be used in future as it may contribute towards changes in the expression of MMP-14 when passaged continuously. A comparative study (Hagemann et al., 2010; Hagemann et al., 2012) between established cell line and primary cells suggested that there is a large variation in the MMPs expression which are changeable with duration of cell culture and are highly dependent of

cell culture conditions and cell-density. This complex microenvironment of GBM pathogenesis is still ambiguous, and it is appealing to speculate that depending on the environment, glioma cells will upregulate different MMP members to help achieve their growth. Such example is from a study on a glioma invasion which suggested that glioma cells exploit their astrocyte environment for the production and activation of MMP-2 which resulted to the increased ability of glioma cells to invade (Lee et al., 2003). Thus, it may not be MMP-14 as the only factor that responsible towards invasive characteristic of the glioblastoma cells studied seen in the invasion assay.

Vascular endothelial growth factor (VEGF) pattern seen in this study is similar to the pattern of MMP-14 level of expression. Three of the glioblastoma cell cultures studied, except MUTC cells were low in the VEGF level compared to normal brain cells thus suggests that they are non-angiogenic. Perhaps, their angiogenic capacity may not solely depend or be attributed by the level of VEGF expression but other factor such as CD44 as discussed earlier. Not only responsible for angiogenesis, VEGF also have a role in mediating invasion activity in tumour cells. From our results on invasion assay *in vitro*, it is suggested that high invasive capacity measured in the three glioblastoma cells (before reduced by curcumin treatment) was due to the low level of VEGF that detected in the flow cytometry analysis. This finding is consistent with other studies when inhibition of VEGF signalling has been reported to increase the invasiveness and metastasis in some preclinical models (Rubenstein et al., 2000; Casanovas et al., 2005; Ebos et al., 2009; Paez-Ribes et al., 2009). The mechanism of the aggressiveness is speculative but participating factors could increase the expression of c-Met, the tyrosine kinase receptor for hepatocyte growth factor (HGF). These findings are supported by the recent discoveries made in glioblastoma and pancreatic cancer studies.

With respect to MUTC cells, our results showed that high level of VEGF was detected in flow cytometry analysis when low invasive capacity was measured using *in vitro* invasion assay. It has been reported that VEGF expression is strongly associated with tumour aggressiveness and early relapse which indicates poor prognosis and shorter survival of glioma patients (Bergers, 2003; Hardee, 2012). However, there is also a recent report that suggested that an overexpressed VEGF suppresses invasion in glioblastoma which provides some initial benefit for patients (McCarthy, 2012). Although this is specifically applied for patients with glioblastoma who express both mesenchymal-epithelial transition (MET) factor and Vascular Endothelial Growth Factor Receptor 2 (VEGFR2), this mechanism of suppression in invasion was also experienced in pancreatic cancers which not only slows tumour growth but also decreases invasion and metastasis by concurrent inhibition of c-Met and VEGF signalling (Sennino et al., 2012). However, it is not known whether MUTC cells express both factors (MET and VEGFR2) in order to have this benefit.

In glioblastoma multiforme cells, it is understood that the balance of angiogenic growth factors is resulted from both activation of oncogenes and inactivation of tumour suppressors which then responsible for the up-regulation of pro-angiogenic pathways (Gatson, 2012). It has been reviewed that solid tumour survival is dependent on angiogenesis which is new blood vessels formation where they gain nutrient and oxygen from and occurs in the presence of angiogenic factor such as vascular endothelial growth factor (Merzak, 1997). Thus it is suggested that, inhibition of VEGF in malignant glioma patients has withholds tumour recurrence together with impressive radiological responses and reduction in peritumoural oedema (Stupp, 2012). Such inhibition is through the treatment with the anti-VEGF monoclonal antibody bevacizumab, which delays progression and prolongs survival of some patients but results in increased vascular co-option (an alternative way to obtain blood vessels through pre-existing vessels).

VEGF is an endothelial cell-specific mitogen that induces not only angiogenesis and permeabilization of blood vessels *in vivo* but also a central role in the regulation of vasculogenesis (Neufeld et al., 1999). Its normal functions include forming new blood vessels following injury and during embryonic development. However, deregulation of VEGF has been reviewed in many cancers which resulted to the development of solid tumours by promoting tumour angiogenesis and inhibition of VEGF signalling that abrogates the development of a wide variety of tumours. For instance, it was reported previously (Neufeld, 1999) that VEGF is abundantly expressed in glioma cells which reside along necrotic areas and this expression is potentiated in response to hypoxia, by activated oncogenes, and by a variety of cytokines.

As demonstrated in this study, the invasive or angiogenic capacity of these glioblastoma cells investigated may not be attributed to one common factor as has been reported before, but perhaps an integration of many factors that overlapping in functions. MMP-14 that is well known for its contribution in promoting invasion may not be always the case as CD44 or NG2 are also have indirect roles in mediating invasion and angiogenesis of the cells. The network signalling transmitted by these factors in the microenvironment is made more complex by the addition of beta-1-integrin with a role that correlates with the invasive behaviour of glioma cells, VEGF that facilitates both angiogenesis and invasion and GD3 with a role in promoting apoptosis.

The reliability of flow cytometry technique against Enzyme-Linked ImmunoSorbent Assay (ELISA) in detecting antigen's expressions could be arguable as both have pros and cons in their system. This study used flow cytometry technique as part of collaboration with Cancer Research UK as well as a continuity and expansion to previous studies (Rooprai et al., 2001; Rooprai, Christidou and Pilkington, 2003; Rooprai et al., 2007; Abdullah Thani et al., 2012). Indeed, flow cytometry technique has been chosen to be the standard analysis but for

different potential therapeutic agent being studied. Flow cytometry provides thousands of cells thus consistency is reliable hence resulting to data that are only cell based. ELISA, which gives a single optical density, requires less cell numbers thus provides more replicates for each assay. Indeed, both techniques are equally manageable but a selection is important thus flow cytometry was chosen over ELISA.

Heterogeneity of glioblastoma cells contributes to sophisticated expression of markers and varied population doubling time

In this study, our result in cell morphology showed that, compared to normal brain cells, the human glioblastoma cells were heterogeneous with different subtypes of varying shapes and sizes seen in a population of cells. It is suggested that the heterogeneity of the astrocytes may be greater than previously thought and this will become evident as molecular markers become more sophisticated. This is likely to impact on ideas about how astrocytes are involved in both health (normal astrocytes) and disease (glioblastoma which is astrocyte origin) (Nedergaard, Ransom and Goldman, 2003). The morphology of normal human brain cells is more homogeneous in nature compared to that of malignant gliomas. CC2565, which is a normal human astrocytic cell line, has clearly depicted more the unicellular morphology of the brain cells. As seen in the photomicrograph (Figure 16A) in the result chapter, the morphology of CC2565 cells was identical in one population of cells and uniform in the shape and size of the cells. Further sub-culturing of CC2565 may have developed increased homogeneity of cell populations which was also observed in a study of glioblastoma cells (Parker and Pilkington, 2006).

However, unlike normal brain cells, glioblastoma cells showed variability in cell morphology (fig 15, section 3.1). It was also demonstrated that astrocytic gliomas exhibited not just heterogeneity as seen in the morphology, but also the molecular heterogeneity. This

molecular heterogeneity provides potential targets for developing molecular targeted therapies (Huang, et al., 2009). Such information has an impact on the glioma management. These include consequences that are reflected in the *in vitro* phenotype such as in the growth rate and sensitivity towards chemotherapeutics (Yung and Shapiro, 1982) and the therapeutic resistance of the tumours to treatment which partly contributed by distinct intratumoural cellular heterogeneity (Hamerlik, Rich and Lathia, 2013).

Glioblastomas are extremely malignant neoplasms which have a high mitotic rate, often comprising pleomorphic astrocytic cells with marked nuclear atypia and necrosis (Pilkington, 2001). Indeed, Glioblastoma Multiforme was named due to its extreme variability in cell morphology and it shows a great variety from patient to patient (Salcman et al, 1995). The word “multiforme” derives from the tumour’s varied morphological features and heterogenous population of cell that present within a single tumour bed. This term represents the histopathologic description of lesions with a high degree of cellular and nuclear polymorphism. Moreover, cells size and shape in glioblastomas are ranged from small, undifferentiated with hyperchromatic nuclei and numerous multinucleated giant cells which coexist with areas of high cellular uniformity (Kleihues, 2000; Kleihues et al., 2007; Ohgaki and Kleihues 2013). In addition, pseudopallisades are associated with necrosis and constantly being a significant feature in GBM (Salcman et al, 1995; Rong et al., 2006). It also distinguishes GBM from lower grade astrocytomas, signalled a transition to more aggressive behaviour of brain tumour hence incorporated in the pathologic definition (Wippold et al., 2006). Indeed, glioblastoma is heterogenous in characteristic compared to other tumours and numerous studies have demonstrated that cells within a glioma differ not only in morphology but also in their genetics and biological behaviour. For example, it was demonstrated that over-expressions of epidermal growth factor receptor (EGFR) in heterogenous tumour of

glioblastoma activated interclonal communication which resulted to an enhancement of the tumour growth (Bonavia et al., 2011).

The heterogeneity seen in these glioblastoma cells likely reflects the individuality of the tumours of origin and genotypes as well as the capacity for a range of phenotypic expression of the cells. In addition, the biopsy reports of these four primary brain tumour cells were different from each other in their histological sections review. Although all four showed typical features of glioblastomamultiforme, i.e. vascular proliferation or necrosis with mitoses and nuclear pleomorphism, the other histological differences noted may contribute to the variation of cytological features and patterns in each primary brain tumour cell cultures. These variations reported include chromosome 1p19q deletion, the presence of some occasional giant cells and addition of gemistocytic astrocytes (see biopsy reports in appendix). Unfortunately, with regards to the pathology reports obtained from King's College Hospital (the origin of the GBM cells, biopsy-derived), no other information was given (unless written in the report). Moreover, it is now impossible to get additional information as it may not have been necessary to have the data routinely at King's College Hospital at the time. Additional information such as EGFR, PDGFR etc. was not available previously (at time the reports were given) but may be added in future for the purpose of research.

Taken together, the difference noted in the morphology between normal brain and glioblastoma cells studied may suggests that there is a relation between the heterogeneity seen with the findings seen in the cell kinetics studied (population doubling time (PDT) assay) and variation in the antigenic expressions determined. Our population doubling time results showed that all four primary brain tumour cell cultures studied had relatively longer population doubling times, up to 208 hours but normal brain cells took only 40 hours to double in number (Fig 16). Unlike primary brain tumour cell cultures that are heterogenous, homogenous established glioma cell lines that have been investigated which include U373

and IPSB-18 had shorter population doubling time of 48 and 16 hours, respectively (unpublished data). As a result, the heterogeneity seen in these primary brain tumour cell cultures may explain the increased population doubling time compared to normal brain cells. In a population of cells, a particular cell that harbours with it different phenotype and genotype may have different capacity of growth and proliferation rates. Hence, several subpopulations of cells that exist in a tumour exhibit a range of doubling times. Furthermore, it is suggested that, as the cells are passaged, lingering cells with the highest growth capacity predominantly influence the PDT in each primary brain tumour cell cultures studied.

From our results, it is observed that the biological behaviour of these malignant glioma cells investigated are not straightforward but difficult to interpret not only because the pattern of antigens expressions in each of them are varied but also overlapping in functions to the cells, i.e. invasion, angiogenesis or induction of apoptosis. Primary cells derived from different patients can behave differently in culture conditions and this is likely to depend on many intrinsic factors such as genetics and age of individuals from whom the tissue was derived. MUBP cells were found to be invasive and had a significant level of CD44 and Beta-1-integrin. These cells showed little or no angiogenic activity and had low levels of VEGF compared to the normal brain cells. It is likely that MUBP invasive activity has overshadowed the angiogenesis event due to strong expressions of both beta-1-integrin and CD44. However, MUBS and MUP cells which were also either low or similar to the VEGF level in the normal brain cells demonstrated increased angiogenic activity. It is possible that the angiogenic activity occurred in these glioma cells was not promoted by VEGF but was instead a consequence of high level of CD44. Significant invasive capacity was also measured in these cell cultures (MUBS and MUP). This activity was possibly enhanced by a combination of high CD44 and NG2 level that were observed. Moreover, high expression of CD44 that was exhibited in MUP cells may responsible for the invasive potential due to the

prominent staining seen compared to the normal brain cells. As a result, the levels of invasion in these two glioblastoma cells were higher than that measured in MUBP or MUTC cells. The latter two cultures were low in NG2 expression.

MUTC cells expressed higher amounts of MMP-14 compared to the other cell cultures. As described earlier MMP-14 (mt-MMP-1) expression is associated with invasive cells. However, in this case it is possible that the high level of VEGF that measured in the cells may neutralize this effect. As discussed earlier, over-expression of VEGF, suppresses invasion in glioma-expressing MET and VEGFR2 hence reduced in the protease level such as MMP-14 in the cells. Although this is not yet known for sure, there is a possibility that both factors may have been expressed in MUTC cells which warrants further investigation.

Conclusions

Taken together, glioblastomas as with other cancers are the results of an accumulation of genetic alterations, leading to the activation of oncogenes and/or the inactivation of tumour suppressor genes. Thus, in this study, these malignant gliomas may have their messenger RNAs (mRNAs) translated into proteins from the abnormal or altered genes, leading to aberrant expressions of some critical proteins.

As seen in this study, the complexity of mixed antigenic expressions yet overlapping in functions in the tumour cells indirectly suggests that not a single but an integrated role of antigens are responsible for a specific functions in tumourigenecity of the cells. Indeed, other findings from other assays of different antigen expression, invasion and angiogenesis are of relevance. One marker might indicate one specific biological behaviour of the cells but this is not always the case in the complex microenvironment of glioblastoma when it is a heterogenous network and dysregulated in cell signalling, as with other cancers. Although curcumin is potentially cytotoxic to these glioblastoma cells which has also experienced by

the established cell line (Abdullah Thani et al., 2012), it has not induced apoptosis to occur, suggesting curcumin killed the cells via non-apoptotic pathway hence warrant further analysis on elucidating the possible pathway involved. Nevertheless, regardless the aberrant expression of antigens studied in relevance to invasion and angiogenesis, curcumin was found to have the potential in inhibiting both angiogenesis and invasion activity in these primary glioblastoma cells.

To our knowledge, there are no studies that have investigated the potential therapeutic mechanism of lycopene (or LycoRed) in gliomas. All previous research either focused on animal studies or other types of human cancer. Although the therapeutic potential of LycoRed was not demonstrated in this study, further studies of this may be worthwhile. Thus, regardless of the findings that LycoRed did not kill the glioblastoma cells studied, it is tempting to know if it has the capability in reducing invasive capacity or inhibiting angiogenesis of the glioma cells. Indeed, a potential mechanism of lycopene in cancers has been documented not only for its well-known anti-oxidant property but also for its effects in modulating growth factors in cell signalling (insulin growth factor (IGF); platelet derived growth factor (PDGF); VEGF), and altering cell cycle progression in prostate cancer (Lo et al., 2007; Ford et al., 2011). Previous studies have also shown that lycopene has a therapeutic effect on breast and prostate cancers (Dorgan et al., 1998; Giovannucci, 1999; Kirsh et al., 2006). Thus further studies of the potential therapeutic properties of Lycopene in glioblastoma may be worthwhile.

Further studies of importance

Treating primary brain tumours has unique challenges such as its difficult access to the tumour site and heterogeneity of tumour response from one malignant glioma case to the next. Hence a larger scale involving different analyses is required to fully evaluate the

potential of both lycoRed and curcumin in the prevention and treatment of glioblastoma. An example is a cell cycle arrest study using flow cytometry analysis which involves DNA replication and cell separation that consists of four distinct phases; G1 (growth and preparation of cells for DNA synthesis), S (DNA synthesis), G2 (preparation for mitosis) and M (mitosis) phases. The main regulatory molecules in the cell cycle phase are cyclins and cyclin dependent kinases (CDKs) which play major roles in verifying (checkpoint) that every requirement has been met before the cell cycle is allowed to proceed to the next step, in which deregulated in cancer cells.

One approach is a single time point measurement of cells when it is based on measurement of DNA content of the cells following cell staining with fluorescent dye such as PI or 4'6'-diamino-2-phenylindole (DAPI), with the addition of ribonucleic acid polymerase A (RNase A) as to remove RNAs from the cells thus preventing from creating artefacts that would distort the results. As a result, the fluorescence intensity of the stained cells reveals distribution of cells in three major phases of the cycle (G1 vs S vs G2/M) and makes it possible to detect apoptotic cells with fractional DNA content (Pozarowski and Darzynkiewicz, 2004). Cell cycle assay is also related to the expression of cyclin D, cyclin E, cyclin A, or cyclin B1 vs DNA content. This allows one to distinguish, for example, G0 from G1 cells, identify mitotic cells, or relate expression of other intracellular proteins to the cell cycle position. Another approach relies on the detection of 5'-bromo-2'-deoxyuridine (BrdU) incorporation to label the DNA-replicating cells. Such examples have involved cell cycle analysis in cancer studies associated with flavonoids as the agents of treatment. A study demonstrated that treatment with resveratrol led to G1 phase cell cycle arrest in bladder cancer cells by downregulation of cyclin D1, cyclin dependent kinase 4, activation of p21 and retinoblastoma protein (Rb) that phosphorylated (Bai et al., 2010).

Another flavonoid study on quercetin demonstrated that the viability of cervical cancer was suppressed by quercetin in a dose dependent manner with cell cycle that arrested at G2/M phase (Priyadarsini et al., 2010). Therefore, cell cycle analysis via flow cytometry would confirm the non-apoptotic event seen in our Annexin V results thus leading to the identification of possible modulation or activation either pro- or anti-apoptotic molecules that might have occurred.

Another approach in targeting apoptosis occurrence is via cleaved caspase 3 assay via flow cytometry technique. Indeed, modulating apoptosis via caspase family of proteins is one obvious target and commonly emphasized in apoptosis analysis. Caspases (cysteine-aspartic acid-specific proteases) are one of the molecular players involved in programmed cell death. Activation of caspases from its inactive state (inactive zymogen) via transcatalytic cleavage and followed by assembly of the product post cleavage is considered to be the point of detection. Caspase 3 is a well-characterised effector in apoptosis. Most caspase-3 substrates' recognition site is DEVD (the single-letter code for amino acid is used) where cleavage occurs after the second D (Thornberry et al., 1997). This polypeptide (DEVD) is linked to rhodamine-110 (a fluorescent). The non-fluorescent bis-substituted peptide derivatives of rhodamine 110 are intracellularly cleaved to green fluorescent monosubstituted rhodamine 110 and free rhodamine 110. This green fluorescent is measured in intact cells (as these substrates are cell-permeable) upon excitation with 488nm laser light of the flow cytometry (Ormerod et al., 2005).

To expand the research of curcumin or LycoRed therapeutic effects on glioblastoma, an additional to cell cycle assay would be western blotting (WB), an assay at the protein level, which is commonly in association with real time polymerase chain reaction (RT-PCR) analysis. It is well established and straightforward in the interpretation. Western blotting allows the proteins in a complex sample such as in solid tumour of a glioblastoma (30 µg

lysates) to be separated according to molecular weight and visualized within a gel matrix and/or, once separated, transferred onto a supporting membrane, where they may be probed for the binding of antibodies or lectins. A glioma study using established cell lines has demonstrated the expressions of EGFR and matrix metalloproteinases which suggested being responsible as causative factors in mediating glioma malignancy (VanMeter et al., 2004). Another quantitative assay would be Real Time-Polymerase Chain Reaction (RT-PCR) when the expression of mRNA of each factor studied would be able to be identified at the molecular level as detected in another glioma study (Hagemann et al., 2010). In relation with WB and other protein detection assays, with RT-PCR, the factors that suggested having roles in the progression of gliomas may be determined at early stage thus assisting in elucidating the prevention and therapeutic potential of either curcumin or LycoRed.

In recent years, epigenetic alterations in glioblastoma multiforme have been a great interest in diagnosing the potential prognostic and response factors towards treatment. Alterations in the chromatin structure and/or DNA methylation without changes in the DNA sequence (Henikoff and Matzke, 1997), epigenetic mechanism in normal cells regulates many cellular processes such as cell differentiation and memory formation. However, disruption of epigenetic processes can lead to altered gene function and malignant cellular transformation. In the state of diseases such as cancers, epigenetic modifications comprises of DNA methylation, post-translational histone modifications (acetylation, methylation, phosphorylation, ubiquitination, sumoylation) and regulation of gene expression by non-coding (nc) RNA including microRNA (Stilling and Fischer, 2011; Choudhuri, 2011). Epigenetic alterations in glioblastoma have involved many genes such as O6-methylguanine methyltransferase (MGMT) and mutL homolog 1 (MLH1) that function in DNA repair, p14ARF (p14), cyclin dependent kinase inhibitor 2B (p15/CDKN2B) and retinoblastoma 1 (RB1) that play roles in cell cycle regulation. For an instance, DNA methylation of MGMT

is frequent in glioblastoma multiforme when it is associated with increased number of mutations and poor outcome hence considered a biomarker of poor prognosis (Komine et al., 2003). In contrast, it has been reported that GBM patients with methylated MGMT respond more positively to temozolomide (TMZ) than patients with unmethylated MGMT (Hegi et al., 2005; Balana et al., 2008). In the unmethylated MGMT, the DNA repair enzyme (MGMT) removes methyl groups from the O⁶-position of guanine and the expression of MGMT is therefore thought to inhibit the cytotoxic effect of TMZ. A recent study (Costa et al., 2010) has reported that there is no association between MGMT promoter methylation and the outcome of GBM treated with TMZ hence additional robust and consistent studies are warranted to clarify this information particularly to use MGMT status in clinical decisions.

The initiation and progression of cancer, is now realized to involve epigenetic abnormalities along with genetic alterations which can substitute for genetic variation later in tumour progression. Therefore, it is important not only to find the key molecular targets that responsible for the initiation of tumourigenesis but also to identify whether curcumin or lycopene may act as inhibitors towards histone deacetylases and histone methyltransferases in improving the current poor prognosis of GBM. These may be facilitated by Histone Methyltransferase and Deacetylase Assays involve the incubation of histone reaction mixtures with curcumin or lycoRed concentrations which then resolved on 15% SDS-PAGE, and subjected to fluorography followed by autoradiography. This has been demonstrated in a cervical cancer cells when histone modifying enzyme (p300/CBP) was inhibited by 3-fold at 100µM of curcumin (Blasubramanyam, et al., 2004). It has also been shown that exposure of human hepatoma cells to curcumin led to a significant decrease of histone acetylation at a range of 50-100 µM of curcumin (Kang et al., 2005). No study has investigated the effect of lycopene (lycoRed) on histone acetylation. However, there are studies that have demonstrated a role for lycopene inducing cell cycle arrest through certain CDKs that decreased in

expression. Inactivated CDKs deactivated Rb phosphorylation which resulted to inhibition in histone acetylation and transcription of genes (Karas et al., 2000; Nahum et al., 2001; Hwang and Bowen, 2004).

With combination of these assays for future studies together with other relevant available assays, the potential therapeutic benefits of curcumin or LycoRed on GBM may be fully discovered and our limitations in understanding on complexities of glioblastoma multiforme may be improved.

References

- Abdullah Thani, N.A., Sallis, B., Nuttall, R. et al. (2012). Induction of apoptosis and reduction of MMP gene expression in U373 cell line by polyphenolics in *Aronia melanocarpa* and curcumin. *Oncol Rep*, 28(4):1435-42.
- Abusnina, A., Keravis, T., Zhou, Q. et al. (2015). Tumour growth inhibition and anti-angiogenic effects using curcumin correspond to combined PDE2 and PDE4 inhibition. *Thromb Haemost.* 113 (2), 319-28.
- Aggarwal, B.B., Bhatt, I.D., Ichikawa, H., Ahn, K.S., Sethi, G., Sandur, S.K., Sundaram, C., Seeram, N., Shishodia, S. (2007). Curcumin-biological and medicinal properties. In: P.N. Ravindran, K.N. Babu, K. Sivaraman, (Eds.) *Turmeric the genus curcuma* (pp. 297-368). New York: CRC Press.
- Aggarwal, B.B., Kumar, A., Bharti, A.C. (2003). Anticancer Potential of Curcumin: Preclinical and Clinical Studies. *Anticancer Research*, 23, 363-398.
- Aggarwal, B.B., Sung, B. (2009). Pharmacological basis for the role of curcumin in chronic diseases: an age-old spice with modern targets. *Trends Pharmacol Sci*, 30, 85-94.
- Aggarwal, S., Takada, Y., Singh, S. et al. (2004). Inhibition of growth and survival of human head and neck squamous cell carcinoma cells by curcumin via modulation of nuclear factor-kB signaling. *Int J Cancer* 111, 679-692.
- Ahsan, H., Parveen, N., Khan, N.U., Hadi, S.M. (1999). Pro-oxidant, anti-oxidant and cleavage activities on DNA of curcumin and its derivatives demethoxycurcumin and bisdemethoxycurcumin. *Chemico-Biological Interactions*, 121, 161-175.
- Aitchison, K., Datla, K., Rooprai, H., Fernando, J., Dexter, D. (2010). Regional distribution of clomipramine and desmethyldomipramine in rat brain and peripheral organs on chronic clomipramine administration. *Journal of Psychopharmacology*, 24(28), 1261-1268.
- Akiyama, Y., Jung, S., Salhia, B., Lee, S., Hubbard, S., Taylor, M. et al., (2001). Hyaluronate receptors mediating glioma cells migration and proliferation. *Journal of Neurooncology*, 53, 115-127.

- Albini, A., Iwamoto, Y., Kleinman, H.K., Martin, G.R., Aaronson, S.A., Kozlowski, J.M. and McEwan, R.N. (1987). A Rapid *in Vitro* Assay for Quantitating the Invasive Potential of Tumor Cells. *Cancer Research*, 47, 3239-3245.
- Anan, P., Sundaram, C., Jhurani, S., Kunnumakkara, A.B., Aggarwal, B.B. (2008). Curcumin and cancer: An “old age” disease with and “age old” solution. *Cancer Letters* 267,133-164.
- Anand, .P, Kunnumakkara, A.B., Newman, R.A., Aggarwal, B.B. (2007). Bioavailability of curcumin: problems and promises. *Mol Pharm* 4,807-818.
- Anto, R.J., Mukhopadhyay, A., Dening, K., Aggarwal, B.B. (2002). Curcumin (diferuloylmethane) induces apoptosis through activation of caspase-8, BID cleavage and cytochrome c release: its suppression by ectopic expression of Bcl-2 and Bcl-xl. *Carcinogenesis*, 23, 143-150.
- Anuchapreeda, S., Limtrakul, P., Thanarattanakorn, P., Sittipreechacharn, S., Chanarat, P. (2006). Inhibitory effect of curcumin on WT1 gene expression in patient leukemic cells. *Arch Pharm Res* 29(1), 80-7.
- Aoki, H., Takada, Y., Kondo, S., Sawaya, R., Aggarwal, B.B., Kondo, Y. (2007). Evidence that curcumin suppresses the growth of malignant gliomas in vitro and in vivo through induction of autophagy: role of Akt and extracellular signal-regulated kinase signaling pathways. *Mol Pharmacol*, 72,29-39.
- Aplin, A.E. et al. (1998). Signal Transduction and Signal Modulation by Cell Adhesion Receptors: The Role of Integrins, Cadherins, Immunoglobulin-Cell Adhesion Molecules, and Selectins. *Pharmacol Rev*, 50(2), 197-264.
- Atsumi, T., Tonosaki, K., Fujisawa, S. (2006). Induction of early apoptosis and ROS generation activity in human gingival fibroblasts (HGF) and human submandibular gland carcinoma (HSG) cells treated with curcumin. *Arch Oral Biol*, 51(10), 913-21
- Auerbach, R.W., Polakowski, I. (1991). Assays for angiogenesis: A review. *Pharmacol. Ther.* 51, 1–11.
- Avgeropoulos, N.G., Batchelor, T.T. (1999). New Treatment Strategies for Malignant Gliomas. *The Oncologist*, 4, 209-224.
- Bachmeier, B.E., Mohrenz, I.V., Mirisola, V. et al. (2008). Curcumin downregulates the inflammatory cytokines CXCL1 and -2 in breast cancer cells via NF-kappaB. *Carcinogenesis* 29,779-789.

- Bae, M.K., Kim, S.H., Jeong, J.W., Lee, Y.M., Kim, H.S., Kim, S.R., Yun, I., Bae, S.K., Kim, K.W. (2006). Curcumin inhibits hypoxia-induced angiogenesis via down-regulation of HIF-1. *Oncology Reports*, 15, 1557-1562.
- Bai, Y., et al. (2010). Resveratrol induces apoptosis and cell cycle arrest of human T24 bladder cancer cells *in vitro* and inhibits tumor growth *in vivo*. *Cancer Science*, 101(2), 488-493.
- Balana, C., Carrato, J., Ramirez, J., et al. (2008). Concordance and clinical value of the MGMT promoter methylation pattern in tissue with paired serum and MGMT protein expression in a series of glioblastoma (GB) patients. *Journal of Clinical Oncology*, 26, 2037.
- Balasubramanyam, K., et al. (2004). Curcumin, a novel p300/CREB-binding protein-specific inhibitor of acetyltransferase, represses the acetylation of histone/nonhistone proteins and histone acetyltransferase-dependent chromatin transcription. *J Biol Chem*, 279, 51163-51171.
- Bar, E.E., Chaudhry, A., Lin, A. et al. (2007). Cyclopamine-mediated hedgehog pathway inhibition depletes stem-like cancer cells in glioblastoma. *Stem Cells*, 25, 2524-2533.
- Batchelor, T.T., Sorenson, A.G., di Tomaso, E., Zhang, W.T., Duda, G., Cohen, K.S., Kozak, K.R., Cahill, D.P., Chen, P.J., Zhu, M. et al. (2007). AZD2171, a pan-VEGF receptor tyrosine kinase inhibitor, normalizes tumour vasculature and alleviates edema in glioblastoma patients. *Cancer Cell*, 11, 83-95.
- Becton Dickinson (BD) Biocoat Angiogenesis System. Retrieved February 20, 2011, from the website: <http://www.bd.com/resource.aspx?IDX=17822>
- Bellail, A.C., Hunter, S.B., Brat D.J., Tan, C., Van Meir, E.G. et al. (2004). Microregional extracellular matrix heterogeneity in brain modulates glioma cell invasion. *The International Journal of Biochemistry & Cell Biology*, 36, 1046-1069.
- Bello L, Francolini M, Marthyn P, et al (2001). Alpha(v)beta3 and alpha(v)beta5 integrin expression in glioma periphery. *Neurosurgery* 49,380-390.
- Bergers, G., Benjamin, L.E. (2003). Tumorigenesis and the angiogenic switch. *Nat Rev Cancer*, 3(6), 401-10.
- Berges, G., Hanahan, D. (2008). Modes of resistance to anti-angiogenic therapy. *Nat Rev Cancer*, 8, 592-603.

- Berra, B., Gaini, S.M., Riboni, L. (1985). Correlation between ganglioside distribution and histological grading of human astrocytomas. *Int J Cancer*, 36, 363-366.
- Bianco, P., Robey, P.G., Simmons, P.J. (2008). Mesenchymal stem cells: revisiting history, concepts, and assays. *Cell Stem Cell*, 3(4), 313–319.
- Bielak-Mijewska, A., Piwocka, K., Magalska, A., Sikora, E. (2004). P-glycoprotein expression does not change the apoptotic pathway induced by curcumin in HL-60 cells. *Cancer Chemother Pharmacol*, 53, 179-185.
- Bigner, D.D., McLendon, R.E., Brunner, J.M. (1998). *Russell and Rubinstein's pathology of tumours of the nervous system* (6th ed.). New York: Oxford University Press.
- Binder, D.K., Berger, M.S. (2002). Proteases and the biology of glioma invasion. *Journal of Neuro-Oncol*, 56, 149-158.
- Binion, D.G., Otterson, M.F., Rafiee, P. (2008). Curcumin inhibits VEGF-mediated angiogenesis in human intestinal microvascular endothelial cells through COX-2 and MAPK inhibition. *Gut*, 57, 1509-1517.
- Biostatus Limited. *DRAQ 7*. Retrieved February 18, 2011, from the website: http://www.biostatus.com/product/draq7_new/features_and_benefits/
- Birks SM, Danquah JO, King L, Vlasak R, Gorecki DC, Pilkington GJ. (2011). Targeting the GD3 acetylation pathway selectively induces apoptosis in glioblastoma. *Neuro Oncol*. 13(9), 950-60.
- Birlik, B., Canda, S., Ozer, E. (2006). Tumour vascularity is of prognostic significance in adult, but not paediatric, astrocytomas. *Neuropathology Applied Neurobiology*, 32, 532-538.
- Bishop, E. T., Bell, G. T., Bloor, S., Broom, I. J. et al. (1999). An in vitro model of angiogenesis: basic features. *Angiogenesis*. 3(4), 335–344.
- Bisht, S., Maitra, A. (2009). Systemic delivery of curcumin: 21st century solutions for an ancient conundrum. *Curr Drug Discov Technol*, 6(3), 192-9.
- Blasi, F., Carmeliet, P. (2002). uPAR: A versatile signalling orchestrator. *Nature Reviews: Molecular Cell Biology*, 3, 932-943.
- Boileau, T., W-M., Boileau, A.C., Erdman Jr., J.W. (2002). Bioavailability of all-*trans* and *cis*-isomers of Lycopene. *Exp Biomed*, 227, 914-919.

- Bonavia, R., Inda, M.D.M., Cavenee, W. and Furnari, F. (2011). Heterogeneity Maintenance in Glioblastoma: a social network. *Cancer Res*, 71(12), 4055–4060.
- Bosetti, C., Talamini, R., Montella, M., Negri, E., Conti, E., Franceschi S, La Vecchia, C. (2004). Retinol, Carotenoids and the risk of prostate cancer: A case control study from Italy. *International Journal of Cancer*, 112,689–692.
- Bourboulia, D. and Stetler-Stevenson, W.G. (2010). Matrix metalloproteinases (MMPs) and tissue inhibitors of metalloproteinases (TIMPs): positive and negative regulators in tumor cell adhesion. *Sem. Can. Biol*, 20,161-168.
- Bouterfa, H., Janka, M., Meese, E., Kerkau, S., Roosen, K., Tonn, J.C. (1997). Effect of changes in the CD44 gene on tumour cell invasion in gliomas. *Neuropathol Appl Neurobiol*, 23,373–379.
- Bradford, R., Koppel, H., Pilkington, G.J., Thomas, D.G.T., Darling J.L. (1997). Heterogeneity of chemosensitivity in six clonal cell lines derived from a spontaneous murine astrocytoma and its relationship to genotypic and phenotypic characteristics. *Journal of Neuro-Oncology* 34,(3), 247-261.
- Brand, K. et al. (2000). Treatment of colorectal liver metastases by adenoviral transfer of tissue inhibitor of metalloproteinases-2 into the liver tissue. *Cancer Research*, 60, 4337-5730.
- Brandes, A.A., Pasetto, L.M. (2000). New therapeutic agents in the treatment of recurrent high-grade gliomas. *FORUM Trends in Experimental and Clinical Medicine*, 10, 121-131.
- Brat, D.J., Castellano-Sanchez, A., Hunter, S.B., Pecot, M.J., Cohen, C., Hammond, E.H., et al., (2004). Pseudopalisading cells in glioblastoma are hypoxic, express extracellular matrix proteases and are formed by an actively migrating population. *Cancer Research*, 64(3), 920-927.
- Brat, D.J., Van Meir, E.G. (2004). Vaso-occlusive and pro-thrombotic mechanisms associated with tumour hypoxia, necrosis and accelerated growth in glioblastoma. *Laboratory Investigation*, 84, 397-405.
- Brekke, C., Lundervold, A., Enger, P.O., Brekken, C., Stalsett, E., Pedersen, T.B., Haraldseth, O., Kruger, P.G., Bjerkvig, R., Chekenya, M. (2006). NG2 expression regulates vascular morphology and function in human brain tumours. *NeuroImage*, 29, 965-976.

- Breyer, R. et al. (2000). Disruption of intracerebral progression of C6 rat glioblastoma by in vivo treatment with anti-CD44 monoclonal antibody. *J Neurosurg*, 92,140-9.
- Briske-Anderson, M.J. et al. (1997). Influence of culture time and passage number on morphological and physiological development of Caco-2 cells. *Proceedings of the Society for Experimental Biology and Medicine*, 214(3), 248-257.
- Brown G.L., Eckley, M., Wargo, K.A. (2010). A Review of Glioblastoma Multiforme. *US Pharm*, 35(5), 3-10.
- Bureyko, T., Hurdle, H., Metclafe, J.B., Clandinin, M.T., Mazurak V.C. (2009). Reduced growth and integrin expression of prostate cells cultured with lycopene, vitamin E and fish oil *in vitro*. *British Journal of Nutrition*, 101, 990-997.
- Burg, M.A. et al. (1997). A central segment of the NG2 proteoglycan is critical for the ability of glioma cells to bind and migrate towards type VI collagen. *Exp Cell Res*, 235, 254-264.
- Burg, M.A. et al. (1998). Expression of the NG2 proteoglycan enhances the growth and metastatic properties of melanoma. *J.Cell Physiol*, 177, 299-312.
- Burger, P., Scheithauer, B.W. (1994). Atlas of tumor pathology: Tumours of the central nervous sytem. Washington DC: Armed Forces Institute of Technology.
- Burgess, L.C. et al. (2008). Lycopene has limited effect on cell proliferation in only two of seven human cell lines (both cancerous and noncancerous) in an *in vitro* system with doses across the physiological range. *Toxicol In Vitro*, 22(5), 1297–1300.
- Burnet, N. (2004). Oncology management of CNS tumours. Retrieved December 26, 2010, from website: <http://www.ecric.org.uk/docs/Burnet070409.pps>
- Capper, D., Mittelbronn, M., Meyermann, R., et al. (2008). Pitfalls in the assessment of MGMT expression and in its correlation with survival in diffuse astrocytomas: Proposal of a feasible immunohistochemical approach. *Acta Neuropathologica*, 115,249–259.
- Carmeliet, P. (2003). Angiogenesis in health and disease. *Nature Medicine*, 9(6), 653-660.
- Carpentier, G. Image analysis and processing tool developments using Image J software. AERES Laboratoire CRRET Universite Paris, April 2008.

- Casanovas, O., Hicklin, D.J., Bergers, G., Hanahan, D. (2005). Drug resistance by evasion of antiangiogenic targeting of VEGF signaling in late-stage pancreatic islet tumors. *Cancer Cell*, 8,299–309.
- Caspani, E.M., Crossley, P.H., Redondo-Garcia, C., Martinez, S. (2014). Glioblastoma: A Pathogenic Crosstalk between Tumor Cells and Pericytes. *PLoS ONE* 9(7), e101402.
- Castellino, R.C., Durden, D.L. (2007). Mechanism of disease: the PI3K-Akt-PTEN signaling node-an intercept point for the control of angiogenesis in brain tumours. *Nat Clin Pract Neurol*, 3, 682-693.
- Ceballos-Salobreña, A., Gaitán-Cepeda, L.A., Ceballos-Garcia, L., and Lezama-Del Valle, D. (2000). *AIDS Patient Care and STDs*, 14(12),627-635.
- Chakrabandhu, K., Huault, S., Garmy, N., Fantini, J., Stebe, E., Mailfert, S., Marguet, D., Hueber, A.O. (2008). The extracellular glycosphingolipid-binding motif of Fas defines its internalization route, mode and outcome of signals upon activation by ligand. *Cell Death Differ.* 15(12), 1824-37.
- Chalabi, N., Corre, L.L., Maurizis, J.C., Bignon, Y.J., Bernard-Gallon, D.J. (2004). The effects of lycopene on the proliferation of human breast cells and *BRCA1* and *BRCA2* gene expression. *European Journal of Cancer* , 40(11) , 1768-1775.
- Chang-Liu, C.M. et al. (1997). Effect of passage number on cellular response to DNA-damaging agents: cell survival and gene expression. *Cancer Letters*, 26(113), 77-86.
- Chekenya, M., Enger, P.O., Thorsen, F., Tysnes, B.B., Al-Sarraj, S., Read, T.A., Furmanek, T., Mahesparan, R., Levine, J.M., Butt, A.M., Pilkington, G.J., Bjerkvig, R. (2002a). The glial precursor proteoglycan, NG2, is expressed in tumour neovasculature by vascular pericytes in human malignant brain tumours. *Neuropathol. Appl. Neurobiol*, 28(5), 367-380.
- Chekenya, M., Hjelstuen, M., Enger, P.O., Thorsen, F., Jacob, A.L., Probst, B., Haraldseth, O., Pilkington, G.J., Butt, A., Levine, J.M., Bjerkvig, R. (2002). NG2 proteoglycan promotes angiogenesis-dependent tumour growth in CNS by sequestering angiostatin. *The FASEB Journal*, 16, 586-588.

- Chekenya, M., Rooprai, H.K., Davies, D., Levine, J.M., Butt, A.M., Pilkington, G.J. (1999). The NG2 chondroitin sulfate proteoglycan: role in malignant progression of human brain tumours. *Int J Dev Neurosci.*, 17(5-6):421-35.
- Chen, H.W., Lee, J.Y. et al. (2008). Curcumin Inhibits Lung Cancer Cell Invasion and Metastasis through the Tumor Suppressor HLJ1. *Cancer Res*, 68, 7428.
- Cheng, A.L., Hsu, C.H., Lin, J.K., et al. (2001). Phase I clinical trial of curcumin, a chemopreventive agent, in patients with high-risk pre-malignant lesions. *Anticancer Res.* 21, 2895–900.
- Chiba, T., Kita, K., Zheng, Y.W., Yokosuka, O., Saisho, H., Iwama, A., Nakauchi, H., Taniguchi, H. (2006). Side Population Purified From Hepatocellular Carcinoma Cells Harbors Cancer Stem Cell-Like Properties. *Hepatology*, 44, 240-251.
- Choe, G., Park, J.K., Jouben-Steele, L., Kremen, T.J., Liao, L. M., Vinters, H.V. et al., (2002). Active matrix metalloproteinase 9 expression is associated with primary glioblastoma subtype. *Clinical Cancer Research*, 8, 2894-2901.
- Choi, H., Chun, Y.S., Kim, S.W., Kim, M.S., Park, J.W. (2006). Curcumin Inhibits Hypoxia-Inducible Factor-1 by Degrading Aryl Hydrocarbon Receptor Nuclear Translocator: A Mechanism of Tumour growth Inhibition. *Molecular Pharmacology*, 70(5), 1664-1671.
- Choudhuri, S. (2011). From Waddington's epigenetic landscapeto small noncoding RNA: some important milestones in the history of epigenetics research. *Toxicol Mech Methods*, 21, 252-274.
- Chung, H., Seo, S., Moon, M., Park, S. (2007). IGF-I inhibition of apoptosis is associated with decreased expression of prostate apoptosis response-4. *J Endocrinol*, 194(1), 77-85.
- Clement, V., Sanchez, P., de Tribolet, N. et al. (2007). Hedgehog-Gli signaling regulates human glioma growth, cancer stem cell self-renewal and tumorigenicity. *Current Biology*, 17, 165-172.
- Colell, A., García-Ruiz, C., Roman, J., Ballesta, A., Fernández-Checa, J.C. (2001). Ganglioside GD3 enhances apoptosis by suppressing the nuclear factor-kappa B-dependent survival pathway. *FASEB J.* 15(6),1068-70.
- Collins, V.P. Brain tumours: Classification and genes. (2004). *J Neurol Neurosurg Psychiatry*, 75(II),ii2-ii11.

- Combs S.E., Wagner, J., et al. (2008). Postoperative Treatment of Primary Glioblastoma Multiforme With Radiation and Concomitant Temozolomide in Elderly Patients. *International Journal of radiation Oncology*Biology*Physics*, 70(4), 987-992.
- Corallini, A., Pagnani, M., Viadana, P., Silini, E., Mottes, M., Milanesi, G., Gerna, G., Vettor, R., Trapella, G., Silvani, V., et al. (1987b). Association of BK virus with human brain tumors and tumors of pancreatic islets. *Int J Cancer* 39,60–67.
- Costa, B.M., Caeiro, C., Guimaraes, I. et al. (2010). Prognostic value of MGMT promoter methylation in glioblastoma patients treated with temozolomide-basedchemoradiation: A Portuguese multicentre study *Oncology Reports*. 23, 1655-1662.
- Da Violante G. et al.(2002). Evaluation of the Cytotoxicity Effect of Dimethyl Sulfoxide (DMSO) on Caco2/TC7 Colon Tumor Cell Cultures. *Biological and Pharmaceutical Bulletin*, 25(12), 1600-1603.
- Daido, S., Kanzawa, T., Yamamoto, A., Takeuchi, H., Kondo, Y., and Kondo, S. (2004) Pivotal role of the cell death factor BNIP3 in ceramide-induced autophagic cell death in malignant glioma cells. *Cancer Res* 64, 4286-4293.
- Daido, S., Yamamoto, A., Fujiwara, K., Sawaya, R., Kondo, S., and Kondo, Y. (2005) Inhibition of the DNA-dependent protein kinase catalytic subunit radiosensitizes malignant glioma cells by inducing autophagy. *Cancer Res* 65, 4368-4375.
- Daley, E., Wilkie, D., Loesch, A., Hargreave,s I.P., Kendall, D.A., Pilkington, G.J., Bates, T.E. (2005). Chlorimipramine: a novel anticancer agent with a mitochondrial target. *Biochemical Biophysical Research Communication*, 328(2), 623-32.
- Darzynkiewicz, Z., Huang, X., Okafuji, M., King, M.A. (2004). Cytometric methods to detect apoptosis. *Methods in Cell Biology*, 75, 307-34.
- Datla, K.P., Christidou, M., Widmer, W.W., Rooprai, H.K. & Dexter, D.T. (2001). Tissue distribution and neuroprotective effects of citrus flavonoid tangeretin in a rat model of Parkinson's disease. *Neuroreport*, 12, (17), 3871-3875.
- Datla, K.P., Zbarsky, V., Dexter, D. (2006). Effects of anaesthetics on the loss of nigrostriatal dopaminergic neurons by 6-hydroxydopamine in rats. *Journal of Neural Transmission*, 113(5), 583-91.

- Daumas-Duport, C., Scheithauer, B., O'Fallon, J., Kelly, P.(1988).Grading of astrocytomas. A simple and reproducible method. *Cancer*, 62(10), 2152-65.
- Deeken, J.F., Loscher, W. (2007). The blood brain barrier and cancer: transporters, treatment and Trojan horses. *Clin Cancer Res*, 13, 1663-1674.
- Deryugina, E. I., Quigley, J.P. (2015). Tumor angiogenesis: MMP-mediated induction of intravasation- and metastasis-sustaining neovasculature. *Matrix Biology*, 44(46), 94-112
- Deryugina, E.I. Soroceanu, L., Strongin, A.Y. (2002). Up-regulation of vascular endothelial growth factor by membrane-type 1 matrix metalloproteinase stimulates human glioma xenograft growth and angiogenesis. *Cancer Res* 62, 580-588.
- Deryugina, E. et al. (1997). Matrix metalloproteinase-2 activation modulates glioma cell migration. *J.Cell Sci*, 110(19), 2473-82.
- Di, G.H., Li, H.C., Shen, Z.Z., Shao, Z.M. (2003). Analysis of anti-proliferation of curcumin on human breast cancer cells and its mechanism. *Zonghua Yi Xue Za Zhi*, 83, 1764-1768.
- Diehn, M., Cho, R.W. Lobo, N.A. et al. (2009). Association of reactive oxygen species levels and radioresistance in cancer stem cells. *Letter Nature*, 458, 780-783.
- Divya, C.S., Pillai, M.R. (2006). Antitumour action of curcumin in human papillomavirus associated cells involves downregulation of viral oncogenes, prevention of NFkB and AP-1 translocation and modulation of apoptosis. *Mol. Carcinog*, 45,320-332.
- Diwadkar-Navsariwala, V., Novotny, J.A., Gustin, D.M., Sosman, J.A., Rodvold, K.A., Crowell, J.A., Stacewicz-Sapuntzakis, M., Bowen, P.E. (2003). A physiological pharmacokinetic model describing the disposition of lycopene in health men. *Journal of Lipid Research*, 44, 1927-1939.
- Dorai, T. and Aggarwal, B.B. (2004). Role of chemopreventive agents in cancer therapy *Cancer Letters*, 215(2), 129–140.
- Dorgan, J. F., Sowell, A., Swanson, C. A. et al. (1998). Relationships of serum carotenoids, retinol, α -tocopherol, and selenium with breast cancer risk: results from a prospective study in Columbia, Missouri (United States). *Cancer Causes and Control*, 9, (1), 89–97.

- Duvoix, A., Roman, B., Delhalle, S., Schnekenburger, M., Morceau, F., Henry, E., Dicato, M., Diederich, M. (2005). Chemopreventive and therapeutic effects of curcumin. *Cancer Letters*, 223,181-190.
- Ebos, J.M., Lee, C.R., Cruz-Munoz, W., Bjarnason, G.A., Christensen, J.G., Kerbel, R.S. (2009). Accelerated metastasis after short-term treatment with a potent inhibitor of tumor angiogenesis. *Cancer Cell*, 15,232–9.
- Egeblad, M., Werb, Z. (2002). New Functions For The Matrix Metalloproteinases In Cancer Progression. *Nature Reviews*, 2, 161-174.
- Egelblad, M. and Werb, Z. (2002). New functions for the matrix metalloproteinases in cancer progression. *Nature Rev*, 2,161-174.
- Elizabeth, K., Rao, M.N.A. (1990). Oxygen radical scavenging activity of curcumin. *Int J Pharmacol*, 58,237-40.
- Espinosa de los Monteros, A., Zhang, M., De Vellis, J. (1993). O2A progenitor cells transplanted into the neonatal rat brain develop into oligodendrocytes but not astrocytes. *Proc Natl Acad Sci USA*, 90(1), 50-54.
- Esquenet, M. et al. (1997). LNCaP prostatic adenocarcinoma cells derived from high and low passage numbers display divergent responses not only to androgens but also to retinoids. *Journal of Steroid Biochemistry and Molecular Biology*, 62,391-399.
- Eyler, C.E., Rich, J.N. (2008). Survival of the Fittest: Cancer Stem Cells in Therapeutic Resistance and Angiogenesis. *Journal of Clinical Oncology*, 26, 17, 2839-2845.
- Faisal, W., O'Driscoll, C.M., Griffin, B.T. Bioavailability of lycopene in the rat: the role of intestinal lymphatic transport. (2010). *Journal of Pharmacy and Pharmacology*, 62, 323-331.
- Fan, T.-P.D. & Polverini, P.J. (1997). *In vivo* models of Angiogenesis. in *Tumor angiogenesis* (eds. Bicknell, R., Lewis, C. E. & Ferrara, N.) 5–18 (Oxford University Press, Oxford).
- Fan, X., Matsui, W., Khaki, L. et al. (2006). Notch pathway inhibition depletes stem cell-like cells and blocks engraftment in embryonal brain tumours. *Cancer Research*, 66, 7445-7452.
- Fan, X., Salford L.G., Bengt, W. (2007). Glioma stem cells: Evidence and limitation. *Seminars in Cancer Biology*, 17, 214-218.

- Fan, X., Salford, L.G., Widegren, B. (2007). Glioma stem cells: Evidence and limitation. *Seminars in Cancer Biology*, 17, 214-218.
- Feldkamp MM, Lau N, Rak J, Kerbel RS, Guha A. (1999). Normoxic and hypoxic regulation of vascular endothelial growth factor (VEGF) by astrocytoma cells is mediated by Ras.. *Int J Cancer*. 81 (1), 118-24.
- Ferrara, N., Hillan, K.J., et al. (2004). Discovery and development of bevacizumab, an anti-VEGF antibody for treating cancer. *Nature Reviews Drug Discovery*, 3, 391-400.
- Ferreira A.L.A., Yeum, K.J., Liu, C., Smith, D., Krinsky, N.I., Wang, X.D., Russell, R.M. (2000). Tissue Distribution of Lycopene in Ferrets and Rats after Lycopene Supplementation. *Journal of Nutrition*, 130, 1256-1260.
- Fidler, I.J., Ellis, L.M. (2004). Neoplastic angiogenesis-not all blood vessels are created equal. *New England Journal of Medicine*, 35, 215-216.
- Fillmore, H.L., VanMeter, T.E., Broaddus, W.C. et al. (2001). Review Membrane-type matrix metalloproteinases (MT-MMPs): expression and function during glioma invasion. *J Neurooncol*, 53(2), 187-202.
- Final Appraisal Determination (2007). Carmustine implants and Temozolomide for the treatment of newly diagnosed high- grade glioma. Retrieved December 26, 2010, from the National Institute for Health and Clinical Excellence (NICE) website: http://www.nice.org.uk/nicemedia/pdf/Glioma_carmustine_FAD.pdf
- Fine, H. (2006). *Overview: Classification and treatment of primary brain tumours; issues and efficacy endpoints in glioma clinical trials*. (FDD/AACR/ASCO, Public Workshop on Brain Tumour Clinical Trial Endpoints). Retrieved December 26, 2010, from website: <http://www.fda.gov/downloads/AboutFDA/CentersOffices/.../ucm120811.pdf>
- Fitting, S., Zhou, S., Chen, W., Vo, P., Hauser, K.F., Knapp, P.E. (2010). Regional heterogeneity and diversity in cytokine and chemokine production by astroglia:differential responses to HIV-1 Tat, gp12- and morphine revealed by multiplex analysis. *J Proteome Res*, 9, 1795-1804.
- Fleischer, A., Ghadiri, A., Frederic, D., Duhamel, M., Rebollo, M.P., Franco, F.A., Rebollo, A. (2006). Modulating apoptosis as a target for effective therapy. *Molecular Immunology*, 43, 1065-1079.

- Folkman, J. (2007). Angiogenesis: an organizing principle for drug discovery? *Nature Review Drug Discovery*, 6, 273-286.
- Folkman, J., Haudenschild, C. (1980). Angiogenesis in vitro. *Nature*. 288 (5791), 551-6.
- Ford, N.A., Elsen, A.C., Zuniga, K., Lindshield, B.L. and Erdman Jr. J.W. (2011). Lycopene and Apo-12'-Lycopenal Reduce Cell Proliferation and Alter Cell Cycle Progression in Human Prostate Cancer Cells. *Nutrition and Cancer* 63(2), 256-263.
- Forsyth, P.A., et al. (1999). Gelatinase-A (MMP-2), gelatinase-B (MMP-9) and membrane type matrix metalloproteinase-1 (MT1-MMP) are involved in different aspects of the pathophysiology of malignant gliomas. *Br J Cancer*, 79,1828–1835.
- Friedman, H.S., Prados, M.D., Wen, P.Y., et al. (2009). Bevacizumab alone and in combination with irinotecan in recurrent glioblastoma. *J Clin Oncol*, 27(28), 4733-4740.
- Fukuda, S., Kato, F., Tozuka, Y., Yamaguchi, M., Miyamoto, Y., Hisatsune, T. (2003). Two distinct subpopulations of nestin-positive cells in adult mouse dentate gyrus. *Journal of Neuroscience*, 23, 9357-9366.
- Gabelloni, P. et al (2010). Inhibition of metalloproteinases derived from tumours: new insights in the treatment of human glioblastoma. *Neuroscience*, 168(2), 514–522.
- Gaini, S.M., Riboni, L., Cerri, C., Grimoldi, N., Sganzerla, E.P., Berra, B. (1988). Ganglioside content and composition in human gliomas. *Acta. Neurochir. Suppl. (Wien)*, 43, 126-129.
- Galati, G., O'Brien, P.J. (2004). Potential toxicity of flavonoids and other dietary phenolics: significance for their chemopreventive and anticancer properties. *Free Radical Biology and Medicine*, 37(3), 287-303.
- Gann, P.H., Ma, J., Giovannucci, E., Willett, W., Sacks, F.M., Hennekens, C.H., Stampfer, M.J. (1999). Lower prostate cancer risk in men with elevated plasma lycopene levels: results of a prospective analysis. *Cancer Res* 59,1225–1230.
- Garcea, G., Berry, D.P., Jones, D.J.L., Singh, R., Dennison, A.R., Farmer, P.B., Sharma, R.A., Steward, W.P., Gescher, A.J. (2005). Consumption of the putative chemopreventive agent curcumin by cancer patients: assessment of curcumin levels in the colorectum and their pharmacodynamic consequences. *Cancer Epidemiol Biomarkers Prev*, 14,120-125.

- Garcea, G., Jones, D.J., Singh, R., Dennison, A.R., Farmer, P.B., Sharma, R.A., Steward, W.P., Gescher, A.J., Berry, D.P. (2004). Detection of curcumin and its metabolites in hepatic tissue and portal blood of patients following oral administration. *Br J Cancer*, 90(5), 1011-1015.
- Gatson, N.N., Chiocca, E.A., Kaur, B. (2012). Anti-angiogenic gene therapy in the treatment of malignant gliomas. *Neurosci Lett*, 527(2), 62-70.
- Gavin, P., Yogev, R. (1999) Central Nervous System Abnormalities in Pediatric Human Immunodeficiency Virus Infection *Pediatr Neurosurg*, 31,115–123.
- Genentech Inc. South San Francisco, CA. (2011). *Avastin (bevacizumab) package insert-prescribing information*. Retrieved December 26, 2010, from Genetech website: <http://www.gene.com/gene/products/information/pdf/avastin-prescribing.pdf>
- Ghashghaei, H.T., Weimer, J.M., Schmid, R.S., Yokota, Y., McCarthy, K.D., Popko, B., Anton, E.S. (2007). Reinduction of ErbB2 in astrocytes promotes radial glial progenitor identity in adult cerebral cortex. *Genes Dev*, 21, 3258-3271.
- Ghosh, M., Ryan, R.O. ApoE enhances nanodisk-mediated curcumin delivery to glioblastoma multiforme cells. *Nanomedicine*, Pages 1-9.
- Giese, A., Westphal, M. (1996). Glioma invasion in the central nervous system. *Neurosurg*, 39,235-252.
- Giovannucci E. (2002). A review of epidemiologic studies of tomatoes, lycopene and prostate cancer. *Studies of tomatoes, lycopene and prostate cancer*, 852-859.
- Giovannucci, E. (1999).Tomatoes, tomato-based products, lycopene, and cancer: review of the epidemiologic literature. *Journal of the National Cancer Institute*, 91, (4), 317–331.
- Gladson, C.L. (1996). Expression of integrin alpha v beta 3 in small blood vessels of glioblastoma tumors. *J Neuropathol Exp Neurol* 55,1143-1149.
- Glas, M., Happold, C., Rieger, J., et al. (2009). Long-term survival of patients with glioblastoma treated with radiotherapy and lomustine plus temozolomide. *Journal of Clinical Oncology*, 27, 1257–1261.
- Goel, A., Kunnumakkara, A.B., Aggarwal, B.B. (2008). Curcumin as Curecumin: from kitchen to clinic. *Biochem. Pharmacol*, 75(4), 787-809.

- Goretzki, L., Lombardo, C.R., Stallcup, W.B. (2000). Binding of the NG2 Proteoglycan to Kringle Domains Modulates the Functional properties of Angiostatin and Plasminogen. *The Journal of Biological Chemistry*, 275(37),28625-28633.
- Gressett, S., Shah, S. (2009). Intricacies of bevacizumab-induced toxicities and their management. *Ann Pharmacother*, 43, 490-501.
- Griffioen, A.W., Coenen, M.J., Damen, C.A. et al (1997). CD44 is involved in tumor angiogenesis; an activation antigen on human endothelial cells. *Blood*, 90(3), 1150-9.
- Grossman, S.A., Batara, J.F. (2004). Current Management of Glioblastoma Multiforme. *Seminars in Oncology*, 31, 635-644.
- Gupta, H., Pawar, D., Riva, A.,Bombardelli, E., Morazzoni, P. (2012). A Randomized, Double-blind, Placebo-controlled Trial to Evaluate Efficacy and Tolerability of an Optimized Botanical Combination in the Management of Patients with Primary Hypercholesterolemia and Mixed Dyslipidemia. *Phytotherapy Research*, 26(2), 265-272.
- Gupta, M., Djalilvand, A., Brat, D.J. (2005). Clarifying the Diffuse Gliomas. An update on the morphologic features and markers that discriminate oligodendroglioma from astrocytoma. *Am J Clin Pathol*, 124,755-768
- Gururaj, A.E., Belakavadi, M., Venkatesh, D.A., Marmé, D., Salimath, B.P. (2002). Molecular mechanisms of anti-angiogenic effect of curcumin. *Biochem Biophys Res Commun*, 297,934-942.
- Gutman, M., Singh, R.K., Xie, K., Bucana, C.D., Fidler, I.J. (1995). Regulation of interleukin-8 expression in human melanoma cells by the organ environment. *Cancer Res*, 55, 2470–5.
- Hadjipanayis, C.G., Van Meir, E.G. (2009). Brain cancer propagating cells: biology, genetics and targeted therapies. *Trends in molecular medicine*. 15(11),519-530.
- Hagemann, C., Anacker, J., Ernestus, R.I., Vince, G.H. (2012). A complete compilation of matrix metalloproteinase expression in human malignant gliomas. *World J Clin Oncol*. 3(5), 67-79.
- Hagemann, C., Anacker, J., Haas, S., Riesner, D., Schomig, B., Ernestus, R.I., Vince, G.H. (2010). Comparative expression pattern of Matrix-Metalloproteinases in human glioblastoma cell-lines and primary cultures. *BMC Research Notes*, 3,293.

- Hakulinen, J., Sankkila, L., Sugiyama, N. et al. (2008). Secretion of active membrane type 1 matrix metalloproteinase (MMP-14) into extracellular space in microvesicular exosomes. *J.Cell Biochem.* 105, 1211-1218.
- Hamerlik, P., Rich, J.N. and Lathia J.D. (2013). News and Views Basic Science: Glioblastoma Stem Cells.*Eur Assoc NeuroOncol Mag*, 3(2), 49-54.
- Han, S.S., Seo, H.J., Surh, Y.J. (2002).Curcumin suppresses activation of NF-kappaB and AP-1 induced by phorbol ester in cultured human promyelocytic leukemia cells.*J Biochem Mol Biol* 35,337-342.
- Haraguchi, N., Utsunomiya, T., Inoue, H., Tanaka, F., Mimori, K., Barnard, G.F., Mori, M. (2006). Characterization of a Side Population of Cancer Cells from Human Gastrointestinal System. *Stem Cells*, 24, 506-513.
- Hardee, M.E. and Zagzag, D. (2012). Mechanisms of glioma-associated neovascularization. *Am J Pathol*, 181(4), 1126-41.
- Hardell, L., Nasma, A., Pahlson, A., et al. (1999). Use of cellular telephones and the risk for brain tumours: a case-control study. *Int J Oncol*, 15, 113-116.
- Hegi M.E. (2005). *MGMT* Gene Silencing and Benefit from Temozolomide in Glioblastoma. *N Engl J Med*, 352,997-1003.
- Henikoff, S, Matzke M.A. (1997). Exploring and explaining epigenetic effects. *Trends Genet*, 13, 293-295.
- Hertog, M.G., Kromhout, D., Aravanis, C., Blackburn, H., Buzina, R., Fidanza, F., Giampaoli, S., Jansen, A., Menotti, A. & Nedeljkovic, S. (1995). Flavonoid intake and long-term risk of coronary heart disease and cancer in the seven countries study. *Archives of Internal Medicine*, 155, 4, 381-386.
- Hide, T., Takezaki, T., Nakamura, H., Kuratsu, J., Kondo, T. (2008). Brain tumour stem cells as research and treatment targets. *Brain Tumour Pathology*, 25, 67-72.
- Higuchi, M., Ohnishi, T., Arita, N., Hiraga, S., Hayakawa, T. (1993). Expression of tenascin in human gliomas: Its relation to histological malignancy. *Acta Neuropathology (Berlin)*, 85, 481-487.
- Hiscox, S., Baruah, B., Smith, C., Bellerby, R., Goddard, L., Jordan, N., Poghosyan, Z., Nicholson, R.I., Barrett-Lee, P., and Gee, J. (2012). Overexpression of CD44 accompanies acquired tamoxifen resistance in MCF7 cells and augments their

sensitivity to the stromal factors, heregulin and hyaluronan. *BMC Cancer*. 12 (12),458.

- Hochstim, C., Deenen, B., Lukaszewicz, A., Zhou, Q., Anderson, D.J. (2008). Identification of positionally distinct astrocyte subtypes whose identities are specified by a homeodomain code. *Cell*, 133, 510-522.
- Hock, S.W., Fan, Z., Buchfelder, M. et al. (2013). Evolution of the Molecular Biology of Brain Tumours and the Therapeutic Implications. *Chapter 4. Brain Tumour-Induced Angiogenesis: Approaches and Bioassays*.p.125-146
- Holland, E.C. (2000). Glioblastoma multiforme: The Terminator. *PNAS*, 97(12), 6242-6244.
- Hood, J.D., Cheresh, D.A. (2002). Role of integrins in cell invasion and migration. *Nature Reviews*, 2, 91-100.
- Hotary, K., Allen, E., Punturieri, A., Yana, .I, Weiss, S.J. (2000). Regulation of cell invasion and morphogenesis in a three-dimensional type I collagen matrix by membrane-type matrix metalloproteinases 1, 2, and 3. *J Cell Biol* , 149, 1309–23.
- Hsu, C.H., Cheng, A.L. (2007). Clinical studies with curcumin. *Adv Exp Med Biol.*, 595, 471-80.
- Hu, A., Huang, J-J., Jin, X-J., et al. (2015). Curcumin suppresses invasiveness and vasculogenic mimicry of squamous cell carcinoma of the larynx through the inhibition of JAK-2/STAT-3 signaling pathway. *American Journal of Cancer Research*. 5(1),278-288.
- Huang, T.T, Sarkaria, S.M., Cloughsey, T.F, Mischel, P.S. (2009). Targeted therapy for malignant glioma patients: lessons learned and the road ahead. *Neurotherapeutics* 6: 500-512.
- Huang, Y., Hoffman, C., Rajappal, P. et al. (2014). Oligodendrocyte Progenitor Cells Promote Neovascularization in Glioma by Disrupting the Blood–Brain Barrier. *Cancer Res* 74, 1011 .
- Hwang, E.S., Bowen, P.E. (2004). Cell cycle arrest and induction of apoptosis by lycopene in LNCaP human prostate cancer cells. *J Med Food*. 7(3),284-9.
- Ibrahim, N., Yu, Y., Walsh, W.R., Yang, J.L. (2012). Molecular targeted therapies for cancer: sorafenib mono-therapy and its combination with other therapies (review). *Oncol Rep.*, 27(5):1303-11.

- Il'yasova, D., McCarthy, B.J., Erdal, S. et al. (2009). Human Exposure to Selected Animal Neurocarcinogens: A Biomarker-Based Assessment and Implications for Brain Tumor Epidemiology. *J Toxicol Environ Health B Crit Rev.* 12(3), 175–187.
- Ireson, C., Jones, D.J.L., Orr, S., Coughtrie, M.W.H., Boocock, D.J., Williams, M.L., Farmer, P.B., Steward, W.P., Gescher, A.J. (2002). Metabolism of the cancer chemopreventive agent curcumin in human and rat intestine. *Cancer Epidemiol Biomarkers Prev*, 11,105-111.
- Ireson, C., Orr, S., Jones, D.J.L., Verschoyle, R., Lim, C.K., Luo, J.L., Howells, L., Plummer, S., Jukes, R., Williams, M., Steward, M.P., Gescher, A. (2001). Characterization of metabolites of the chemopreventive agent curcumin in human and rat hepatocytes and in the rat in vivo and evaluation of their ability to inhibit phorbol ester-induced prostaglandin E-2 production. *Cancer Research*, 61,1058-1064.
- Ishida, B.K., Turner, C., Chapman, M.H., McKeon, T.A. (2004). Fatty Acid and Carotenoid Composition of Gac (*Momordica cochinchinensis* Spreng) Fruit. *J. Agric. Food Chem.*, 52 (2), 274–279.
- Ito, H., Daido, S., Kanzawa, T., Kondo, S., and Kondo, Y. (2005) Radiation-induced autophagy is associated with LC3 and its inhibition sensitizes malignant glioma cells. *Int J Oncol* 26, 1401-1410.
- Jain, R.K. et al. (2007). Angiogenesis in brain tumours. *Nature Reviews Neuroscience* 8, 610–622
- Jain, R.K., di Tomaso, E., Duda, D.G., Loeffler, J.S., Sorensen, A.G., Batchelor, T.T. (2007). Angiogenesis in brain tumours. *Nat Rev Neurosci*, 8,610-622.
- Jain, R.K., Tong, R.T., Munn, L.L. (2007). Effect of vascular normalization by antiangiogenic therapy on interstitial hypertension, peritumour edema and lymphatic metastasis; insights from a mathematical model. *Cancer Research*, 67, 2729-2735.
- Jian, L., Du, C.J., Lee, A.H., Binns, C.W. (2005). Do dietary lycopene and other carotenoids protect against prostate cancer? *International Journal of Cancer*, 113, 1010–4.
- Jin, S.G., Jeong, Y.I., Jung, S. (2009). The effect of hyaluronic Acid on the invasiveness of malignant glioma cells : comparison of invasion potential at hyaluronic Acid hydrogel and matrigel. *J Korean Neurosurg Soc.* 46(5),472-8

- Jo, G.H., Bogler, O., Chwae, Y-J. et al. (2015). Radiation-Induced Autophagy Contributes to Cell Death and Induces Apoptosis Partly in Malignant Glioma Cells. *Cancer Research and Treatment : Official Journal of Korean Cancer Association* 47(2), 221-241.
- Jones, J.L., Walker, R.A. (1999). Integrins: a role as signalling molecules. *Mol Path*, 52,208-213.
- Jung, Y.D., Ahmad, S.A., Akagi, Y., et al. (2000). Role of the tumor microenvironment in mediating response to anti-angiogenic therapy. *Cancer Metastasis Rev*,19,147–57
- Jurenka, J.S. (2009). Anti-inflammatory properties of curcumin, a major constituent of *Curcuma longa*: a review of preclinical and clinical research. *Altern Med Rev*,14,141-153.
- Kamat, A.M., Sethi, G., Aggarwal, B.B. (2007). Curcumin potentiates the apoptotic effects of chemotherapeutic agents and cytokines through down-regulation of nuclear factor kappa-B and nuclear factor-kappa-B-regulated gene products in IFN-alpha-sensitive and IFN-alpha-resistant human bladder cancer cells. *Molecular Cancer Therapy*, 6, 1022-1030.
- Kanai, M., Yoshimura, K., Asada, M. et al. (2011). A phase I/II study of gemcitabine-based chemotherapy plus curcumin for patients with gemcitabine-resistant pancreatic cancer. *Cancer Chemotherapy and Pharmacology*, 68(1), 157–164.
- Kang, J. et al. (2005). Curcumin-induced histone hypoacetylation: the role of reactive oxygen species. *Biochem Pharmacol*, 69, 1205-1213.
- Kanzawa, T., Germano, I.M., Komata, T., Ito, H., Kondo, Y., and Kondo, S. (2004) Role of autophagy in temozolomide-induced cytotoxicity for malignant glioma cells. *Cell Death Differ* 11,448-457.
- Kapoor, S., Priyadarsini, K.I. (2001). Protection of radiation-induced protein damage by curcumin. *Biophysical Chemistry*, 92,119-126.
- Karas, M., Amir, H., Fishman, D., Danileko, M., Segal, S., Nahum, A., Koifmann, A., Giat, Y., Levy, J., Sharoni, Y. (2000). Lycopene Interferes With cell Cycle Progression and Insulin-Like Growth Factor I Signaling in Mammary Cancer Cells. *Nutrition and Cancer*, 36(1), 101-111.

- Ka-Wei, T., Alaei-Mahabadi, B., Samuelsson, T. et al. (2013). The Landscape of Viral Expression and Host Gene Fusion and Adaptation in Human Cancer. *Nature Communications* 4: 2513.
- Kenig, S., Alonso, M.B., Mueller, M.M., Lah, T.T. (2010). Glioblastoma and endothelial cells cross-talk, mediated by SDF-1, enhances tumour invasion and endothelial proliferation by increasing expression of cathepsins B, S, and MMP-9. *Cancer Letters*, 289(1), 53-61.
- Khafif, A., Hurst, R., Kyker, K., Fliss, D.M., Gil, Z., Medina, J.E. (2005). Curcumin: a new radio-sensitizer of squamous cell carcinoma cells. *Otolaryngol Head Neck Surg*, 132, 317–21.
- Khanbolooki, S., Nawrocki, S.T., Arumugam, T., Andtbacka, R., Pino, M.S., Kurzrock, R., Logsdon, C.D., Abbruzzese, J.L., McConkey, D.J. (2006). Nuclear factor kappa-B maintains TRAIL resistance in human pancreatic cancer cells. *Molecular Cancer Therapy*, 5, 2251-2260.
- Khaw, A.K., Hande, M.P., Kalthur, G., Hande, M.P. (2013) Curcumin inhibits telomerase and induces telomere shortening and apoptosis in brain tumour cells. *J Cell Biochem* 114, 1257–1270
- Kim, H. Y., Park E. J., Joe E. H., and Jou, I. (2003). Curcumin suppresses Janus kinase-STAT inflammatory signaling through activation of Src homology 2 domain-containing tyrosine phosphatase 2 in brain microglia. *J. Immunol.* 171, 6072–6079.
- Kim, O. S., Park, E. J., Joe, E. H., and Jou, I. (2002). JAK-STAT signaling mediates gangliosides-induced inflammatory responses in brain microglial cells. *J. Biol. Chem.* 277, 40594–40601.
- Kim, W.Y., Lee, H.Y. (2009). Brain angiogenesis in developmental and pathological processes: mechanism and therapeutic intervention in brain tumours. *FEBS Journal*, 276, 4653-4664.
- Kim, Y., Kumar, S. (2014). CD44-Mediated Adhesion to Hyaluronic Acid Contributes to Mechanosensing and Invasive Motility. *Mol Cancer Res* 12; 1416 .
- Kim, Y., Kumar, S. (2014). The Role of Hyaluronic Acid and Its Receptors in the Growth and Invasion of Brain Tumors. *Tumors of the Central Nervous System* 13, 253-266 .

- Kirsh, V.A., Mayne, S. T., Peters, U., et al. (2006). A prospective study of lycopene and tomato product intake and risk of prostate cancer. *Cancer Epidemiology, Biomarkers & Prevention*, 15, (1), 92–98.
- Kleihues, P. et al. (2007). The 2007 WHO Classification of Tumours of the Central Nervous System. *Acta Neuropathol.* 114(2), 97–109.
- Kleihues, P., Burger, P.C., Scheithauer, B.W.(1993). The New WHO classification of brain tumours. *Brain Pathology*, 3,255-268.
- Kleihues, P., Cavenee, W. (2000). *World health organization classification of tumours: Pathology and genetics of tumours of the nervous system*. Lyon: International Agency for research on Cancer: IARC Press.
- Kleihues, P., Ohgaki, H. (2013). The Definition of Primary and Secondary Glioblastoma. *Clin Cancer Res* 19, 764.
- Kleinman, H.K., et al. (1993). In Rohrbach, D.H. and Timpl, Reds. *Molecular and Cellular Aspects of Basement Membranes* Academic Press, 309-326.
- Knott, J.C., Edwards, A.J., Gullan, R.W., Clarke, T.M., Pilkington, G.J. (1990). A human glioma cell line retaining expression of GFAP and gangliosides, recognized by A2B5 and LB1 antibodies, after prolonged passage. *Neuropathol Appl Neurobiol*, 16(6), 489-500.
- Knupfer, M.M. et al.(1999). CD44 expression and hyaluronic acid binding of malignant glioma cells. *Clinical and Experimental Metastasis*, 17(1),81-86.
- Komine, C. et al. (2003). Promoter hypermethylation of the DNA repair gene) 6-methylguanine-DNA methyltransferase is an independent predictor of shortened progression free survival in patients with low-grade diffuse astrocytomas. *Brain Pathol*, 13, 176-84.
- Kondraganti, S., Mohanam, S., Chintala, S.K., Kin, Y., Jasti, S.L., Nirmala, C., Lakka, S.S., Adachi, Y., Kyritsis, A.P., Ali-Osman, F., Sawaya, R., Fuller, G.N., Rao, J.S. (2000). Selective Suppression of Matrix Metalloproteinase-9 in Human Glioblastoma Cells by Antisense Gene Transfer Impairs Glioblastoma Cell Invasion. *Cancer Research*, 60, 6851-6855.
- Koochekpour, S., Pilkington, G.J. (1996). Vascular and perivascular GD3 expression in human gliomas. *Cancer Letters*, 104, 97-102.

- Koochekpour, S., Pilkington, G.J., Merzak, A. (1995). Hyaluronic acid/CD44H interaction induces cell detachment and stimulates migration and invasion of human glioma cells in vitro. *International Journal of Cancer*, 63,450-454.
- Kouhata, T., Fukuyama, K., Hagihara, N., Tabuchi, K. (2001). Detection of simian virus 40 DNA sequence in human primary glioblastomas multiforme. *J. Neurosurg.*, 95: 96-101.
- Krakstad, C. and Chekenya, M. (2010). Survival signalling and apoptosis resistance in glioblastomas: opportunities for targeted therapeutics. *Molecular Cancer*, 9:135.
- Kreisl, T.N., Kim, L., Moore, K., et al. (2009). Phase II trial of single-agent bevacizumab followed by bevacizumab plus irinotecan at tumor progression in recurrent glioblastoma. *J Clin Oncol*, 27, 740-745.
- Kunwar, A., Barik, A., Mishra, B., Rathinasamy, K., Pandey, R., Priyadarsini, K.I. (2008). Quantitative cellular uptake, localization and cytotoxicity of curcumin in normal and tumour cells. *Biochimica et Biophysica Acta*, 1780, 673-679.
- Kuttan, R., Bhanumathy, P., Nirmala, K., George, M.C. (1985). Potential anticancer activity of turmeric (*Curcuma longa*). *Cancer Lett* 29(2), 197-202.
- Lakka, S.S. et al. (2002). Adenovirus-mediated expression of antisense MMP-9 in glioma cells inhibits tumor growth and invasion. *Oncogene*, 21(52), 8011-8019.
- Le, D.M., Besson, A., Fogg, D.K. (2003). Exploitation of astrocytes by glioma cells to facilitate invasiveness: a mechanism involving matrix metalloproteinase-2 and the urokinase-type plasminogen activator-plasmin cascade. *J Neurosci.* 23(10),4034-43
- Lee, M.H. and Murphy, G. (2004). Matrix metalloproteinases at a glance. *Journal of Cell Science* 117, 4015-4016.
- Lee, S. M., Lee, E. J., Ko, Y. H., et al. (2009). Prognostic significance of O6-methylguanine DNA methyltransferase and p57 methylation in patients with diffuse large B-cell lymphomas. *APMIS*, 117, 87-94.
- Leon, S.P., Folkerth, R.D., Black, P.M. (1996). Microvessel density is a prognostic indicator for patients with astroglial brain tumours. *Cancer*, 77, 362-372.
- Liotta, L.A. (1986). Tumor invasion and metastases-role of the extracellular matrix: Rhoads Memorial Award lecture. *Cancer Res* ,46, 1-7 .

- Liu, E., Wu, J., Cao, W., Zhang, J., Liu, W., Jiang, X., Zhang, X. (2007). Curcumin induces G2/M cell cycle arrest in a p53-dependent manner and upregulates ING4 expression in human glioma. *Journal of Neuro-Oncology*, 85(3), 263-270.
- Lo, H.M., Feng-Hung, C., Tseng, Y.L., Chen, B.H., Shian Jian, J., Wu, W.B. (2007). Lycopene binds PDGF-BB and inhibits PDGF-BB-induced intracellular signalling transduction pathway in rat smooth muscle cells. *Biochemical Pharmacology*, 74, 54-63.
- Louis, D.N., Ohgaki, H., Wiestler, O.D., Cavenee, WK., Burger, P.C., Jouvet, A., Scheithauer, BW., Kleihues, P.(2007).The 2007 WHO Classification of Tumours of the Central Nervous System. *Acta Neuropathol*, 114, 97-109.
- Luque-García, J. L., Martínez-TorreCuadrada, J. L., Epifano, C., Cañamero, M., Babel, I. and Casal, J. I. (2010). Differential protein expression on the cell surface of colorectal cancer cells associated to tumor metastasis. *Proteomics* 10, 940–952.
- Maher, E.A. et al. (2001).Malignant glioma: genetics and biology of a grave matter. *Genes and Dev*, 15, 1311-1333.
- Maheshwari, R., Singh, A., Gaddipati, J., Srimal, R. (2006). Multiple biological activities of curcumin: a short review. *Life Sci*, 78, 2081-2087.
- Maiani, G., Periago Caston, M.J., Catasta, G., Toti, E., Cambrodon, I.G., Bysted, A. et al. (2009). Carotenoids/; actual knowledge on food sources, intakes, stability and bioavailability and their protective role in humans. *Mol Nutr Food Res*, 53, S194-S218.
- Marczylo, T.H., Verschoyle, R.D., Cooke, D.N., Morazzoni, P., Steward, W.P., Gescher, A.J. (2007). Comparison of systemic availability of curcumin with that of curcumin formulated with phosphatidylcholine. *Cancer Chemotherapy and Pharmacology*, 60(2), 171-177.
- Marin, Y.E., Wall, B.A., Wang, S., Namkoong, J., Martino, J.J., Suh, J., Lee, H.J., Rabson, A.B., Yang, C.S., Chen, S., Ryu, J.H. (2007). Curcumin dowregulates the constitutive activity of NF-kappa B and induces apoptosis in novel mouse melanoma cells. *Melanoma Res*, 17,274-283.
- McCarthy, N. (2012). Migration: VEGF suppresses invasion. *Nature Reviews Cancer*, 12(9), 581-581.

- McKinney, P.A. Brain tumours: Incidence, survival and aetiology. (2004). *Journal of Neurology and Neurosurgery and Psychiatry*, 75, 1-12.
- Merchant, T.E., Pollack, I.A., Loeffler, J.S. (2010). Brain Tumors Across the Age Spectrum: Biology, Therapy and Late Effects. *Seminars in Radiation Oncology*, 20(1), 58-66.
- Merzak, A., Koocheckpour, S., Pilkington, G.J. (1994). CD44 mediates human glioma cell adhesion and invasion *in vitro*. *Cancer Res*, 54, 3988–3992.
- Merzak, A., Pilkington, G.J. Molecular and cellular pathology of intrinsic brain tumours. (1997). *Cancer and Metastasis Reviews*, 16, 155-177.
- Mikkelsen, T., Bjerkvig, R., Laerum, O.D. et al. (eds) (1998). Brain Tumor Invasion. United States of America: Wiley-Liss.
- Miller, A.L. (1997). Antioxidant Flavonoids: Structure, Function and Clinical Usage. *Alternative Medicine Review*, 1(2), 103-111.
- Mohan, R., Sivak, J., Ashton, P., Russo, L.A., Pham, B.Q., Kasahara, N., Raizman, M.B., Fini, M.E. (2000). Curcuminoids inhibit the angiogenic response stimulated by fibroblast growth factor-2, including expression of matrix metalloproteinase gelatinase B. *J Biol Chem*, 275, 10405-10412.
- Morga, E., Faber, C., Heuschling, P. (1999). Regional heterogeneity of the astroglial immunoreactive phenotype: effect of lipopolysaccharide. *J Neurosci Res*, 57, 941-952.
- Mukherjee Nee Chakraborty, S., Ghosh, U., Bhattacharyya, N.P., Bhattacharya, R.K., Dey, S., Roy, M. (2007). Curcumin induced apoptosis in human leukemia cell HL-60 is associated with inhibition of telomerase activity. *Mol. Cell. Biochem*, 297, 31-39.
- Murai, T. et al. (2004). Engagement of CD44 promotes Rac activation and CD44 cleavage during tumor cell migration. *J Biol Chem*, 279, 4541–50.
- Murray, D., Morrin, M., McDonnell, S. (2004). Increased Invasion and Expression of MMP-9 in Human Colorectal Cell Lines by a CD44-dependent Mechanism *ANTICANCER RESEARCH* 24, 489-494
- Morello, V. et al. (2011). β 1 integrin controls EGFR signaling and tumorigenic properties of lung cancer cells. *Oncogene*, 30(39), 4087-96.
- Murakami, D. et al, (2003). Presenilin-dependent γ -secretase activity mediates the intramembranous cleavage of CD44. *Oncogene*, 22, 1511–16.

- Nabors, L.B., Mikkelsen, T., Rosenfeld, S.S., Hochberg, F., Akella, N.S., Fisher, D.D., Cloud, G.A., Zhang, Y., Carson, K., Wittemer, S.M. et al. (2007). Phase I and correlative biology study of cilengitide in patients with recurrent malignant glioma. *J Clin Oncol*, 25, 1651-1657.
- Nahum, A., Hirsch, K., Danilenko, M., et al. (2001). Lycopene inhibition of cell cycle progression in breast and endometrial cancer cells is associated with reduction in cyclin D levels and retention of p27Kip1 in the cyclin E-cdk2 complexes. *Oncogene*, 20, (26), 3428–3436, 2001.
- Nakada, M. et al. (2001). Roles of membrane type 1 matrix metalloproteinases and tissue inhibitor of metalloproteinases 2 in invasion and dissemination of human malignant glioma. *J. Neurosurg* 94, 464-473.
- Nakada, M., Nakamura, H., Ikeda, E., Fujimoto, N., Yamashita, J., Sato, H., Seiki, M., Okada, Y. (1999). Expression and tissue localization of membrane-type 1, 2, and 3 matrix metalloproteinases in human astrocytic tumors. *Am J Pathol*. 154, 417–428.
- Naor, D., Nedvetzki, S., Golan, I., Melnik, L., Faitelson, Y. (2002). CD44 in cancer. *Crit Rev Clin Lab Sci*, 39(6), 527-579.
- Narayan, S. Cu (2004). Curcumin, a multi-functional chemopreventive agent, blocks growth of colon cancer cells by targeting beta-catenin-mediated transactivation and cell-cell adhesion pathways. *J Mol Histol*, 35, 301–7.
- Nedergaard, M., Ransom, B., Goldman, S.A. (2003). New roles for astrocytes: redefining the functional architecture of the brain. *Trends Neurosci*, 26, 523-530.
- Neufeld, G. et al (1999). Vascular endothelial growth factor (VEGF) and its receptors. *The FASEB Journal*, 13(1), 9-22
- Nghiemphu, P.L., Liu, W., Lee, Y., et al. (2009). Bevacizumab and chemotherapy for recurrent glioblastoma: a single-institution experience. *Neurology*, 72, 1217-1222.
- Nikkah, G., Tonn, J.C., Hoffmann, O., Kraemer, H.P., Darling, J.L., Schahenmayr, W., Schonmayr, R. (1992). The MTT assay for chemosensitivity testing of human tumours of the central nervous system. *Journal of Neuro-Oncology*, 13, 13-24.
- Noack, J., Richter, K., Kopp-Schneider, A. et al. (2014). A sphingosine kinase inhibitor combined with temozolomide induces glioblastoma cell death through accumulation of dihydrosphingosine and dihydroceramide, endoplasmic reticulum stress and autophagy. *Cell Death and Disease* 5, e1425

- Norden, A.D., Young, G.S., Setayesh, K., et al. (2008). Bevacizumab for recurrent malignant gliomas: efficacy, toxicity, and patterns of recurrence. *Neurology*, 70, 779-787.
- Nuttall, R.K., Pennington, C.J, Taplin, J., Wheal, A., Yong, V.W., Forsyth, P.A. and Edwards, D.R. (2003). Elevated membrane-type matrix metalloproteinases in gliomas revealed by profiling proteases and inhibitors in human cancer cells. *Mol Cancer Res* 1:333-345.
- Ogiso, M., Ohta, M., Harada, Y., Kubo, H., Hirano, S. (1991). Developmental change in ganglioside expression in primary culture of rat neurons. *Neuroscience*. 41, 167–176.
- Ohgaki, H., Kleihue, P. (2007). Genetic Pathways to Primary and Secondary Glioblastoma. *Am J Pathol*. 170(5), 1445–1453.
- Ohka, F., Natsume, A., Wakabayashi, T. (2012). Current Trends in Targeted Therapies for Glioblastoma Multiforme *Neurology Research International* 2012.
- Ohkawa, Y., Momota, H., Kato, A. et al. (2015). Ganglioside GD3 enhances invasiveness of gliomas by forming a complex with platelet-derived growth factor receptor alpha and Yes. *J Biol Chem*. pii: jbc.M114.635755.
- Okada, H., et al. (1996). Suppression of CD44 expression decreases migration and invasion of human glioma cells. *Int J Cancer*, 66, 255–60.
- Okada, K. et al. (2001). Curcumin and especially Tetrahydrocurcumin ameliorate oxidative stress-induced renal injury in mice. *J.Nutr*, 131(8), 2090-2095.
- Okomoto, I. et al (1999). CD44 cleavage induced by a membrane-associated metalloprotease plays a critical role in tumor cell migration. *Oncogene*, 18, 1435–46.
- Okomoto, I. et al. (2001). Proteolytic release of CD44 intracellular domain and its role in the CD44 signaling pathway *J Cell Biol*, 155, 755–62.
- Olson, A.K., Dimberg, A., Kreuger, J., Claesson-Welsh, L. (2006). VEGF receptor signaling-in control of vascular function. *Nature Review: Molecular Cell Biology*, 7, 359-371.
- Omoni, A.O., Aluko, R.E. (2005). The anti-carcinogenic and anti-atherogenic effects of lycopene: a review. *Trends in Food Science & Technology*, 16(8), 344-350.
- Onishi, M., Ichikawa, T., Kurozumi, K., Date, I. (2011). Angiogenesis and invasion in glioma. *Brain Tumour Pathology*, 28(1), 13-24.

- Orian-Rousseau, V., Chen, L., Sleeman, J.P., Herrlich, P., Ponta, H. (2002). CD44 is required for two consecutive steps in HGF/c-Met signaling. *Genes Dev*, 16(23), 3074-3086.
- Ormerod, MG. (ed). (2005). *Flow Cytometry*. 3rd edition. New York. Oxford University Press.
- Pae, H.O., Jeong, S., Jeong, G.S., Kim, K.M., Kim, H.S., Kim, S.A., Kim, Y.C., Kang, S.D., Kim, B.N., Chung, H.T. (2007). Curcumin induces pro-apoptotic endoplasmic reticulum stress in human leukemia HL-60 cells. *Biochem Biophys Res Commun*, 353, 1040-1045.
- Paez-Ribes, M., Allen, E., Hudock, J., Takeda, T., Okuyama, H., Vinals, F., et al. (2009). Antiangiogenic therapy elicits malignant progression of tumors to increased local invasion and distant metastasis. *Cancer Cell*, 15, 220–31.
- Panicker, S.R., Kartha, C.C. (2010). Curcumin attenuates glucose-induced monocyte chemoattractant protein-1 synthesis in aortic endothelial cells by modulating the nuclear-factor kappaB pathway. *Pharmacology* 85, 18-26.
- Park CC, Zhang H, Pallavicini M, Gray JW, Baehner F, Park CJ, Bissell MJ. (2006). Beta1 integrin inhibitory antibody induces apoptosis of breast cancer cells, inhibits growth, and distinguishes malignant from normal phenotype in three dimensional cultures and in vivo. *Cancer Research*. 66 (3), 1526–1535.
- Park, D., Kim, Y. et al. (2012). Hyaluronic acid promotes angiogenesis by inducing RHAMM-TGFβ receptor interaction via CD44-PKCδ. *Mol Cells*, 33(6):563-74.
- Parker, K.A., Pilkington, G.J. (2006). Apoptosis of human malignant glioma-derived cell cultures treated with clomipramine hydrochloride, as detected by Annexin-V assay. *Radiol Oncol*, 40(2), 87-93.
- Paulus, W. et al. (1996). Diffuse brain invasion of glioma cells requires beta1 integrins. *Lab Invest* 75, 819-826.
- Peng, L., Wang, B., Ren, P. (2005). Reduction of MTT by flavonoids in the absence of cells. *Colloids and Surfaces Biointerfaces*; 45, 108-111.
- Perry, M.-C., Demeule, M., Régina, A., Mouldjian, R. and Béliveau, R. (2010). Curcumin inhibits tumor growth and angiogenesis in glioblastoma xenografts. *Mol. Nutr. Food Res*, 54, 1192–1201.

- Peters, M.D., Davis, S.K., Austin, S. (1990). Clomipramine: an antiobsessional tricyclic antidepressant. *Clin Pharm*, 9, 165-178.
- Pfister, S., Hartmann, C., Korshunov, A. (2009). Histology and Molecular Pathology of Pediatric Brain Tumors. *J Child Neurol* 24(11), 1375-1386 .
- Pierpoint, W.S. (1990). PQQ in plants. *Trends in biochemical sciences*, 15, 8, 299.
- Pilkington G.J. (1996). The role of the extracellular matrix in neoplastic glial invasion of the nervous system. *Braz J Med Biol Res*. 29,1159–1172.
- Pilkington, G.J. (1994). Tumour cell migration in the central nervous system. *Brain Pathology*, 4, 157-166.
- Pilkington, G.J. (2001). Brain tumours in the elderly. In D. Ed, T. De La (Eds.), *Pathology of the Aging Human Nervous System* (pp.408-428).Oxford: Oxford University Press.
- Pillai, G.R., Srivastava, A.S., Hassanein, T.I., Chauhan, D.P., Carrier, E. (2004). Induction of apoptosis in human lung cancer cells by curcumin. *Cancer Letters*, 208,163-170.
- Ponta, H., Sherman, L., Herrlich, P.A. (2003). CD44: From adhesion molecules to signalling regulators. *Nature Reviews: Molecular Cell Biology*, 4, 33-45.
- Ponta, H., Sherman, L., Herrlich, P.A. (2003). CD44: from adhesion molecules to signalling regulators. *Nat Rev Mol Cell Biol*, 4(1), 33-45.
- Popescu, A.M., Purcaru, S.O., Stoleru, B. et al. (2013). Angiogenesis and Vascular Endothelial Growth Factor in malignant gliomas. *Current Health Sciences Journal* 39, (1).
- Pozarowski, P., Darzynkiewicz, Z. (2004). Analysis of cell cycle by flow cytometry. *Methods Mol Biol.*, 281, 301–311.
- Preusser, M., de Ribaupierre, S., Wohrer, A. et al. (2011). Current concepts and management of glioblastoma. *Ann Neurol*. 70(1), 9-21.
- Priyadarsini, R.V., Senthil Murugan, R., Maitreyi, S., Ramalingam, K., Karunakaran, D., Nagini, S. (2010). The flavonoid quercetin induces cell cycle arrest and mitochondria-mediated apoptosis in human cervical cancer (HeLa) cells through p53 induction and NF-κB inhibition. *European Journal of Pharmacology*, 649 (1–3), 84-91.

- Puré, E., Cuff, C.A. (2001). A crucial role for CD44 in inflammation. *Trends Mol Med*, 7(5), 213-221.
- Radotra, B., McCormick, D. (1997). CD44 is involved in migration but not spreading of astrocytoma cells *in vitro*. *Anticancer Res*, 17, 945–949.
- Raff, M.C., Miller, R.H., Noble, M. (1983). A glial progenitor cell that develops in vitro into an astrocyte or oligoendrocyte depending on culture medium. *Nature*, 303(5916), 390-396.
- Rahmani, A.H., Al Zohairy, M.A., Aly, S.M. et al.(2014). Curcumin: A Potential Candidate in Prevention of Cancer via Modulation of Molecular Pathways. *BioMed Research International* 2014, Article ID 761608, 15 pages
- Rampling, R., James, A., Papanastassiou, V. (2004). The Present and Future Management of Malignant Brain Tumours: Surgery, Radiotherapy and Chemotherapy. *Journal of Neurosurgery Psychiatry*, 75 (II), 24-30.
- Ranuncolo, S.M. et al (2002). CD44 expression in human gliomas. *Journal of Surgical Oncology*, 79(1), 30-36.
- Rao, J.S. (2003). Molecular mechanisms of glioma invasiveness: The role of proteases. *Nature Reviews, Cancer*, 3, 489-501.
- Rao, J.S., Steck, P.A., Mohanam, S., Stetler-Stevenson, W.G., Liotta, L.A., Sawaya, R. (1993). Elevated levels of M(r) 92,000 type IV collagenase in human brain tumour. *Cancer Research*, 53(10), 2208-2211.
- Rasheed, S, Nelson-Rees WA, Toth EM, Arnstein P, Gardner MB. (1974). Characterization of a newly derived human sarcoma cell line (HT-1080). *Cancer*. 33 (4), 1027–1033.
- Ray, S, Chattopadhyay N, Mitra, A, Siddiqi, M, Chatterjee, A (2003). Curcumin exhibits antimetastatic properties by modulating integrin receptors, collagenase activity and expression of Nm23 and E-cadherin. *J Environ Pathol Toxicol Oncol*, 22(1), 49-58.
- Readon, D.A., Dejdardins, A., Vredenburgh, J.J., et al. (2009). Metronomic chemotherapy with daily oral etoposide plus bevacizumab for recurrent malignant glioma: a phase II study. *Br J Cancer*, 101, 1986-1994.

- Reddy, S., Rishi, A.K., Xu, H., Levi, E., Sarkar, F.H., Majumdar, A.P. (2006). Mechanisms of curcumin and EGF-receptor related protein (ERRP)-dependent growth inhibition of colon cancer cells. *Nutritional Cancer*, 55,185-194.
- Regina, A., Demeule, M., Laplante, A., et al. (2001). Multidrug resistance in brain tumours: Roles of the blood-brain barrier. *Cancer and Metastasis Review*, 20, 13-25.
- Reich, P., Shwachman,H. and Craig, M.N. (1960). Lycopenemia-A Variant of Carotenemia. *J. Engl J Med*, 262 (6), 263-269.
- Rong, Y., Durden, D.L., Van Meir, E.G., Brat, D.J. (2006). Pseudopalisading' necrosis in glioblastoma: a familiar morphologic feature that links vascular pathology, hypoxia, and angiogenesis. *J Neuropathol Exp Neurol*. 65(6), 529-39.
- Rooprai, H., Vanmeter, T., Panou, C., et al. (1999). The role of integrin receptors in aspects of glioma invasion in vitro. *Int J Dev Neurosci*, 17,613–623.
- Rooprai, H.K. et al., (2000). The effects of exogenous growth factors on matrix metalloproteinase secretion by human brain tumour cells. *Br J Cancer*, 82(1), 52–55.
- Rooprai, H.K., Christidou, M., Pilkington, G.J. (2003). The potential for strategies using micronutrients and heterocyclic drugs to treat invasive gliomas. *Acta-Neurochirurgica*, 145(8), 613-4.
- Rooprai, H.K., Kandaneeratchi, A., Maidment, S.L., Christidou, M., Trillo-Pazos, G., Dexter, D.T., Rucklidge, G., Widmer, W.W., Pilkington, G.J. (2001). Evaluation of the effects of swainsonine, captopril, tangeretin and nobiletin on the biological behaviour of brain tumour cells in vitro. *Neuropathology and Applied Neurobiology*, 27, 29-39.
- Rooprai, H.K., Kyriazis, I., Nuttall, R.K., Edwards, D.R., Zicha, D., Aubyn, D., Davies, D., Gullan, R., Pilkington, G.J. (2007). Inhibition of invasion and induction of apoptosis by selenium in human malignant brain tumour cells in vitro. *International Journal of Oncology*, 30(5), 1263-71.
- Roth, V. (2006). <http://www.doubling-time.com/compute.php>
- Rubenstein, J.L., Kim, J., Ozawa, T., Zhang, M., Westphal, M., Deen, D.F., et al. (2000). Anti-VEGF antibody treatment of glioblastoma prolongs survival but results in increased vascular cooption. *Neoplasia*, 2,306–14.

- Sabeh, F., Ota, I., Holmbeck, K., et al. (2004). Tumor cell traffic through the extracellular matrix is controlled by the membrane-anchored collagenase MT1-MMP. *J Cell Biol*, 167, 769–81.
- Salcman, M. (1995). Glioblastoma and malignant astrocytoma. In: Andrew H Kaye, Edward R Laws Jr. Brain Tumours. New York: Churchill Livingstone.p. 449-478.
- Sambuy Y et al. (2005). The Caco-2 cell line as a model of the intestinal barrier; influence of cell and culture related factors on Caco-2 cell functional characteristics. *Cell Biology and Toxicology*, 21,1-26.
- Sathornsumetee, S., Rich, J. (2007). Antiangiogenic therapy in malignant glioma: promise and challenge. *Curr Pharm*, 13, 3545-3558.
- Sato, R., Helzlsouer, K.J., Alberg, A.J., Hoffman, S.C., Norkus, E.P., Comstock, G.W. (2002). Prospective study of carotenoids, tocopherols and retinoid concentrations and the risk of breast cancer. *Cancer Epidemiology Biomarkers Prev*, 11, 451-457.
- Schering-Plough Corp. Kenilworth, NJ. (2008). Temodar (temozolomide) package insert-pharmacist information. Retrieved December 26, 2012, from the Schering-Plough Corp/Merck & Co. website: <http://www.spfiles.com/pharmtemodar.pdf>
- Schindler, R., Mentlein, R. (2006). Flavonoids and vitamin E reduce the release of the angiogenic peptide vascular endothelial factor from human tumour cells. *Journal of Nutrition*, 136, 1477-1482.
- Schlessinger, J. (2000).Cell signaling by receptor tyrosine kinases. *Cell*, 103:211–225.
- Sen, S., Sharma, H., Singh, N. (2005). Curcumin enhances vinorelbine mediated apoptosis in nsccl cells by the mitochondrial pathway. *Biochem Biophys Res Commun*. 331, 1245–52.
- Senft, C., Polacin, M. et al (2010). The nontoxic natural compound Curcumin exerts anti-proliferative, anti-migratory, and anti-invasive properties against malignant gliomas *BMC Cancer*, 10, 491.
- Sennino, B. et. al. (2012). Suppression of tumour invasion and metastasis by concurrent inhibition of c-Met and VEGF signalling in pancreatic neuroendocrine tumours. *Cancer Discovery*, 2(3),270-87.

- Seo, J. H., Jeong, K. J., Oh, W. J., Sul, H. J., Sohn, J. S. et al. (2010). Lysophosphatidic acid induces STAT3 phosphorylation and ovarian cancer cell motility: their inhibition by curcumin. *Cancer Lett.* 288, 50–56.
- Seol, D.W., Chen, Q., Zarnegar R. (2000). Transcriptional activation of the hepatocyte growth factor receptor (c-met) gene by its ligand (hepatocyte growth factor) is mediated through AP-1. *Oncogene*, 19(9), 1132-7.
- Shanmugam, M.K., Rane, G., Kanchi, M.M. et al. (2015). The multifaceted role of curcumin in cancer prevention and treatment. *Molecules*. 20(2), 2728-69.
- Shao, Z.M., Shen, Z.Z., Liu, C.H., Sartippour, M.R., Go, V.L., Heber, D., Nguyen, M. (2002). Curcumin exerts multiple suppressive effects on human breast carcinoma cells. *International Journal of Cancer*, 98, 234-240.
- Sharma, R.A., Gescher, A.J., Steward, W.P. (2005). Curcumin: the story so far. *European Journal of Cancer*, 41, 1955-1968.
- Sharma, R.A., Ireson, C.R., Verschjoyle, R.D., Hill K.A., Williams, M.J.L., Leuratti, C., Manson, M.M., Marnett, L.J., Steward, W.P., Gescher, A.J. (2001a). Pharmacodynamic effects of dietary curcumin on glutathione S-transferase and malondialdehyde-DNA adducts in rat liver and colon mucosa: relationship with drug levels. *Clin Cancer Res* 7, 1452–1458.
- Sharma, R.A., McLelland, H.R., Ireson, C.R., Hill, K.A., Euden, S.A., Manson, M.M., Primohamde, M., Marnett, L.J., Gescher, A.J., Steward, W.P. (2001b). Pharmacodynamic and pharmacokinetic study of oral *Curcuma* extract in patients with colorectal cancer. *Clin Cancer Res* 7, 1894–1900.
- Shehzad, A., Wahid, F., Lee, Y.S. (2010). Curcumin in Cancer Chemoprevention: Molecular Targets, Pharmacokinetics, Bioavailability, and Clinical Trials. *Archiv der Pharmazie*, 343(9), 489–499.
- Shi, M., Cai, Q., Yao, L., Mao, Y., Ming, Y., Ouyang, G. (2006). Antiproliferation and apoptosis induced by curcumin in human ovarian cancer cells. *Cell Biology International*, 30(3), 221-226.
- Shi, P., Chen, W.W., Hu, X.Y., Yu, C.X., Zhang, P.J., Jiang, A., Zhang, J.Y. (2006). Up-regulates the expression of maspin gene in prostate cancer cell line LNCaP. *Yao Xue Xue Bao*, 41, 1152-1156.

- Shi, Q., Bao, S., Song, L. et al. (2007). . Targeting SPARC expression decreases glioma cellular survival and invasion associated with reduced activities of FAK and ILK kinases. *Oncogene* 26, 4084–4094
- Simon, A., Allais, D.P., Durox, J.L., Basly, J.P., Durand-Fontainer, S., Delage, C. (1998). Inhibitory effect of curcuminoids on MCF-7 cell proliferation and structure-activity relationships. *Cancer Letters*, 129,111-6.
- Singh, S.K., Howkins, C., Clarke, I.D., et al. (2004). Identification of human brain tumour initiating cells. *Nature*, 432, 396-401.
- Siwak, D.R., Shishodia, S., Aggarwal, B.B., Kurzrock, R. (2005). Curcumin induced antiproliferative and pro-apoptotic effects in melanoma cells are associated with suppression of Ikappa B kinase and nuclear factor kappaB activity and are independent of the B-Raf/mitogen activated/extracellular signal regulated protein kinase pathway and the Akt pathway. *Cancer*, 104,879-890.
- Skommer, J., Wlodkowic, D., Pelkonen, J. (2006). Cellular foundation of curcumin induced apoptosis in follicular lymphoma cell lines. *Exp Hematol*, 34,463-474.
- Sneath, R.J., Mangham, D.C. (1998).The normal structure and function of CD44 and its role in neoplasia. *Mol Pathol*, 51(4),191-200.
- Sofroniew, M.V., Vinters, H.V. (2010). Astrocytes: biology and pathology. *Acta Neuropathol*, 119, 7-35.
- Sohail, A., Sun, Q., Zhao, H., Bernardo, M.M., Cho, J.A., Fridman, R.(2008). MT4-(MMP17) and MT -(MMP25), a unique set of membrane-anchored matrix metalloproteinases:properties and expression in cancer. *Cancer and Metastasis reviews*, 27(2), 289-302.
- Sokoloski, J.A., Shyam, K., Sartorelli, A.C. (1997). Induction of the differentiation of HL-60 promyelocytic leukemia cells by curcumin in combination with low levels of Vitamin D3. *Oncology research*, 9,31-39.
- Srejayan, N., Rao, M.N.A. (1994). Curcuminoids as potent inhibitors of lipid peroxidation. *The Journal of Pharmacy and Pharmacology*, 46, 1013-1016.
- Stilling, R.M., Fischer, A. (2011). The role of histone acetylation in age-associated memory impairment and Alzheimer's disease. *Neurobiol Learn Mem*, 96, 19-26.
- Stivarou, T., Patsavoudi, E. (2015). Review Extracellular Molecules Involved in Cancer Cell Invasion *Cancers* 7, 238-265

- Stojic, J. et al (2008). Expression of matrix metalloproteinases MMP-1, MMP-11 and MMP-19 is correlated with the WHO-grading of human malignant gliomas. *Neurosci Res*, 60, 40–49.
- Strimpakos, A.S., Sharma, R.A. (2008). Curcumin: Preventive and therapeutic properties in laboratory studies and clinical trials. *Antioxidants & Redox Signaling*, 10(3), 511-538.
- Stupp, R., Mason, W.P., van den Bent, M.J. et al. (2005). Radiotherapy plus concomitant and adjuvant temozolomide for glioblastoma. *N Eng J Med*, 352, 987-96.
- Stupp, R., Wong, E.T., et al. (2012). NovoTTF-100A versus physician's choice chemotherapy in recurrent glioblastoma: a randomised phase III trial of a novel treatment modality. *Eur J Cancer*, 48(14), 2192-2202.
- Sun, M., Yang, Y., Li, H., Su, B., Lu, Y., Wei, Q., Fan, T. (2004). The effect of curcumin on bladder cancer cell line EJ in vitro. *Zhong Yao Cai*, 27, 848-850.
- Szaakacs, G., Gottesman, M.M. (2004). Comparing Solid Tumour with Cell Lines: Implications for Identifying Drug Resistance Genes in Cancer. *Molecular Interventions*, 4(6), 323-325.
- Szotek, P.P., Pieretti-Vanmarcke, R., Masiakos, P.T., Dinulescu, D.M., Connolly, D., Foster, R., Dombkowski, D., Preffer, F., MacLaughlin, D.T., Donahoe, P.K. (2006). Ovarian cancer side population defines cells with stem cell-like characteristics and Mullerian Inhibiting Substance responsiveness. *Proceedings of the National Academy of Sciences of the United States of America*, 103(30), 11154-11159.
- Taherian, A.A. et al. (2011). Differences in integrin expression and signalling within human breast cancer cells. *BMC Cancer*, 11, 293.
- Taiwo, B.O. (2000). AIDS-related primary CNS lymphoma: a brief review. *AIDS Read*. 10 (8), 486-91.
- Takano, S., Yamashita, T., Ohneda, O. (2010). Molecular Therapeutic Targets for Glioma Angiogenesis. *Journal of Oncology*, 2010, 1-11.
- Taub, M., Wang, Y., Szczesny, T.M., Kelnman, H.K. (1990). Epidermal growth factor or transforming growth factor alpha is required for kidney tubulogenesis in Matrigel cultures in serum-free medium. *Proc Nat l Acad Sci USA*, 87, 4002-4006.

- Teodoro, A.J., Oliveira, F.L., Martins, N.B. et al. (2012). Effect of lycopene on cell viability and cell cycle progression in human cancer cell lines. *Cancer Cell International* 12,36
- Thompson, K.H., Bohmerle, K., Polishchuk, E., Martins, C., Toleikis, P., Tse, J., Yuen, V., Mcneill, J.H., Orvig, C. (2004). Complementary inhibition of synoviocyte, smooth muscle cell or mouse lymphoma cell proliferation by a vanadyl curcumin complex compared to curcumin alone. *J Inorg Biochem*, 98, 2063-2070.
- Thornberry, N.A., Rano, T.A., Peterson, E.P. et al. (1997). A combinatorial approach defines specificities of members of the caspase family and granzyme B. Functional relationships established for key mediators of apoptosis. *J.Biol Chem* 272(29), 17907-17911.
- Tourneau, C.L., Faivre, S., Raymond, E. (2008). New developments in multitargeted therapy for patients with solid tumours. *Cancer Treatment Reviews*, 34, 37-48.
- Trimble, M.R. (1990). Worldwide use of clomipramine. *J Clin Psychiat*, 51(Suppl), 51-54.
- Trumbo, P.R. (2005). Promises and Perils of Lycopene /Tomato Supplementation and Cancer Prevention. Are there Adverse Effects of Lycopene Exposure? *Journal of Nutrition*, 135, 2060S-2061S.
- Tu, H., Xu, C., Zhang, W. et al. (2010). GABA_B Receptor Activation Protects Neurons from Apoptosis via IGF-1 Receptor Transactivation. *The Journal of Neuroscience*, 30(2), 749-759.
- Tu, Y., Zhong, Y. et al (2011). Activation of JAK/STAT signal pathway predicts poor prognosis of patients with gliomas. *Medical Oncology*, 28(1), 15-23.
- Tysnes, B.B. et al. (1996). Stimulation of glioma-cell migration by laminin and inhibition by anti-alpha3 and anti-beta1 integrin antibodies. *Int J Cancer* 67, 777-784.
- VanMeter, T.E. et al. (2001). The role of matrix metalloproteinase genes in glioma invasion: co-dependent and interactive proteolysis. *J Neurooncol*, 53,213–235.
- VanMeter, T.E. et al. (2004). Induction of membrane-type-1 matrix metalloproteinase by epidermal growth factor-mediated signaling in gliomas. *Neuro-oncol*, 6(3), 188–199.

- Verhaak, et al. (2010). Integrated genomic analysis identifies clinically relevant subtypes of glioblastoma characterized by abnormalities in PDGFRA, IDH1, EGFR, and NF1. *Cancer Cell*, 17(1), 98-110.
- Vermes, I., Haanen, C., Steffens-Nakken, H., Reutelingsperger, C., (1995) A novel assay for apoptosis. Flow cytometric detection of phosphatidylserine expression on early apoptotic cells using fluorescein labelled Annexin V. *J Immunol Methods*, 184, 29-51.
- Von Deimling, A., Eibl, R.H., Ohgaki, H., Louis, D.N., von Ammon, K., Petersen, I., Kleihues, P., Chung, R.Y., Wiestler, O.D., Seizenger, B.R. (1992). p53 mutations are associated with 17p allelic loss in grade II and grade III astrocytoma. *Cancer Research*, 52, 2987-2990.
- Vredenburgh, J.J., Desjardins, A., Herndon, J.E. II, Dowell, J.M., Reardon, D.A., Quinn, J.A., Rich, J.N., Sathornsumetee, S., Gururangan, S., Wagner, M. et al. (2007). Phase II trial of bevacizumab and irinotecan in recurrent malignant glioma. *Clin Cancer Research*, 13, 1253-1259.
- Vredenburgh, J.J., Desjardins, A., Herndon, J.E. II, et al. (2007). Bevacizumab plus irinotecan in recurrent glioblastoma multiforme. *J Clin Oncol*, 25, 4722-4729.
- Wang, L., Ye, X., Cai, X. et al. (2015). Curcumin suppresses cell growth and invasion and induces apoptosis by down-regulation of Skp2 pathway in glioma cells. *Oncotarget* 5,1-11
- Wang, W., Abbruzzese, J.L., Evans, D.B., Larry, L., Cleary, K.R., Chiao, P.J. (1999). The nuclear factor-kappa B RelA transcription factor is constitutively activated in human pancreatic adenocarcinoma cells. *Clinical Cancer Research*, 5, 119-127.
- Wang, W.Z., Zhang, B.Y. (2009). Effect of curcumin on JAK-STAT signalling pathway in hepatoma cell lines. *Yao Xue Xue Bao*, 44(12), 1434-9.
- Weber, E.L., Goebel, E.A. (2005). Cerebral edema associated with Gliadel wafers: Two case studies. *Neuro-Oncology*, 7, 84-89.
- Wei, M.Y., and Giovannucci, E.L. (2012). Lycopene, Tomato Products, and Prostate Cancer Incidence: A Review and Reassessment in the PSA Screening Era. *Journal of Oncology*, 2012. Article ID 271063, 7 pages.
- Wei, K.C. et al. (2010). Evaluation of the prognostic value of CD44 in glioblastoma multiforme. *AntiCancer Res*, 30, 253-260.

- Weissenberger, J., Priester, M. et al (2010). Dietary Curcumin Attenuates Glioma Growth in a Syngeneic Mouse Model by Inhibition of the JAK1,2/STAT3 Signaling Pathway. *Clin Cancer Res*, 16, 5781.
- Wen, P.Y., Kesari, S. (2008). Malignant gliomas in adults. *N Engl J Med*, 359,492-507
- Wenger SL et al. (2004). Comparison of established cell lines at different passages by karyotype and comparative genomic hybridization. *Bioscience Reports*, 24(6): 631-639.
- Westphal, M., Hilt, D.C., Bortey, E., Delavault, P., Olivares, R., Warnke, P.C., Whittle, I.R., Jaaskelainen, J., Ram, Z. (2003). A phase 3 trial of local chemotherapy with biodegradable carmustine (BCNU) wafers (gliadel wafers) in patients with primary malignant glioma. *Neuro-oncology*, 5, 79-88.
- Westphal, M., Ram, Z., Riddle, V., Hilt, D., Bortey, E. (2006). Gliadel wafer in initial surgery for malignant glioma: long -term follow –up of a multicenter controlled trial. *Acta Neurochir*, 148, 269-275.
- Wilken, R., Veena, M.S., Wang, M.B. et al. (2011). Curcumin: A review of anti-cancer properties and therapeutic activity in head and neck squamous cell carcinoma. *Molecular Cancer* 10,12.
- Wilken, R., Veena, M.S., Wang, M.B. and Srivatsan, E.S. (2011). Curcumin: A review of anti-cancer properties and therapeutic activity in head and neck squamous cell carcinoma. *Molecular Cancer*, 10(12), 1-19.
- Wippold, F.J., Lammie, M., Anatelli, F., Lennerz, J., Perry, A. (2006). Neuropathology for the Neuroradiologist: Palisades and Pseudopalisades. *AJNR Am J Neuroradiol*, 27, 2037-2041.
- Wiranowska M., Rojiani M. V. (2011). Extracellular matrix microenvironment in glioma progression, in Glioma – Exploring Its Biology and Practical Relevance, ed. Anirban Ghosh, editor. (Shanghai: InTech;), 257–284
- Wiranowska, M. et al. (2006). CD44 adhesion molecule and neuro-glial proteoglycan NG2 as invasive markers of glioma. *Brain Cell Biol*, 35(2-3):159-72.
- Wiranowska, M., Ladd, S. et al. (2010). Modulation of hyaluronan production by CD44 positive glioma cells. *International Journal of Cancer*, 127(3), 532-542.

- Wiranowska, M., Ladd, S., Moscinski, C. et al. (2010). Modulation of hyaluronan production by CD44 positive glioma cells. *International Journal of Cancer* 127(3), 532–542.
- Wu, C., Alman, B.A. (2008). Side population cells in human cancers. *Cancer Letters*, 268(1), 1-9.
- Wu, Y., Chen, Y., Xu, J., Lu, L. (2002). Anticancer activities of curcumin on human Burkitt's lymphoma. *Zhonghua Zhong Liu Za Zhi*, 24,348-352.
- Wyss, A., Wirtz, G. M., Woggon, W. D., Brugger, R., Wyss, M. (2001). Expression pattern and localization of beta,beta-carotene 15,15'-dioxygenase in different tissues. *Biochem J*, 354,521–529.
- Xie, J. (2000). PDGF Pathways and Growth of Basal Cell and Squamous Cell Carcinomas [Electronic version]. Austin (TX): Madame Curie Bioscience Database.
- Ye, M-X., Li, Y., Yin, H., Zhang, J. (2012). Curcumin: Updated Molecular Mechanisms and Intervention Targets in Human Lung Cancer. *International Journal of Molecular Sciences*. 13(3), 3959-3978.
- Yeum, K.J., Russel, R.M. (2002). Carotenoid Bioavailability and Bioconversion. *Annual Review of Nutrition*, 22, 483-504.
- Yoysungnoen, P., Wirachwong, P., Bhattarakosol, P., Niimi, H., Patumraj, S. (2006). Effects of curcumin on tumor angiogenesis and biomarkers, COX-2 and VEGF, in hepatocellular carcinoma cell-implanted nude mice. *Clin Hemorheol Microcirc* 34,109-115.
- Yu Q., Stamenkovic, I. (2000). Cell surface-localized matrix metalloproteinase-9 proteolytically activates TGF-beta and promotes tumor invasion and angiogenesis. *Genes Dev*, 14(2), 163-176.
- Yu, H. et al. (1997). Evidence for diminished functional expression of intestinal transporters in Caco-2 cell monolayers at high passages. *Pharmaceutical Research*, 14(6), 757-762.
- Yu, J., Ustach, C. and Choi Kim, H.R. (2003). Platelet-derived Growth Factor Signaling and Human Cancer. *Journal of Biochemistry and Molecular Biology*, 36(1), 49-59.

- Yu, Q., Stamenkovic, I. (1999). Localization of matrix metalloproteinase 9 to the cell surface provides a mechanism for CD44-mediated tumour invasion. *Genes Development*, 13, 35-48.
- Yung, W.A., Shapiro, J.R. and Shapiro, W.R. (1982). Heterogeneous chemosensitivities of subpopulations of human glioma cells in culture. *Cancer Research*, 42, 992–998.
- Yvonne, G.L., et al., (2007). Curcumin Inhibits Tumor Growth and Angiogenesis in Ovarian Carcinoma by Targeting the Nuclear Factor- κ B Pathway. *Clin Cancer Res* 13, 3423.
- Zagzag, D., Friedlander, D.R., Dosik J., Chikramane, S., Chan, W., Greco, M.A. et al., (1996). Tenascin-C expression by angiogenic vessels in human astrocytoma and by human brain endothelial cell in vitro. *Cancer Research*, 56, 182-189.
- Zbarsky, V., Datla, K.P., Parkar, S., Rai, D.K., Aruoma, O.I. & Dexter, D.T. (2005). Neuroprotective properties of the natural phenolic antioxidants curcumin and naringenin but not quercetin and fisetin in a 6-OHDA model of Parkinson's disease. *Free radical research*, 39(10), 1119-1125.
- Zhang, Y., Barres, B.A. (2010). Astrocyte heterogeneity: an underappreciated topic in neurobiology. *Current Opinion in Neurobiology*, 20, 588-594.
- Zheng, L.D., Tong, Q.S., Wu, C.H. (2002). Inhibitory effects of curcumin on apoptosis of human ovary cancer cell line A2780 and its molecular mechanism. *Ai Zheng*, 21, 1296-1300.
- Zheng, L.D., Tong, Q.S., Wu, C.H. (2006). Growth inhibition and apoptosis inducing mechanisms of curcumin on human ovarian cancer cell line A2780. *Chin J Integr Med*, 12, 126-131.
- Zuniga, R.M., Torcuator. R., Jain, R., et al. (2009). Efficacy, safety and patterns and recurrence in patients with recurrent high grade gliomas treated with bevacizumab plus irinotecan. *J Neurooncol*, 91, 329-336.

Appendices

Appendix 1: Curcumin C3 Complex Certificate of Analysis and LycoRed
Nutritional Information



SABINSA CORPORATION

20 Lake Drive,
East Windsor,
New Jersey - 08520
Tel: 732-777-1111
Fax: 732-777-1443

Sabinsa Utah,
750 South Innovation Circle,
Payson, UT 84651
Tel: 801-465-8400
Fax: 801-465-8600

PACKING SLIP

Ship To : **SAMPLE REQUEST CUSTOMER**
Dept. of Natural Sciences
School of Health and Social Sciences
Middlesex University
Room HG29, Hatchcroft Building

The Burroughs, Hendon
London NW4 4BT
United Kingdom

Sold To : **SAMPLE REQUEST CUSTOMER**
Dept. of Natural Sciences
School of Health and Social Sciences
Middlesex University
Room HG29, Hatchcroft Building

The Burroughs, Hendon
London NW4 4BT
United Kingdom

Date Of Shipment : **December 05, 2011**

Shipped From : **NEW JERSEY**

Ship Via :

Service : **COLLECT**

Packing	Product Name	Lot No.	Quantity
1 x 0.1 Kg	CURCUMIN C3 COMPLEX®	J110235	0.100 Kg

Comments :

RETURNS: We hope that you are happy with this order. However, if you need to return this material, Please contact customer service at 1-732-777-1111 or 1-801-465-8400 and obtain a return authorisation number before returning. Please mention RA no. on all return paperwork to expedite replacements or credits. Material(s) received without a RA no. may not be credited in your account.



SABINSA CORPORATION

*Pharmaceuticals *Phytochemicals
*Fine Chemicals *Herbal Extracts
*Cosmeceuticals *Specialty Chemicals

CERTIFICATE OF ANALYSIS

Page 1 of 3

Product Name CURCUMIN C3 COMPLEX®
Product Code 0330
Batch No. J110235
TR No. DB11F0134
Date of Manufacture September 2011
Date of Expiry August 2016



Sold To : SAMPLE REQUEST CUSTOMER

Quantity : 0.100 KG

Botanical/Scientific name Curcuma longa
CAS No 84775-52-0
Plant part Rhizomes
Preparation type Extraction
Solvent used for extraction Ethyl acetate
Solvent used in manufacture Isopropyl alcohol
Final extract ratio 50:1 to 60:1
Standardization Curcuminoids
Excipient Used None

Parameters	Result	Limit	Reference
PHYSICAL			
Description	Complies	Orange yellow powder*	Organoleptic
Identification	Complies	To comply by HPLC	HPLC, SLL/STP-C-012**
Loss on drying	0.7 % w/w	Not more than 2.0% w/w (dried at 105°C)	USP <731>
Residue on ignition	0.2 % w/w	Not more than 1.0% w/w	USP <281>
Tapped bulk density	0.57 g/ml	Between 0.50g/ml and 0.90/ml	USP <616>
Loose bulk density	0.33 g/ml	Between 0.30g/ml and 0.50g/ml	USP <616>
Sieve Test (Passes Through)			USP <786>
- 20 Mesh	100 % w/w	Not less than 95% w/w	
- 40 Mesh	97.65 % w/w	Not less than 95% w/w	
- 80 Mesh	94.43 % w/w	Not less than 75% w/w	
CHEMICAL			
Assay			
-Content of total curcuminoids by HPLC	95.3 % w/w	Not less than 95.0% w/w and not more than 102.0% w/w on dry basis	HPLC, SLL/STP-C-012**

20 Lake Drive
East Windsor
New Jersey - 08520
Tel: 732-777-1111
Fax: 732-777-1443

Our Innovation Is Your Answer®
www.sabinsa.com

Sabinsa Utah
750 South Innovation Circle
Payson, UT - 84651
Tel: 801-465-8400
Fax: 801-465-8600



SABINSA CORPORATION

*Pharmaceuticals *Phytochemicals
*Fine Chemicals *Herbal Extracts
*Cosmeceuticals *Specialty Chemicals

CERTIFICATE OF ANALYSIS

Page 2 of 3

Product Name CURCUMIN C3 COMPLEX®
Product Code 0330
Batch No. J110235
TR No. DB11F0134
Date of Manufacture September 2011
Date of Expiry August 2016



Purity by HPLC

-Bisdemethoxycurcumin	6.5 %	Not less than 2.5% and not more than 6.5%	HPLC, SLL/STP-C-012**
-Demethoxycurcumin	19.83 %	Not less than 15.0% and not more than 25.0%	HPLC, SLL/STP-C-012**
-Curcumin	73.67 %	Not less than 70.0% and not more than 80.0%	HPLC, SLL/STP-C-012**

OTHERS

Total heavy metals	10 ppm (µg/g)	Not more than 20ppm (µg/g)	USP <231> Method II
Lead	0.67 ppm (µg/g)	Not more than 2ppm (µg/g)	ICP-OES,SLL/STP-H-006**
Arsenic	<0.2 ppm (µg/g)	Not more than 1ppm (µg/g)	ICP-OES,SLL/STP-H-006**
Cadmium	<0.2 ppm (µg/g)	Not more than 1ppm (µg/g)	ICP-OES,SLL/STP-H-006**
Mercury	<0.02 ppm (µg/g)	Not more than 0.1ppm (µg/g)	ICP-OES,SLL/STP-H-006**
Residual solvents	Complies	To comply as per USP	USP <467>
Residual pesticides	Complies	To comply as per USP	Pesticide Analytical Manual

MICROBIAL

Total plate count	<100 cfu/g	Not more than 5000cfu/g	USP <2021>
Yeast and mould count	<10 cfu/g	Not more than 100cfu/g	USP <2021>
Escherichia coli	Complies	Negative/10g	USP <2022>
Salmonella	Complies	Negative/10g	USP <2022>
Staphylococcus aureus	Complies	Negative/10g	USP <2022>
Pseudomonas aeruginosa	Complies	Negative/10g	USP <62>
Enterobacteriaceae	Complies	Negative/10g	USP <2021>

ADDITIONAL INFORMATION

Sanitizing treatment	Non irradiated and not treated with ETO
Certification status (Kosher/Halal)	Kosher certified, Halal certified

20 Lake Drive
East Windsor
New Jersey - 08520
Tel: 732-777-1111
Fax: 732-777-1443

Our Innovation Is Your Answer®
www.sabinsa.com

Sabinsa Utah
750 South Innovation Circle
Payson, UT - 84651
Tel: 801-465-8400
Fax: 801-465-8600



SABINSA CORPORATION

*Pharmaceuticals *Phytochemicals
*Fine Chemicals *Herbal Extracts
*Cosmeceuticals *Specialty Chemicals

CERTIFICATE OF ANALYSIS

Page 3 of 3

Product Name CURCUMIN C3 COMPLEX®
Product Code 0330
Batch No. J110235
TR No. DB11F0134
Date of Manufacture September 2011
Date of Expiry August 2016



Genetic Modification Status GMO free
BSE/TSE status BSE/TSE free
Country of origin India
Cultivated or wild crafted Cultivated
Storage condition Store at room temperature
Manufactured By Sami Labs Limited
19/1,19/2 I Main, II Phase, Peenya Industrial Area, Bangalore - 560058, Karnataka, India
Manufactured At Sami Labs Limited - Dobaspet
Plot No.4B/4C, KIADB Industrial Area, Dobaspet, Somapura Hobli, Nelamangala, Bangalore Rural Dist.-562111
Patent Information CURCUMIN C3 COMPLEX® is Patented Product from Sabinsa Corporation, US#5861415, EP#0839037
Remarks
*Since it is a herbal product, there is likely to be minor colour variation because of the geographical and seasonal variations of the raw material
*Natural products can be hygroscopic and tend to agglomerate sometimes. It is suggested to sift before use


Camille Somaru
Manager QC/QA

The above certificate of analysis is based on **Specifications Issue No: 13.0 Dated: August 22, 2011**

****In-House developed and validated methods**


NAP: Not Applicable

NAV: Not Available

20 Lake Drive
East Windsor
New Jersey - 08520
Tel: 732-777-1111
Fax: 732-777-1443

Our Innovation Is Your Answer®
www.sabinsa.com

Sabinsa Utah
750 South Innovation Circle
Payson, UT - 84651
Tel: 801-465-8400
Fax: 801-465-8600

		LycoRed Ltd. Hebron Road, Industrial Zone P.O.Box 320, Beer-Sheva 84102, Israel Tel: ++972 8 6296994, Fax: ++972 8 6236310 www.lycored.com info@lycored.com
NUTRITIONAL INFORMATION		Date: February 18 th , 2007
Product:	Tomat-O-Red® 10% CWD	Catalogue no: 400301

Lycopene	10%
Total Calories	376 cal./100gr
Calories from Fat	149.4 cal./100gr
Total Fat	16.6%
Saturated Fat	3.3%
Cholesterol	-
Sodium	197 ppm
Potassium	2530 ppm
Total Carbohydrates	35.1%
Dietary Fiber	20%
Soluble Fiber	20%
Insoluble Fiber	-
Total Fibers	20%
Sugars	-
Protein	-
Calcium	-
Iron	18.5 ppm
Moisture	5%
Sucrose Ester	13.3%